THE UNIVERSITY
of EDINBURGH

NOVEL APPROACH TO CANCER THERAPEUTICS USING COMPARATIVE CANCER BIOLOGY

Bhindu Revi

Doctor of philosophy

The University of Edinburgh

December 2017

DECLARATION

I hereby declare that I am the author of this thesis. The work described in this thesis is my own and any contribution by others has been clearly indicated and acknowledged. I can also confirm that no part of this thesis has been previously submitted for any other degree or professional qualification.

Bhindu Revi
December 2017

"Dream, Dream Dream.
Dreams transform into thoughts
And thoughts result in action."

- A.P.J. Abdul Kalam

Acknowledgements

My PhD would have been impossible without the invaluable help from many people and no words can express my gratitude to all. First and foremost my appreciation goes to Prof David argyle for giving me this opportunity and always providing me with great support, it was indeed great honour to work and get guidance from you throughout my PhD. Many thanks are due to Kathryn for believing in me, for introducing me into the beautiful world of MDM2 and IRF-1. I am very grateful to her for giving me the opportunity to join her research group and sharing her passion for science with me in endless discussions. Thank you for all your patience during the 3 years in supervising me and also in proof reading my thesis. Thank you for always giving me the freedom to explore and plan my own experiment and refining me into a better scientist. Thanks are also due to Ted for his brilliant ideas and his ability to always see the positives in all experimental data. Thanks for all the proof reading and for being very approachable for any doubts. Many thanks goes to Lisa for proof reading my thesis chapter. Borek for all his help while my trip to Brno. Many thanks to everyone in my thesis committee especially Donald Yool for all the support.

Finally, none of this would have been possible without the continuous support and encouragement from my ever inspiring husband Hari and also the cuddles of my little daughter Jia which acted like stress buster for all the bad science days. A big thanks to my fav 3 ☺ my Mother, Father and mother in law who helped out in looking after Jia throughout my PhD, I owe a lot to them. Many thanks to my dear sisters Ragi and Smitha who have always been a great support throughout the PhD and always trusting in me. My best friend Ambily even though she's miles away she made sure she was always there for me when I needed her the most. Many thanks to Philip for all the help with his expertise in chaperone and always being a silent reminder for my thesis. Thanks to all the members of Hupp ball group especially Maria Gil, Maria Gomez, Aiman, and Ashita. Jia, thanks for always keeping me company in lab and in trips. Many thanks to Moon and her mom for all the delicious meals and time we spend together in Edinburgh. Many thanks to Liz and Kalai for being there in lab and out of Lab Company.

Abbreviations

aa	Amino acid
ARF	alternate reading frame protein
AMP	Adenosine monophosphate
ATP	Adenosine triphosphate
Bp	Base pair
BSA	Bovine serum albumin
CHIP	C-terminus of Hsc70-interacting protein
Co-IP	Co-immunoprecipitation
CNVs	copy number variations
DAPI	4', 6-diamino-2-phenylindole
DMSO	Dimethyl sulphoxide
DNA	Deoxyribonucleic acid
DTT	Dithiothreitol
E.coli	*Escherichia coli*
EGFR	Epidermal growth factor receptor
EDTA	Ethylenediaminetetraacetic acid
FBS	Foetal bovine serum
FACS	Fluorescence-Activated Cell Sorting
FASP	Filter-Aided Sample Preparation
GAPDH	Glyceraldehyde-3-Phosphate Dehydrogenase
HEPES	4-(2-hydroxyethyl)-1-piperazineethanesulfonic acid
HSP	heat shock protein
His	Histidine

HRP	Horse radish peroxidase
IFN	Interferon
ITPG	Isopropyl-β-thio-galactoside
INDELS	insertions or deletions
IF	Immunofluorescence
IR	Ionising radiation
kDa	Kilodalton
mAb	Monoclonal antibody
mRNA	Messenger RNA
NGS:	next-generation sequencing
OD	Optical density
ORF	Open reading frame
OSA	Osteosarcoma
pAb	Polyclonal antibody
p53	Tumour suppressor protein 53
PAGE	Polyacrylamide gel electrophoresis
PD1	programmed cell death protein 1
PDL-1	programmed death ligand 1
RNA	Ribonucleic acid
rpm	Revolutions per minute
SBP	Streptavidin-Binding Peptide
SNVs	single nucleotide variants
STS	soft tissue sarcomas
SDS	Sodium dodecyl sulphate
siRNA	Short interfering RNA

Tris	2-amino-2-hydroxymethyl-propane-1, 3-diol
TMT	Tandem Mass Tagging
wt	Wild type
WES	whole exome sequence
WGS	whole genome sequence

Abstract

Developing personalized cancer therapies based on cancer genomics methodologies forms the basis for future cancer therapeutics. A genomics platform was developed based on canine cancer to produce a proof-of-concept for personalized genomics led therapeutic choices but also developing personalized therapeutics for canine cancer patients themselves. The platform identified the genetic state of a canine cancer patient within two drugable pathways; p53 and HSP90/IRF1. The former gene was wild-type p53 thus directing the use of p53 activating molecules. The latter mutations in both HSP90 and IRF1 suggested an investigation into HSP90 and interferon signalling molecules as drug leads. Drugs that target both of these pathways were subsequently used to measure drug effects in cell line models but also to identify novel biomarkers of drug responses.

My study focused on the effect of the HSP90-inhibitor Ganetespib had on its client proteins, particularly IRF-1. Briefly my results indicated the following:(i) Ganetespib downregulated IRF-1 protein levels in A375 cell lines and this attenuation was not mediated by either MDM2 or CHIP (E3 ligase). IFNγ- induced IRF-1 was also observed to be downregulated when Ganetespib was used in combination therapy.(ii) Insitu proximity ligation assay showed induced HSC70 upregulation upon HSP90 inhibition by Ganetespib and HSC70/MDM2 complexes were seen to be stabilized compared to the usage of MDM2/p53 inhibitor-nutlin. I hypothesize that MDM2/HSC70 complex might chaperon IRF-1 into lysosome for degradation via chaperon mediated autophagy pathway. (iii) My results also indicate that Ganetespib can downregulate IFN γ- induced PDL-1 expression in melanoma cell lines. Pre-sensitizing the cells with Ganetespib prior to the addition of IFNγ could attenuate PDL-1 to basal levels. (iv) My results also showed that the downregulation of PDL-1 by Ganetespib is an IRF-1 dependent mechanism. Therefore, my results suggest that HSP90 represents an important emerging target for cancer therapy because its inactivation results in the simultaneous blockade of multiple signalling pathways and can also sensitize tumor cells to other anticancer agents. Targeting HSP90 could also help to disrupt PD1/PDL-1 interaction and activate immune system to recognise tumor cells. I conclude that HSP90 and IRF-1 play a critical role in types II interferon pathways and these findings establish a novel basis for the design of future Ganetespib-based combinatorial approaches to improve patient outcomes in this disease. These approaches finally demonstrate that cancer genomics can stratify choice of cancer drugs used on patients but also provide evidence that cancer patient samples can be used for the specific stratification of cancer drug choice based on cancer genomics data.

Lay summary

Melanoma is the deadliest form of skin cancer. Although it comprises less than 5% of skin cancer cases, melanoma accounts for the great majority of skin cancer-related deaths. HSP90 is protein that assists in the maintenance of several essential proteins in human body and aids in protein degradation. It also stabilisers proteins which are required for cancer (tumor growth). Hence drugs that target (inhibit) HSP90 is of great value for cancer therapeutics and has been widely studied in the past 20 years. My project comprises the study of one such novel HSP90 inhibitor drug called Ganetespib in melanoma cell lines. My results indicated that using this drug in cancer cell lines decreased a protein called PDL-1(also known as immune checkpoint target) which is usually seen elevated in patients with this cancer type. Hence by lowering this protein, it is possible to enable the body's own immune system to fight cancer. My results also indicated that using Ganetespib in combination with other anticancer drugs may provide a more powerful and effective method to treat melanoma patients.

Contents

DECLARATION ii
Acknowledgements iv
Abbreviations v
Abstract viii
1.1 Chapter 1 Introduction 1
1.1 Molecular Chaperone proteins 1
1.1.1 Chaperone machinery 3
1.1.2 The HSP90 family and their subcellular localization 5
1.1.3 The HSP90 machinery 7
1.1.3.1 Structure 7
1.1.3.2 Function 7
1.1.4 HSP70 9
1.1.5 HSF1 9
1.2 Chaperones and cancer 10
1.2.1 Targeting HSP90 in cancer therapy 10
1.2.1.1 Escaping Antigrowth Signals 11
1.2.1.2 Limitless Proliferation and Avoidance of Senescence 11
1.2.1.3 Angiogenesis 12
1.3 HSP90 drugs in clinics 14
1.3.1 RETASPIMYCIN 17
1.3.2 NVP-AUY922 17
1.3.3 AT13387 18
1.3.4 Ganetespib 18
1.4 Combination Phase I/II trial 21
1.5 Clients of HSP90 24
1.5.1 The IRF family 24
1.5.2 Evolution of the IRF family 25
1.5.3 Interferons and the interferon signalling pathway 25
1.5.4 Overview of the human IRF family members 28
1.5.4.1 IRF-1 28

1.5.4.2 IRF-2 28
1.6 SARCOMA 30
1.6.1 P53 32
1.6.2 MDM2 32
1.6.3 Mutations of TP53, expression levels of MDM2 32
1.7 Comparative oncology 33
1.8 Canine Model 33
1.9 Canine Sarcoma 34
1.9.1.1 Osteosarcoma 36
1.9.1.2 Genetic Heterogeneity 36
1.9.1.3 Chromosomal Abnormalities 36
1.9.2 Tumour Suppressors 37
1.9.2.1 Rb Pathway 37
1.9.2.2 p53 Pathway 37
1.9.3 Other Tumour Suppressors 38
1.9.3.1 Oncogenes 38
1.9.4 Advantages over other models 39
1.9.5 Limitations of the dog model 40
1.9.6 Current Drugs on clinics 42
1.10 Bioinformatics in comparative oncology 44
1.11 THESIS AIMS 45
2 Methods and materials 46
2.1 Plasmids, chemicals and reagents 46
2.2 General microbiological techniques 46
2.2.1 Maintaining bacterial cultures 46
2.2.2 Glycerol stocks 47
2.2.3 Preparation of competent cells by heat shock method 47
2.2.4 Transforming bacterial cells 48
2.3 General molecular biology techniques 48
2.3.1 Plasmid DNA amplification, extraction and quantification 48
2.3.2 Agarose gel electrophoresis of DNA 49
2.4 General biochemical techniques 49
2.4.1 Protein quantification 49
2.4.2 SDS-PAGE 50
2.4.3 Coomassie staining of SDS-PAGE gels 51

2.4.4 Western blotting 52
2.4.5 Stripping nitrocellulose blots 55
2.5 Cell culture 56
2.5.1 Cell lines 56
2.5.2 Sub-culturing of cells 58
2.5.3 Freezing and thawing cells 58
2.5.4 Transient transfection of DNA and siRNA 59
2.5.5 Harvesting cells 59
2.5.6 Mammalian cell lysis 60
2.5.7 Drug treatments 61
2.6 Microscopy 63
2.6.1 Proximity ligation assay (PLA) 63
2.7 Other assays 64
2.7.1 Co-immunoprecipitation (Co- IP) 64
2.7.2 SBP-tagged pull down 64
2.8 Immunofluorescence 65
2.9 Sample Preparation for Mass Spectrometry and result Analysis 66
2.9.1 Mass Spectrometry 66
2.9.1.1 Sample preparation for mass-spectrometry 66
2.9.1.2 Lysis of cell pellets 66
2.9.1.3 FASP digestion 67
2.9.1.4 TMT labelling 68
2.9.1.5 Peptide purification 69
2.9.2 Flow Cytometry 70
2.10 General Biochemical Techniques 71
2.10.1 Bradford Assay for Protein quantification 71
2.11 Cell-based assays 71
2.11.1 Cell cytotoxicity Assay 71
2.12 Bioinformatics 71
2.12.1 Canine Osteosarcoma DNA and RNA purification 71
2.12.2 Sequencing of OSA31 DNA 72
2.12.3 Sequencing of OSA31 RNA 72
2.12.4 Data analysis 72
2.12.4.1 Input files into CLC workbench 72
2.12.4.2 Downloading the canine reference 72

..... 73
2.12.4.3 Map reads to contig and variant detections for OSA31 tumor DNA and Normal DNA..... 76
2.12.4.4 Compare Normal to OSA31 seq data 76
..... 81
2.12.4.5 Detection of expressed somatic mutations in the RNAseq..... 83
3 Results: Comparative oncology: canine model..... 87
3.1 The use of a Canine Osteosarcoma cancer cell as a model for personalizing anti-cancer therapeutics 87
3.1.1 Cell models used for nucleic acid sequencing. 88
3.1.2 DNA seq analysis of the OSA31 genome. 89
3.1.3 Non-synonymous mutations and types of mutations by comparing tumour to normal tissue 89
3.1.4 Identifying expressed mutations by comparing tumour RNA to tumour DNA 91
3.1.5 Defining the commonly mutated genes..... 95
3.2 Characterization of a canine osteosarcoma cell as a model for developing next generation proteogenomics..... 99
3.2.1 Characterisation of canine osteosarcoma cell lines for p53 activation in response to Nutlin-3 99
3.2.2 Characterisation of canine osteosarcoma cell lines for HSP70 responsiveness to HSP90 inhibitors. 101
3.2.3 Characterisation of canine osteosarcoma cell lines for IRF1 response to HSP90 inhibition. 103
3.2.4 Proteomics on drug-treated canine osteosarcoma cell lines to develop biomarkers of drug responsiveness 106
3.2.5 Summary of the Ganetespib treatment responses..... 108
3.2.6 Upregulated proteins with Ganetespib treatment 108
3.2.7 Downregulated proteins upon treatment with Ganetespib 115
3.2.8 Proteomic changes upon Nutlin-3 treatment. 119
3.2.9 Summary of characterisation of the OAS31 cell line as a model for drug testing. 125
4 MDM2 interactome..... 128
4.1 Introduction 128
4.2 Results 131
4.2.1 MDM2 interactome and p53 ubiquitination..... 131

4.2.2 Ewing sarcoma and HSP90 inhibitors 135
4.2.3 Characterisation of osteosarcoma cell lines in association with MDM2 expression 137
4.2.4 Ganetespib stabilises HSP/C 70 and MDM2 interaction 139
4.2.5 Validation of HSC/P70 and MDM2 interaction 142
4.2.6 Combinatorial treatment of Ganetespib with nutlin 145
4.2.7 Cell viability with Ganetespib and nutlin treatments 149
4.2.8 Discussion 151
5 Mechanism of downregulation of IRF-1 with ganetespib 152
5.1 Introduction 152
5.1.1 IRF-1 152
5.1.2 Molecular chaperons and IRF-1 152
5.2 Results 154
5.2.1 Inhibition of HSP90 leads of reduction of client protein levels 154
5.2.2 Attenuation of IRF-1 is p53-independent 158
5.2.3 Downregulation of IRF-1 is affected by proteasome inhibitors 160
5.2.4 Role of E3 ligases in IRF-1 downregulation 162
5.2.5 CHIP and MDM2 Knock-down 168
5.2.6 Chaperone mediated autophagy 172
5.2.7 HSP90 inhibitors and autophagy 176
5.2.8 Proteomic screen 182
5.2.8.1 Effects of Ganetespib treatment on A375 proteome 184
5.2.8.2 Effects of Nutlin treatment on the A375 proteome 188
5.2.8.3 Effects of combinatorial treatment on the A375 proteome 193
5.2.8.4 UBA 3 analysis 198
5.3 Discussion 200
6 HSP90 inhibitors in immune surveillance 202
6.1 Introduction 202
6.1.1 The Interferon system 202
6.1.1.1 Interferon γ 202
..... 205
6.1.2 Therapeutic targets for cancer immunotherapy 205
6.1.2.1 Immune checkpoints 205
6.1.2.2 Combined therapies 207
6.1.3 HSP90 and the immune system 209

6.2 Aim 209
6.3 Results 210
6.3.1 Ganetespib downregulates IFNγ -induced IRF-1 expression 210
6.3.2 Upregulation in IRF-1 expression with IFNγ is dose and time dependent 212
6.3.3 Downregulation of IFNγ-induced PD-L1 expression by Ganetespib 216
6.3.4 Ganetespib inhibits PD-L1 expression induced by INFγ pre-treatment 220
6.3.5 Loss of PD-L1 is via an IRF-1-dependent pathway 222
6.3.6 The dose dependency of PD-L1 expression on Ganetespib depends on cell type 225
6.3.7 PD-L1 expression is regulated by the autophagy protein ATG5 227
6.3.8 HSP90 inhibitors in IFNα signalling 230
6.4 Discussion 233
7 Conclusion and future work 239
8 Bibliography 245

List of Figures

FIGURE 1 CHAPERONE PROTEINS 2
FIGURE 2 CHAPERONE MACHINERY 4
FIGURE 3HSP90 SUB-FAMILY 6
FIGURE 4 HSP90 STRUCTURE 8
FIGURE 5 HALLMARKS OF CANCER 13
FIGURE 6 FIRST AND SECOND GENERATION HSP90 INHIBITORS 15
FIGURE 7 CLINICAL TRIALS 16
FIGURE 8 STRUCTURE AND MECHANISM OF ACTION OF GANETESPIB 20
FIGURE 9 ONGOING COMBINATION TRIALS OF GANETESPIB WITH OTHER THERAPEUTIC AGENTS 23
FIGURE 10 IFN SIGNALLING PATHWAYS 27
FIGURE 11 CLASSIFICATION OF SARCOMA 31
FIGURE 12 INTEGRATED AND COMPARATIVE DRUG TRIAL MODEL 35
FIGURE 13 HUMAN AND CANINE CANCER CELLS ARE SIMILARLY SENSITIVE TO CHEMOTHERAPY 41
FIGURE 14 NUTLIN ACTION ON MDM2-P53 COMPLEX 43
FIGURE 15IMPORTING FILES TO WORKBENCH 73
FIGURE 16 DOWNLOADING THE CANINE REFERENCE GENOME 74
FIGURE 17 DOWNLOADING CANINE REFERENCE GENOME CONTINUED 75
FIGURE 18 MAP READS TO CONTIGS/REFERENCE 77

FIGURE 19BASIC VARIANT DETECTION 78
FIGURE 20VARIANT DETECTION CONTINUED 79
FIGURE 21COMPARE TUMOR OSA31 TO NORMAL TISSUE 80
FIGURE 22ANNOTATE 81
FIGURE 23AMINOACID CHANGES 82
FIGURE 24 COMPARE VARIANT DNA AND RNA SEQ FROM OSA31 84
FIGURE 25COMPARE VARIANT DNA AND RNA SEQ FROM OSA31 CONTINUED 85
FIGURE 26 CREATING TRACKS 86
FIGURE 27MUTATION SIGNATURE 90
FIGURE 28 BROWER EXAMPLE FOR MUTATION SIGNATURES OBSERVED IN OSA31 GENOME 93
FIGURE 29KEY GENES MUTATED IN OSTEOSARCOMA 94
FIGURE 30 HIGHEST GENES FOUND BOTH IN DNA AND RNA TUMOUR 96
FIGURE 31 PROGNOSTIC BIOMARKERS 97
FIGURE 32 POTENTIAL CANINE VACCINE LIST 98
FIGURE 33 PANEL OF CANINE CANCER OSTEOSARCOMA CELL LINES TESTED FOR LEVELS OF HSP70, HSP90, P53, AND MDM2 PROTEINS. 100
FIGURE 34 CHARACTERISATION OF P53 AND HSP70 102
FIGURE 35OSA AND D17 TREATED WITH GANETESPIB AND NUTLIN 104
FIGURE 36 PLA SYSTEM DETECTS CANINE HSP/C70/MDM2 INTERACTIONS 105
FIGURE 37 WESTERN BLOT ANALYSIS OF PROTEOMICS SAMPLES 107
FIGURE 38 SCATTER PLOT INDICATING PROTEINS UPREGULATED/DOWNREGULATED WITH GANETESPIB TREATMENT 111
FIGURE 39 UPREGULATED PROTEINS IN A CANINE OSTEOSARCOMA CELL LINE TREATED WITH GANETESPIB 113
FIGURE 40 UPREGULATED PROTEINS WITH GANETESPIB 114
FIGURE 41 DOWNREGULATED PROTEINS IN OSA31 CELLS WITH GANETESPIB TREATMENT 117
FIGURE 42 DOWNREGULATED PROTEINS IN OSA31 CELLS WITH GANETESPIB TREATMENT 118
FIGURE 43 SCATTER PLOT INDICATING GENES UPREGULATED/DOWNREGULATED WITH NUTLIN TREATMENT 121
FIGURE 44 UPREGULATED GENES WITH NUTLIN TREATMENT IN OSA31 CELLS 122
FIGURE 45 UPREGULATED PROTEINS IN OSA31 CELLS WITH NUTLIN TREATMENT 123
FIGURE 46 DOWNREGULATED GENES WITH NUTLIN IN OSA31 CELLS 124
FIGURE 47 MDM2 INTERACTOME AND P53 UBIQUITINATION 132
FIGURE 48 COMPONENTS REGULATING P53 UBIQUITINATION 134
FIGURE 49 EWING SARCOMA AND HSP90 INHIBITORS 136
FIGURE 50 CELL DENSITY INFLUENCES MDM2 PROTEIN EXPRESSION LEVELS 138
FIGURE 51 GANETESPIB STABILISES HSP/C70 AND MDM2 COMPLEXES. 140
FIGURE 52 MDM2 AND HSP70 LOCALISATION WITH DRUG TREATMENTS 141
FIGURE 53 VALIDATION OF HSC/P 70 AND MDM2 INTERACTION 144
FIGURE 54 COMBINATORIAL EFFECTS OF NUTLIN AND GANETESPIB ON IRF-1 DEPLETION 147

FIGURE 55 EFFECT OF COMBINATORIAL TREATMENT ON IRF-1 LOCALISATION 148
FIGURE 56 CELL VIABILITY WITH NUTLIN AND GANETESPIB TREATMENTS. 150
FIGURE 57 HSP90 INHIBITOR DOWNREGULATES CLIENT PROTEINS..... 156
FIGURE 58 HSP90 LOCALISATION IN A375 CELL LINES 157
FIGURE 59 LOSS OF IRF-1 IS A P53 INDEPENDENT MECHANISM 159
FIGURE 60 ATTENUATION OF IRF-1 IS POST-TRANSLATIONAL 161
FIGURE 61PROXIMITY LIGATION ASSAY SYSTEM DETECTS INDUCED HSP70 AND MDM2 INTERACTION WITH GANETESPIB 164
FIGURE 62 PROXIMITY LIGATION ASSAY SYSTEM DETECTS HSP70 AND CHIP INTERACTION WITH GANETESPIB AND NUTLIN TREATMENT..... 165
FIGURE 63 PLA SYSTEM DETECTS MDM2 AND CHIP INTERACTION WITH GANETESPIB AND NUTLIN TREATMENT 166
FIGURE 64 LOCALISATION OF MDM2 AND CHIP WITH GANETESPIB AND NUTLIN TREATMENT 167
FIGURE 65 ROLE OF CHIP AND MDM2 IN DOWNREGULATION OF IRF-1 WITH GANETESPIB TREATMENT 170
FIGURE 66 PROXIMITY LIGATION ASSAY DETECTS INDUCED HSC70/MDM2 INTERACTION WITH GANETESPIB TREATMENT 171
FIGURE 67 IRF-1 AND HSP70 INTERACTIONS WITH GANETESPIB TREATMENT 174
FIGURE 68 CHAPERONE MEDIATED AUTOPHAGY..... 179
FIGURE 69 PROXIMITY LIGATION ASSAY DETECTION OF HSC70/MDM2 WITH AUTOPHAGY AND PROTEASOME INHIBITORS 181
FIGURE 70 TMT MASS SPECTROMETRY 183
FIGURE 71 SCATTER PLOT INDICATING GENES UPREGULATED/DOWNREGULATED WITH GANETESPIB TREATMENT 185
FIGURE 72UPREGULATED GENES WITH GANETESPIB 186
FIGURE 73 DOWNREGULATED GENES WITH GANETESPIB..... 187
FIGURE 74 SCATTER PLOT INDICATING GENES UPREGULATED/DOWNREGULATED WITH NUTLIN TREATMENT..... 190
FIGURE 75 UPREGULATED GENES WITH NUTLIN 191
FIGURE 76 DOWNREGULATED GENES WITH NUTLIN 192
FIGURE 77 SCATTER PLOT INDICATING GENES UPREGULATED/DOWNREGULATED WITH COMBINATORIAL TREATMENT.. 195
FIGURE 78 UPREGULATED GENES WITH COMBINATORIAL TREATMENT 196
FIGURE 79 DOWNREGULATED GENES WITH COMBINATORIAL TREATMENT 197
FIGURE 80 WESTERN BLOT ANALYSIS OF THE ROLE OF UBA-3 AS POTENTIAL E1 LIGASE 199
FIGURE 81 CYTOKINES INDUCE JANUS KINASE/SIGNAL TRANSDUCERS AND ACTIVATORS OF TRANSCRIPTION (JAK/STAT) PATHWAY ACTIVATION..... 204
FIGURE 82 IMMUNE CHECKPOINT PATHWAYS 208
FIGURE 83 GANETESPIB DOWNREGULATES IFNΓ-INDUCED IRF-1 EXPRESSION IN MELANOMA CELLS. 211
FIGURE 84 IRF-1 ACTIVATION VIA IFNΓ IS DOSE AND TIME DEPENDENT 214
FIGURE 85 IRF-1 LOCALISATION WITH IFNΓ TIME COURSE 215
FIGURE 86 GANETESPIB DOWNREGULATES IFNΓ INDUCED PD-L1 EXPRESSION. 218

FIGURE 87 LOCALISATION OF PD-L1 219
FIGURE 88 GANETESPIB DOWNREGULATES PRE-TREATED IFNΓ-INDUCED PD-L1 EXPRESSION. 221
FIGURE 89 IFNΓ-INDUCED EXPRESSION OF PD-L1 IS IRF-1 DEPENDENT 223
FIGURE 90 IRF-1 LOCALISATION AFTER IFNΓ STIMULATION 224
FIGURE 91 ATTENUATION OF IFN-INDUCED PD-L1 IS CELL TYPE DEPENDENT 226
FIGURE 92 DOWNREGULATION OF IFNΓ-INDUCED PD-L1 BY GANETESPIB IS REGULATED VIA THE ATG5 GENE 229
FIGURE 93 IFNA INDUCED PD-L1 DOWNREGULATION BY GANETESPIB 232
FIGURE 94 SUMMARY FOR POTENTIAL EFFECTS OF GANETESPIB ON TUMOUR CELLS 238
FIGURE 95CHAPERON MEDIATED AUTPHAGY 244
FIGURE 96 UPREGULATED WITH GANETESPIB 270
FIGURE 97 UPREGULATED WITH NUTLIN 272
FIGURE 98 DOWNREGULATED WITH GANETESPIB 273
FIGURE 99DOWNREGULATED WITH NUTLIN 274
FIGURE 100GAN+NUT UPREGULATED 275
FIGURE 101NUTLIN+GAN DOWNREGULATED 276

List of Tables

TABLE 1 ANTIBODIES 55
TABLE 2 CELL LINES AND CULTURE MEDIA 58
TABLE 3 DRUGS: PRINCIPAL EFFECTS AND WORKING CONCENTRATIONS 63
TABLE 4 SAMPLES FOR TMT 68

1.1 Chapter 1 Introduction

1.1 Molecular Chaperone proteins

Heat-shock protein (HSP) or chaperone proteins are a family of proteins that are produced by cells in response to exposure to stressful conditions. Many members of this group perform chaperone functions by stabilising new proteins to ensure correct folding, or by helping to refold proteins that have been damaged by cellular stress. Increase in HSP expression is transcriptionally regulated. The dramatic upregulation of heat shock proteins is a key part of the heat shock response and is induced primarily by heat shock factor (HSF).Figure 1a illustrates the basic molecular chaperones expressed by cells in a state of stress, and some of their key functions (Stuart K. Calderwood, 2016) (Workman, 2003).

Heat-shock proteins are named according to their molecular weight. The small 8 kilodalton protein, ubiquitin, which marks proteins for degradation, also has features of a heat shock protein. The principal heat-shock proteins that have chaperone activity belong to five conserved categories eg.HSP33,HSP60,HSP70,HSP90,HSP100, and the small heat-shock proteins (sHSP)Figure 1-b (Félix Sauvage a, 2017).In my thesis I will focus predominantly on HSP90 and HSP70 proteins.

(a)

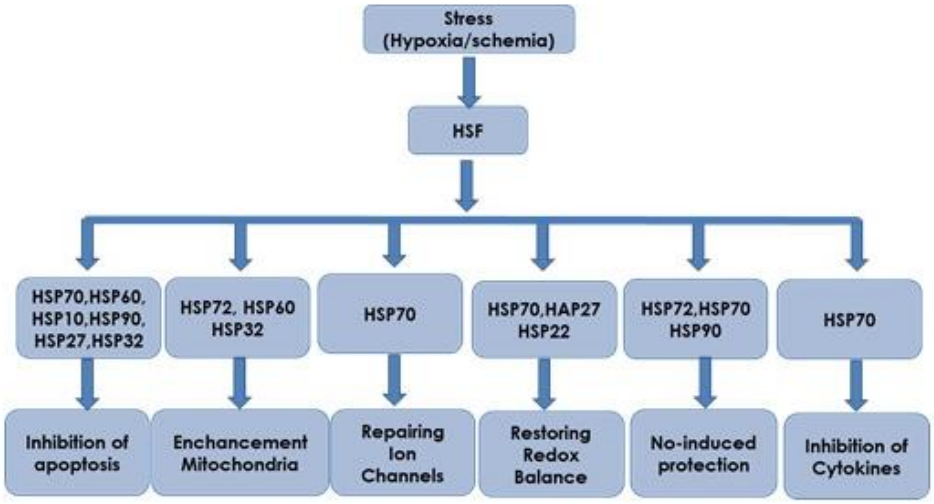

(b)

Protein	Function	Co-Chaperones
Small HSP (Hsp27)	chaperone	None
HSP60	Chaperonin	Hsp10
HSP70	chaperone	Hsp40,Grpe,Bag1,Bag3,Hip,Hop,CHIP
HSP90	chaperone	P23,Aha1,Hop,FKBP51,FKBP52,Cyp40,Cdc37
HSP110	Holdase,Co-Chaperone	None

Figure 1 Chaperone proteins

(a) Heat shock response pathways and hypoxia adaptive responses; adapted from (Neil C Chi, 2004) (b) These are the major HSPs induced by heat shock. Their roles in cancers of various morphologies have been reviewed previously. Co-chaperones HSP10, HSP40, Grpe, Bag1, Bag3, Hip, Hop, CHIP, p23, Aha1FKBP51 and FKBP52, Cyp40, and Cdc37 facilitate interactions of the primary chaperone with client proteins. (Stuart K. Calderwood, 2016)

1.1.1 Chaperone machinery

The chaperone machinery consists of HSP90 associated with co-chaperones (including HSP40, HSP27, HOP, Cdc37, p23 and Aha1) (Figure 2). Each co-chaperone has a specific role in assisting HSP90 to repair and refold proteins. Many other proteins also play a role in the chaperone cycle and oncogenesis, including immunophilins and the peptidylprolyl cis-trans isomerases FKBP1 and 2. Most of the HSP90 co-chaperones are tetratricoprotein repeat (TPR) proteins and interact with a specific sequence in the C-terminal domain of HSP90 (MEEVD motif). HOP was the first HSP90 ATPase regulatory co-chaperone to be described. It is responsible for the coupling of HSP70 and HSP90 for the activation of steroid hormone receptors mediated by HSP90. The Cdc37 adaptor is another kinase-specific co-chaperone that can arrest the ATPase cycle of HSP90. Its N-terminal region interacts with protein kinases (as client proteins) and its central and C-terminal domains interact with HSP90. This interaction maintains an open conformation of HSP90 by preventing N-domain dimerization, and the N-M domain docking required for ATP hydrolysis. In this way, Cdc37 inhibits ATP hydrolysis and contributes to the prolonged association of HSP90 dimers with client proteins and to effective chaperone action. Aha1 is a recently discovered co-chaperone that interacts with HSP90 at the level of the M- and N-domains in presence or in absence of bound nucleotide. This interaction stimulates the ATPase activity of HSP90. Aha1 and p23 have opposing effects on HSP90, as p23 inhibits the ATPase activity, while Aha1 triggers the release of client protein by stimulating ATP hydrolysis (Rappa F, 2012) (Félix Sauvage a, 2017).

Within the cell, proteins associated with Hp27 are passed on to HSP70–co-chaperone complexes. Finally, the HSP70-bound clients are passed to HSP90 complexes, which carry out the finishing touches, producing a folded and functional client protein. Inhibition of any of these stages prevents the folding reaction. Activation of proteins complexed to HSP90 generally leads to their release; the released client is then transiently functional before it’s unfolding and deactivation (Rappa F, 2012).

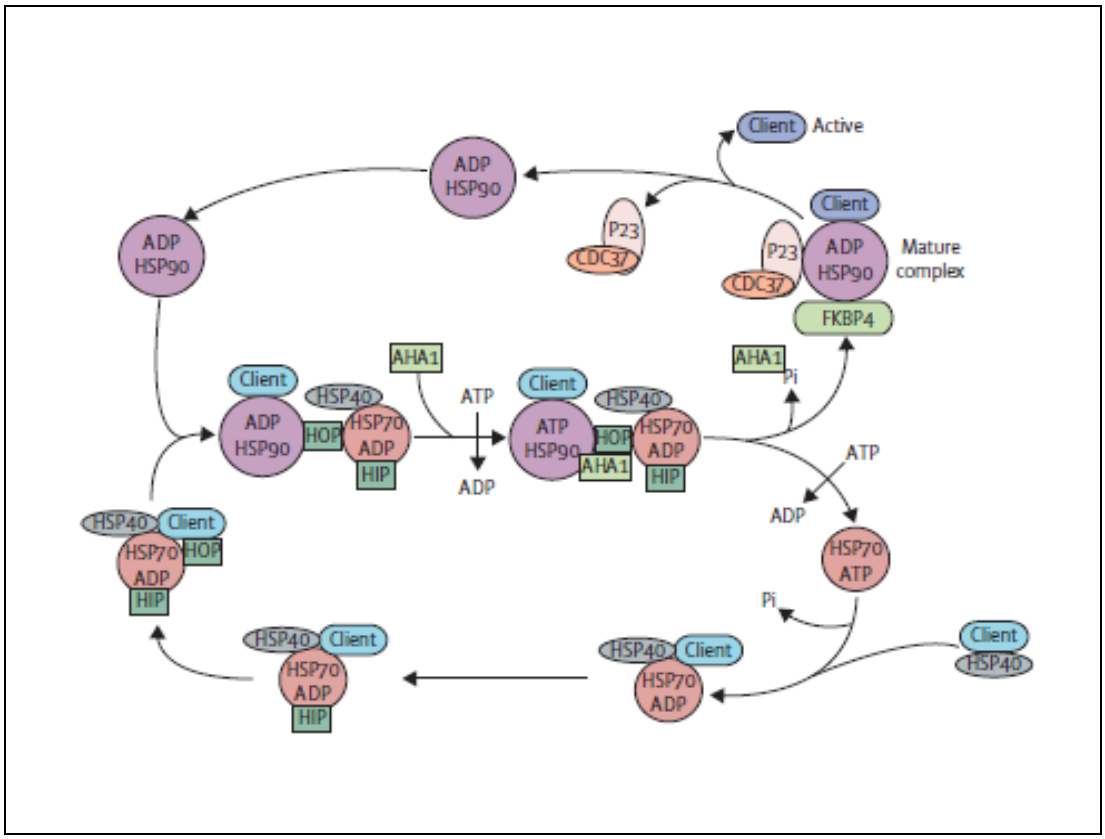

Figure 2 Chaperone machinery

HSP70, HSP40, and a client protein form an early complex. The client protein is transferred from HSP70 to HSP90 through the adaptor protein HOP (STI1). Binding of HOP is sufficient to stabilise the open conformation of HSP90. HSP90 adopts the ATPase-active (closed) conformation upon binding of ATP. P23 (SBA1) stabilises the closed state of HSP90, which weakens the binding of HOP and promotes its exit from the complex, hydrolysing ATP and liberating one phosphate molecule (Pi). Potentially, an immunophilin-type protein (FKBP4) associates to form a late complex, together with HSP90 and P23. After hydrolysis of ATP, P23 and the folded client are released from HSP90. The cofactors CDC37, HOP, AHA1, and P23 accelerate or slow specific steps of the cycle (Garcia-Carbonero R, 2013).

1.1.2 The HSP90 family and their subcellular localization

The HSP90 family in mammalian cells consists of four major homologues (Figure 3) ((Sreedhar, 2004) (Whitesell L, 2005). HSP90a (inducible form/major form) and HSP90b (constitutive form/minor form) are mostly found in the cytoplasm and the nucleus. HSP90a and HSP90b share 86 % amino acid identity and are ubiquitously expressed in all nucleated cells. In addition to HSP90a and HSP90b, there are two organelle-residing isoforms, the 94 kDa glucose-regulated protein (Grp94) and tumour necrosis factor (TNF) receptor-associated protein 1 (Trap1). Grp94 is localised to the endoplasmic reticulum while Trap1 resides in the mitochondrial matrix and the inner membrane space. Additionally, there are cell-surface-bound or secreted HSP90s residing outside the cytoplasm, generally referred to as extracellular HSP90 (eHSP90) (Tsutsumi S N. L., 2007). The eHSP90 is not an isoform of the HSP90 family but is actually an HSP90 that is cell-surface-bound or secreted from the cytoplasm. Each individual isoform possesses a unique biological function, and participates in various physiological and pathological processes (Sreedhar, 2004).

family	subcellular location	subfamily	gene	protein
HSP90A	cytosolic	HSP90AA (inducible)	HSP90AA1	Hsp90-α_1
			HSP90AA2	Hsp90-α_2
		HSP90AB (constitutively expressed)	HSP90AB1	Hsp90-β
HSP90B	Endoplasmic reticulum		HSP90B1	Endoplasmin/ GRP-94
TRAP	mitochondrial		TRAP1	TNF Receptor - Associated P rotein 1

Figure 3HSP90 sub-family

Sub-families of HSP90 and their localisation in cells.

1.1.3 The HSP90 machinery

1.1.3.1Structure

The HSP90 monomer consists of three main domains: a N-terminal domain, the binding site for ATP the hydrolysis of which, mediated by HSP90 and its co-chaperones, is the driving force for HSP90 function; a middle domain (M) where client proteins and co-chaperones bind, and a C-terminal domain; another binding site for co-chaperones, responsible for HSP90 dimerization. Substrate binding to the middle domain induces conformational changes of HSP90 via interaction with co-chaperones and ATP hydrolysis leading to a "closed" conformation (Figure 4). In this state, HSP90 can exert its activity (Félix Sauvage a, 2017).

1.1.3.2Function

HSP90 is a ubiquitous, well conserved and abundant dimeric protein that facilitates the repair and proper refolding of proteins that have undergone stress (such as pH changes, temperature variations, hypoxia or cytokine release resulting from tissue injury) that could modify their structure and thereby their function. HSP90 has a very important role in cell homeostasis and cytoprotection in various stress situations. HSP90 plays a vital role in the activation of multiple pathways important for tumour growth and resistance to cytotoxic therapies. HSP90 is an abundant and evolutionarily conserved protein that functions in a dynamic multi-chaperone complex to stabilise and activate over 200 client proteins, including those that are involved with the adaptive response to stress and necessary for constitutive cell signalling. HSP90s are ATPases that exert their chaperone role through a complex cycle regulated by the binding and hydrolysis of ATP, and by several co-chaperones. In addition to the ATP regulatory cycle, HSP90 can be regulated post-translation by phosphorylation, nitrosylation, and acetylation.

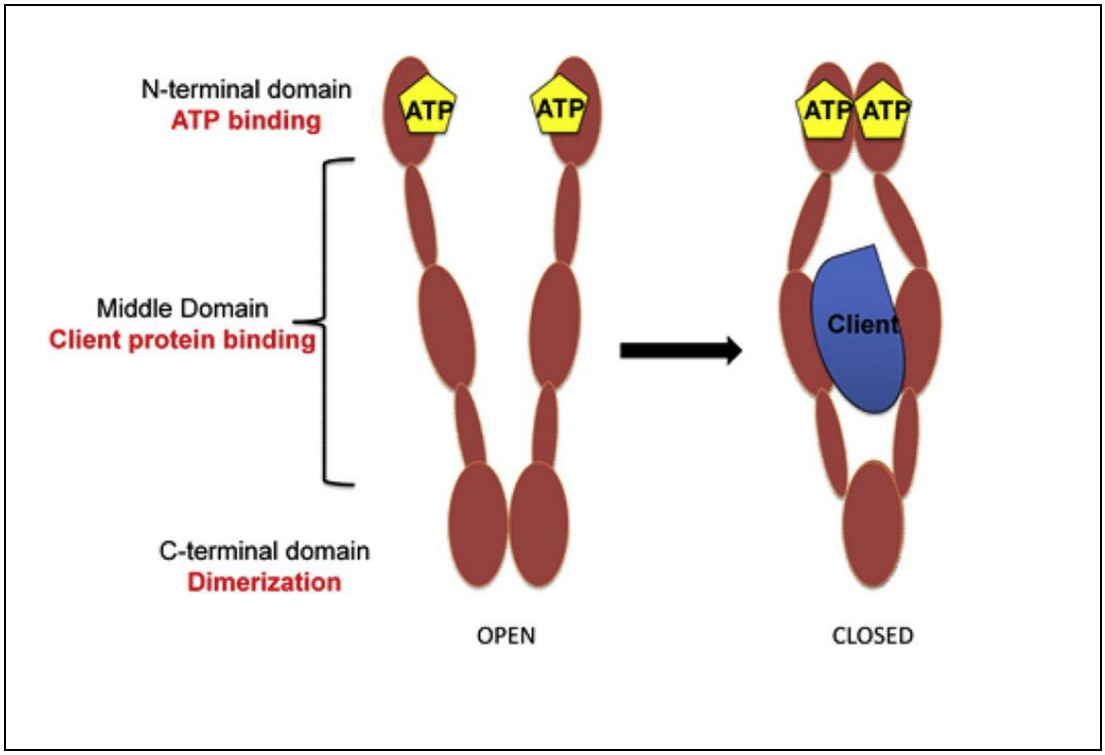

Figure 4 HSP90 structure

Schematic representation of the structure of HSP90. Substrate binding to the middle domain induces conformational changes of HSP90 *via* interaction with co-chaperones and ATP hydrolysis leading to a "closed" conformation.

1.1.4 HSP70

HSP70 contains two major functional domains, including a C-terminal peptide-binding sequence and an N-terminal ATPase domain that permits the folding of denatured client proteins. In brief, HSP70 is able to bind to unfolded proteins, and enable their folding. HSP70 is then released from the folded client when ATP bound to the N-terminal domain is hydrolysed, by utilizing its intrinsic ATPase activity. It should be noted that, within the environment of the cell, most chaperones require the aid of several co-chaperones to amplify the rates of client association, ATPase activity, and nucleotide exchange (Félix Sauvage a, 2017) (Gabai, 2015) (Matthias P. Mayer, 2000).

By contrast, HSP70 association was shown to lead to loss of activity in the client protein partner through partial unfolding and, thus, HSP70 could function as an inhibitor of some processes. Elevated levels of HSP70 inhibit the apoptotic cascade by such a mechanism. The coordinate induction of individual HSPs by stress suggested a shared mechanism regulating their expression (Gabai, 2015).

1.1.5 HSF1

When cells are undergoing stress and in some other situations such as treatment with N-terminal HSP90 inhibitors, a heat shock response (HSR) is triggered. This phenomenon involves the induction of several heat shock proteins, including HSP70 and HSP27, and is regulated at the transcriptional level by heat shock factor 1 (HSF-1), which acts as the "conductor" of the HSR.

In normal situations, HSF-1 is bound to HSP90 in the form of inactive monomers. Under stress situations, this complex dissociates and HSF-1 is released, hyperphosphorylated and binds to DNA in the form of an active trimer, resulting in the transcription of HSP genes. During recovery periods, when the stress situation is over, activated HSF-1 is repressed by the pool of chaperones. There are several hypotheses regarding this phenomenon, including that some chaperones (HSP70, HSP90 and HSP40) act as sensors and are thus able to induce a negative regulation of the HSR after stress periods. This suggests that accumulated chaperones may have a repressive activity on transcription to allow a return to homeostasis. Therefore, HSF-1 plays a central role in the response to inhibitors (Félix Sauvage a, 2017)

1.2 Chaperones and cancer

In cancer, growth control is deregulated and proliferation resumes. When growth is required, normal cells receive instruction for proliferation from secreted growth factors. The factors then bind to high-affinity receptor proteins that have extracellular binding surfaces as well as intracellular signalling domains. Thus, receptors accept the growth signal and transmit it into the interior of the cell. Signals then pass through a series of relay proteins that amplify the message, leading ultimately to cell proliferation. Deregulation at each of the signal transduction stages can be oncogenic due to unscheduled proliferation. Most of the receptors and enzymes that constitute the cascade are oncogenic when expressed at elevated levels or activated through mutation. Many of these proteins are clients of HSP90; therefore, amplification of HSP90 is permissive for unrestrained proliferation. Thus, HSP90 chaperone complexes maintain the signalling circuitry that underlies the capacity of many cancers for independent growth (Figure 5) (Stuart K. Calderwood, 2016).

1.2.1 Targeting HSP90 in cancer therapy

Among HSP90 client proteins, several are involved in the so-called “hallmarks of cancer”, first proposed by Hanahan and Weinberg and therefore contribute to tumorigenic cell stabilization (Hanahan, 2011) Figure 5. These proteins have a major role in cancer, and include protein kinases, telomerases and steroid hormone receptors as well as transcription factors. Therefore, proliferation, apoptosis and metabolism pathways are all concerned in the chaperoning of HSP90. The accumulation of mutated and dysregulated oncoproteins has been associated with modification of HSP90 properties. Finally, as client oncoproteins display stable association with HSP90, the latter is more activated in tumour cells hence a higher affinity for inhibitors. These singular properties make the targeting of HSP90 a highly promising approach to cancer therapy since the inhibition of a single target can result in multiple effects on oncogenesis-associated phenomena. When the function of HSP90 is inhibited, the client protein cannot be properly stabilized and will be targeted to the proteasome by the ubiquitin-ligase system. The extent and duration of protein degradation with HSP90 inhibition might vary substantially for specific client proteins, with HER2 and ALK–EML4 showing the highest sensitivity. (workman, 2004)

As a result, oncogenic proteins involved in the cancer hallmarks are degraded, leading to the possibility of various anticancer effects such as cell growth arrest and apoptosis induction. HSP90 inhibition has also been known to be radiation sensitising on tumour cells (Yifan Wang, 2016)

Some of major roles of chaperones in the tumour environment are mentioned below.

1.2.1.1Escaping Antigrowth Signals

One of the principal factors that control the development of cancer is p53, a protein with a role in mediating growth arrest and apoptosis in response to DNA damage. Inactivating mutations in Tp53 (the gene encoding p53) appear to be dominant to the other, normal allele. Expression of HSP70 and HSP90 increases to high levels in tumours with mutated p53, and both chaperones may have roles in stabilising the altered conformation of mutant p53. HSP27 interacts with wild-type p53 in a pathway that leads to functional inactivation and interruption of senescence (Hanahan, 2011) (Félix Sauvage a, 2017)

1.2.1.2Limitless Proliferation and Avoidance of Senescence

HSPs are also effective at interrupting another pathway of cell inactivation, in this case by inhibiting cell senescence. Normal cells resist transformation by having a limited number of permitted divisions. This system is based on the lack of replication of chromosome ends at each cell division; the capping structures at the chromosome ends become progressively shortened, leading to arrest of further division and cell senescence.

Cancer cells evade the senescence programme by deploying the enzyme telomerase, which replaces the shortening ends of telomeres. HSP90 binds to telomerase and is required for its efficient function. Thus, HSP90 might deter senescence by chaperoning telomerase and overcoming the erosion of telomeres over time when expressed to high levels, as in cancer. Indeed, chemical targeting of HSP90 inhibits telomerase function, confirming a role for the chaperone in limiting senescence in cancer. In addition, HSP27 and HSP70 inhibit the effector arm of the senescence pathway by reducing the effectiveness of p53 in promoting cell senescence. p53 transcriptionally upregulates cell cycle protein p21, which directly arrests proliferation, and this process is inhibited by high levels of HSP70. Thus, the exaggerated levels of HSPs in cancer provide an environment that is conducive to maintaining the status of the potentially immortal cancer cell (Stuart K. Calderwood, 2016).

1.2.1.3Angiogenesis

Growing tumours inevitably outgrow the local blood supply as they increase in size, and begin to become starved of oxygen. However, tumour cells are able to deploy hypoxia inducible factors (HIF), proteins that can sense the low oxygen environment and mediate the expression of growth factors, such as vascular endothelial growth factor (VEGF), which increase the growth of the tumour capillary network. Recent reports also indicate that HSP27 becomes proangiogenic when released from tumour cells and can bind to receptors, stimulating VEGF transcription through an alternative pathway involving the factor NF-kB. Extracellular HSP27 also exerts proangiogenic properties through direct interactions with VEGF in the medium. (Stuart K. Calderwood, 2016)

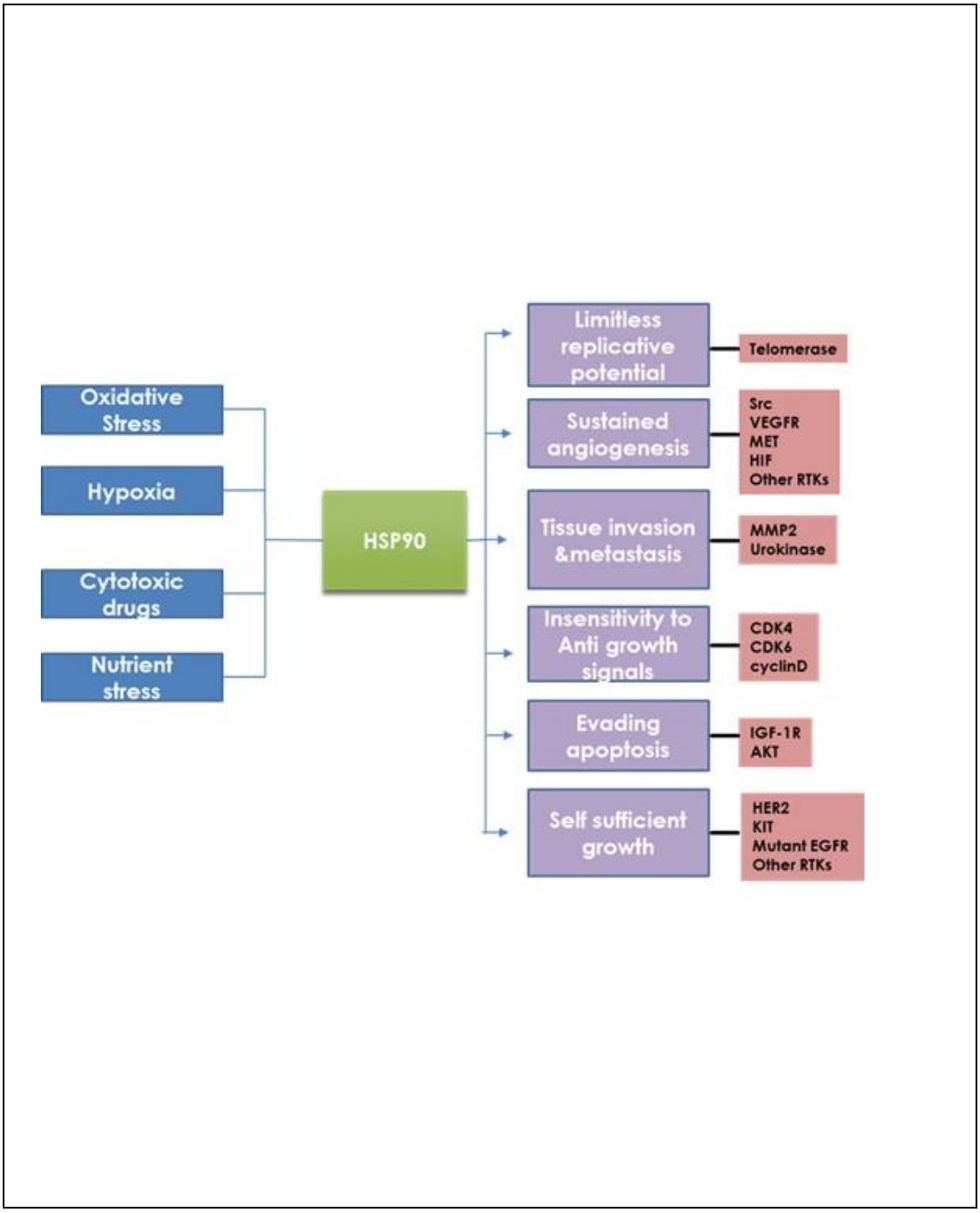

Figure 5 Hallmarks of cancer

HSP90 function is required for the establishment and maintenance of the hallmarks of cancer. HSP90 function is also critical for cancer cells to survive the genetic instability on which acquisition of the above hallmarks depends, and the environmental stresses to which they are frequently subjected. Adapted from (Len Neckers, 2015)

1.3 HSP90 drugs in clinics

Compared with normal cells, neoplastic cells exhibit greater dependence on chaperone proteins, which play a critical role in signal transduction, cell cycle regulation, and apoptosis (S. Parimi, 2014). As a result, HSP90 represents an attractive target for cancer therapy.

HSP90 can be targeted by different families of inhibitors, which act mainly on the N-terminal or the C-terminal domain. The N-terminal domain containing the ATP binding site has been shown to be the binding site of the antitumour antibiotics geldanamycin (GA) and radicicol (Félix Sauvage a, 2017) .The first and second generation HSP90 inhibitors are mentioned in Figure 6.

The prototype HSP90 inhibitor geldanamycin provided proof-of-concept for HSP90 inhibition. However, geldanamycin and its derivatives [17-AAG] and [17-DMAG]) could not be fully developed due to a number of safety and pharmacological limitations. Consequent efforts using a variety of different chemical scaffolds have led to the development of highly potent, second-generation, small molecule HSP90 inhibitors with improved pharmacological properties and safety profiles (Komal Jhaveri, 2015).

Trials of early-generation HSP90 inhibitors in oncology demonstrated limited efficacy (especially when administered as monotherapy), poor solubility, and dose-limiting toxicities (including hepatotoxicity); however, encouraging progress has been made with newer-generation inhibitors. Here, I focus on some of promising HSP90 inhibitors, retaspimycin, ganetespib, AT13387 and NVP-AUY922, that are currently under evaluation, either as monotherapy or in combination therapy, for lung and breast cancers (Figure 7), and I will discuss their potential relevance for future clinical practice. (S. Parimi, 2014) (Komal Jhaveri, 2015)

HSP90 inhibitors	Class	Pharmaceutical company
First-generation HSP90 inhibitors		
Tanespimycin (17-AAG, KOS-953)	Geldanamycin derivative	Kosan Biosciences/Bristol-Myers-Squibb
Alvespimycin (17-DMAG)	Geldanamycin derivative	Kosan Biosciences/Bristol-Myers-Squibb
Retaspimycin (IPI-504)	Geldanamycin derivative	Infinity Pharmaceuticals
IPI-493	Geldanamycin derivative	Infinity Pharmaceuticals
Second-generation HSP90 inhibitors		
CNF2024/BIIB 021	Purine	Biogen Idec
MPC-3100	Purine	Myriad Pharmaceuticals/Myrexis
Debio 0932 (CUDC-305)	Purine-like	DebioPharm
PU-H71	Purine	Samus Therapeutics
Ganetespib (STA-9090)	Resorcinol–Triazole	Synta Pharmaceuticals
NVP-AUY922 (VER-52269)	Resorcinol–Isoxazole	Novartis
NVP-HSP990	Not reported	Novartis
KW-2478	Resorcinol	Kyowa Hakko Kirin Pharma
AT13387	Resorcinol	Astex
SNX-5422	Indazol-4-one	Serenex/Pfizer
DS-2248	Not reported	Daiichi Sankyo Inc
XL888	Not reported	Exelixis

Figure 6 first and second generation HSP90 inhibitors

Drug name	Trial information	Stratification	End point	ORR	Comments
Ganetespib	NCT01031225 n=99 Phase II	Cohort A: mutant *RAS* Cohort B: mutant *EGFR* Cohort C: wild type	PFS at 16 weeks Cohort A: 13.3% Cohort B: 5.9% Cohort C: 13.9%	4% (only seen in patients with ALK translocation)	Two deaths (one cardiac arrest and one renal failure)
	GALAXY-1 NCT01348126 n=255 Phase II Combination drug: docetaxel	LDH *RAS* mutation Time since advanced disease Performance status Smoking	OS: HR 0.69 PFS: HR 0.70	15% in the combination arm 11% in stand-alone arm	Best response achieved in patients with >6 months since advanced diagnosis (HR 0.41)
AUY922	NCT01922583 n=112 Phase II	*EGFR*-mutated *KRAS*-mutated ALK-rearranged Wild type	ORR and SD at 18 weeks Overall: 13%	EGFR: 18% KRAS: 0% ALK: 25% Wild type: 13%	SD achieved in some crizotinib-resistant patients
Retaspimycin (IPI-504)	NCT00431015 n=76 Phase II	EGFR wild-type *EGFR*-mutated	ORR of 7%	EGFR wild-type: 10% *EGFR*-mutated: 4%	Grade 3 liver dysfunction in 11% of patients

Drug	Clinical trial number	Phase	Adjunct drug	Mutation selection
Ganetespib	GALAXY-2 (NCT01798485)	III	Docetaxel	–
	NCT01348126	IIB/III	Docetaxel	–
	NCT01031225	II	–	–
	NCT01562015	II	–	–
	NCT01579994	I	Crizotinib	ALK
	NCT02261805 (small-cell lung cancer)	I	Doxorubicin	–
	NCT01590160 (mesothelioma)	I/II	–	
AUY922	NCT01922583	II	–	
	NCT01854034	II	–	EGFR exon 20
	NCT01752400	II	–	ALK
	NCT01646125	II	Vs pemetrexed/docetaxel	EGFFR
	NCT01124864	II	–	EGFR/ALK/W^{+}
	NCT02276027	II	–	
	NCT01259089	I/II	Erlotinib	EGFR
	NCT01772797	IB	LDK378	ALK
	NCT01784640	I	Pemetrexed	–
IPI-504	NCT01362400	II	Docetaxel	–
	NCT01228435	II	–	ALK
	NCT01427946	IB/II	Everolimus	–
	NCT00431015	I/II	–	–
AT13387	NCT01712217	I/II	Crizotinib	ALK

Figure 7 Clinical trials

Current list of clinical trails with hsp90 inhibitors (esfahani K, 2015)

1.3.1 RETASPIMYCIN

Retaspimycin (IPI-504) is a benzoquinone ansamycin antibiotic and second-generation (water soluble) HSP90 inhibitor. Like other HSP90 inhibitors, retaspimycin uses the ubiquitin–proteasome pathway to break down key client proteins important in oncogenesis. Unlike its first-generation predecessors (geldanamycin, tanespimycin (17AAG), alvespimycin), which had disappointing results in clinical trials or were associated with dose-limiting toxicities (or both), retaspimycin is associated with better water solubility, greater potency, and fewer toxicities. Nonetheless, as with other second-generation HSP90 inhibitors, retaspimycin is administered intravenously and poses a risk of hepatotoxicity (S. Parimi, 2014).

Retaspimycin has been evaluated in malignancies such as chronic myelogenous leukemia, multiple myeloma, gastrointestinal stromal tumour, non-small-cell lung cancer (NSCLC), and breast cancer. Based on early-phase clinical trial results to date, retaspimycin has demonstrated the most promise in the NSCLC population, especially for tumours that harbour the *ALK* rearrangement. Pre-clinically, antitumour effects were observed for retaspimycin, both as a single agent and in combination with trastuzumab or lapatinib, in HER2 -positive disease resistant to standard therapies. Retaspimycin has also been evaluated in combination with taxanes in patients with metastatic NSCLC in an expansion of a Phase IB trial. (esfahani K, 2015)

1.3.2 NVP-AUY922

NVP-AUY922 is another resorcinol derivative and second-generation HSP90 inhibitor currently under clinical investigation. As an isoxazole amide, it is considered one of the most potent HSP90 inhibitors developed to date. In a phase I trial in 96 patients with advanced solid tumours, disease stabilisation was observed in 16 patients, the drug was reasonably well tolerated, with the main adverse effects being diarrhoea, nausea and vomiting, fatigue, and ocular toxicities (S. Parimi, 2014).

Like other HSP90 inhibitors in development, NVP-AUY922 appears to hold the greatest promise in NSCLC. In a phase II trial in 112 treatment-refractory patients with advanced NSCLC , promising clinical activity was observed, with partial responses observed in 13 of 101 patients (13%), including 2 of 8 who were ALK -positive, 6 of 33 with *EGFR* mutation, and 4 of 30 with wild-type *EGFR, KRAS,* and *ALK* (S. Parimi, 2014)

In preclinical studies, it has been shown to have clinical activity in lung cancer cells with MET- and AKL-mediated resistance. AUY922 treatment effectively suppressed proliferation and induced cell death in both resistant cell lines by downregulating EGFR, MET, and AXL expression, which led to decreased AKT-pathway activation. AUY922 has also been shown to act as a radio-sensitiser to cell lines with acquired resistance to EGFR inhibitors. These cell-line studies have been replicated in animals with NSCLC xenograft tumours with MET- and AXL-mediated resistance. AUY922 has also been combined with trastuzumab in patients with HER2-amplified or *HER2*-mutated NSCLC. (esfahani K, 2015)

1.3.3 AT13387

AT13387 is a potent second-generation nonansamycin HSP90 inhibitor. It has been shown to have effects in NSCLC cell lines, as well as in mouse xenograft models. Its long duration of action has enabled once-weekly dosing. AT13387 has also shown clinical efficacy in ALK-rearranged cell lines, as well as in mouse xenograft models injected with those cells (esfahani K, 2015).

1.3.4 Ganetespib

Ganetespib (STA-9090) is a resorcinol-containing triazole that has shown greater potency, improved tumour penetration, and a more favourable toxicity profile than tanespimycin in preclinical models. Ganetespib inhibits HSP90 protein by acting on the ATP-binding domain at the N-terminus Figure 8a (Ziyan Y. Pessetto, 2017). Overall, ganetespib seems to be well tolerated, with no reports of severe ocular, cardiac, liver, or renal toxic effects. (Rocio Garcia-Carbonero, 2013).
Ganetespib has been safely used in thousands of patients in over 60 clinical trials internationally. Ganetespib has been evaluated in a number of malignancies, including melanoma, chronic myelogenous leukaemia, gastrointestinal stromal tumour, and colorectal, lung, and breast cancers. (esfahani K, 2015)

Ganetespib has greater potency and potential efficacy against several NSCLC subsets, including those harbouring *EGFR* or *ERBB2* mutations. Treatment with ganetespib resulted in decreased downstream signalling through the PI3K–AKT–mTOR and RAF–MEK–ERK pathways (Figure 8b). Ganetespib also overcame multiple forms of crizotinib resistance,

including secondary *ALK* mutations. Additionally, ganetespib lacks the ocular toxicity that has been reported with NVP-AUY922. Taken together, these promising results suggest that ganetespib may be more potent in its antitumour activity compared with first-generation inhibitors and has an optimal safety profile that predicts for a superior therapeutic index. This has provided a compelling rationale to further develop this agent clinically. (Komal Jhaveri, 2015)

(a)

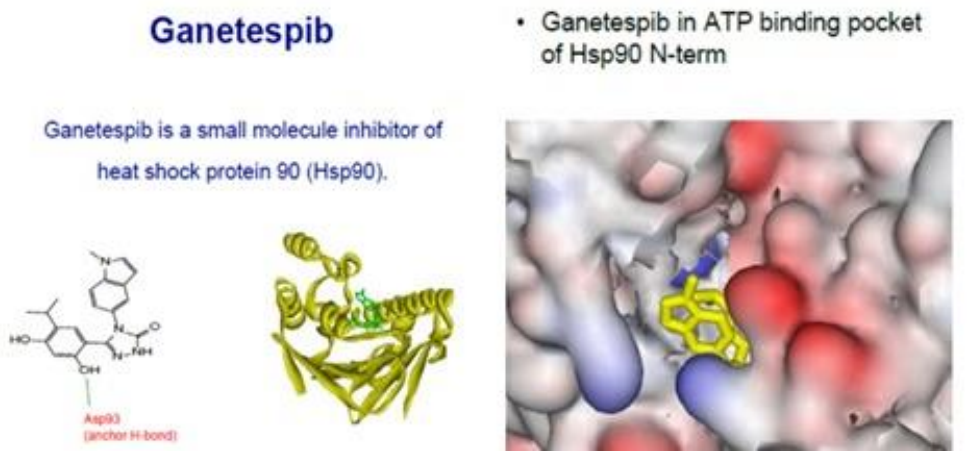

(b)

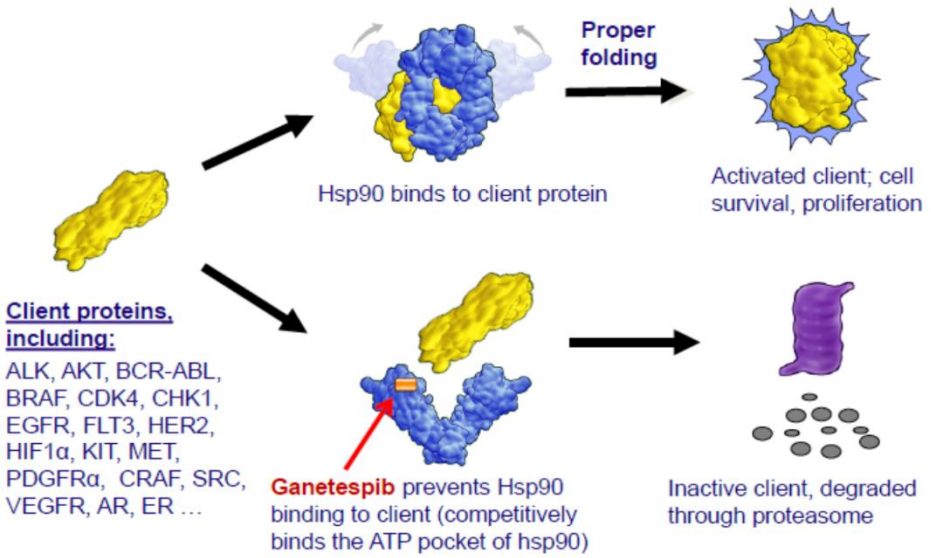

Figure 8 Structure and mechanism of action of ganetespib

(syntapharmaceuticals, 2016)

1.4 Combination Phase I/II trial

Figure 9 lists several ongoing combination trials of ganetespib with cytotoxic agents such as taxanes and doxorubicin, radiation, fulvestrant, and other targeted agents such as sirolimus, crizotinib, Ziv-Aflibercept, and bortezemib for several tumour types. Antitumour activity has been observed with ganetespib both as monotherapy and in combination with other agents, including synergistic effects in combination with taxanes and etoposide. A completed phase II randomized trial in stage IV NSCLC combining ganetespib with docetaxel compared with docetaxel alone has demonstrated efficacy signal in a subgroup of patients, and therefore it was further tested in a phase III randomized trial (GALAXY II; NCT01798485) (Yifan Wang, 2016) (esfahani K, 2015).

The combination of docetaxel and ganetespib is in advanced clinical testing in NSCLC based on the results from the Phase IIb GALAXY-I (Study of Ganetespib + Docetaxel in Advanced NSCLC) trial. Preliminary results from a Phase I trial of ganetespib plus paclitaxel and trastuzumab, a humanized monoclonal antibody against HER2, were recently presented at the San Antonio Breast Cancer Symposium. There were no grade 3 toxicities attributable to ganetespib. (Komal Jhaveri, 2015).
Together, these compelling preclinical studies have formed the rationale for many Phase I/II clinical trials in combinations with ganetespib as a way to optimize efficacy and delay or limit acquired resistance.

Phase	Disease	Combination	Dose and schedule	Primary endpoint	ClinicalTrials.gov Identifier
I	Multiple myeloma	Ganetespib +/– bortezemib	Ganetespib IV days 1, 4, 8, 11 every 3 weeks Bortezomib IV or subcutaneous days 1, 4, 8, 11 every 3 weeks	MTD	NCT01485835
I/II	Phase 1 includes multiple sarcoma subtypes and Phase 2 MPNST	Ganetespib plus sirolimus	Ganetespib 150 mg/m^2 IV on days 1, 8, and 15 IV over 1 hour Sirolimus 4 mg taken orally once daily on a continuous dosing schedule	Toxicity/clinical benefit	NCT02008877
I	Rectal cancer	Ganetespib, capecitabine, and radiation	Ganetespib 60 mg/m^2 once weekly ×2 weeks prior to starting XRT and then on days 1, 8, 15 for cycle 1 and then on days 29 and 36 for cycle 2 Capecitabine at 825 mg/m^2 twice daily for the entire duration of radiation therapy	Response rate	NCT01554969
I	HER2+ metastatic breast cancer	Ganetespib, paclitaxel, and trastuzumab	Ganetespib IV over 1 hour on days 1, 8, and 15 Trastuzumab IV over 30 minutes, and paclitaxel IV over 1 hour on days 1, 8, 15, and 22	MTD	NCT02060253
II	Neoadjuvant breast cancer (I-SPY 2)	Ganetespib + paclitaxel	Ganetespib 150 mg/m^2 once weekly for 3 out of 4 weeks Paclitaxel: 80 mg/m^2 IV weekly ×12 weeks	pCR	NCT01042379
Randomized Phase II	HR+ breast cancer	Arm A: Fulvestrant Arm B: Fulvestrant + ganetespib Arm C: Crossover from Arm A to Arm B at progression	Fulvestrant 1M on day 1 and 15 of cycle 1, day 1 of cycle 2 and each subsequent cycle Ganetespib IV over 1 hour on days 1, 8, and 15 of each cycle	PFS	NCT01560416

I	ALK positive lung cancers	Crizotinib and ganetespib	Ganetespib IV over 1 hour on days 1 and 8 of a 21-day cycle Crizotinib 250 mg orally twice daily continuously	MTD and PFS	NCT01579994
I/II	Solid tumors/refractory small-cell lung cancer	Ganetespib + doxorubicin	Ganetespib 100 mg/m^2 or 150 mg/m^2 IV on days 1 and 8 of a 21-day cycle Doxorubicin 50 mg/m^2 IV on day 1 of a 21-day cycle	MTD/ORR	NCT02261805
Phase I/II	Malignant pleural mesothelioma (MESO-02)	For Phase II: Ganetespib + cisplatin/pemetrexed Or Ganetespib + carboplatin/ pemetrexed	Ganetespib IV on day 1 and day 15 of each cycle Cisplatin 75 mg/m^2, day 1 every 21 days Pemetrexed 500 mg/m^2, day 1 every 21 days Carboplatin AUC5, day 1 every 21 days Pemetrexed 500 mg/m^2, day 1 every 21 days	DLT, MTD/PFS	NCT01590160
I/randomized II	Metastatic, p53-mutant, platinum-resistant ovarian cancer (GANNET53)	For Phase II: Arm A: ganetespib plus paclitaxel Arm B: paclitaxel	Ganetespib IV once weekly for 3 out of 4 weeks Paclitaxel 80 mg/m^2, given IV once weekly for 3 out of 4 weeks	PFS	NCT02012192
I/II	Recurrent ovarian, fallopian tube, or primary peritoneal cancer	Paclitaxel and ganetespib	Paclitaxel and ganetespib IV over 1 hour on days 1, 8, and 15	DLT, RP2D, PFS at 6 months, RR	NCT01962948
I	Refractory gastrointestinal carcinomas, non-squamous non-small-cell lung carcinomas, urothelial carcinomas, and sarcomas	Ganetespib and Ziv-Aflibercept	Ganetespib IV weekly on days 1, 8, and 15 of a 28-day cycle Ziv-Aflibercept IV every 2 weeks, on days 1 and 15, of a 28-day cycle	MTD, safety	NCT02192541

Abbreviations: MTD, maximum tolerated dose; IV, intravenous; MPNST, malignant peripheral nerve sheath tumors; HER2+, human epidermal growth factor receptor 2 positive; DLT, dose limiting toxicity; RP2D, recommended Phase 2 dose; PFS, progression-free survival; RR, response rate; HR+, hormone-receptor positive; IM, intramuscular; ORR, objective response rate; pCR, pathologic complete response; ALK, anaplastic lymphoma kinase.

Figure 9 Ongoing combination trials of Ganetespib with other therapeutic agents

(Komal Jhaveri, 2015)

1.5 Clients of HSP90

As mentioned previously HSP90 has over 200 client proteins. In my thesis I will focus predominantly on IRF-1, which was lately discovered as a client of HSP90 (Narayan, 2009)

The vertebrate immune system comprises two major parts - the innate and adaptive components. The innate response forms the first line of defence in a vertebrate and is a quick response that targets a broad range of pathogens. The adaptive response, on the other hand, is the specific response directed against a foreign particle that is mediated by T- and B-lymphocytes, and has the remarkable feature of immunological memory. While the adaptive response is specific to vertebrates, innate defence mechanisms have been observed in some of the earliest living eukaryotes (Viau, 2005) (Bartl, 2003).

The interferon regulatory factor (IRF) family of transcription factors has been intimately linked with the vertebrate immune response. Members of the IRF family play a crucial role in the development of the antiviral state and have been shown to perform a variety of other functions in host defence, particularly with respect to the innate immune response (Takaoka A. T., 2008). This thesis focuses on the founding member of this family, IRF-1, and describes the identification of novel IRF-1 binding proteins in an attempt to better understand how IRF-1 mediates its cellular functions.

1.5.1 The IRF family

Ten IRF family members (IRF-1 to IRF-10) have been described in vertebrates, with IRF-10 being non-functional in humans and mice. A characteristic feature of IRF-1 family members is an N-terminal DNA binding domain (DBD) that contains five invariant tryptophan residues spaced at 10–18 amino acid intervals. Additionally, the IRF family members also contain a C-terminal IRF association domain (IAD; IAD1 or IAD2) that allows them to interact with other IRF family members or other transcription factors (Takaoka A. T., 2008).

Based on phylogenetic studies and evolutionary history, the 10 IRF family members have been divided into two super groups – the IRF-1 and IRF-4 super groups. The IRF-1 super group contains IRF-1 and IRF-2, which share a C-terminal IAD2 domain that does not structurally resemble any other known domains. The IRF-4 super group is further divided into three groups

– the IRF-3 group consisting of IRF-3 and IRF-7, the IRF-4 group comprising IRF-4, IRF-8, IRF-9 and IRF-10, and the IRF-5 group containing IRF-5 and IRF-6. The eight members of the IRF-4 super group share a C-terminal IAD1 domain that resembles the C-terminal MH2 domain of the Smad proteins (Takaoka A. T., 2008).

1.5.2 Evolution of the IRF family

Early studies showed the absence of *IRF* genes in *Drosophila* and *Caenorhabditis* genomes, and thus the IRF family was thought to have developed in deuterostomes. A recent study, however, suggests that the origin of the *IRF* genes coincides with the origin of multicellularity and underwent a turbulent evolution. The study demonstrates the presence of *IRF* family genes in all five major metazoan groups, and traces the evolution of the family up to higher vertebrates (Nguyen H, 1997).

Based on evolutionary history, although IRFs underwent a massive reduction or were completely lost or severely mutated in some organisms, the IRF family once again expanded to four members close to the appearance of the first vertebrate. These four members – the predecessors of the 4 IRF groups (1, 3, 4 and 5) – then evolved into the 10 vertebrate IRFs possibly as a result of 2-fold duplication of the entire genome

1.5.3 Interferons and the interferon signalling pathway

Interferons (IFNs) belong to a class of proteins called cytokines, which are secreted by cells of the immune system and function primarily in cell–cell communication and signalling. IFNs have been studied in detail in the context of host defence against viral infections and the term ‘interferon’ was coined to reflect their role in interfering with and preventing viral replication in host cells (Nehyba, 2009).

IFNs are of three types – Type I, II, and III. Type I IFNs are produced by a variety of cells upon viral infection and include IFN-α, -β, -ω, -ε, and –κ. The sole member of Type II IFNs is IFN-γ, which is produced by activated T cells and natural killer (NK) cells. The recently-discovered Type III IFNs, or IFN-λs, (IFN-λ1-3 or IL-28A, IL-28B and IL-29 respectively) are, like Type I IFNs, produced by virus-infected cells. However, they are structurally different from Type I IFNs and they bind to their own distinct set of IFN-receptors (Nehyba, 2009).

Classic IFN signalling involves the JAK-STAT pathway. The IFNs bind to their respective receptors – IFN-α/β receptor or IFNAR for IFN-α/β, IFN-γ receptor or IFNGR for IFN-γ, and IFN-λR1 or IL-28Rα for IFN-λs (Figure 10). These receptors comprise of at least two distinct

subunits, denoted 1 and 2. The binding of the IFN to its respective receptor activates the Janus protein tyrosine kinases (Jak PTKs) associated with the receptors (Tyk2 and Jak1 for IFNAR, and Jak1 and Jak2 for IFNGR) through auto and/or trans phosphorylation of specific residues. The activated Jak PTKs then phosphorylate their downstream targets, namely the signal transducers and activators of transcription (STAT) family members STAT1 and STAT2. Activation of the STATs leads to the formation of the transcriptionally active complexes IFN-α-activated factor (AAF; also called IFN-γ-activated factor or GAF), and/or IFN-stimulated gene factor 3 (ISGF3). GAF is a homodimer of activated Stat1, while ISGF3 is a heterotrimer of activated STATs-1 and -2, and IRF-9/p48/ISGF3γ. These activated complexes then move into the nucleus, where they bind to specific DNA elements, namely the IFN-γ-activated sequence or GAS for GAF, and the IFN-stimulated regulatory element or ISRE for ISGF3. This results in the transcriptional activation of the promoter containing the GAS or ISRE sequence. IRF-1 induction is primarily through the IFN-γ-activated pathway (Takaoka A. a., 2006) (Nehyba, 2009)

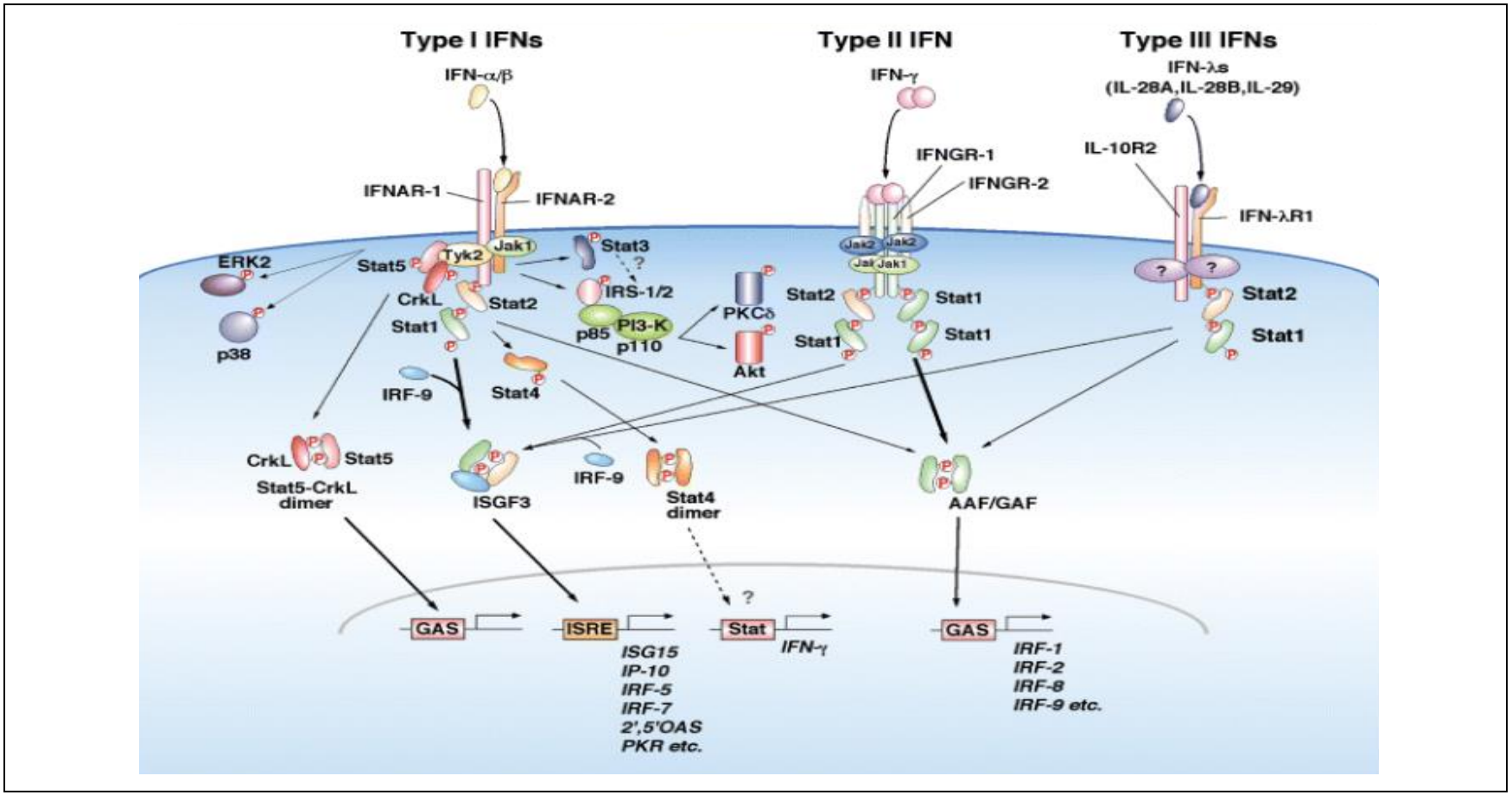

Figure 10 IFN signalling pathways

Activation of cardinal Jak-Stat pathway and additional signalling cascades by three types of IFNs. IFNs are categorized into three types on the basis of the type of receptor. Type I IFNs (only IFN-α and IFN-β are shown for simplicity), type II IFN (IFN-γ) and type III IFNs (IFN-λ1/IL-29, IFN-λ2/IL-28A and IFN-λ3/IL-28B) bind to their corresponding distinct receptor complex as indicated. All of them activate the canonical Jak-Stat pathway (see text for further explanation).
(Takaoka A. a., 2006)

1.5.4 Overview of the human IRF family members

The human IRF family comprises nine members (IRF-1 to IRF-9). Initially identified as regulators of the interferon system, the IRFs have since been shown to possess a variety of other cellular functions. A brief description of the human IRF-1 and IRF-2 is given below.

1.5.4.1IRF-1

The founding member of the IRF family, IRF-1 was initially identified as a positive regulator of the *IFNβ* gene. It has subsequently been shown to regulate other IFN and IFN-responsive genes, and plays a crucial role in host defence [37, 38]. In addition to its role in regulating the IFN genes and the antiviral response, IRF-1 has important functions in the T cell response, the DNA damage response, the cell cycle and apoptosis, and tumour suppression (Nehyba, 2009).

1.5.4.2IRF-2

Cross-hybridisation experiments with the IRF-1 cDNA revealed a structurally similar molecule, sharing a 62% homology with the N-terminal half of IRF-1; this molecule was named IRF-2. Further analyses revealed that both IRF-1 and IRF-2 bind to the same DNA element, the interferon regulatory factor response element or IRF-E with consensus sequence G (A) AAAG/CT/CGAAAG/CT/C that is almost identical to the interferon-stimulated response element or ISRE with consensus sequence A/GNGAAANNGAAACT (where N is any base). Later, the crystal structure of the IRF-2 DNA-binding domain in complex with DNA was determined (Figure 1.5) [9]. In the structure, IRF-2 was found to specifically contact the AANNGAA sites on DNA (contact sites are underlined; N is any base) (Harada, 1989).

IRF-2 has been shown to have an antagonistic function to IRF-1 and represses IRF-1 induced transcriptional activation of *IFNβ*. The IRF-2 protein is much more stable than IRF-1 (half-life of > 8 h vs 30 min respectively), and since both IRF-1 and IRF-2 bind to the same DNA elements with similar affinities this results in a relative repression of promoters under IRFs (Harada, 1989). However, upon induction by virus, dsRNA, IL-1, IL-6 etc., IRF-1 levels increase markedly, thereby changing the IRF-1: IRF-2 ratio in favour of IRF-1 and allowing activation of IRF-1 target genes. Additionally, the C-terminus of the IRF-2 protein contains a repressor domain, and the deletion of this domain converts IRF-2 into a transcriptional activator.

IRF-2 has also been described as an oncogene, as its over-expression in NIH 3T3 cells results in oncogenic transformation, which can be reverted by over-expression of IRF-1. The exact mechanism by which IRF-2 functions in oncogenesis is unknown – it could exert its effects by perturbing IRF-1 mediated tumour suppression; by competing with other IRFs for binding to the same IRF-E; or by activating genes such as Histone H4, which have been implicated in cell cycle progression and oncogenesis. In a recent study using breast cancer tissue microarrays, tumours were found to maintain expression of IRF-2 if there was coincident expression of IRF-1, suggesting that IRF-2 blocks the tumour suppressive function of IRF-1 in these cases, thereby promoting oncogenesis (Huang, 2007) (Xi, 1999).

Interestingly, some studies have suggested a tumour suppressive function for IRF-2 in addition to its role in oncogenesis In one case, IRF-2 and IRF-1 were shown to synergistically activate the class II transactivator (CIITA) promoter, and a pancreatic tumour cell line expressing a mutant IRF-2 was identified in which CIITA induction by IFN-ɣ was absent (Xi, 1999).

Thus, while IRFs plays a major role in the innate immune response – particularly in antiviral defence – they also function in cell differentiation, cell growth inhibition and induction of apoptosis.

1.6 SARCOMA

Sarcomas constitute a heterogeneous group of bone and soft tissue malignancies that account for approximityly 15% of all paediatric, and 1% of all adult, cancers. Sarcomas affect about 11,000 individuals in the US and 200,000 individuals worldwide each year. There has been great impact on approaches to treat these cancers, as it is now clear that unlike most epithelial tumours, which are defined by the organ of origin, sarcomas can be defined by their molecular pathology. (Helman LJ, 2003) (Mohamed T Hafez, 2012) (Eva Wardelmanna, 2012) (Taylor BS, 2011)

Many sarcoma subtypes are resistant to cytotoxic agents, and even for those subtypes that are chemo-sensitive, long term responders are rarely seen due to cumulative toxicity and a therapeutic ceiling that has now been reached. Overall five-year survival rates for patients diagnosed with soft tissue sarcomas remains at 60%, highlighting the pressing need for new targeted systemic therapies particularly for those patients with recurrent or advanced disease (Frith, Hirbe et al. 2013).

Soft tissue sarcoma (STS) can be divided into the following groups (Figure 11) having:

- reciprocal translocations accounting for 15–20% of cases (e.g. synovial sarcoma, Ewing sarcoma)
- specific mutations (e.g. gastrointestinal stromal tumour (GIST)) or deletions (e.g.,rhabdoid tumour) amplifications (e.g., well differentiated liposarcoma)
- Complex genomic profiles

Liposarcomas are malignant soft tissue sarcomas that arise from adipose tissue, classically defined by their morphologic appearance into five classes: well-differentiated liposarcoma (WDLPS), dedifferentiated liposarcoma (DDLPS), myxoid liposarcoma, round cell liposarcoma and pleiomorphic liposarcoma. The histologic subtypes have significant differences in their clinical behaviour, such as their tendency to metastasize and to respond to treatment. WDLPS generally have a low metastatic rate and do not respond to chemotherapy, whereas the round cell variant of myxoid liposarcoma has a high propensity to metastasize but is much more sensitive to chemotherapy and radiation (Frith AE, 2013)

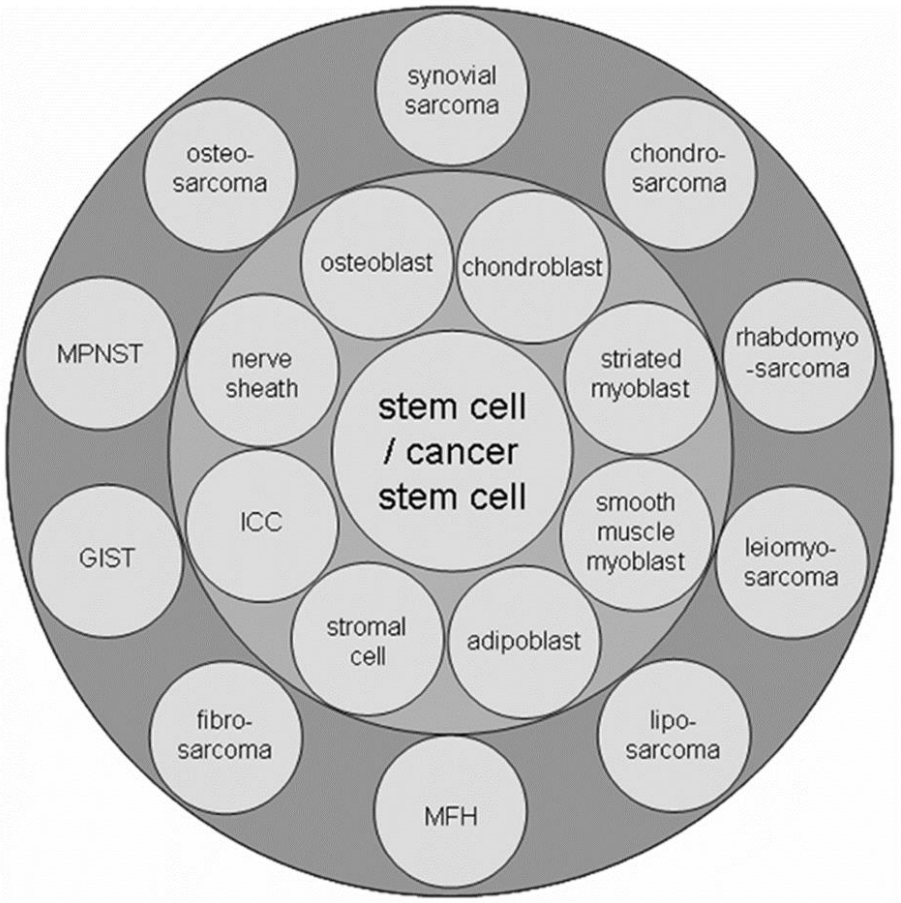

Figure 11 Classification of sarcoma

Schematic classification of the various sub types of sarcoma

1.6.1 P53

The tumour suppressor p53 is a potent transcription factor that controls a major pathway protecting cells from malignant transformation. In response to stress, the cellular level of p53 is elevated by a posttranslational mechanism, leading to cell cycle arrest or apoptosis (Lyubomir T. Vassilev, 2004). Under non-stressed conditions, p53 is tightly controlled by the MDM2 protein, through an autoregulatory feedback loop. p53 is also regulated by other gene products as such ARF. The ARF tumour suppressor is a protein that is transcribed from an alternate reading frame of the INK4a/ARF locus (CDKN2A). MDM2 inhibits p53 activity, while ARF inhibits MDM2. Overexpression of MDM2, or loss of ARF/p53, is observed in many cancers (Wang, 2012).

1.6.2 MDM2

MDM2 (Mouse double minute 2 homologue) encodes a negative regulator of the tumour suppressor p53, and is a member of the E3 ubiquitin ligases that acts to target p53 for proteasomal degradation. The MDM2 locus 12q14.3-q15 is part of a frequent focal amplification peak region in cancers. MDM2 amplification differentiates between benign and malignant tumour groups and is nearly considered a diagnostic marker for WDLPS or DDLPS (Frith AE, 2013).

1.6.3 Mutations of TP53, expression levels of MDM2

Relatively few sarcomas harbour TP53 mutations, but in many cases, amplification of MDM2 effectively inactivate p53. The p53 pathway activity can also be affected by normal genetic variation. Mutations in TP53 are less frequent and more heterogeneous in sarcomas than in other cancer types and in addition to the amplification and overexpression of MDM2, other mechanisms, including MDM4 amplification (Ohnstad, Castro et al. 2013). In general, it is estimated that while p53 inactivating mutations are present in approximityly 50% of all cancers, the remaining cancers should have other alterations to the pathway, it is seen that mutations in TP53 are frequent in leiomyosarcomas and osteosarcomas. In contrast to mutations in the CDKN2A and TP53 genes, amplification of MDM2 was seen frequently in STS (Ito M, 2011).

1.7 Comparative oncology

In the US, cancer is diagnosed in almost one million dogs per year, and the incidence is rising. Dedicated pet owners strive to provide the highest level of health care to their companion dogs and actively seek out novel treatment options in the form of experimental therapies and clinical trials when available. These factors provide a unique opportunity to advance the care and understanding of cancer in both man and companion dogs. Out of this symbiotic relationship developed the discipline of comparative oncology, which integrates the study of naturally occurring tumours in animals into studies of human cancer biology and therapeutics. Treatment of many tumour types, such as osteosarcoma, lymphoma, melanoma, etc. have directly benefited from this approach (R. Timothy Bentley, 2016).

During the past four decades, an increased number of similarities between canine tumours and human cancer have been reported: molecular, histological, morphological, clinical and epidemiological, which lead to comparative oncological studies. One of the most important goals in human and veterinary oncology is to discover potential molecular biomarkers that could detect cancer in an early stage and to develop new effective therapies (VISAN, 2015).

1.8 Canine Model

Domestic dogs are divided into over 175 breeds, with members of each breed sharing significant phenotypes. The breed barrier enhances the utility of the model, especially for genetic studies where small numbers of genes are hypothesized to account for the breed cancer susceptibility. These facts, combined with recent advances in high-throughput sequencing technologies allows for an unrivalled ability to use pet dog populations to find often subtle mutations that promote cancer susceptibility and progression in dogs as a whole (Davis, 2014) (Jin Zhang, 2009).

Most types of cancer observed in humans are found in dogs, suggesting that canines may be an informative system for the study of cancer genetics. The comparative oncology approach, specifically referring to the study of pet dogs with spontaneous cancer, offers a potential

solution to the lingering questions about cancer drugs, its metabolites, and their accumulation in tumours (Corey Saba, 2016) (Davis, 2014).

1.9 Canine Sarcoma

A number of haematologic and solid tumour types in humans are also seen in companion animals such as dogs, including lymphoma, mammary carcinoma, melanoma and soft tissue sarcoma (STS). In canines, STS is a prevalent disease that comprises 15% of all reported cancers and, like the human disease, it can arise from several cellular origins and in multiple body locations including the limbs, trunk or head and neck. The range of STS tumour types include fibrosarcomas, peripheral nerve sheath tumours, hemangiopericytoomas, myxosarcomas, perivascular wall tumours, liposarcomas, leiomyosarcomas and other poorly differentiated tumours. (J. P. Frazier, 2016)

Gemcitabine has been investigated and used in human patients with advanced or metastatic STS as a single agent or in combination with other drugs. The lack of response in gemcitabine-treated xenograft tumours is consistent with clinical studies of this drug in canine solid tumours, in which single agent gemcitabine has demonstrated limited antitumour activity. Establishment of more canine models will allow researchers to rigorously test hypotheses prior to the initiation of, and in parallel to, comparative oncology trials in dogs. Frazier and group demonstrated the feasibility of generating preclinical models of disease from a dog with cancer, an effort that could be expanded to create larger libraries of canine xenograft models. The reduced cost and relatively easy access to tissues derived from dogs with cancer provides a great opportunity for generating a large collection of preclinical models that capture the heterogeneity of a disease like STS. Such models will be instrumental in supporting translational work in companion animals and promoting further work to establish and characterize new laboratory models of disease like STS Figure 12. (J. P. Frazier, 2016)

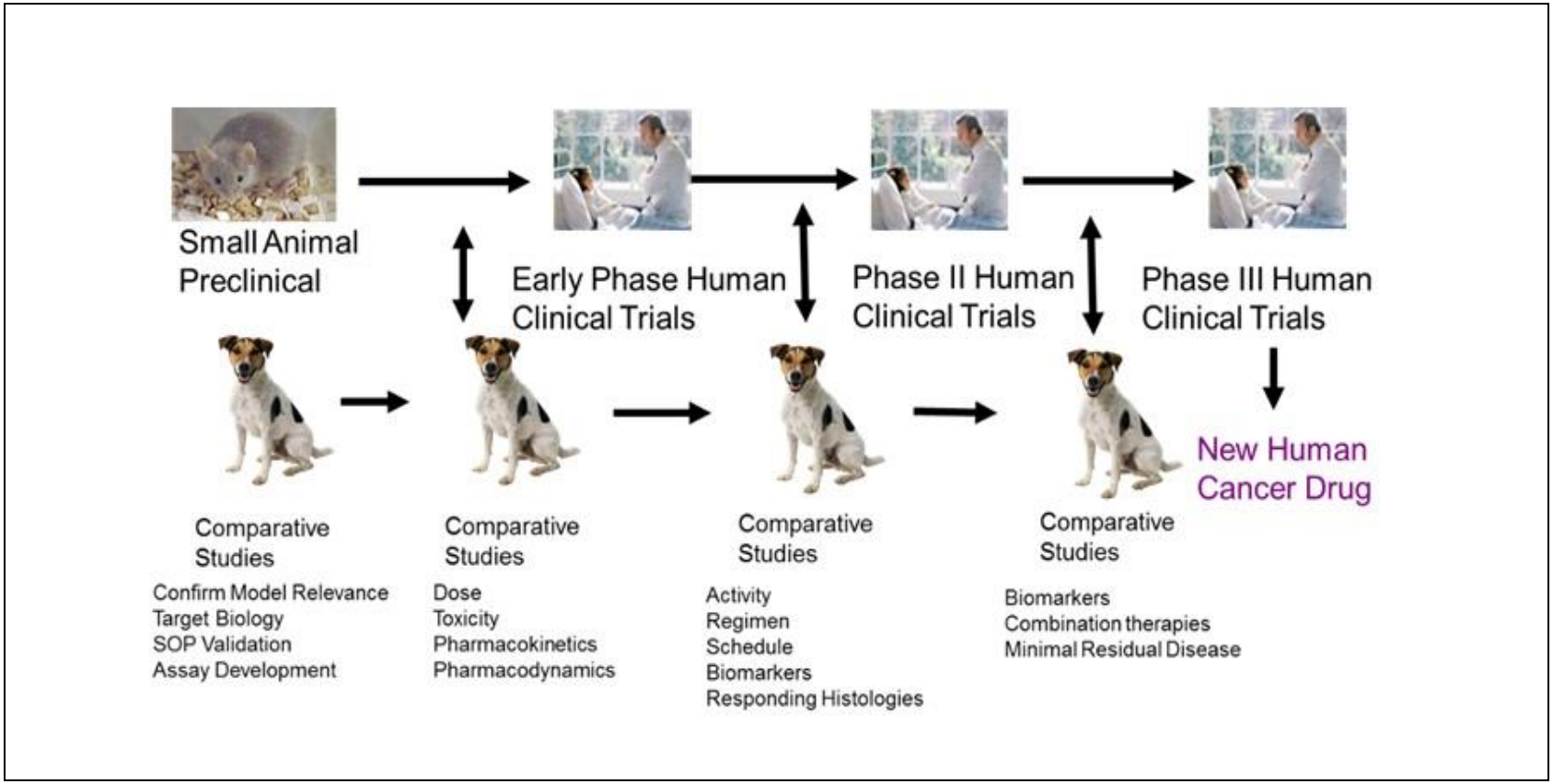

Figure 12 Integrated and Comparative Drug trial model

Most preclinical studies that progress to human clinical trials fail at phaseI/II stage. This failure is most likely to the large translational gap between a orthotopic xenograft murine model and a complex immuncompetent human host, Comparative oncology provides an ideal platform to bridge this gap. (R. Timothy Bentley, 2016)

1.9.1.1Osteosarcoma

Osteosarcoma is the most common primary bone tumour of both children and dogs. It is an aggressive tumour in both species with a rapid clinical course leading ultimately to metastasis. Companion studies with dogs especially osteosarcoma have been studied for more than a decade showing similar p53 mutation in human and canine osteosarcoma. In dogs and children, distant metastasis occurs in 80% of individuals treated by surgery alone. Both canine and human osteosarcoma has been shown to contain a sub-population of cancer stem cells (CSCs), which may drive tumour growth, recurrence and metastasis, suggesting that naturally occurring canine osteosarcoma could act as a preclinical model for the human disease (Pang, 2014) (Leeuwena, 1997).

1.9.1.2Genetic Heterogeneity

The mutational landscape of osteosarcoma is highly complex and varies significantly between tumours. This high degree of inter-tumour heterogeneity confounds our understanding of the molecular pathogenesis of osteosarcoma and may explain some of the difficulty in identifying therapeutic agents that are likely to improve outcomes for the spectrum of patients with osteosarcoma.

1.9.1.3Chromosomal Abnormalities

A hallmark of osteosarcoma is chromosomal instability (CIN), a form of genome-wide alteration characterized by a high degree of losses and gains of full chromosomes or chromosomal segments. CIN has been shown to result from a loss of function in cell cycle checkpoint and DNA damage response pathways.

Osteosarcoma is a cancer typified by widespread and heterogeneous abnormalities in chromosomal number and substructure. Osteosarcoma ploidy can range from haploidy to hexaploidy. While myriad chromosomal losses/gains have been identified, chromosome 1 is most often gained and chromosomes 9, 10, 13, and 17 are most often lost. The most common copy number alterations are deletions of portions of chromosomes 3, 6, 9, 10, 13, 17, and 18 and amplifications of portions of chromosomes 1, 6, 8, and 17. These regions encode a number of tumour suppressors and oncogenes, respectively.

1.9.2 Tumour Suppressors

1.9.2.1Rb Pathway

Retinoblastoma (Rb) is a critical regulator of the G_1-to-S cell cycle transition. In the absence of mitogenic stimuli, Rb remains dephosphorylated and binds to E2F family transcription factors, preventing their activation of cell cycle progression. During normal mitosis, this is reversed via Rb phosphorylation by CDK4. Loss-of-function *Rb* mutations remove this cell cycle checkpoint. The CDKN2A locus (also known as INK4A) encodes two functionally and structurally distinct genes via alternative splicing. The first, $p16^{INK4a}$, is a negative regulator of CDK4. The second, $p14^{ARF}$, is a key regulator of p53. Loss of $p16^{INK4a}$ function alleviates negative regulation of CDK4, resulting in Rb inactivation. Thus, mutations in the *CDKN2A* gene can phenocopy loss-of-function *Rb* mutations.

With pathophysiological similarities to its human counterpart, canine OS represents an ideal model for comparison of conserved regions of genomic instability that may be disease associated rather than genomic passengers. Their study used tools to identify disease-associated genome-wide DNA copy number aberrations in canine and human OS (Angstadt, 2012).

1.9.2.2 p53 Pathway

p53 is a transcription factor that regulates critical genes in DNA damage response, cell cycle progression, and apoptosis pathways. p53 acts as a tumour suppressor in essentially all tumour types, and its function can be affected by mutations to the gene itself or by mutations to up- or downstream mediators of its activity. p53, the most commonly mutated gene in human cancers, is found to be altered in dog cancers. However, little is known about the role of p53 in dog tumourigenesis. p53 mutations and MDM2 amplification has been demonstrated in canine soft-tissue sarcomas. The principle role of mdm2 is to act as a negative regulator of p53 function. The frequency of mdm2 amplifications correlates to that described for human tumours of similar histological sub-types (Jin Zhang, 2009) (Khanna, 2015).

$p14^{ARF}$ normally acts to sequester the E3 ubiquitin ligase MDM2 in the nucleolus, preventing it from promoting p53 degradation. $p14^{ARF}$ is expressed from the same *CDKN2A* locus that encodes $p16^{INK4a}$. Loss-of-function mutations in the $p14^{ARF}$gene can phenocopy mutations to *TP53*.

Loss-of-function *TP53* mutations occur in as many as three-fourths of osteosarcoma cases. These mutations include allelic loss (75–80%), rearrangements (10–20%), and point mutations (20–30%).Nasir and group demonstrated that 6 of 30 canine cases had p53 mutations (20%) (Nasir L. , 2001). Jin Zhang and group demonstrated that, upon exposure to DNA damage agents or Mdm2 inhibitor nutlin-3, canine p53 is accumulated and capable of inducing its target genes, MDM2 and p21. Taken together, these results indicate that canine p53 family proteins have biological activities similar to their human counterparts. These similarities make the dog as an excellent out-bred spontaneous tumour model and the dog can serve as a translation model from bench-top to cage-side and then to bedside (Jin Zhang, 2009).

1.9.3 Other Tumour Suppressors

Other tumour suppressors associated with deletions or loss of heterozygosity in osteosarcoma include: *APC*, *BUB3*, *FGFR2*, *LSAMP*, *RECQL4*, and *WWOX*.

1.9.3.1Oncogenes

1.9.3.1.1 Rb Pathway

E2F3 and CDK4, both of which counteract Rb control of cell cycle progression, have been estimated to possess gain-of-function mutations in 60% and 10% of tumours, respectively.

1.9.3.1.2 p53 Pathway

MDM2 is an E3 ubiquitin ligase that acts as a negative regulator of p53 .The *MDM2* gene is amplified in 3–25% of osteosarcoma tumours. COPS3 also promotes proteosomal degradation of p53 and is estimated to cause gain-of-function mutations in 20–80% of osteosarcomas.

1.9.3.1.3 c-Myc

The transcription factor c-Myc is a key factor that acts as a general amplifier of gene expression, enhancing the transcription of essentially all genes with active promoters in a given cell, and is a well-described oncogene with gained function in most tumour types. *c-Myc* is amplified in 7–67% of osteosarcoma tumours and overexpressed in at least 34% of tumours.

1.9.3.1.4 Other Oncogenes

Other oncogenes associated with amplifications in osteosarcoma include: *CDC5L*, *MAPK7*, *MET*, *PIM1*, *PMP22*, *PRIM1*, *RUNX2* and *VEGFA*. Collectively, the finding that near ubiquitous alterations in the Rb and p53 pathways function in osteosarcoma through both gain- and loss-of-function mutations indicates that loss of cell

cycle control and inappropriate DNA damage response are key drivers of osteosarcoma development (Khanna, 2015).

1.9.4 Advantages over other models

There is a large “translational gap” between highly artificial, xenograft models in generally immunodeficient rodents of clonal origin versus spontaneously developing, highly heterogeneous, and constantly evolving natural human cancer model. Moreover, the small size of these rodents limits imaging and is prohibitive to testing novel therapeutic strategies in conjunction with surgical resection, a key component of current standard of care. Pet dogs share the same environment as their human counterparts and are also susceptible to various spontaneous malignancies that affect the human population. These naturally occurring tumours in pet dogs are very similar to their human counterparts regarding their clinical presentation and pathophysiology. They carry similar natural history and prognosis condensed into the approximityly seven times shorter overall lifespan of dog (R. Timothy Bentley, 2016).

An ethical advantage of this approach over the experimental rodent model is that treatment studies do not involve induction of a disease state but rather involves treating a spontaneous disease and therefore ameliorating suffering and extending survival. Murine models can also be used for dog cancer xenograft models to parallel the studies of human xenografts and delineate the molecular biology, including role of specific genes in regulating canine cancer (R. Timothy Bentley, 2016).Toxicities initially encountered in human phase I/II trials are not often initially identified in rodent studies, thus utilizing pet dogs may facilitate early detection of such side effects and save the larger cost associated with failed human clinical trials. Although canine cancer studies are more expensive and time-consuming compared with rodent models, they are within the cost range of other large animal toxicity studies necessitated for investigational new drug applications and may be more cost-effective if the cost of failed human clinical trials due to weak preclinical data is taken into consideration (R. Timothy Bentley, 2016). There are several comparative studies recently for example towards a comparative canine-human model system, Hupp and group developed a novel anti-CD20 monoclonal antibody (NCD1.2) that binds both human and canine CD20 (Saurabh Jain, 2016). Extensive pedigrees of canine cancer cases may provide a valuable model for human hereditary cancers. Also due to the unique characteristics of inbred dog populations, a far smaller number of animals and DNA markers are needed (S. Hugen, 2016).

In addition to the similarities in drug metabolism, the large size of pet dogs and their naturally-occurring, biologically heterogeneous malignancies allow for the collection of repeated blood and tissue samples to study drug PK and biodistribution. Human and canine cancer cells are also similarly sensitive to chemotherapy (Figure 13). Such critical questions, when answered by the tumour-bearing dog model, add value to the current approaches during drug development (Corey Saba, 2016).

1.9.5 Limitations of the dog model

Limited knowledge of the recorded histories of dog breeds and, more importantly, exercise no control over their maintenance. Dog breeds are not mouse or rat strains, and the geneticist is somewhat at the mercy of the breed club for access to phenotypes and DNA samples. One of the limitations of spontaneous canine cancer is that unlike the transgenic mouse model, it is not useful for studying the effect of single gene mutations and has limited experimental manipulation potential. Another limitation of using a canine model for regular oncology studies is the availability of an adequate number of dogs for the studies on a regular basis (R. Timothy Bentley, 2016).

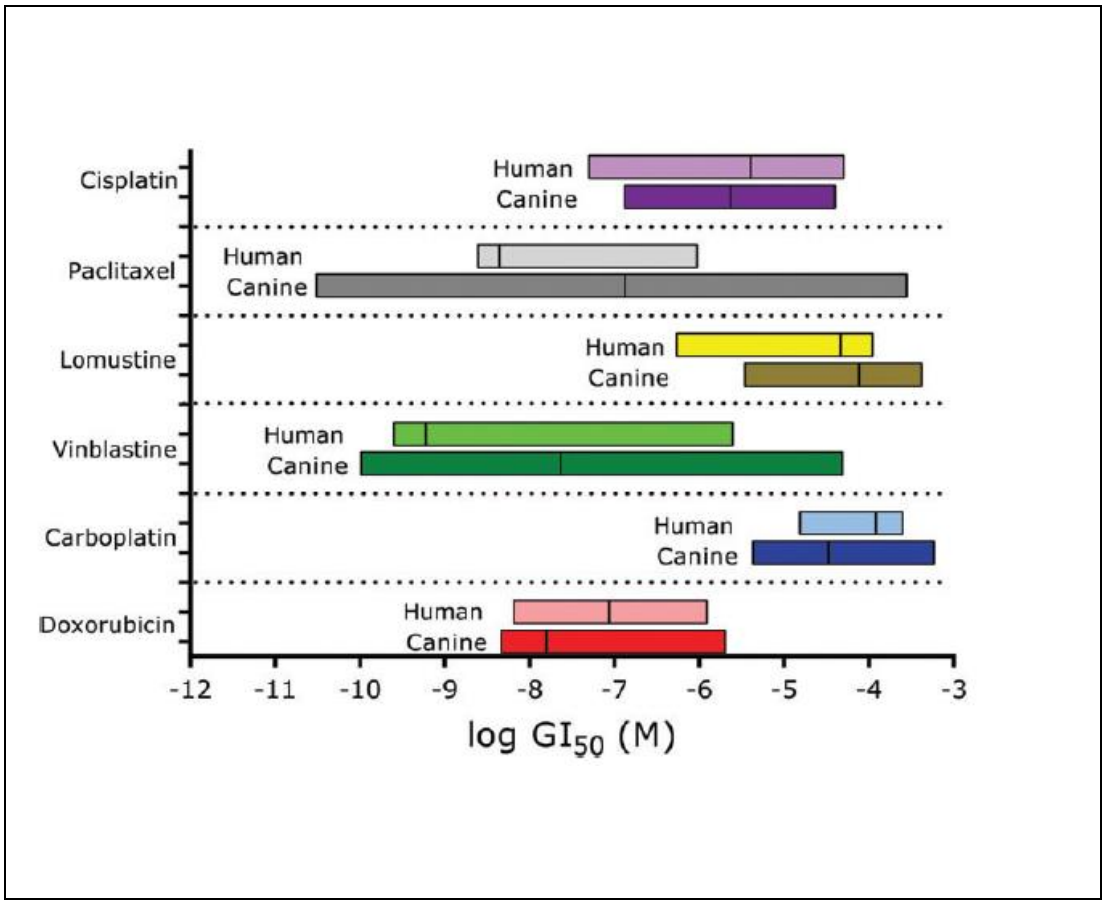

Figure 13 Human and canine cancer cells are similarly sensitive to chemotherapy

GI50 ranges of the human NCI60 panel to six chemotherapeutics were compared with the ranges generated in the canine FACC (The Flint Animal Cancer Center)
Panel (J. S. Fowles, 2016)

1.9.6 Current Drugs on clinics

The treatment of sarcoma has relied on cytotoxic chemotherapies with such drugs as doxorubicin, ifosfamide and dacarbazine in the neoadjuvant, adjuvant and palliative settings that have low response rates. With the rapid development of targeted agents and better molecular understanding of the individual subtypes of sarcoma, the development of either subtype or pathway specific therapies is evolving. (Frith AE, 2013)

Nutlin-3A, an inhibitor of MDM2 (Figure 14) has been shown to induce apoptosis in vitro and in vivo in the p53 wild-type MDM2-amplified osteosarcoma (OS) cell lines. (Duhamel LA, 2012). Characterizing the relative frequencies of mutations affecting CDKN2A, MDM2, and TP53 in sarcomas becomes important for the clinical development of MDM2 antagonists such as Nutlin-3.The crystal structure of MDM2–nutlin complexes revealed that nutlins project functional groups into the binding pocket that mimic the interaction of the three p53 amino acids critical for the interaction: Phe19, Trp23 and Leu26Figure 14 (Lyubomir T. Vassilev, 2004). RG7112 is a member of the nutlin family and is the first MDM2 antagonist to be assessed clinically. It is a potent inhibitor of P53–MDM2 binding that effectively stabilises P53 protein, activates P53 signalling, and inhibits cancer cell growth. It has an imidazoline structure and acts by binding to MDM2 resulting in unbound active p53. (Lyubomir T. Vassilev, 2004).The number of patients with high-grade OS who are likely to benefit from Nutlin-3A is low, because p53 is mutated in a significant proportion of such tumours. Since this drug can induce cell cycle arrest in vitro in the non-MDM2-amplified cell line U2OS, implies that a subset of central OS may benefit from this treatment. (Duhamel LA, 2012)There has been a proof of mechanism neoadjuvant trial using RG7112 (Roche, Nutley, NJ) in WDLPS and DDLPS that demonstrated p53 up regulation and reactivation. (Frith AE, 2013).There are additional MDM2 antagonists that are for human use. One is MI-219 (Ascenta Therapeutics, Malvern, PA) which has a spiro-oxindole structure that also binds to MDM2 to inhibit p53 binding, which allows for p53 activation in tumour cell lines with wild-type p53. There is a new class of small molecules (for example RO-5963, Roche, Nutley, NJ) that inhibit p53 interactions with both MDM2 and MDMX by inducing the dimerisation of MDM2 to MDMX, which restores p53 activity in cancer cells. It has similar p53-MDM2 inhibitory activity to Nutlin-3, but has nearly equivalent p53-MDMX inhibitory activity as well. (Frith AE, 2013)

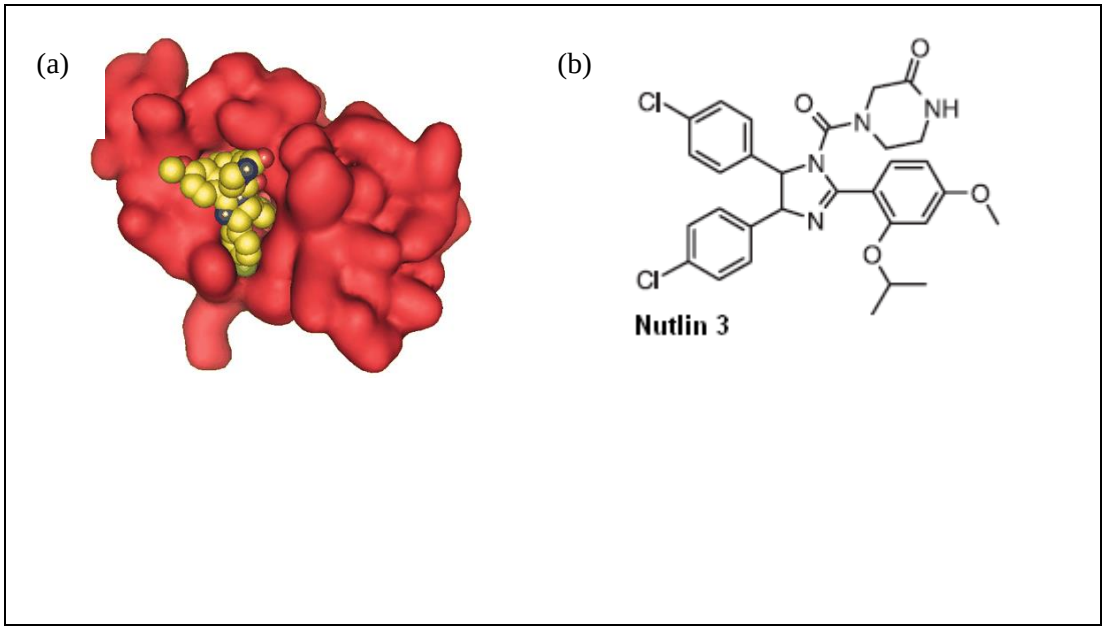

Figure 14 Nutlin action on MDM2-p53 complex

(a) Nutlin 3 bound at p53 pocket on MDM2 (b) structure of Nutlin 3 (Valeria Azzarito, 2012)

1.10 Bioinformatics in comparative oncology

In this new genomics era for cancer research, combining genotypic, phenotypic and pharmacologic data to reveal novel relationships has been essential for the many recent discoveries that have culminated in improved clinical outcomes. With these new tools, the possibilities for comparative and translational applications with human cancer research are becoming readily apparent. Dogs with cancer can potentially benefit from new discoveries made in human oncology, and conversely, human research can benefit through the integration of canine cancer models for pre-clinical validation studies. Sequencing would be an invaluable tool in identifying potential mutations and/or deletions in oncogenes and tumour suppressors across the entire genome. The integration of multiple types of genomic data will facilitate identification of the most significant drivers in canine cancer (J. S. Fowles, 2016).

Chi and group demonstrated that canine tumours can provide information generalizable to human tumours. Spontaneous canine soft tissue sarcomas exhibit inter-tumoural heterogeneity due to multiple mutations in oncogenes and tumour suppressor genes, varying environmental conditions, and inherited germline variations. The combination of these factors leads to immense natural heterogeneity in tumour phenotypes, disease outcomes, and response to therapies. (Chi, 2012)

Genomics-based predictors of drug response have the potential to improve outcomes associated with cancer therapy. Osteosarcoma (OS), the most common primary bone cancer in dogs, is commonly treated with adjuvant doxorubicin or carboplatin following amputation of the affected limb. Fowles and group demonstrated that gene expression-based modelling using canine datasets or a combination of human and canine datasets could accurately predict clinical outcome in canine osteosarcoma patients treated with adjuvant DOX and/or CARBO therapy. These results are important for human and canine cancer research for two main reasons:

1. Shows the potential of an advanced animal translational model for testing genomic methods of personalized cancer treatment in a clinical setting
2. Shows the potential for canine cancer research to expand in this genomic era through the incorporation of human genomic data into their model development design, which is currently much more prevalent and available than canine datasets (Fowles, 2016)

1.11 THESIS AIMS

The aims of my thesis were first to begin to use next generation sequencing of a canine cancer (osteosarcoma) to identify potential druggable targets using currently available drugs as a concept develop in personalized therapies. This led to the focus on pathways where two classic druggable targets exist: MDM2 and HSP90. Secondly, I characterize inhibitors of these pathways in a range of cell models to define mode of action and to discover new biomarkers. Together, my thesis shows the value in genomics-led, personalized drug treatment strategies in both human and canine cancer cells. The data also reveal how biomarkers can be discovered whose inhibition can augment such anti-cancer drugs and lead to new drug discovery platforms.

2 Methods and materials

2.1 Plasmids, chemicals and reagents

pcDNA3-IRF-1 WT and Flag IRF-1 WT were from Kathryn Ball; WT and mutant SBP-Hsp70 were from Philip, Brno Czech republic. All general chemicals and reagents were from Sigma or BDH unless otherwise indicated.

2.2 General microbiological techniques

All microbiological techniques were carried out using sterile apparatus and media under aseptic conditions.

2.2.1 Maintaining bacterial cultures

Bacterial cultures were grown in Luria-Bertani (LB) broth unless otherwise indicated in an incubator-shaker maintained at 37°C, 220 rpm. Suitable sterile containers with capacities of at least 4X the volume of the culture being grown were used to allow for adequate aeration. If required, selective antibiotics were added to the LB medium at the following final concentrations: 100 μg/ml ampicillin

Luria-Bertani (LB) broth

25 g LB medium (Miller) was dissolved in 1 litre of distilled water and sterilised by autoclaving at 121°C for 15-20 min. Final concentrations of the individual components in the broth were:

1% (w/v) Tryptone

0.5% (w/v) Yeast extract

1% (w/v) NaCl

LB Agar

40 g LB-Agar (Miller) was dissolved in 1 litre of distilled water and sterilised by autoclaving at 121°C for 15-20 min. Final concentrations of the individual components were:

1% (w/v) Tryptone

0.5% (w/v) Yeast extract

1% (w/v) NaCl

1.5% (w/v) Agar

LB-agar plates were prepared by pouring LB-agar that was liquefied by heating (and subsequently cooled to about 40°C) into 90 mm petridishes (Sterilin). If required, selective antibiotic was added to the liquefied LB-agar immediately prior to pouring into the petridishes. The agar was further cooled until it solidified, and the plates were dried at 37°C for up to 1 h prior to use.

2.2.2 Glycerol stocks

Glycerol stocks for long term storage of bacteria were prepared by adding 200 µl sterile glycerol to 800 µl mid-log phase bacterial culture in a cryotube (Nunc). The stocks were mixed by gentle agitation, snap frozen in liquid nitrogen and stored at -80°C.

2.2.3 Preparation of competent cells by heat shock method

Bacterial cells (DH5α or BL21) from glycerol stocks were inoculated into 2 ml of LB medium (without antibiotic) and incubated overnight in an incubator-shaker at 37oC and 220 rpm. An aliquot of the overnight culture (250 µl) was added to 50 ml fresh LB and further incubated until its OD600nm was approximityly 0.4. The culture was centrifuged at 4000 g for 15 min at 4oC and the pellet resuspended in 16 ml of ice-cold buffer I. Following a 10 min incubation on ice the cells were centrifuged again as above. The cell pellet was then gently resuspended in 2 ml of ice-cold buffer II, incubated on ice for 10 min and aliquotted (30 µl) into pre-chilled sterile microcentrifuge tubes. The aliquots were snap-frozen in liquid nitrogen and stored at -80oC.

Buffer I

60 mM CH3COOK

100 mM RbCl

10 mM CaCl2

40 mM MgCl2

15% (v/v) glycerol

Adjust to pH 5.8 with CH3COOH and sterilise by filtration

Buffer II

10 mM MOPS

10 mM RbCl

75 mM CaCl2

15% (v/v) glycerol

Adjust to pH 6.5 with NaOH and sterilise by filtration

2.2.4 Transforming bacterial cells

Plasmid DNA (50-250 ng; usually 100 ng) was mixed with an aliquot of freshly thawed competent cells (30 µl) and incubated for 30 min on ice. The cells were then heat shocked at 42ºC for 45 seconds and cooled on ice for 2 min. LB broth without antibiotic (0.2 ml) was added and the mixture was incubated at 37ºC for 60 min with shaking. Aliquots (10 µl and 50 µl) were plated onto LB-agar plates containing the appropriate selective antibiotic and incubated overnight at 37ºC.

2.3 General molecular biology techniques

2.3.1 Plasmid DNA amplification, extraction and quantification

A single bacterial colony from a stock LB-Agar plate was inoculated into 5 ml of LB broth containing selective antibiotic if required and incubated at 37ºC for 6-8 hours with shaking (220 rpm). This ‘starter culture’ was then diluted into 250 ml LB broth (containing antibiotic if necessary) and incubated overnight as above. Cells were collected by centrifuging at 6000 g for 20 min at 4ºC and plasmid DNA extracted using the Qiagen HiSpeed Maxi-prep kit according to the manufacturer’s instructions. DNA was eluted in 0.5 ml nuclease-free water and stored at -20ºC. If required, plasmid DNA was extracted directly from the 5 ml starter culture using the Qiagen Mini-prep kit. DNA was quantified using a NanoDrop ND-1000 spectrophotometer against a nuclease-free water blank.

2.3.2 Agarose gel electrophoresis of DNA

Agarose gel electrophoresis was used to separate DNA fragments, to test the purity of DNA preps, and to purify DNA. 1-2% agarose gels were prepared as required by dissolving electrophoresis-grade agarose (Invitrogen) in 1X TAE and then allowing the dissolved agarose to solidify by cooling. To aid in visualising the DNA, the fluorescent intercalating dye sybr safe was added to the agarose solution at a final concentration of 0.10 μg/ml immediately prior to pouring. DNA samples were mixed with 5X DNA loading dye at a 4:1 ratio of sample:dye and loaded onto the agarose gel, which was subsequently run at 75-100 V for approximityly 1 h (12 V/cm x distance between the electrodes in cm).

1X TAE Buffer

40 mM Tris

1 mM EDTA

Adjust pH to 8 with glacial acetic acid

6X DNA Loading Dye

0.25% bromophenol blue

0.25% xylene cyanol

15% glycerol

2.4 General biochemical techniques

2.4.1 Protein quantification

Protein concentration was estimated using Bradford's reagent (Bio-Rad) as indicated, according to the manufacturer's instructions. Absorbance (595 nm) was measured using the Victor 3 plate reader (Perkin Elmer).

2.4.2 SDS-PAGE

10% Separating Gel

Reagent	*Final conc.*
H2O	as required
30% acrylamide mix#	10%
1.5 M Tris (pH 8.8)	0.39 M
10% (w/v) SDS	0.1%
10% (w/v) APS	0.1%
TEMED (v/v)	0.04%

12% Separating Gel

Reagent	*Final conc.*
H2O	as required
30% acrylamide mix#	10%
1.5 M Tris (pH 8.8)	0.39 M
10% SDS	0.1%
10% APS	0.1%
TEMED (v/v)	0.04%

 # Acrylamide Mix (Protogel, National Diagnostics) consists of 30% (w/v) acrylamide and 0.8% (w/v) bis-acrylamide.

5% Stacking Gel

Reagent	*Final conc.*
H2O	as required
30% acrylamide mix	5%
1 M Tris (pH 6.8)	0.13 M
10% (w/v) SDS	0.1%
10% (w/v) APS	0.1%
TEMED (v/v)	0.1%

1X Running Buffer

192 mM Glycine

25 mM Tris

0.1% (w/v) SDS

Polyacrylamide gels were prepared using the recipes listed above as described by Laemmli (Laemmli, 1970)using the Bio-Rad Mini-Protean kit. The separating gel was poured first, and overlaid with water. The purpose of adding the water is two-fold: on the one hand, it evens out the upper surface of the separating gel as the water now forms the meniscus instead of the gel. The water overlay also cuts off the oxygen supply, thereby allowing the acrylamide to polymerise evenly. After polymerisation of the separating gel, the overlay was removed, and the stacking gel cast. Prior to loading, samples were mixed with an equal volume of 2X sample buffer or with 5X sample buffer at a 4:1 ratio of sample to buffer. The mix was then heated at 85ºC for 3 minutes, and subsequently loaded onto the gel. Pre-stained protein standards (Fermentas) were loaded as size markers. Gels were run at 150 V for approximityly 1 h in 1X running buffer, until the dye front reached the bottom of the gel.

2X Sample Buffer

300 mM Tris (pH 6.8)

5% (w/v) SDS

25% (v/v) glycerol

400 mM DTT

A few grains of bromophenol blue Mix, aliquot and store at -20°C Mix, Final concentrations when 2X sample buffer is mixed with sample at a 1:1 ratio are 150 mM Tris, 2.5% SDS, 12.5% glycerol and 200 mM DTT

2.4.3 Coomassie staining of SDS-PAGE gels

Fix

50% (v/v) methanol

10% (v/v) glacial acetic acid

Stain

50% (v/v) methanol

10% (v/v) glacial acetic acid

0.2% (w/v) coomassie brilliant blue R-250

Destain

7.5% (v/v) methanol

10% (v/v) glacial acetic acid

To visualise proteins by Coomassie brilliant blue staining, SDS-PAGE gels were fixed for 5-10 min at room temperature, and stained with coomassie blue stain for 20-30 min. Stained gels were then destained as required (from 30 min to overnight), washed in water and dried using a heated vacuum gel dryer (Gel Master Model 1426, Welch Rietschle Thomas).

2.4.4 Western blotting

1X Transfer Buffer

192 mM Glycine

25 mM Tris

20% (v/v) methanol

Proteins separated by SDS-PAGE were transferred onto 0.2 μm nitrocellulose membranes (Protran, Schleicher & Schuell Biosciences) using Bio-Rad transfer apparatus. The transfer was carried out in tanks containing agitated transfer buffer and an ice pack to prevent over-heating at 120 V for 1 h or 15 V overnight.

Post transfer, membranes were rinsed in phosphate-buffered saline (PBS) containing 0.1% (v/v) Tween-20 (PBST) three times (5-6 min each). The membrane was then blocked using blocking solution [5% (w/v) semi-skimmed milk powder (Marvel) in PBST] for 1 h, and was subsequently incubated with the primary antibody in blocking solution for 1 h at room temperature or overnight at 4ºC. The membrane was then washed as above and incubated with

horse radish peroxidise (HRP) conjugated secondary antibody [Dako Cytomation; used at 1:2000 dilution in blocking solution] for 1 h at room temperature. The membrane was again rinsed three times with PBST and antibody signal detected using enhanced chemiluminescence (ECL) reagent. Blots were overlaid with a mixture of ECL solutions I and II at a 1:1 ratio (mixed immediately prior to use) for 2 min, blotted dry, exposed to Hyperfilm ECL (Amersham) or X-Ray film (SLS) for the required period of time, and then developed using a Konica Medical Film Processor (Model SRX-101A).

ECL Solution I

100 mM Tris (pH 8.5)

2.5 mM Luminol

0.4 mM p-Coumaric acid

ECL Solution II

100 mM Tris (pH 8.5)

0.02% (v/v) H2O2

The primary antibodies used in this thesis, together with the working dilution and clone (if known) are listed in Table 1

Antibody to	type	Clone/Name	Supplier/Reference	dilution
CHIP	Mouse Monoclonal	v3.1	Gift from B.Vojtesek	1:1000
GAPDH	Mouse Monoclonal	8245	Abcam	1:3000

Hsp/c70	Mouse monoclonal	2.1	Gift from B.Vojtesek	1:2000
Hsp70	Mouse Monoclonal Rabbit Polyclonal	SPA-810 SPA-812	Stressgen	1:1000 1:1000
Hsc70	Rabbit Polyclonal	SPA-816	Stressgen	1:2000
Hsp90	Rabbit Polyclonal		Gift from B.Vojtesek	1:500
Hsp90phospho (GDD)		8.2	Gift from B.Vojtesek	1:2000
Hsp90 (alpha +beta)		EEV 1	Gift from B.Vojtesek	1:4000
IRF-1	Mouse monoclonal	612047	BD bioscience	1:1000
IRF-1	Rabbit polyclonal	C20	Santa cruz	1:500
p53	Mouse monoclonal	DO-1	Gift from B.Vojtesek	1:1000
p53	Rabbit polyclonal	VP-P956	vector	1:1000
Fli-1	Mouse monolconal	G146-222	BD bioscience	1:1000

LC3	Rabbit monoclonal	D11	Cell signalling technology	1:1000
Mdm2	Mouse monoclonal	4b2	Gift from B.Vojtesek	1:1000
Mdm2	Rabbit polyclonal		Gift from B.Vojtesek	1:1000
Lamb2A	Mouse monolconal	25631(H4B4)	abcam	1:1000
PDL-1 (for FACS)	APC Mouse monoclonal	M1H1(563741)	BD bioscience	1:100
PDL-1	Rabbit monoclonal	E1L3N	Cell signalling	1:1000
UBA3	Mouse monoclonal	F10	Santa cruz	1:1000
CDK4	Rabbit polyclonal	H22	Santa cruz	1:1000
Cyclin D1	Mouse monoclonal	Ab-3	Calbiochem	1:1000

Table 1 Antibodies

2.4.5 Stripping nitrocellulose blots

Stripping Buffer

62.5 mM Tris (pH 6.8)

2% (w/v) SDS

0.6% (v/v) β-mercaptoethanol

To strip antibodies off nitrocellulose membranes so that other antibodies could be subsequently added, the membranes were incubated with stripping buffer for 30 min at 50°C with gentle agitation. Blots were then rinsed thoroughly with PBST, blocked in 5% milk/PBST for 1 h and incubated with alternative antibodies as required.

2.5 Cell culture

All tissue culture disposables such as culture plates, flasks and pipettes were from TPP or Greiner-Cellstar unless otherwise indicated.

2.5.1 Cell lines

Cell line	Origin	Growth conditions	Culture media	Media supplements
A375	Human (malignant melanoma)	10% CO2, 37ºC	DMEM	10% (v/v) FBS, 1% (v/v) P/S
A375 p53-/- CRISPR	Human (malignant melanoma)	10% CO2, 37ºC	DMEM	10% (v/v) FBS, 1% (v/v) P/S
A549 CRISPR control WT	Human Carcinoma	10% CO2, 37ºC	DMEM	10% (v/v) FBS, 1% (v/v) P/S
A549 ATG5-/-CRISPR	Human Carcinoma	10% CO2, 37ºC	DMEM	10% (v/v) FBS, 1% (v/v) P/S
A549 ATG5 Rescue	Human Carcinoma	10% CO2, 37ºC	DMEM	10% (v/v) FBS, 1% (v/v) P/S

HCT116	Human colorectal carcinoma	5% CO2, 37ºC	Mc Coy's 5A (Gibco, Invitrogen)	10% (v/v) FBS, 1% (v/v) P/S
TC32	Human(Primitive neuroectodermal tumor (PNET)	5% CO2, 37ºC	DMEM	10% (v/v) FBS, 1% (v/v) P/S
TC71	Human (Ewing's Sarcoma)	5% CO2, 37ºC	DMEM	10% (v/v) FBS, 1% (v/v) P/S
OSA 31	Canine osteosarcoma, primary	5% CO2, 37ºC	DMEM	10% (v/v) FBS, 1% (v/v) P/S
OSA 75	Canine osteosarcoma, primary	5% CO2, 37ºC	DMEM	10% (v/v) FBS, 1% (v/v) P/S
OSA 78	Canine osteosarcoma, primary	5% CO2, 37ºC	DMEM	10% (v/v) FBS, 1% (v/v) P/S
D17	Canine osteosarcoma, primary metastatic lung	5% CO2, 37ºC	DMEM	10% (v/v) FBS, 1% (v/v) P/S

Normal 57	Canine normal bone	5% CO2, 37ºC	DMEM	10% (v/v) FBS, 1% (v/v) P/S

Table 2 Cell lines and culture media

Key:

DMEM: Dulbecco's Minimal Essential Medium (Gibco)

FBS: Fetal Bovine Serum (Autogen Bioclear)

P/S: Penicillin/Streptomycin mix (Invitrogen)

Note: All canine cell lines provided by Prof Geoffrey Wood, university of Guelph

2.5.2 Sub-culturing of cells

Cells were sub-cultured at approximityly 80-90% confluence (2-3 times a week, as required) into sterile tissue culture plates at a 1:10 dilution in fresh medium. In brief, the medium was discarded and the cells were rinsed in sterile PBS. Trypsin-EDTA (Invitrogen) was added (2 ml for a 10 ml culture dish) and the cells were incubated at 37°C for 5 minutes. Fresh culture medium (8 ml for a 10 ml culture dish) was added to deactivate the trypsin-EDTA, the cells were mixed by pipetting, and the required volume (1 ml for a 1:10 dilution) was plated onto a new culture dish containing pre-warmed fresh medium.

2.5.3 Freezing and thawing cells

Freezing Medium

50% (v/v) FBS

10% (v/v) DMSO

40% (v/v) culture medium

Prior to freezing, cells were grown in 10 cm culture dishes and trypsinised as above at 90-95% confluence. Trypsinised cells were collected by centrifugation (200 g, 3 min, and room

temperature) and the cell pellet resuspended in 3 ml freezing medium. The resuspended cells were then transferred to cryotubes (Nunc; 1 ml per tube) and frozen gradually in a Nalgene cryo-freezing container overnight. The frozen cells were then transferred to liquid nitrogen for long-term storage.

Frozen cells were recovered by warming to 37ºC and transferring into a sterile culture dish containing fresh pre-warmed medium. The medium was replaced with fresh medium the following day.

2.5.4 Transient transfection of DNA and siRNA

Cells were transfected at approximityly 70-80% confluence using Attractene (Qiagen) according to the manufacturer's instructions and harvested 24 h post transfection. Within an experiment, DNA levels between samples were normalised using empty vector. For transfection of siRNA (Dharmacon) into cells in 6 well plates, Dharmafect (Dharmacon) was used according to the manufacturer's instructions. In brief, 60 nmol siRNA was diluted to 200 µl with serum and antibiotic free medium. In parallel, 6 µl Dharmafect was added to 194 µl serum and antibiotic free medium in a separate tube and incubated for 5 min at room temperature. The diluted siRNA and Dharmafect were then mixed (400 µl total volume) and incubated for 20 min at room temperature. During the incubation, the cells (at approximityly 70% confluence) were rinsed in PBS and fresh medium containing serum but no antibiotic (1600 µl) was added to each well. Following the incubation, the 400 µl siRNA mix was gently added to the cells, and the cells were incubated at 37°C for 24-72 h (as required) prior to harvesting.

2.5.5 Harvesting cells

At the time of harvesting the cells were placed on ice, following which the medium was discarded. The cells were rinsed with ice-cold PBS (1 ml/well for a 6-well plate and 10 ml for a 10 cm plate) and then harvested in a further 1 ml ice-cold PBS using a cell scraper. In some cases, cells in 10 cm plates were scraped directly into 1 ml lysis buffer (see below). Harvested cells were transferred to a microfuge tube and centrifuged at 2500 g for 5 min at 4ºC. The supernatant was discarded, and the cell pellet was either snap-frozen in liquid nitrogen (and then stored at -80ºC) or immediately lysed using the appropriate lysis buffer.

2.5.6 Mammalian cell lysis

Approximityly two volumes (with respect to the size of the cell pellet) of lysis buffer were added to the harvested cell pellet. Alternately, adherent cells were rinsed in ice-cold PBS and scraped directly into lysis buffer (1 ml per 10 cm plate). Samples were vortexed briefly, incubated on ice for 20 min, and then centrifuged at 16000 g for 15 min at 4ºC. The supernatant (lysate) was transferred to a fresh tube, snap-frozen in liquid nitrogen and stored at -80º (or at -20ºC after addition of sample buffer). The recipes for the lysis buffers used commonly in this thesis are detailed below:

1% NP40 Lysis Buffer

25 mM HEPES (pH 7.5)

1% (v/v) NP40

150 mM KCl

50 mM NaF

5 mM DTT

1X protease inhibitor mix

0.4% Triton X-100 Lysis Buffer

50 mM HEPES (pH 7.5)

0.4% (v/v) Triton X-100

150 mM NaCl

10 nM NaF

2 mM DTT

0.1 mM EDTA

1XProtease inhibitor Mix

Urea Lysis Buffer

8 M Urea

50 mM HEPES (pH 7.6)

5 mM DTT

1 mM benzamidine

50 nM NaF

Protease Inhibitor Mix (10X stock)

200 μg/ml leupeptin

10 μg/ml aprotinin

20 μg/ml pepstatin

10 mM benzamidine

100 μg/ml soybean trypsin inhibitor

20 mM pefabloc

10 mM EDTA

2.5.7 Drug treatments

For the experiments described in this thesis, cells were treated with various drugs and chemicals prior to lysis. Table 3 summarises the drugs used, the concentration and duration of

treatment and the principal effects of the drug. The actual use of each drug in a particular experiment is described in the relevant section where it is used

Drug	Function (with respect to its use in this thesis)	Concentration used at (in cell culture media)	Time(duration of treatment)
MG-132	Inhibits the 26S proteasome by binding reversibly to the N-terminal Thr residue of the β1 subunit	50μM	2 hours
17 AAG	Inhibits Hsp90 by binding to the ATP-binding site and blocking Hsp90 ATPase activity	100nM	6hours/16 hours
Ganetespib	Inhibits Hsp90	100nM	6hours/16 hours
Nutlin	Inhibits P53/Mdm2 interaction	10μM	6 hours
Radicicol	Inhibits Hsp90 by binding to the ATP-binding site and blocking Hsp90 ATPase activity	100nM	6hours/16 hours
Cyclohexi mide	Inhibits protein synthesis by binding to cytoplasmic (80S) ribosomes and blocking translational elongation	30μM	Various time points

IFNγ	Soluble cytokine that is the only member of the type II class of interferons.	100ng/ml	Various time points

Table 3 Drugs: Principal effects and working concentrations

2.6 Microscopy

2.6.1 Proximity ligation assay (PLA)

Cells were grown onto glass coverslips in a 6 well dish until they reached around 50% confluency. After treatment (as indicated in the figure legends), cells were fixed by addition of 4% formaldehyde solution for 10 minutes and then permeabilised using 1% Triton X-100 in PBS. Next Duolink® II (green) assay from Olink® Bioscience was carried out following suppliers instructions. Briefly, any unspecific antibody binding sites were blocked using 3% BSA (w/v) in PBS for 1 hour at room temperature (24°C), next primary antibodies were diluted in the supplied antibody diluent and added to cells and incubated over-night at 4°C. As a control one slide was incubated with only single mAb and no second primary antibody. Next PLA probes conjugated to secondary antibodies anti- mouse and anti-rabbit respectively were added to the cells for 1 hour at 37 °C and ligation and amplification was carried out as detailed by the supplier. In the last step an amplification reaction produces a fluorescent signal that can be detected using a fluorescent microscope with a green filter (488nm). Results were visualised using an Axioplan2 (Zeiss) fluorescent microscope with Planneofluar objectives, a 100W Hg source (Carl Zeiss, Welwyn Garden City, UK) and Chroma #89014ET single emission filters (Chroma Technology Corp., Rockingham, VT) using 40x or 100x magnification Zeiss lense and a Hamamatsu Orca AG CCD camera (Hamamatsu Photonics (UK) Ltd, Welwyn Garden City, UK).The single excitation and emission filters are installed in motorised filter wheels (Prior Scientific Instruments, Cambridge, UK). ImageJ software was used for analysis.

4% formaldehyde solution
4% (v/v) formaldehyde

100 mM PIPES (pH)

10 mM EDTA

1 mM MgCl2

2.7 Other assays

2.7.1 Co-immunoprecipitation (Co- IP)

To provide further evidence of MDM2/HSP70 complex formation in cells, I captured endogenous MDM2 from A375 cells. 1 µg of 4B2 (MDM2 MAb) was added to 2 mg of total protein in the pre-cleared lysate and, in a final volume of 1 ml, incubated for 1 hour at 4°C with gentle rotation. Then, 15 µl of protein G SepharoseTM 4 FastFlow (GE Healthcare; washed 4 times in PBS) was added to the above samples and incubated over-night at 4°C with gentle rotation. Beads were washed four times with 500 µl of IP buffer. Samples (before and after controls) were then eluted by addition of 50 µl of 2X SDS sample buffer and incubation at 95°C for 5 minutes. The eluate was collected by centrifugation and analyzed by SDS-PAGE/Immunoblot for HSP70.

IP buffer 5
0.3 M NaCl

1% (v/v) Triton X-100

50 mM HEPES pH 7.6

2.7.2 SBP-tagged pull down

A375 cells were cultured in 10 cm plates and transfected with 2 µg of the SBP-tag vector, empty, wt HSP70 and mutant HSP70 using attractene. Post transfection cells were treated with either Nutlin or Ganetespib for further 6 hours and the below described steps was followed.

1. Culture media aspirated, wash cells 2X with PBS

2. Cells lysed using lysis buffer (3X the cell pellet)

3. Sonication (3X 15 sec pulse)

4. Spin down cells 15mins 12000g

5. Streptavidin agarose beads were washed in lysis buffer without (PIM and avidin 1:100)

6. Divide lysates into two, add to beads, one lysate with ATP, one without.

7. Precipitate for one hour at room temperature.

8. Wash 3X (200ul) with wash buffer

9. Elute in 35ul elution buffer (wash buffer +2mM Biotin)

10. Spin down and collect 30ul without beads.

Lysis buffer

50mM Hepes (pH 7.6)
150mM KCL
2mM MgCL2
PIM
Avidin (1:100)
+/- Nutlin (10uM) or Ganetespib (100nM)

Wash buffer

50mM Hepes (pH 7.6)
150mM NaCL
50mM KCL
2mM MgCL2
+/- ATP

2.8 Immunofluorescence

Immunostaining of cells was done by growing the mammalian cells in a six well plate containing a glass coverslip per well. Cells were seeded and treated with appropriate drug for either 6 or 6 hours. The cells were washed thrice in PBS (five minutes on shaker for each wash) and then fixed using formaldehyde fixing solution (3.7% formaldehyde, 10mM EGTA pH-8.0, 100mM PIPES pH-6.8, 1mM MgCl2 and 0.2% Triton X-100) at room temperature, followed by washing and permeabilisation of cells with 1% Triton x-100. These permeabilised cells were then washed as before and blocked with 3% BSA for 30 minutes and then probed with the primary antibodies and left overnight at 4◦C in humidity chamber. Then the chambers were washed thrice with PBS and secondary antibody (Rabbit anti-mouse 488 nm) diluted 1:1000 in antibody diluent was added to the chambers with an incubation period of 1 hour in humidity chamber at RT. The chambers were again washed thrice with PBS and were prepared for mounting. For mounting, 1 µl of DAPI fluorescent stain was made up in 10 drops of

mounting medium (DAKO) and placed onto the slides before placing the chambers on it. The chambers were then placed with cells facing the slides and stored in the dark until dried. Once the slides containing the chambers had dried, slides were ready for imaging.

2.9 Sample Preparation for Mass Spectrometry and result Analysis

2.9.1 Mass Spectrometry

2.9.1.1 Sample preparation for mass-spectrometry

When handling samples for mass spectrometry analysis the utmost care was taken to avoid contamination of the samples by keratin. The solutions used for the reactions were filtered before use where possible, gloves and a lab coat were worn at all times and most of the work was performed in a fume hood. Mass spectrometric analysis by TMT tagging was used to determine the differential expression of the proteins as TMT mass spectrometric analysis can give a ratio of proteins in a mixture of samples. A375 cells were grown in a 150mm plates to reach confluency (1 x106 cells per ml) and treated with either Ganetespib (100nM for 16hours) or Nutlin (10uM for 6 hours) prior to harvesting. The cells were grown in triplicate set, one was used to run SDS gel while other two were used as biological replicates for mass spectrometry. I performed the following steps at Masaryk Memorial Cancer Institute, Brno.

Samples

- DMSO treated
- Ganetespib treated
- Nutlin treated
- N+G(Nutlin+Ganetespib) treated

2.9.1.2Lysis of cell pellets

Lysis buffer: 8 M urea in 0.1 M Tris-Cl (pH 8)

1. Lyse the cells by adding five cell-pellet volumes of Lysis Buffer with protease inhibitors (i.e., 200 µL of Lysis Buffer for a 20 µL cell pellet).
2. Mix by pipetting and store in freezer at -20 °Cover night.
3. Sonication and centrifugation at 14,000 × g for 30 minutes at 4°C.
4. Carefully separate the supernatant and transfer into a new tube and store at -20 °C.
5. Determine the protein concentration of the supernatant with RCDC kit.

2.9.1.3FASP digestion

Chemicals and solutions

- UA: 8 M Urea in 0.1 M Tris pH 8
- ABC: 100 mM NH_4HCO_3 in H_2O ,50 mM NH_4HCO_3 in H_2O
- 5 % TFA: 190 ul H_2O + 10 ul TFA (here used about 30% TFA for ph balance 1 to 2 ul)

- 100 mM TCEP in deionized water(tris 2 carboxyethyl phosphine hydrochloride-C4706 sigma)
- 300 mM iodacetamid in deionized water
- Trypsin

FASP Procedure

1. Add 100 µl UA to the filter unit.
2. Add 50ug – 100 µg of sample to the filter.
3. Mix by pipet tip, do not touch the filter.
4. Centrifuge for 15 min, 14 000 g, 20 °C.
5. Discard the flow-through from the collection tube.
6. Add 100 µl UA and 20 ul 100 mM TCEP, mix by pipet tip.
7. Incubate in thermomixer for 30 min, 600 rpm, 37 °C.
8. Centrifuge for 15 min, 14 000 g, 20 °C.
9. Discard the flow-through from the collection tube.
10. Add 100 µl UA and 20 µl 300 mM IAA, mix by pipet tip.(light sensitive)
11. Incubate in thermo-mixer in dark for 20 min, 20 °C.
12. Centrifuge for 15 min, 14 000 g, 20 °C.

13. Discard the flow-through from the collection tube.
14. Add 100 µl 100 mM ABC, mix by pipet tip.(ammonium bicarbonate)
15. Centrifuge for 20 min, 14 000 g, 20 °C.
16. Discard the flow-through from the collection tube.
17. Add 100 µl 100 mM ABC, mix by pipet tip.
18. Centrifuge for 20 min, 14 000 g, 20 °C.
19. Discard the flow-through from the collection tube.
20. Transfer the filter units to new collection tubes.
21. Add 100 µl 50 mM ABC and trypsin (17 ul of 0, 2 ug/ul Trypsin (Promega V511A)), mix at 600 rpm in a thermo-mixer for 1 min.
22. Incubate the units in a wet chamber at 37 °C for 4 - 18 hours.
23. Centrifuge for 15 min, 14 000 g, 20 °C (elution of peptides!!).
24. Repeat step 23.
25. Added 30% TFA 1ul to make the ph between 2 and 4 and then dried the samples in vaccum

2.9.1.4TMT labelling

Used the thermoscientific TMT10plex mass tag labelling kit (CAT: 90110)

Sample	TMT labelling
A375 DMSO1	126
A375 DMSO2	127N
A375 Ganetespib1	127C
A375 Ganetespib2	128N
A375 N+G1	128C
A375 N+G2	129N
A375 Nutlin1	129C
A375 Nutlin2	130N

Table 4 samples for TMT

1. Immediately before use, equilibrate the TMT Label Reagents to room temperature. For the 0.8 mg vials, add 41 µL of anhydrous acetonitrile to each tube. Allow the reagent to dissolve for 5 minutes with occasional vortexing.
2. Briefly centrifuge the tube to gather the solution.
3. Carefully add 41µL of the TMT Label Reagent to each 25-100µg sample.
4. *Note*: A 100 µL glass syringe or positive displacement pipette may be necessary to accurately measure and dispense TMT Reagents in volatile acetonitrile solvent.
5. *Note*: Wash the syringe 3x with miliQ H2O and 3x with anhydrous ACN after each label
6. Incubate the reaction for 1 hour at room temperature.
7. Add 8 µL of 5% hydroxylamine to the sample and incubate for 15 minutes to quench the reaction.
8. Combine samples in a new microcentrifuge tube at equal amounts dry at RT in speed vac and store at -80°C.

2.9.1.5Peptide purification

Chemicals and solutions

100% acetonitrile (ACN) with 0.1% FA

50% ACN with 0.1% FA

80% ACN with 0.1% FA

deionized water with 0.1% FA

I had 50ug per sample and combined all 8 together so 400ug in total. 20ul of the combined sample was topped with 80ul 0.1%FA

Procedure

1. use microSpin columns C-18 (https://www.harvardapparatus.com/Guide+to+C18_SpinColumns.pdf)
2. condition the column 2x with 200 ul 100% ACN with 0.1% FA in the microspin column
3. centrifuge for 3 min, 100 g, 20 °C
4. rinse the column 200 ul water with 0.1% FA

5. centrifuge for 3 min, 300 g, 20 °C
6. add 200 ul water with 0.1% FA, hydrated for 15 min
7. centrifuge for 3 min, 300 g, 20 °C
8. discard the flow-through from the collection tube
9. add sample into the microspin column
10. centrifuge for 3 min, 500 g, 20 °C
11. add 3x 200 µl water with 0.1% FA
12. centrifuge for 3 min, 500 g, 20 °C
13. transfer the microspin column to new collection tubes
14. add 200 µl 50% ACN with 0.1% FA
15. centrifuge for 3 min, 500 g, 20 °C
16. add 200 µl 80% ACN with 0.1% FA
17. centrifuge for 3 min, 500 g, 20 °C
18. transfer the microspin column to new collection tubes, discard the flow-through from the collection tube
19. add 200 µl 100% ACN with 0.1% FA
20. centrifuge for 3 min, 500 g, 20 °C
21. both collection tubes evaporate using SpeedVac

2.9.2 Flow Cytometry

A minimum of 10,000 events were gated to exclude dead cells, and analysis was performed with BD accuri. A375 or A549 cells were treated with either DMSO, Ganetespib, Nutlin or IFNγ for 16 hours or as indicated. Post treatment the cells were washed in ice cold PBS. The cells were trypsinized. The cells were pelleted and 10^8 cells were gently mixed into 400 µL of ice cold PBS and washed thrice at 300 g for 3 min at 4°C. The supernatant was discarded and the cells were resuspended in 100ul PBS and 1ul of PDL-1 antibody (APC conjugated Antibody) or 6ul of isotype antibody was added and cells incubated for 1 hour at room temp. The cells were washed thrice at 300 g for 3 min at 4°C and the supernatant was discarded. The cells were either fixed using PFA (final 2%) or resuspend the pellet in 500ul PBS for FACS analysis. untreated cell controls were also used. The relative binding affinity of the antibody was analyzed using the FlowJo7 and the FACSDiva 6 software (BD FACSAria™ II SORP (BD Biosciences, USA).

2.10 General Biochemical Techniques

2.10.1 Bradford Assay for Protein quantification

The protein concentration in the cell lysate was estimated using the Bradford reagent (#5000006, Bio-Rad) as suggested by the manufacturer's instructions. The plate was shaken on a Microplate shaker (Jencons Scientific Ltd, UK) for 5 min at room temperature and the absorbance was measured 595nmOD using the Victor3 1420 Multilaber Counter (PerkinElmer, USA). The BSA standards from 0 μg/μL (blank) to 4 μg/μL was used to generate a linear standard curve. Using the standard values, the readings of the unknown samples were converted into concentrations in mg/mL for each individual lysate.

2.11 Cell-based assays

2.11.1 Cell cytotoxicity Assay

The assay was carried out in 96 well tissue culture plates. The cells were treated with either Ganetespib, 17AAG or Nutlin for 16 hours.

1. Add 1/10th volume of alamarBlue® reagent directly to cells in culture medium (10ul into 100ul)
2. Incubate for 1 to 4 hours at 37°C in a cell culture incubator, protected from direct light.
3. The absorbance was measured at 560 nm using the Victor 3 plate reader. The cell growth curve was mapped by plotting the absorbance values against time.

2.12 Bioinformatics

2.12.1 Canine Osteosarcoma DNA and RNA purification

OSA31 is a canine osteosarcoma cell line belonging to male Bullmastiff. All the cell lines are kind gift from Prof Geoffrey Wood from university of Guelph. DNA was extracted from the OSA31 tumour cell line and their matched normal tissues using the ChargeSwitch gDNA Mini Tissue kit from Invitrogen following the manufacturer's protocol. RNA was extracted from

tumour OSA31 cell line using RNeasy RNA extraction kit from Qiagen following the manufacturer's protocol.

2.12.2 Sequencing of OSA31 DNA

Exome Sequencing was performed using Agilent V5+UTR Exome Capture Kit (75Mb); Illumina, 100bp paired-end reads using a coverage of Tumour: Normal pairs (100X/30X). Paired de-multiplexed fastq files were generated using CASAVA software (Illumina) and initial quality control was performed using FastQC.

2.12.3 Sequencing of OSA31 RNA

RNA sequencing was performed using Illumina HiSeq2500 100bp paired-end reads. DNA seq and RNA next generation sequencing were performed by otogenetics ltd.

2.12.4 Data analysis

The results from the WES were analysed using bioinformatics software CLC genomics workbench 8.5.1 (Qiagen).The following steps were involved for the input and analysis of the next generation sequencing files.

2.12.4.1 Input files into CLC workbench

The schematic steps involved in inputting the fasta files into workbench is described in Figure 15. The illumine option under input files was selected. The files were imported together as paired-end reads.

2.12.4.2 Downloading the canine reference

As Canine reference is not installed in the software by default, canine reference genome was downloaded using the steps mentioned in Figure 16 and Figure 17

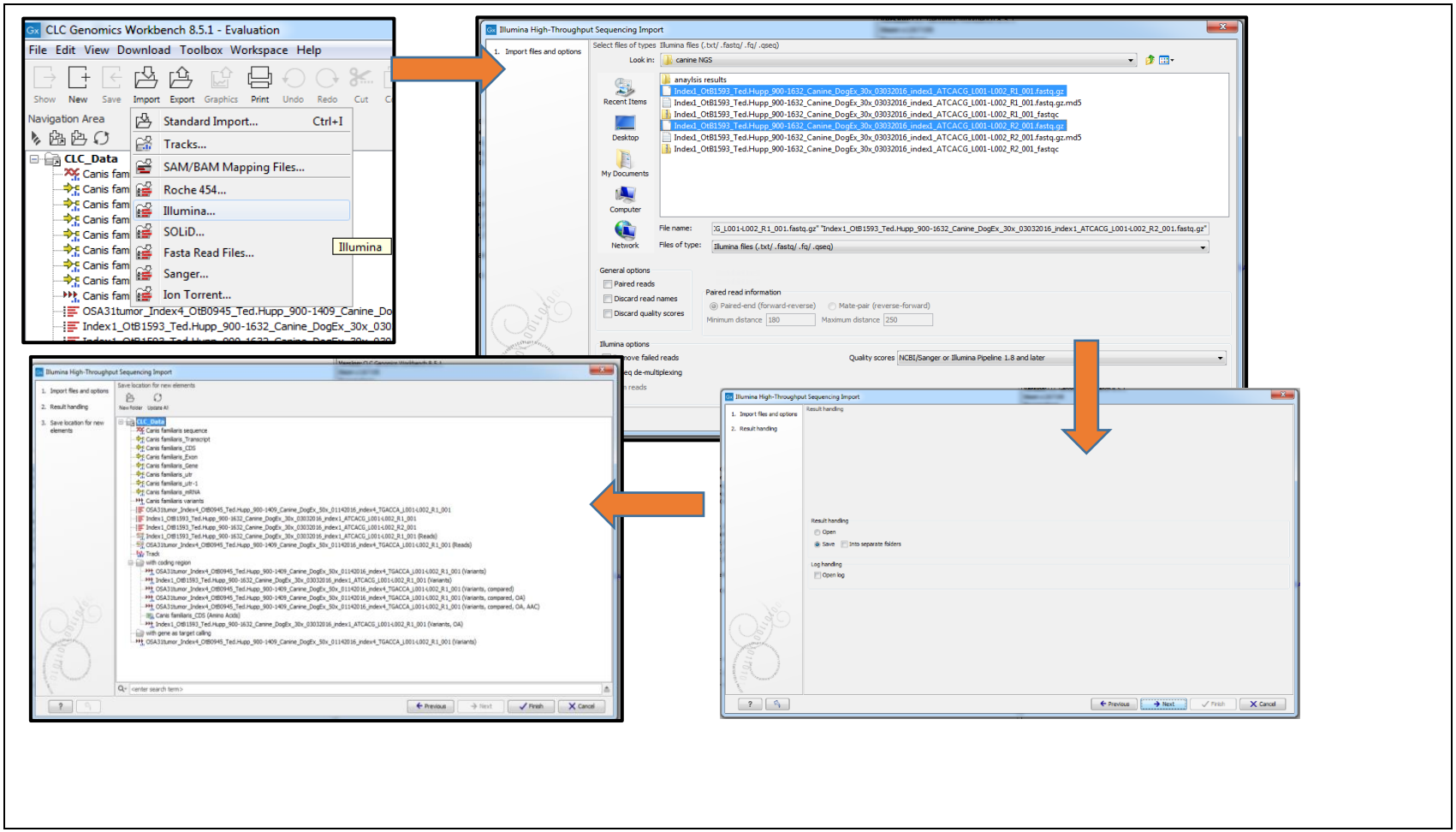

Figure 15importing files to workbench

The tumour reads from each paired-end read were selected. The index26 represents the tumour WES. Illumina option was selected under the import tab, then the paired read files were selected together and saved the paired read file into CLC workbench

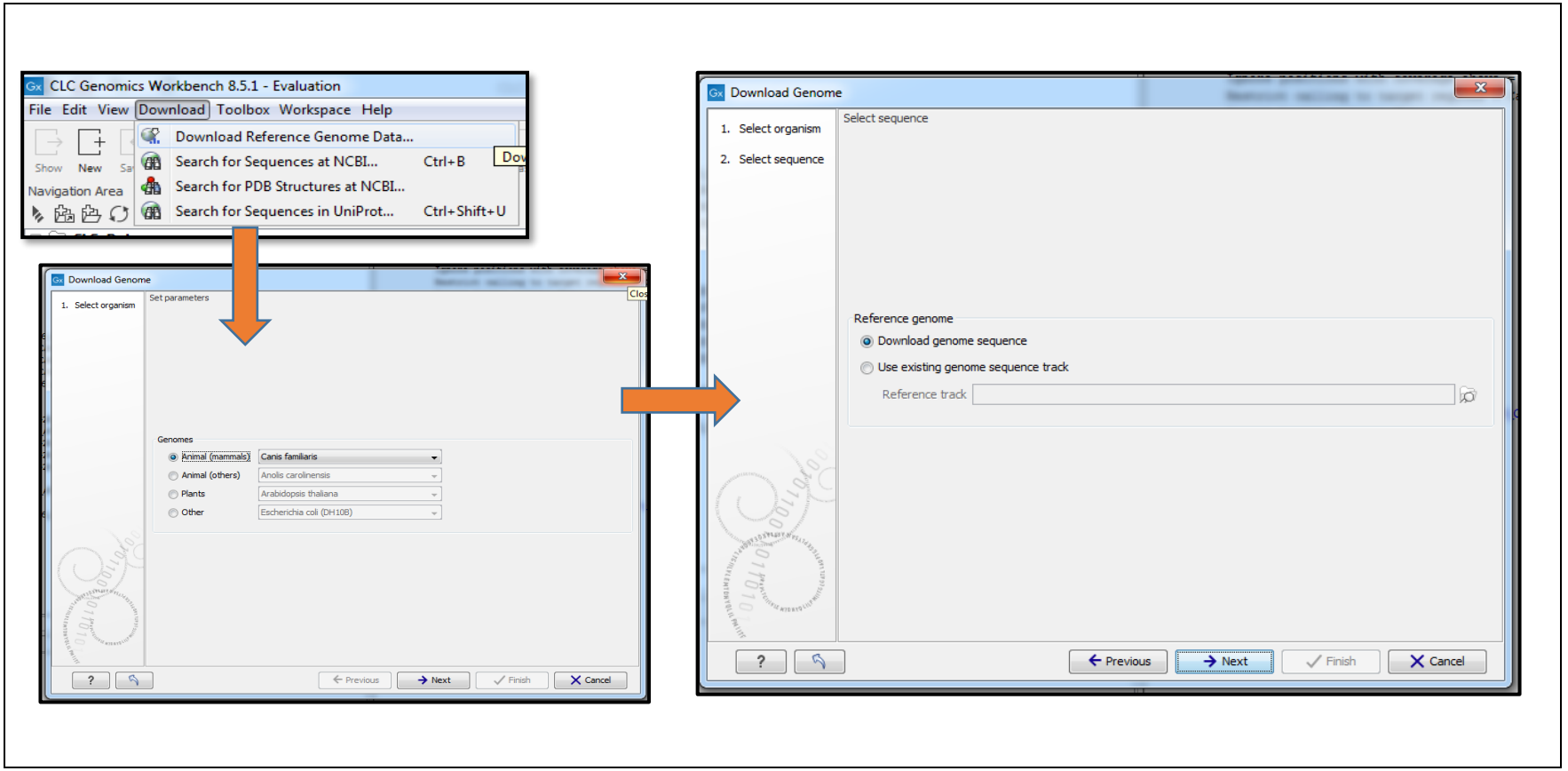

Figure 16 downloading the canine reference genome

In the workbench 8.5.1 under download section canis familaris was selected for set parameters (animal –mammals).Under reference genome select download genome sequence.

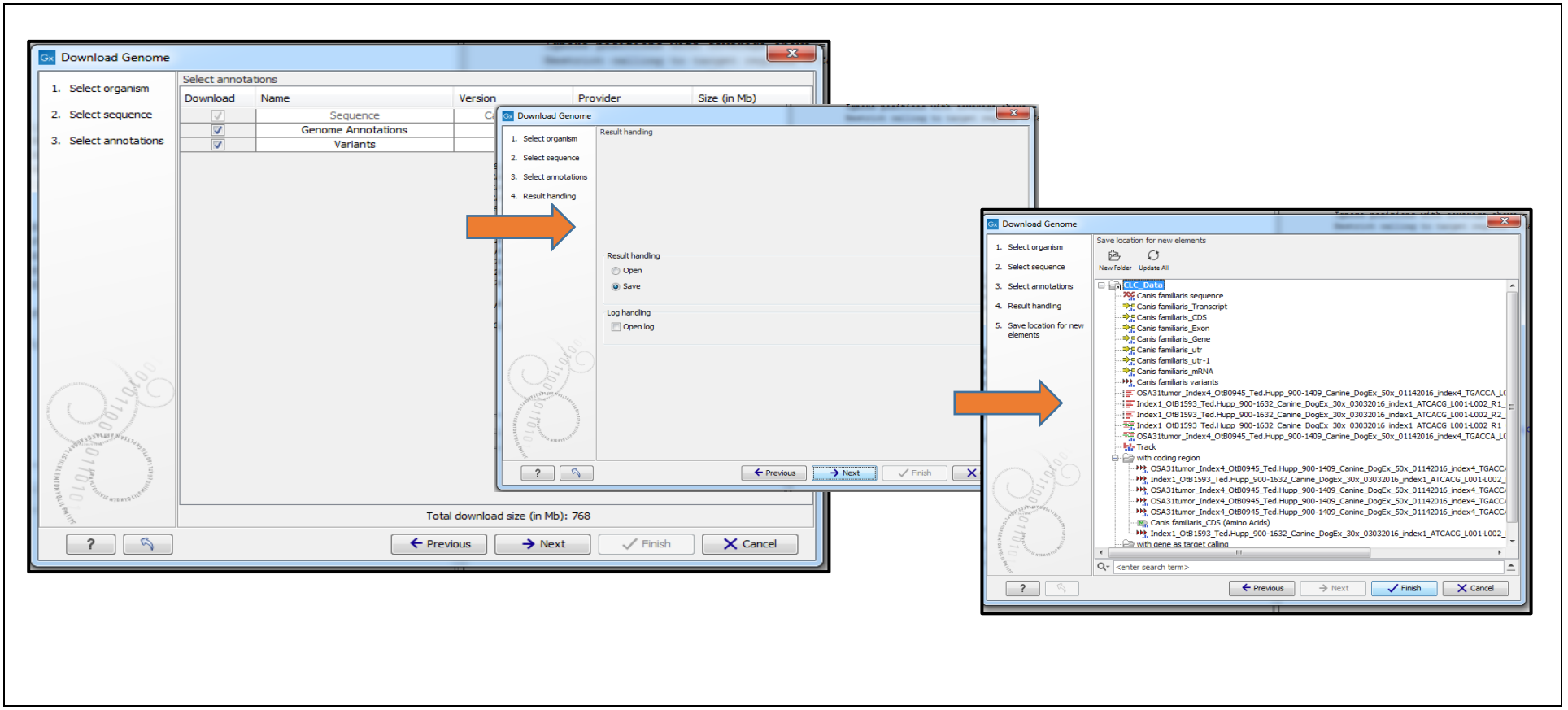

Figure 17 Downloading canine reference genome continued

Genome annotation and variant tick box was selected and the genome files saved under CLC workbench folder.

2.12.4.3 Map reads to contig and variant detections for OSA31 tumor DNA and Normal DNA

Canis familaris was selected as the contig for mapping the DNA seq file. Each of the Tumor DNA and Normal DNA is mapped to canis familaris contig. The workflow for mapping is described in Figure 18. Basic variants is detected in both the tumor and Normal DNA seq file using the procedure as per Figure and Figure. Variants were detected in the exome data using the following parameters: Minimum coverage (number of reads) = 5; Minimum frequency = 5%; Minimum number of variants = 2; Variants in normal germline DNA=0, and the coverage in the germline DNA should be at least 5 reads at the variant site.

2.12.4.4 Compare Normal to OSA31 seq data

The variant file from each of the normal and OSA31 tumor DNA seq file is compared to detect for somatic mutations. The steps involved are as described in Figure 21. In order to visualise the aminoacid changes in the tumor and the respective genes, the variant files are annotated and aminoacid changes added as per Figure 22 and Figure 23 respectively.

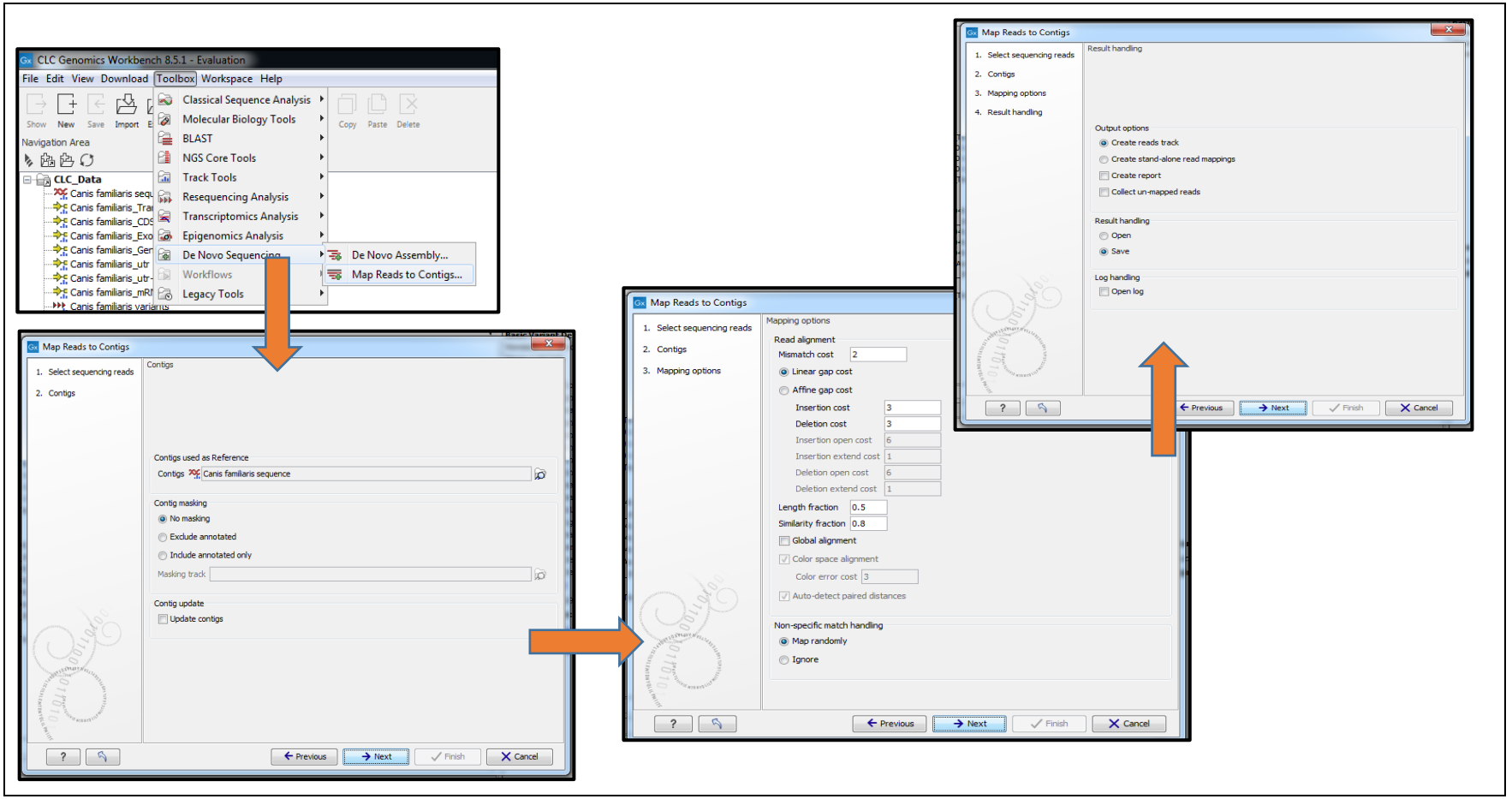

Figure 18 map reads to contigs/reference

Denovo sequencing option is selected from toolbox, then Map reads to contigs where canis familaris is selected as contig. Linear gap count and map randomly selected.

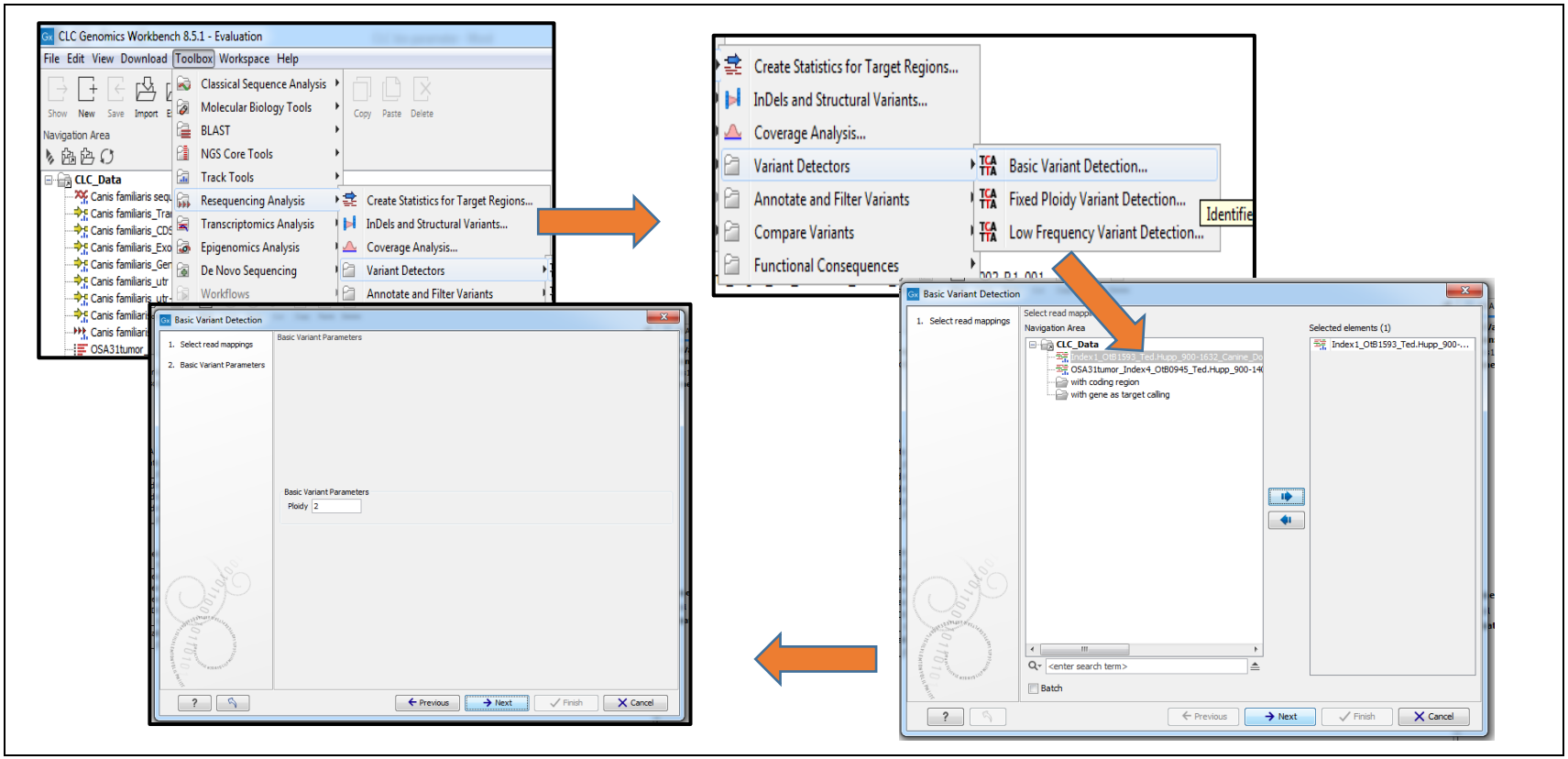

Figure 19basic variant detection

Resequencing analysis is selected form the toolbox menu. Variant detectors and then basic variant detection. After the file is selected ploidy 2 is selected in the basic variant parameters

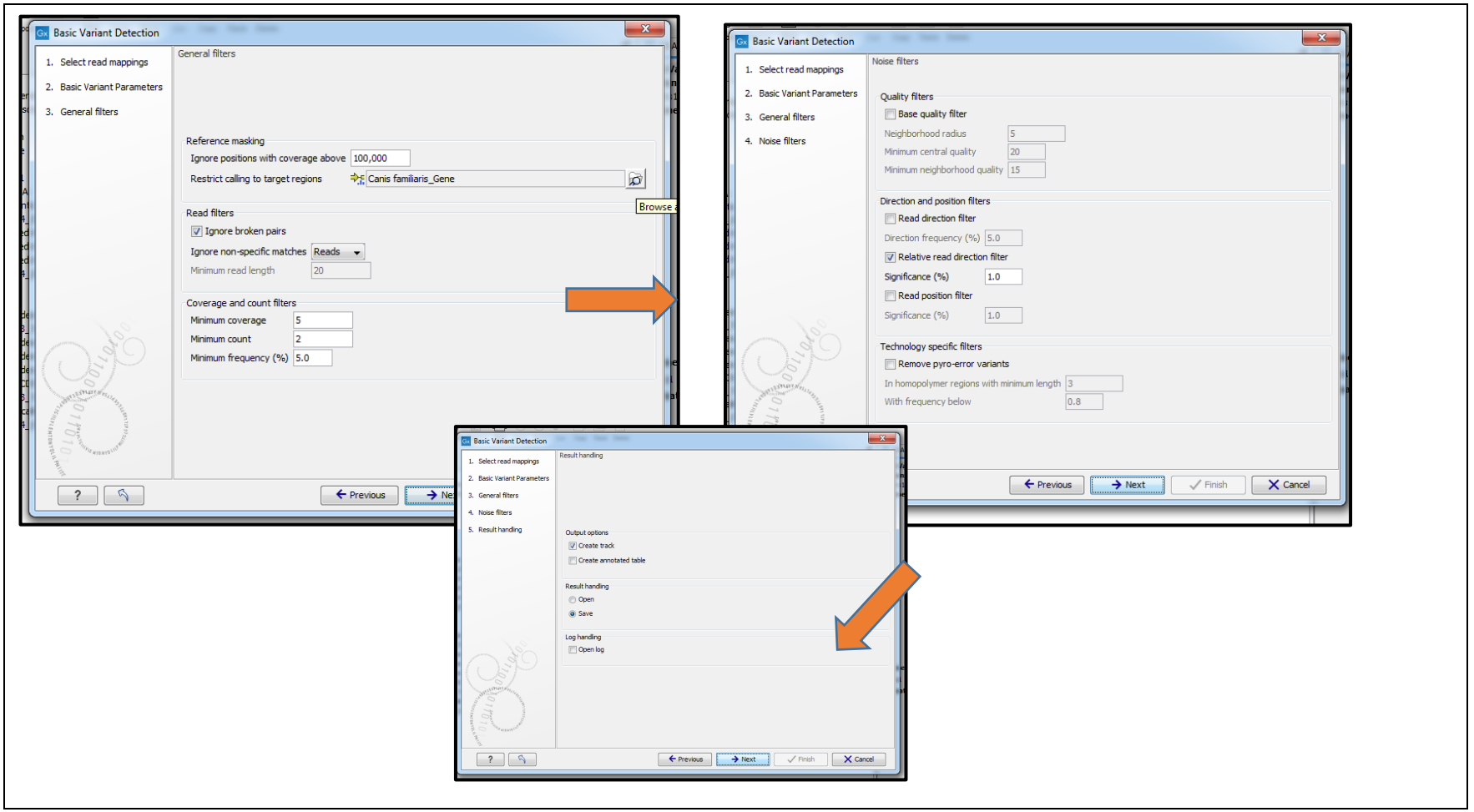

Figure 20variant detection continued

In general filters target region was selected as canis familaris gene and coverage above 100,000 was ignored. Broken pairs were also ignored. Coverage, count and frequency was selected as 5, 2and 5 respectively. For noise filter relative read direction was selected

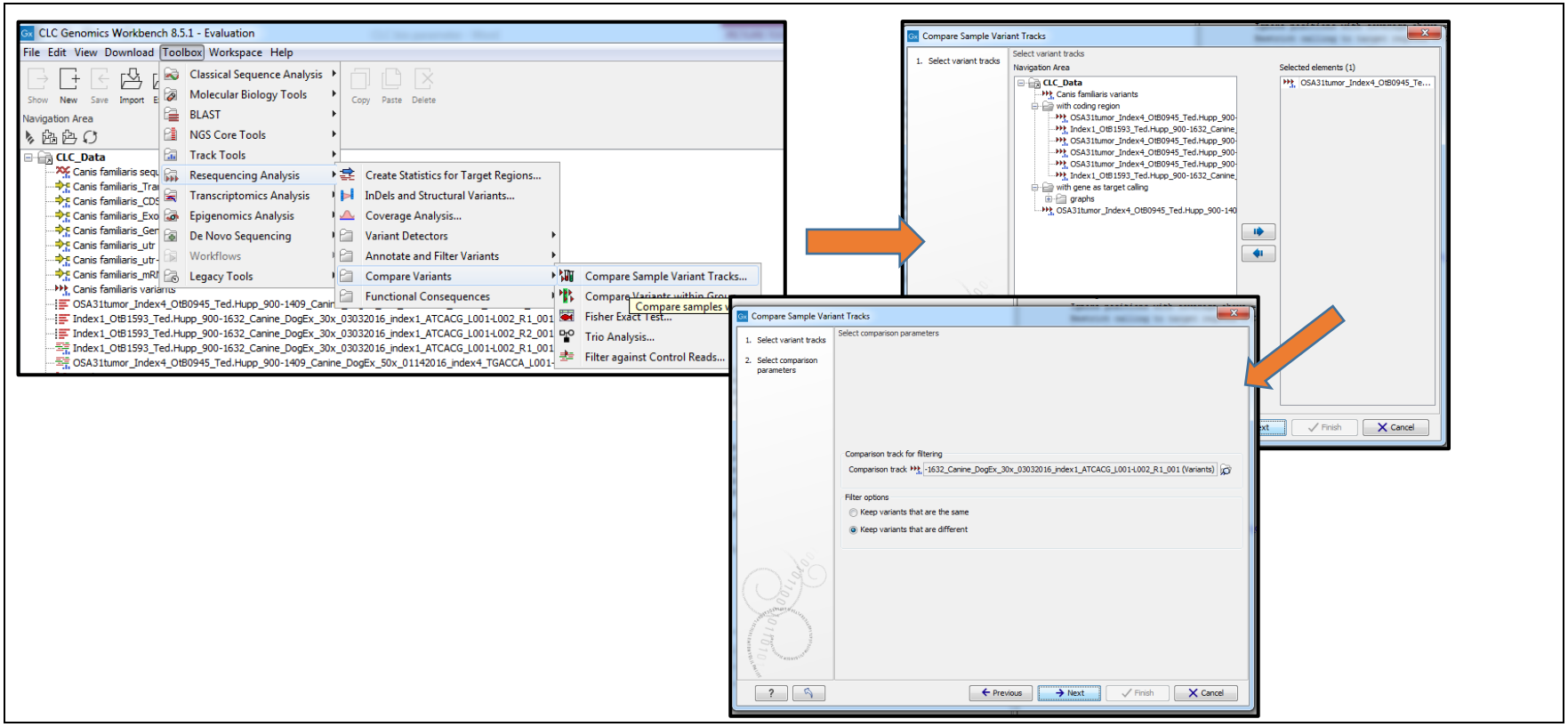

Figure 21compare Tumor OSA31 to normal tissue

Compare variants selected in Resequencing analysis then compare sample variant tracks was selected.OSA31 file selected and normal DNA from OSA31 dog was used as comparison track. Keep variants that are different was selected.

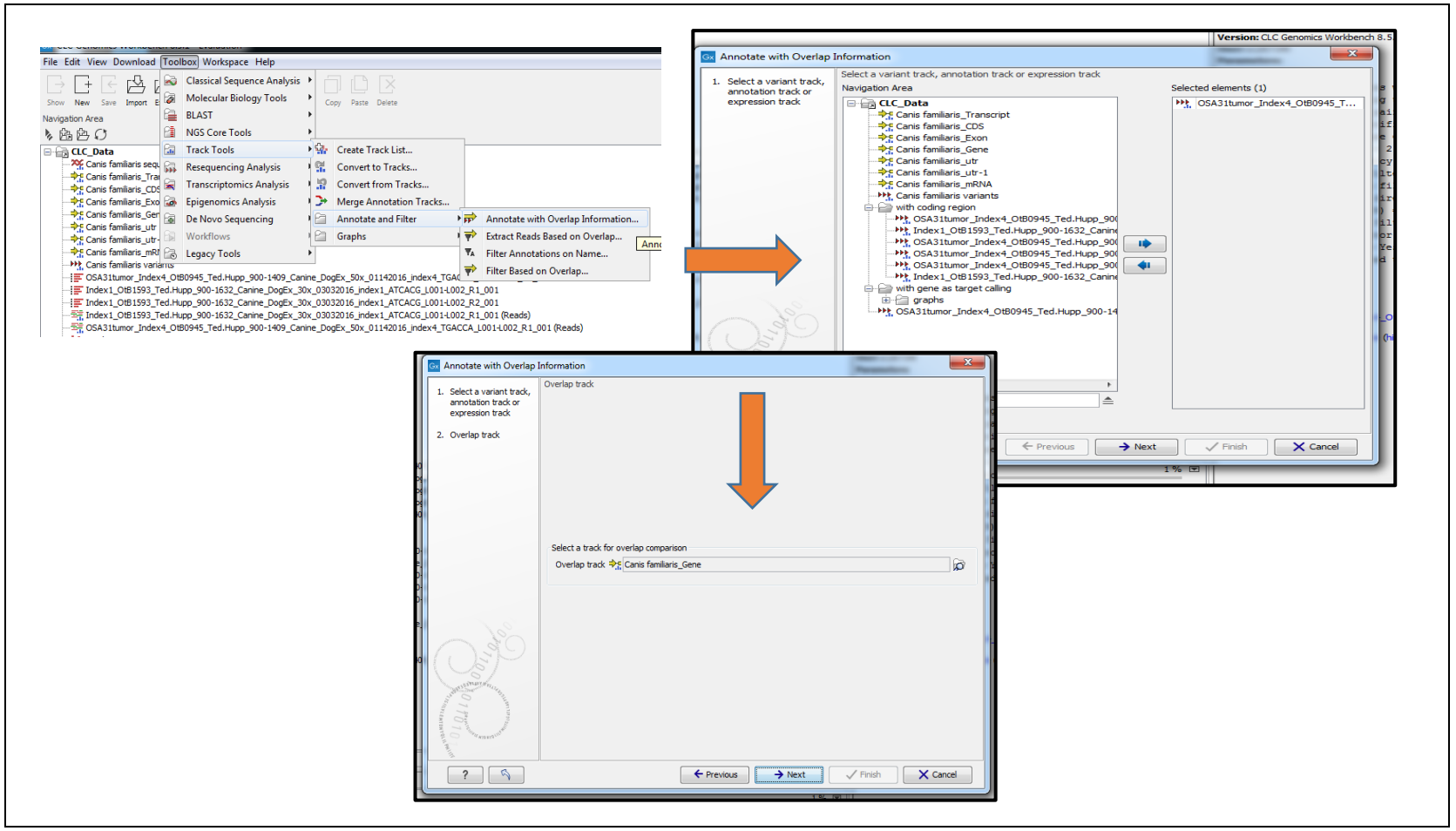

Figure 22annotate

Track tools was selected from tool and then annotate and filter-annotate with overlap information. Overlap track was canis familaris gene. The compared variant file was selected and file saved onto workbench

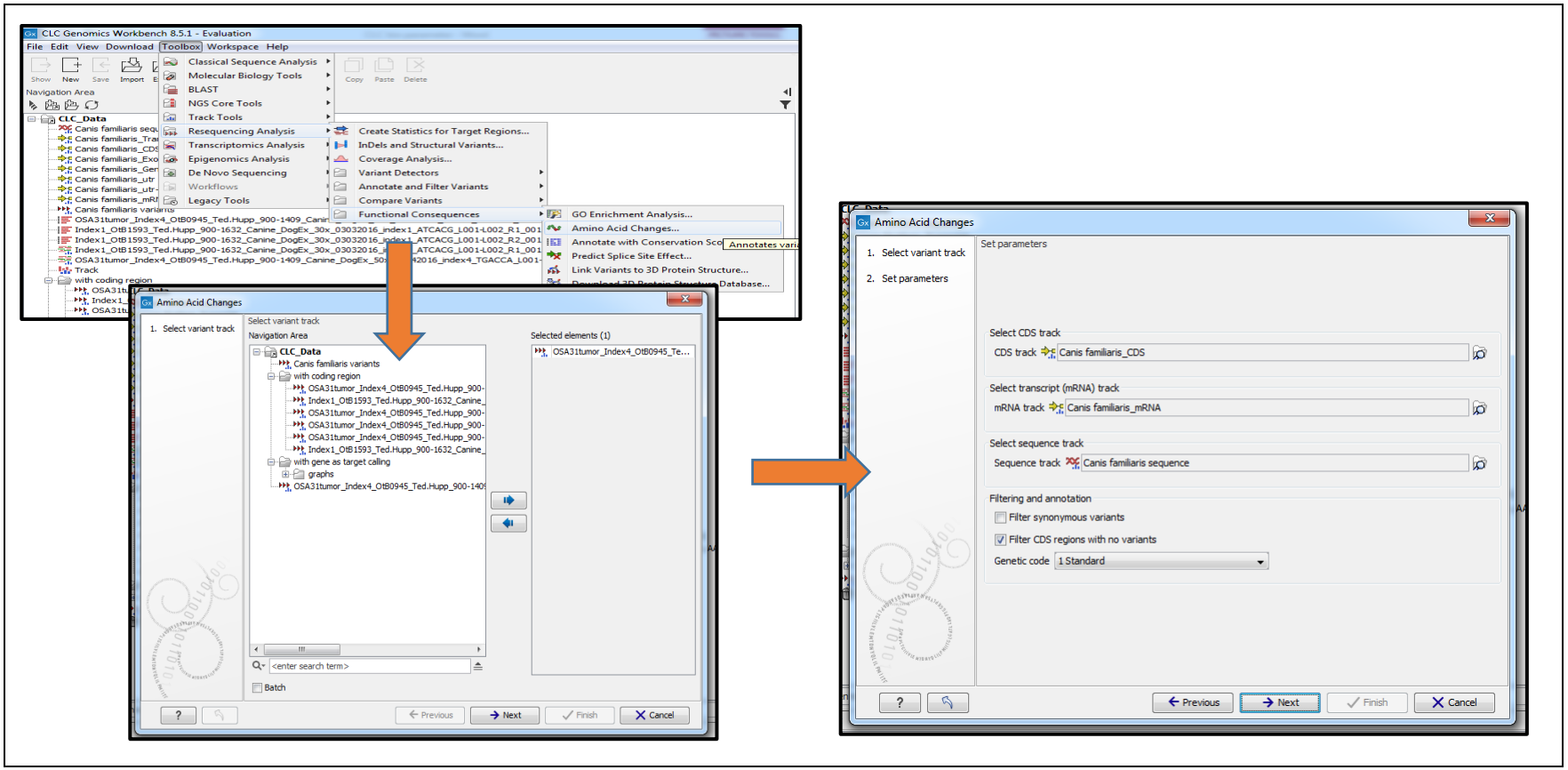

Figure 23aminoacid changes

Resequencing analysis was selected from toolbox, then functional consequences-aminoacid changes, the compared and annotated DNA file is selected with CDS region with no variant designated. CDS, mRNA and sequence files are selected from respective canis familaris files. The files are saved onto CLC workbench folder.

2.12.4.5 Detection of expressed somatic mutations in the RNAseq

Map reads to contigs for RNA seq was performed same as for the DNA seq. Variant detection was also performed on the RNA seq file as per Figure 19 and Figure 20.In order to detect the expressed somatic mutations in the RNA, the tumour RNAseq was compared to the tumour DNAseq of OSA31.

The minimum coverage and number of variants were set to 1 in the RNA reads, while in the DNA the parameters were not changed and left as 5 for minimum coverage and 2 for the minimum number of variants. The respective variants from RNA seq and DNA seq were compared to detect expressed summative mutations. Comparison track is the variant annotated DNA tumor seq and in the filter options “keep variants that are same” is selected Figure 24 and Figure 25. To visualise the specific chromosome and location, tracks were created as per Figure 26.

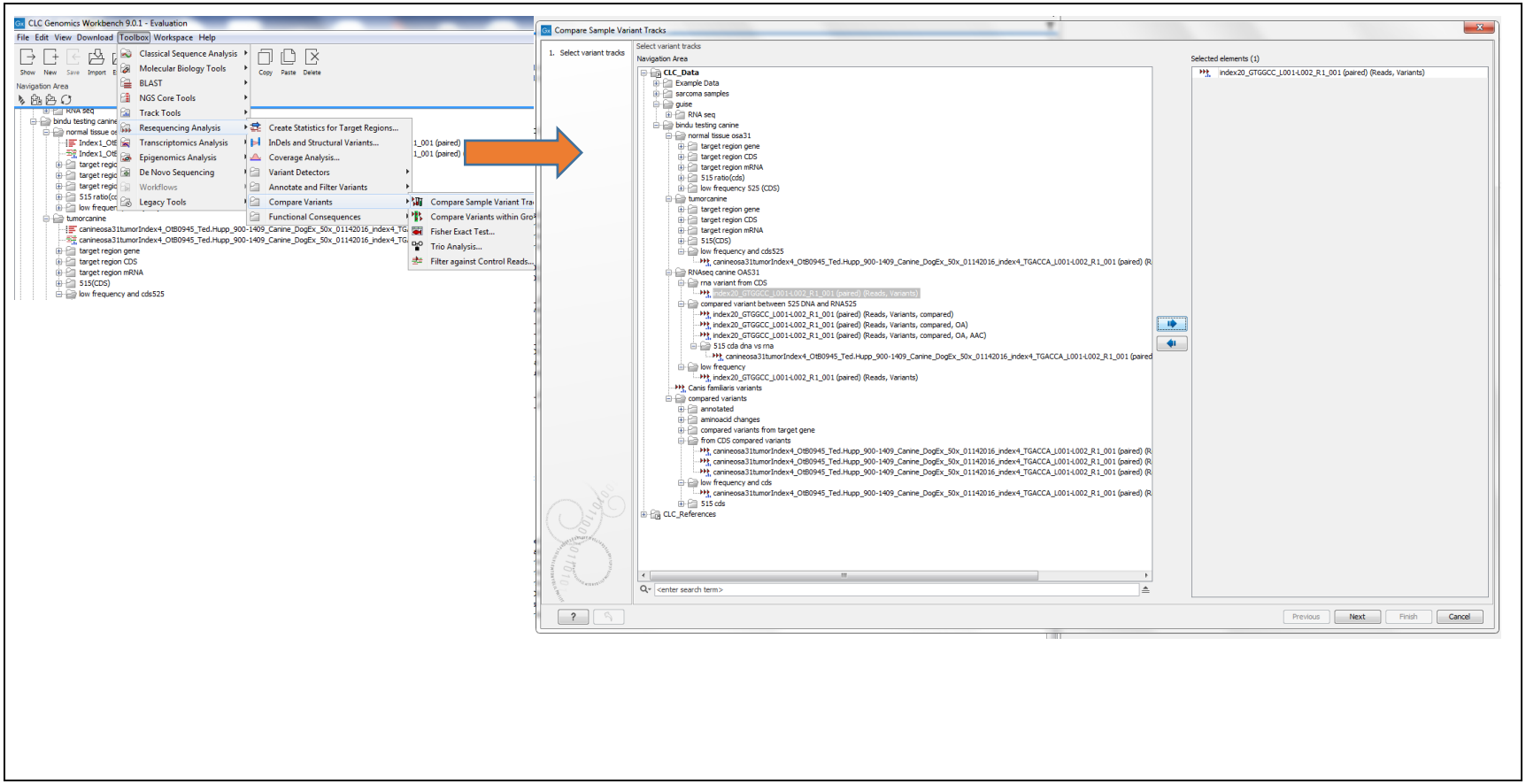

Figure 24 compare variant DNA and RNA seq from OSA31

Compare variants is selected from resequencing analysis options and compare sample variants is designated. Variant RNA seq file is selected.

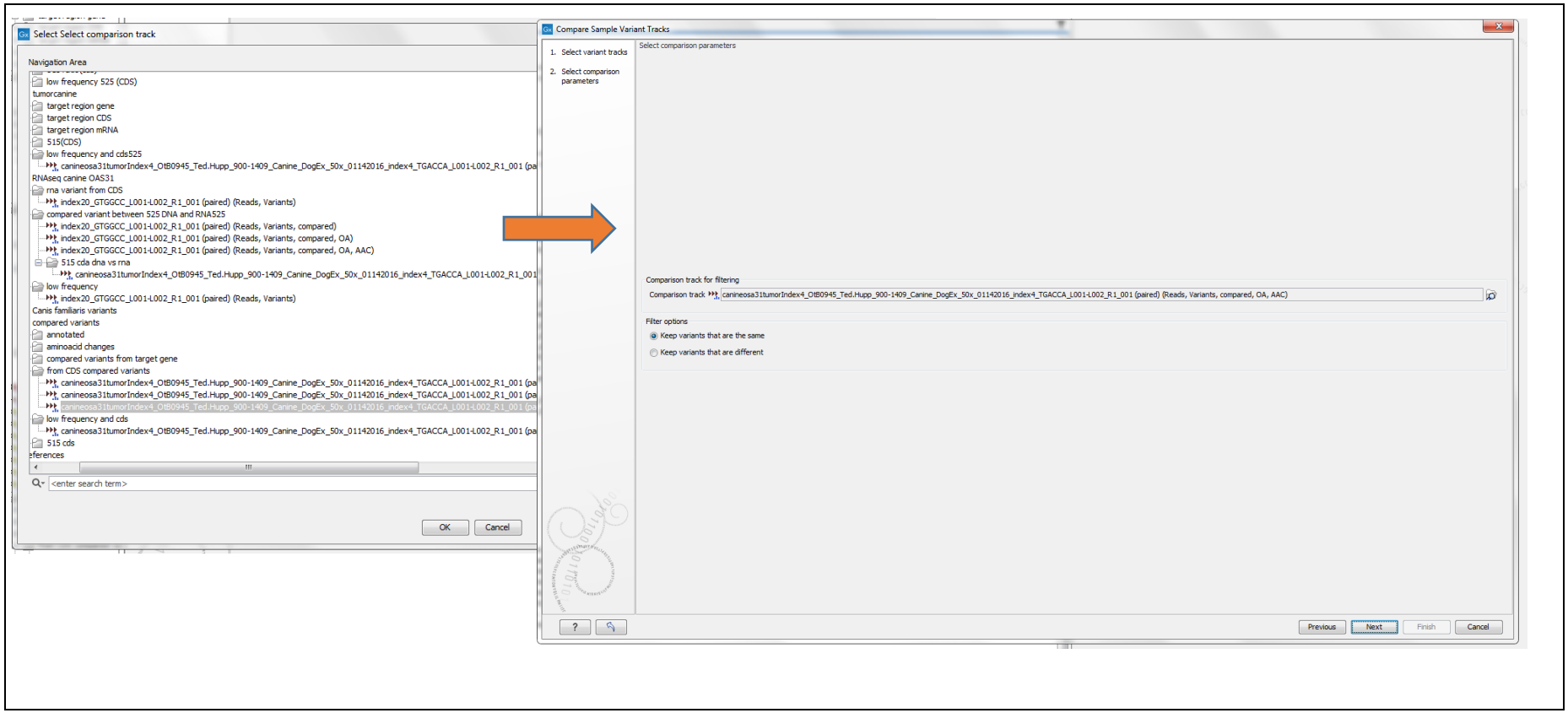

Figure 25compare variant DNA and RNA seq from OSA31 continued

Comparison track here is the variant annotated DNA tumor seq and in the filter options keep variants that are same is selected

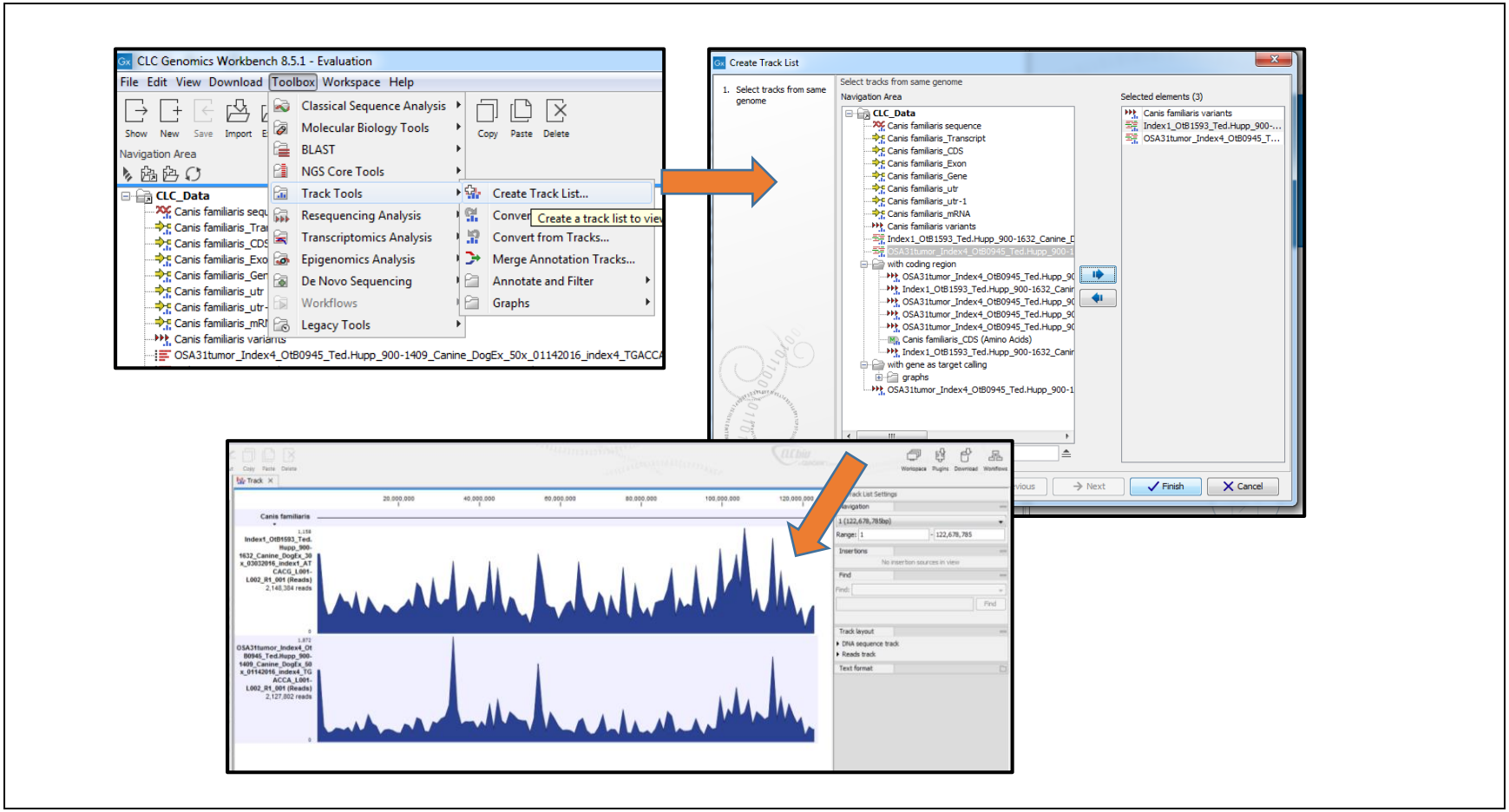

Figure 26 Creating tracks

Create track list is selected from track tools-toolbox options, then the canis familaris variants along with OSA31 variant and normal DNA variant is selected as input files. The required location and chromosome can be added onto the tool bar located at the right to observe the changes in respective track

3 Results: Comparative oncology: canine model

There are relatively few immune competent animal models that can accurately predict drug responses in human cancer patients. The emerging view is that canine cancers (companion animal cancers) provide a spontaneous, age-dependent, immune-competent cancer model can be a test-bed for whether veterinary medicine can produce more accurate models for testing human cancer drugs. In this chapter, I present a strategy to use and characterize one such cell model derived from canine osteosarcoma. This cancer type in dogs has been shown to be a robust physiologically relevant model for the human equivalent. The aim was to use genetic screening to identify genetically mutated pathways and use this as a strategy to develop cancer therapeutics.

3.1 The use of a Canine Osteosarcoma cancer cell as a model for personalizing anti-cancer therapeutics

The past decade has seen immense number of studies seeking to understand how genetic variability contributes to disease. These population-based studies, known as genome-wide association studies, aim to detect genetic variants—most commonly single nucleotide polymorphisms (SNPs)—that are associated with complex traits in populations (e.g., susceptibility to cancer). Recent studies of humans and dogs with osteosarcoma revealed multiple SNPs associated with risk for development of osteosarcoma, and these SNPs have been linked to biological pathways with known relevance to osteosarcomagenesis, but their statistical power has been limited by small sample sizes because of the rarity of this cancer type (Khanna, 2015).

Pet dogs develop osteosarcomas that share many features with the human disease, including tumour histology, gene expression, response to chemotherapy, and risk for pulmonary

metastasis. Accordingly, the dog with osteosarcoma provides a valuable model for the study of cancer-associated genes, drug development, and prognostic markers. Loss-of-function Rb mutations occur in up to 70% of osteosarcoma cases. In one study, 70% of patients possessed deletions or rearrangements in the CDKN2A gene (Khanna, 2015). Nevertheless, these genetic studies have failed to produce robust therapeutic options for improving survival of cancer patients.

What has emerged in recent years, however, is the concept that cancer treatment can be personalized by the identification of mutated proteins produced by the cancer genome. In addition to identification of "driver" pathways that might impact on drug use, a proportion of these mutated proteins can be processed to produce peptides that are presented by the MHC Class I/II system. It is by this process that emerging cancers produce mutated neoantigens, activation of T-cells through cross-presentation, and tumour rejection. However, tumours evolve to escape this process either by dampening the T-cells' themselves or supressing MHC Class I presentation in the tumour cell. Both concepts will be discussed below. This chapter will focus on how we can identify mutated genes using next generation sequencing technologies and how we can use this information for therapeutic approaches. This will help towards development of canine personalized models to identify and test drug leads or neoantigen vaccines, based on the patient-specific genetic signatures,

3.1.1 Cell models used for nucleic acid sequencing.

I analysed the whole exome DNA sequence of tumours (canine osteosarcoma OSA31), and the normal tissue from the same dog as a germline reference, using the CLC genomic workbench 8.1. Total RNA from the OSA31 cell line was also sequenced and compared to the tumour DNA sequence to look for expressed mutations in these tumours. Both methods have advantages and disadvantages, but the combined use of DNAseq and RNAseq is thought to increase the depth of mutated gene identification.

3.1.2 DNA seq analysis of the OSA31 genome.

Genomic DNA and RNA were extracted using commercially available kits. The samples were processed using an Illumina sequencing platform by Otogenetics Ltd. For the tumour samples the HiSeq2500 PE100-125 kit was used to sequence the whole exome from gDNA, paired-end 2x100-125 or PE100-125 (read length). The estimated average on-target DNA sequencing coverage is 100x for the tumour. The estimated average on-target coverage is 30x for the normal genome. The HiSeq2500 system uses sequencing by synthesis (SBS) technology. The SBS technology supports massively parallel sequencing using a proprietary fluorescently labelled reversible terminator method that enables detection of single bases as they are incorporated into growing DNA strands. A fluorescently labelled terminator is imaged as each dNTP is added and then cleaved to allow incorporation of the next base. Since all four reversible terminator-bound dNTPs are present during each sequencing cycle, natural competition minimizes incorporation bias. SBS technology supports both single read and paired-end libraries. (https://www.otogenetics.com/, 2017). The DNA and RNA sequences of OSA31 were imported as fastq files and analysed in the CLC genomics workbench 8.5.1.

3.1.3 Non-synonymous mutations and types of mutations by comparing tumour to normal tissue

To outline the non-synonymous mutations the variants were detected to identify mutated protein drivers. Data analysis indicated that the highest rate of mutations was observed in chromosome 1 followed by chromosomes 2, 3 and 8 respectively (Figure 27a). Figure 27 a also highlights the number of the somatic non-synonymous mutations detected in OSA31 and the mutation signature. The majority of the mutations were SNV (single nucleotide variations) followed by MNV (multiple nucleotide variations), deletions, insertions and replacements respectively (Figure 27b). Using cut-off thresholds of 5_2_5, meaning there must be 5 reads, 2 of which must be mutated, and with a 5% frequency of mutation, we detected 19,636 non-synonymous mutations. This is an unusually large number of mutations, relative to the reference germline and suggests the cell line might be very heterogeneously mutated and/or that passaging the cell line created additional variants. We changed the cut-off frequency to 40% more of the total reads being a mutation and this produced a more usual number of mutations-4,653 (data not shown).

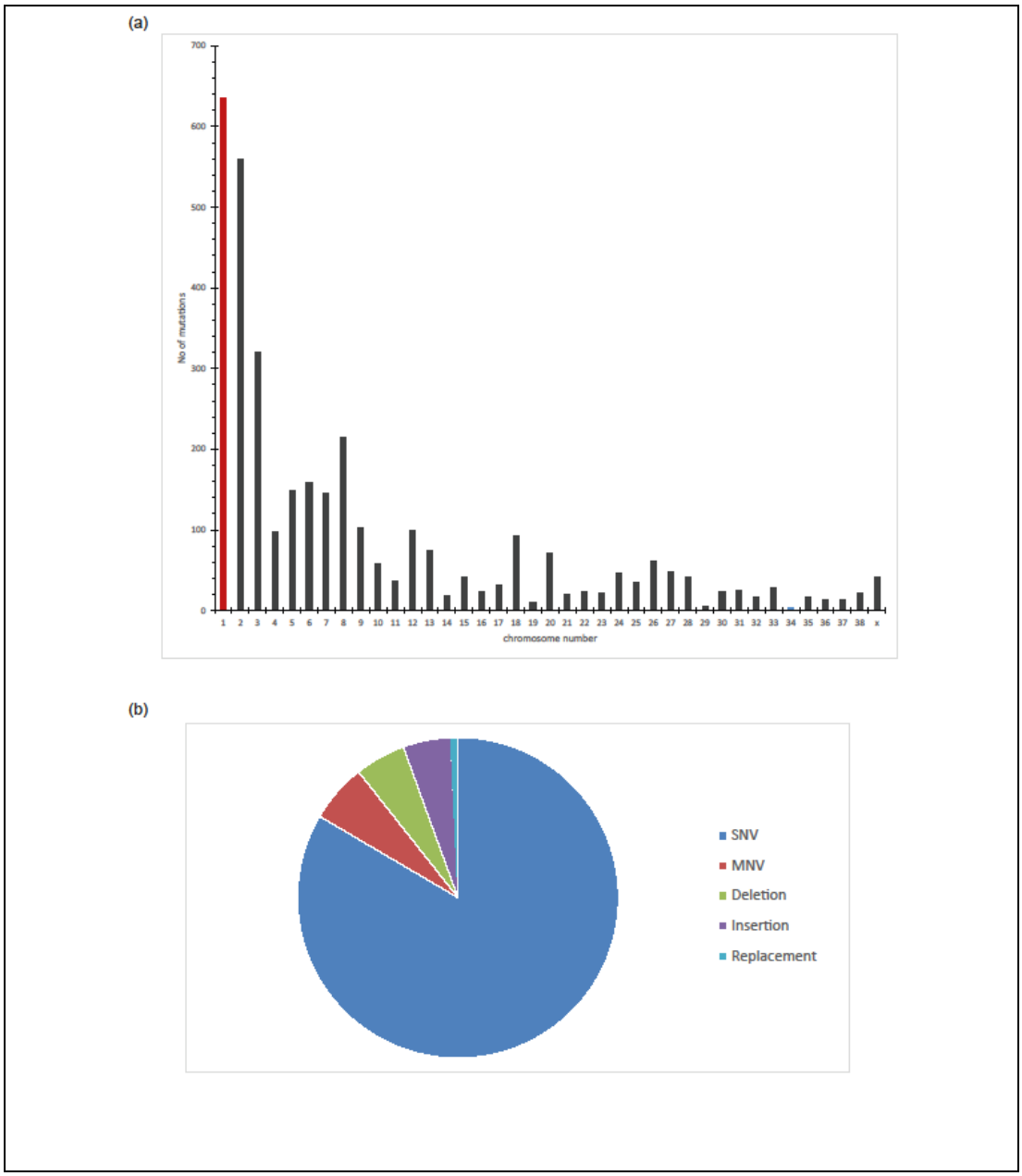

Figure 27Mutation signature

Mutation frequency per chromosome in OSA31 (a) and mutation signature from the DNA seq analysis. Data analysed by CLC workbench.

The gene mutations in OSA31 were wide-ranging. The CLC genomics workbench produced a table containing coverage, count, frequency, chromosome number, variant region, gene name and amino acid change for each of the variant. An example of the browser view is shown in (figure 28).PDGFRB (platelet-derived growth receptor) shows an insertion of TGA. One of the interesting germline mutations observed was in RBM10 (RNA binding motif protein 10), which acts like a tumour suppressor (Jordi Hernández, 2016). Gene sequencing revealed a deletion in CCNB1IP1. The study performed by Confalonieri and group indicated that the levels of Ub ligases such as CCNB1IP1 correlated significantly with relevant prognostic factors, and with clinical outcome (Confalonieri S, 2009). However, there are so many mutations identified for this one patient's tumour that orthogonal assays need to be performed in order to stratify the mutated genes and to focus on developing potential therapeutic strategies.

3.1.4 Identifying expressed mutations by comparing tumour RNA to tumour DNA

DNA sequencing can identify thousands of genomic variants in a single cancer genome, especially if the sample is heterogeneous. Differentiating a genomic variant that causes a selective growth or survival advantage to the tumour is a challenging task (Zhang S. J., 2014). The detected somatic variant frequently occurs in a single allele, and the impact of a heterozygous mutation will depend on whether the mutation-containing allele is transcribed to RNA. The mutation detected in the genomic DNA may not be transcribed into RNA if the wild-type allele is selectively transcribed. Furthermore, the mutation-containing transcript could activate RNA surveillance mechanisms and cause rapid degradation of the mutation-containing transcript. Nonsense-mediated decay (NMD) surveillance, for example, scans transcripts for the presence of premature termination codons before the last exon and, when found, initiates degradation of such transcripts (Castle, 2014.). Therefore, defining "active" somatic genome mutations using RNAseq is very important for judging whether or not the DNA mutation is expressed and/or advantageous to tumour development at the time of disease presentation.

In order to stratify the 19,636 non-synonymous mutations further, we focused on determining how many of these genes have detectable mutated mRNA produced at a relatively high

frequency. To test for the expressed genomic mutations, I compared the variants between the tumour DNA and the RNA. In order to detect all the expressed somatic mutations, I set the parameters of coverage and count of the mutation in the RNAseq to 1. A large number of mutations were detected. All the germline variants found in normal control were eliminated.

Some of the examples of expressed mutations in key genes are shown in

Figure 29. IRF-1, CDKN2A and HSP90ab1 all expressed with an SNV. These all form druggable target pathways that could be used in our strategy to match drug leads to mutated expressed pathways.

When the non-synonymous mutations in the DNA were compared to the expressed mutations in the RNA seq, I observed that all the expressed RNA mutations were listed within the subset of DNA mutations (Figure 30a). This might be expected since we kept the thresholds for DNA sequencing the same and confirms the software output is within the set parameters. The number of the expressed somatic mutations in OSA31 is very low compared to the number of somatic mutations detected in the tumour DNA. Shah and group have shown that only 36% of validated somatic SNVs were observed in the transcriptome sequence when RNAseq data compared with the genomes/exomes data in breast cancer. However, many variants had been missed because there were no reads in the RNA at the position of the variants. Alternatively, these mutant genes might not have been expressed at the time of surgery and resection. (Shah, 2012). Some of the detected expressed somatic non-synonymous mutations with a minimum of five coverage reads in the DNA reads are listed in Figure 30b-d.

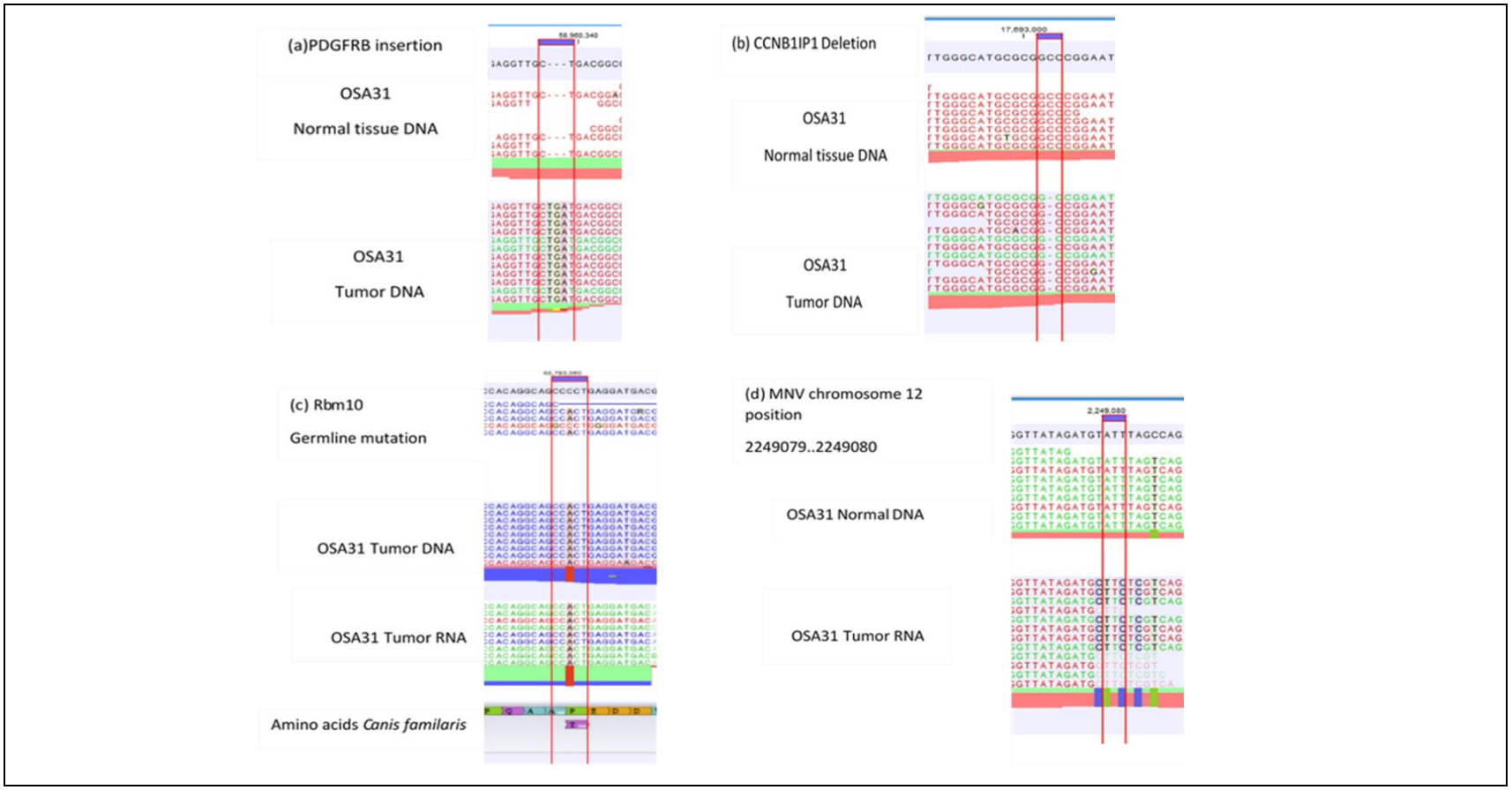

Figure 28 Brower example for mutation signatures observed in OSA31 genome

Examples of expressed somatic mutations in (a) insertion of TGA in PDGFRB (b) deletion of C in CCNB1IP1 (c) germline mutation in RBM10 (d) MNV on chromosome 12. The reference canine genome *Canis familaris* is shown at the top of the image. Colours are: the consensus and reference sequence is black per default; forward reads (single reads) is green per default; reverse reads (single reads) is red per default; paired reads is blue per default, in this case, because the original fastq files were not imported together as paired-end reads, then only individual strands are analysed and there is no fusion to produce paired-end reads (blue).

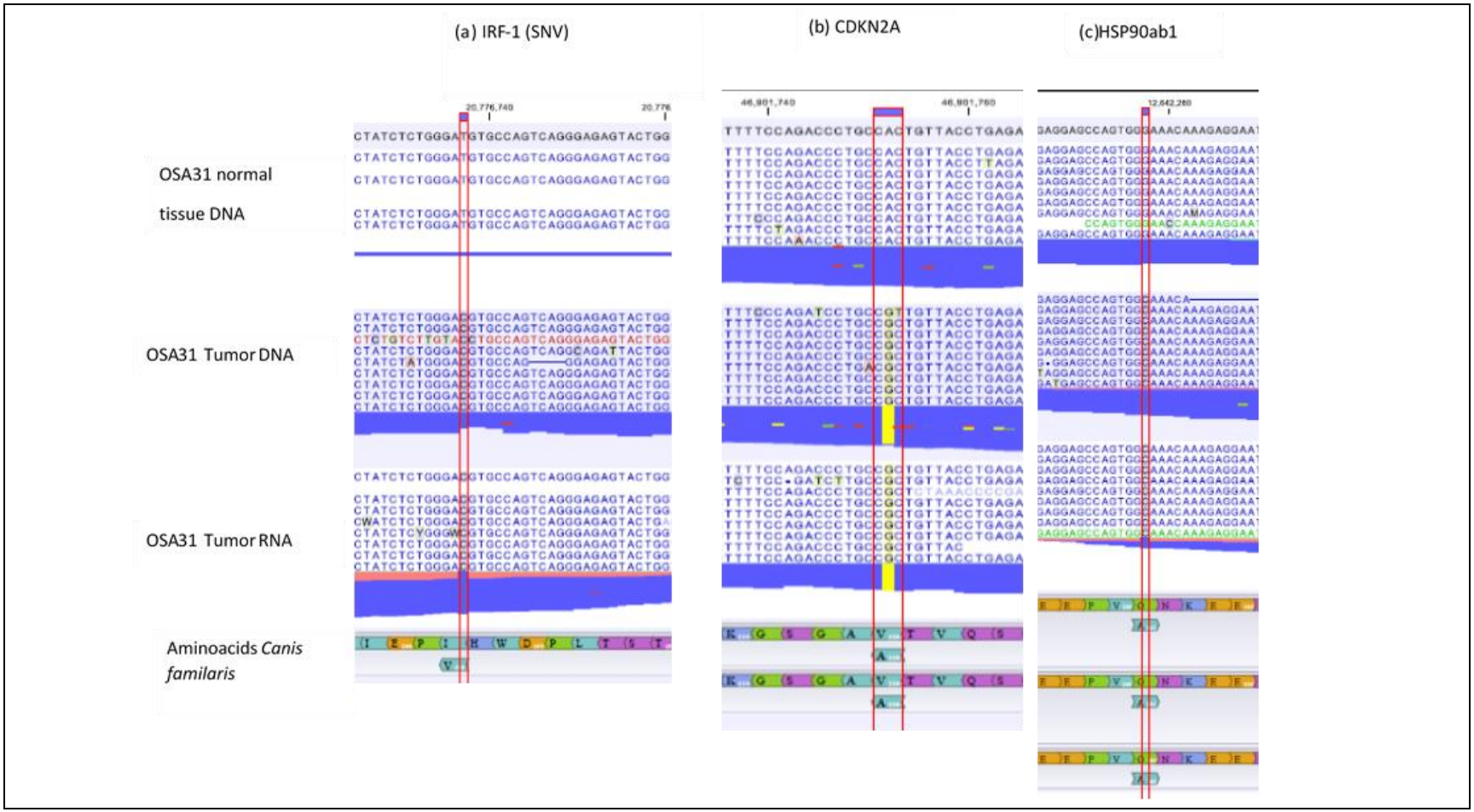

Figure 29key genes mutated in osteosarcoma

(a) IRF-1 SNV amino acid change of I to V (b) CNKN2A amino acid change of V to A (c) HSP90ab1 amino acid change of C to A

3.1.5 Defining the commonly mutated genes

To restrict the list of potential biomarkers I applied cut-offs to increase stringency. I selected only the mutated genes with highest coverage/count and frequency. Some of the mutated expressed genes are listed in Figure 30-c and their expression profile in figure 31. Some of the commonly-mutated genes observed in either human or canine which are also seen in my study are listed in Figure 30-b ((Khanna, 2015) (Angstadt, 2012). The SNP with the strongest association with osteosarcoma development in greyhounds was located 150 kilobases upstream of the CDKN2A/B genes, which are known to play a key role in osteosarcoma development and progression. The most common SNP in Rottweilers and Irish Wolfhounds alters an evolutionarily constrained enhancer element that was also active in human osteosarcoma cells. Loci among all breeds were enriched for genes with key functions in bone differentiation and development (Khanna, 2015). It is challenging to determine the driver gene among the mutated genes. A driver gene is responsible for the initiation or progression of a cancer, or a gene with a mutation that occurs more often than expected by chance. Many of the mutations detected in the cancer genome have no effect on the development of the cancer and are called referred to as passenger mutations. These are attributed to the inherent instability of the cancer genome (Hayes, 2015). Other than statistical significance, there are other factors to be considered when selecting driver mutations. These include whether the mutation is at a specific functional position of the gene, and whether the gene has been reported in any other cancer. The shortlisted expressed mutated genes, along with proteins that were highly expressed in OSA31 by mass spectrometry analysis (74 genes in total), are listed in the Figure 32.

(a)

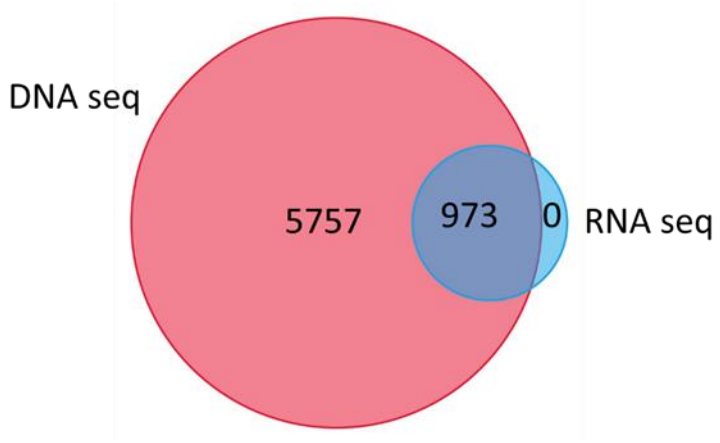

(b)

Chromosome	Region	Type	Reference	Allele	Zygosity	Frequency	Read count	Read coverage	Canis familiaris_Gene
4	5246927	SNV	G	A	Heterozygous	94.92	78	84	IRF2BP2
4	8960338^5896033	Insertion	-	TGA	Heterozygous	82.76	25	30	PDGFRB
5	29056403	SNV	T	C	Heterozygous	6.16	26	478	MMP27
5	28986104	SNV	T	C	Heterozygous	92.71	101	108	MMP1
6	9493824	SNV	A	T	Heterozygous	63.87	184	292	MCM7
6	19268170	SNV	G	A	Homozygous	100	24	24	IL4R
6	38869469	SNV	G	A	Homozygous	90	12	13	TSC2
11	20776737	SNV	T	C	Homozygous	98.78	120	122	IRF1
12	12642277	SNV	G	C	Homozygous	97.14	43	44	HSP90AB1
15	17676565	SNV	G	N	Heterozygous	5.26	0	50	CCNB1IP1
16	46901752	SNV	A	G	Homozygous	97.06	49	50	CDKN2AIP
18	48094324	SNV	G	C	Homozygous	100	19	19	FADD
26	16859142	SNV	G	A	Heterozygous	66.67	23	35	C12orf43
27	22277975	SNV	G	A	Heterozygous	48.39	23	50	KRAS
32	0164110..3016411	MNV	GG	AA	Heterozygous	34.41	88	274	EGF
37	1662590	SNV	C	T	Heterozygous	41.67	5	12	STAT1

(c)

Chromosome	Region	Type	Reference	Allele	Zygosity	Frequency	Read count	Read coverage	Canis familiaris_Gene
6	7532376^7532377	Insertion	-	G	Homozygous	100	98	98	YWHAG
7	79047592	SNV	T	G	Homozygous	100	133	133	ACAA2
9	1481960	SNV	C	T	Homozygous	100	65	65	RNF213
10	16837324	SNV	C	A	Homozygous	100	43	43	SBF1
20	54332848	SNV	G	A	Homozygous	100	48	48	LONP1
21	26063004	SNV	A	G	Homozygous	100	67	67	NUMA1
22	58933648	SNV	C	T	Homozygous	100	48	48	COL4A2, CARS2
28	1579447..1579448	MNV	CA	TG	Homozygous	100	115	115	OGDHL
29	10953422	SNV	T	G	Homozygous	100	57	57	RAB2A
X	91523733	SNV	T	G	Homozygous	99.31	243	244	SLC25A5

(d)

Name
Ras GTPase-activating-like protein **IQGAP1**
Complement **C3**
Neuroblast differentiation-associated protein **AHNAK**
Probable ATP-dependent RNA helicase **DDX17**
E3 ubiquitin-protein ligase **HUWE1**

Figure 30 highest genes found both in DNA and RNA tumour

(a)Venn diagram indicating the number of mutations observed in OSA31 DNA and RNA, data analysed by funrich software (b) common upregulated genes found in both human and canine which was detected in OSA31. (c)A list of genes detected with somatic mutations in both DNA and RNA with highest mutation frequency (coverage). (d) Key high expressed genes.

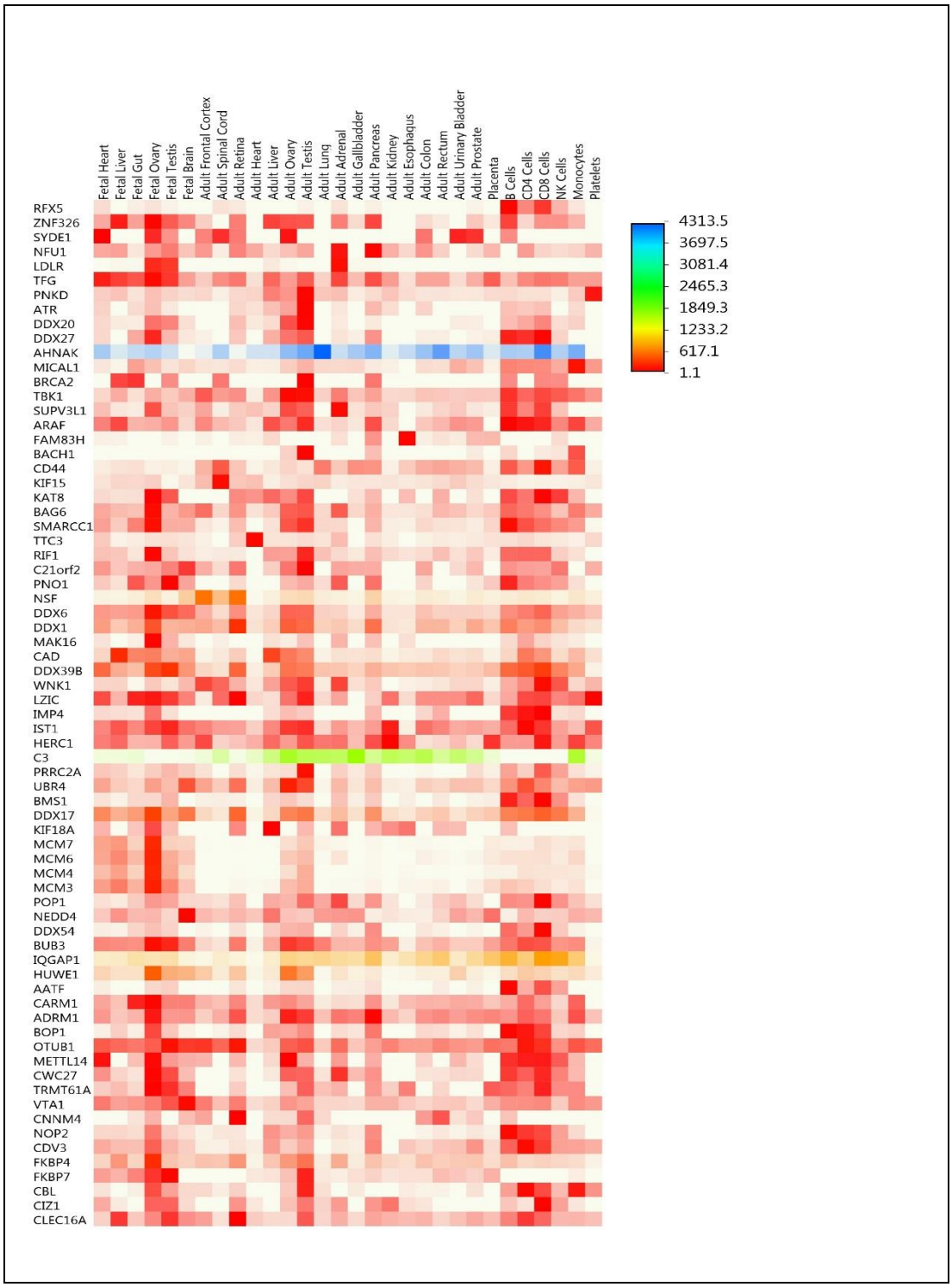

Figure 31 Prognostic biomarkers

Heat map of hit list of genes found both in DNA and in RNA of OSA31 and their location of expression.Heat map demonstrates the expression pattern of genes.upregulated genes are colored in the order blue,green,yellow,orange and red(min color).Each gene is normalised and the color range is 60% used.The Heat map is genereated by funrich software based on the input datasets.

No.	Gene symbol	Gene description
1	AHNAK	AHNAK nucleoprotein
2	ARAF	A-Raf proto-oncogene, serine/threonine kinase
3	ATR	ATR serine/threonine kinase
4	BACH1	BTB and CNC homology 1, basic leucine zipper transcription factor 1
5	BMS1	BMS1 ribosome biogenesis factor
6	BRCA2	breast cancer 2, early onset
7	CBL	Cbl proto-oncogene, E3 ubiquitin protein ligase
8	CDV3	CDV3 homolog (mouse)
9	CIZ1	CDKN1A interacting zinc finger protein 1
10	CLEC16A	C-type lectin domain family 16, member A
11	CNNM4	cyclin M4
12	CWC27	CWC27 spliceosome-associated protein homolog (S. cerevisiae)
13	DDX20	DEAD (Asp-Glu-Ala-Asp) box polypeptide 20
14	DDX54	DEAD (Asp-Glu-Ala-Asp) box polypeptide 54
15	RIF1	replication timing regulatory factor 1
16	C21orf2	chromosome 21 open reading frame 2
17	FAM83H	family with sequence similarity 83, member H
18	FKBP7	FK506 binding protein 7
19	GCN1	GCN1 eIF2 alpha kinase activator homolog
20	HERC1	HECT and RLD domain containing E3 ubiquitin protein ligase family member 1
21	KAT8	K(lysine) acetyltransferase 8
22	KIF15	kinesin family member 15
23	KIF18A	kinesin family member 18A
24	LDLR	low density lipoprotein receptor
25	MCM3	minichromosome maintenance complex component 3
26	MCM7	minichromosome maintenance complex component 7
27	METTL14	methyltransferase like 14
28	MICAL1	microtubule associated monooxygenase, calponin and LIM domain containing 1
29	NFU1	NFU1 iron-sulfur cluster scaffold homolog (S. cerevisiae)
30	NOP2	NOP2 nucleolar protein
31	PNKD	paroxysmal nonkinesigenic dyskinesia
32	POP1	processing of precursor 1, ribonuclease P/MRP subunit (S. cerevisiae)
33	PRRC2A	proline-rich coiled-coil 2A
34	RFX5	regulatory factor X, 5 (influences HLA class II expression)
35	HGH1	HGH1 homolog (S. cerevisiae)
36	BOP1	block of proliferation 1

No.	Gene symbol	Gene description
37	SUPV3L1	suppressor of var1, 3-like 1 (S. cerevisiae)
38	SYDE1	synapse defective 1, Rho GTPase, homolog 1 (C. elegans)
39	TRMT61A	tRNA methyltransferase 61 homolog A (S. cerevisiae)
40	TTC3	tetratricopeptide repeat domain 3
41	MAK16	MAK16 homolog (S. cerevisiae)
42	WNK1	WNK lysine deficient protein kinase 1
43	IMP4	IMP4, U3 small nucleolar ribonucleoprotein
44	C3	complement component 3
45	ZNF326	zinc finger protein 326
46	DDX39B	DEAD (Asp-Glu-Ala-Asp) box polypeptide 39B
47	OTUB1	OTU deubiquitinase, ubiquitin aldehyde binding 1
48	BAG6	BCL2-associated athanogene 6
49	DDX1	DEAD (Asp-Glu-Ala-Asp) box helicase 1
50	UBR4	ubiquitin protein ligase E3 component n-recognin 4
51	TBK1	TANK-binding kinase 1
52	TIGAR	TP53-inducible glycolysis and apoptosis regulator
53	MCM4	minichromosome maintenance complex component 4
54	NEDD4	precursor cell expressed, developmentally down-regulated 4, E3 ubiquitin protei
55	CD44	CD44 molecule (Indian blood group)
56	SMARCC1	related, matrix associated, actin dependent regulator of chromatin, subfamily c, r
57	AATF	apoptosis antagonizing transcription factor
58	CARM1	coactivator-associated arginine methyltransferase 1
59	HUWE1	HECT, UBA and WWE domain containing 1, E3 ubiquitin protein ligase
60	NSF	N-ethylmaleimide-sensitive factor
61	TFG	TRK-fused gene
62	DDX6	DEAD (Asp-Glu-Ala-Asp) box helicase 6
63	IST1	increased sodium tolerance 1 homolog (yeast)
64	FKBP4	FK506 binding protein 4, 59kDa
65	VTA1	vesicle (multivesicular body) trafficking 1
66	DDX27	DEAD (Asp-Glu-Ala-Asp) box polypeptide 27
67	ADRM1	adhesion regulating molecule 1
68	IQGAP1	IQ motif containing GTPase activating protein 1
69	DDX17	DEAD (Asp-Glu-Ala-Asp) box helicase 17
70	BUB3	BUB3 mitotic checkpoint protein
71	CAD	arbamoyl-phosphate synthetase 2, aspartate transcarbamylase, and dihydroorota
72	PNO1	partner of NOB1 homolog (S. cerevisiae)
73	MCM6	minichromosome maintenance complex component 6
74	LZIC	leucine zipper and CTNNBIP1 domain containing

Figure 32 Potential canine vaccine list

A list of genes detected with somatic mutations in DNA, RNA seq and seen in proteomics with ≥ 30% mutation frequency (count / coverage)

3.2 Characterization of a canine osteosarcoma cell as a model for developing next generation proteogenomics

We approached the use of genetics to identify drugable pathways as a personalized approach by focussing on the p53 and HSP90/IRF1 pathways. In the former case, the p53 gene was not mutated and therefore this sarcoma could, in principle, be treated with the p53-activating ligand Nutlin-3. In the case of IRf1 and hSP90, we have previously published that IRF1 is under exquisite control by HSP90, and that HSP90 targeted drugs might be used to impact on this mutated pathway (Narayan, 2009). Below, I set out to characterise whether the OSA31 cell line does or does not respond to the p53-activating drug or the HSP90-inhibiting drug.

3.2.1 Characterisation of canine osteosarcoma cell lines for p53 activation in response to Nutlin-3

Perturbation of the MDM2 and p53 protein network plays a central role in the development of many human cancers. However, improvement of MDM2 targeted therapeutics that activate p53 function is hampered by the absence of robust spontaneous immune-competent preclinical cancer models. Dogs spontaneously develop tumours and are considered a physiological model for comparative oncology initiatives. Various canine tumours involve increased expression of MDM2 in association with decreased expression of WT p53. Thus, dogs may be important models for studying advanced malignancies and the study of p53 activation therapeutics (Rivera-Calderón LG1, 2016). Osteosarcoma is considered one of the canine malignancies of most interest that form such a model as it shows striking similarities in tumour biology and behaviour to its human counterpart (Romanucci, 2012). I wanted to determine if studying canine osteosarcoma would pave the way to accelerate human cancer drug/vaccine targets including MDM2 targeted therapeutics. I studied a panel of OSA cell lines along with normal and primary cell line of the same dog. A panel of cell lines was initially tested, by Prof Geoffrey Wood (University of Guelph), for MDM2, P53 and HSP70 (Figure 33)

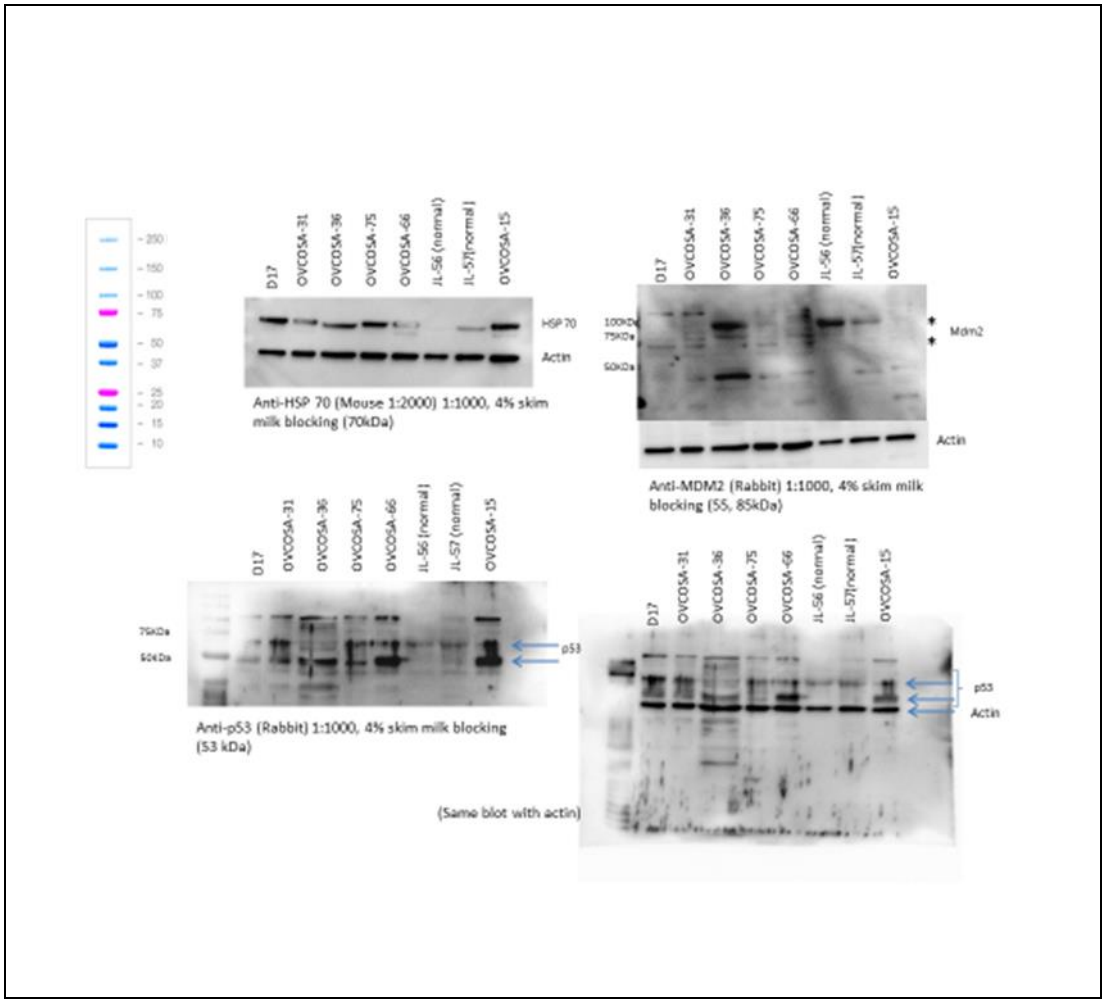

Figure 33 Panel of canine cancer osteosarcoma cell lines tested for levels of hsp70, hsp90, p53, and MDM2 proteins.

The panel of osteosarcoma canine cell lines including OSA31, OSA15, OSA75 ,OSA36 and OSA66 were tested along with controls JL56 (normal), JL57(normal), D17 (commercial canine osteosarcoma) for the expression of the indicated proteins. The loading control is also highlighted.

I selected OSA31 cell line for further study as it appeared to give the best MDM2 induction with Nutlin, suggesting that the cell line was a WT p53 cell line. D17 was selected as a control cell line. Primary cell lines (OSA75 and OSA78) were also tested alongside. Immunoblotting with the p53-specific monoclonal antibodies D01 and 240 gave an immunoreactive protein band of the correct size for p53 (Figure 34a), further highlighting the utility of these cells for examining MDM2-targeted drugs that activate p53.

3.2.2 Characterisation of canine osteosarcoma cell lines for HSP70 responsiveness to HSP90 inhibitors.

I characterised both primary and metatastic cell lines in response to various HSP90 inhibitors. The canine D17 line was used as a control in the assays. JL 75 (OSA75) and JL 78 (OSA78) are primary cell lines and OSA31 is the metatastic cell line. The primary cell lines were treated with the HSP90 inhibitor Ganetespib for 16 hours and cell lysates tested for expression of HSP70 protein. HSP70 induction is considered as a biomarker for HSP90 inhibition. (Dakappagari N, 2009). Cheryl and group have demonstrated that Ganetespib can kill canine tumour cell lines in vitro, and inhibit tumour growth in murine xenografts (Cheryl A London, 2011).

My results indicated that even the lowest dose of 10nM Ganetespib induced HSP70 protein, compared to DMSO or no treatment controls, providing a biomarker of inhibition of HSP90 protein (Figure 34b). Both cell lines responded very similarly to treatment of Ganetespib. GAPDH was used as a loading control and was similar across all the samples. The IC50 of DOX for the OSA75 cell line was 4.1 µM in a cell viability assay (Figure 34c). The cell viability assay was performed by Professor Geoffrey Wood (University of Guelph).

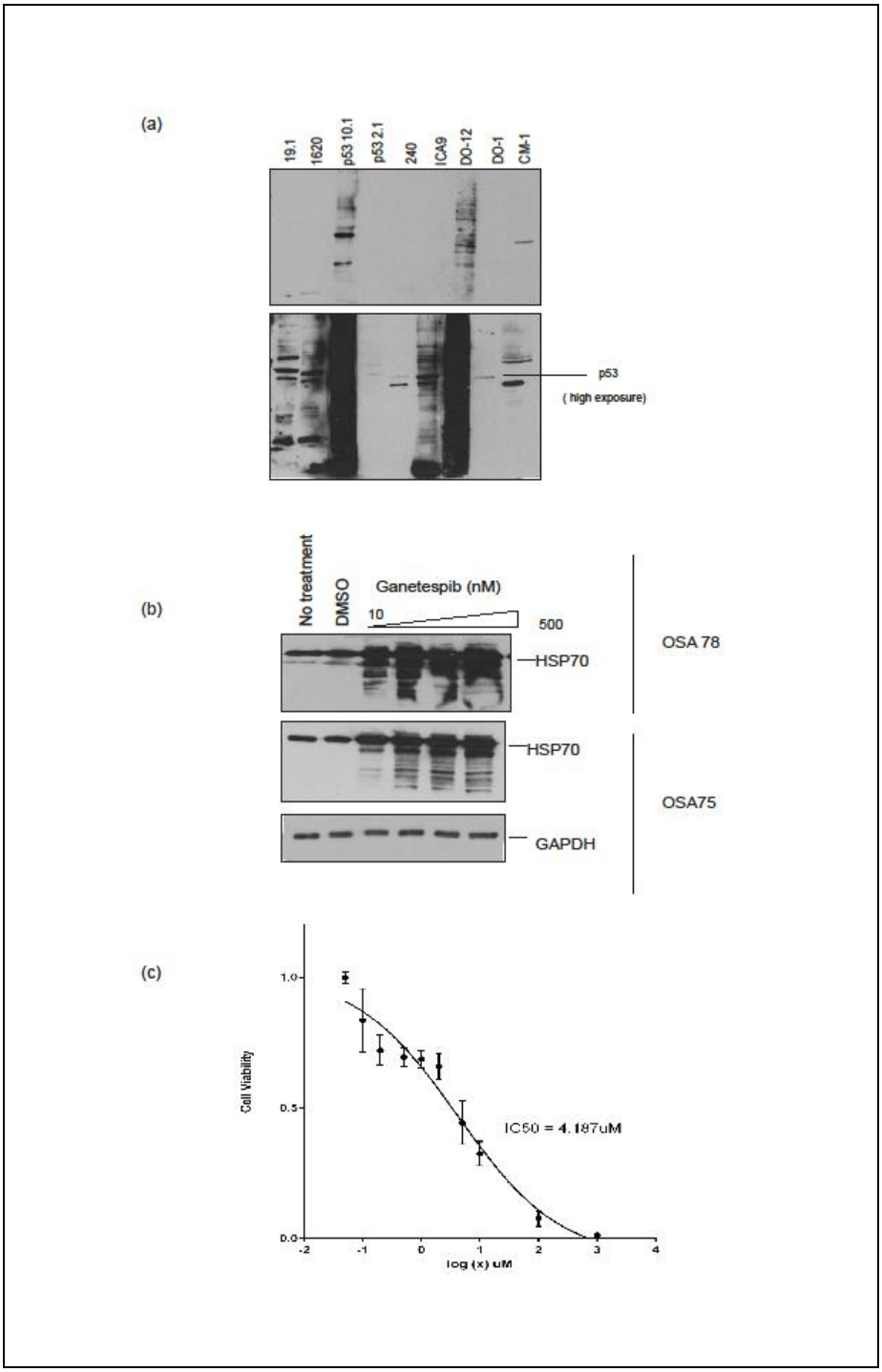

Figure 34 Characterisation of p53 and hsp70

(a) P53 Antibody optimisation for OSA 31 cell lysates using various p53 monoclonal and polyclonal antibodies targeting different epitopes of human p53. (b) Primary cell lines OSA 78 and OSA 75 treated with either Ganetespib (0,10,50,100,500nM) or DMSO for 16 h. Total cell lysates analysed for HSP70 and GAPDH by Western blotting. The data are representative of at least three independent experiments. (c) Cell viability assay performed by prof Geoffrey A wood (university of Guelph)for OSA 75 cells with DOX, IC50 4.1 µM.

3.2.3 Characterisation of canine osteosarcoma cell lines for IRF1 response to HSP90 inhibition.

Having established a baseline of MDM2 or HSP90 inhibition of pathway biomarkers, I next evaluated the impact of both treatments in parallel. Both the metastatic cell line OSA31and control D17 lines were treated with a titration of Nutlin for 6 hours. The results indicated that even the lowest dose of nutlin (5μM), induced MDM2 in both the cell lines as compared to the DMSO controls (Figure 35a). The two cell lines were also treated with a titration of Ganetespib for 16 hours. The results indicated that all doses of Ganetespib induced Hsp70 for both the cell lines (Figure 35b). I wanted to evaluate the effect of Ganetespib on IRF-1 protein. For this, I probed the cell lysates for IRF-1 and the results indicated that there was loss of IRF-1 with the higher doses of Ganetespib (100 and 500nM) for both the cell lines, as compared to the DMSO control. For human cell lines Ganetespib could downregulate IRF-1 even at 50nM, indicating that sensitivity of the drug might vary with cell lines.

Based on this result I also wanted to determine if Ganetespib could lower IFNγ-induced IRF-1 in canine cell lines. OSA31 cells were treated with Ganetespib and IFNγ, either alone or in combination, for 16 hours. The results indicated that IFNγ induced IRF-1 expression levels as compared to controls and Ganetespib could downregulate this IFNγ-induced IRF-1 expression (Figure 35c). The IFNγ induction was not as high as that observed in human cancer cell lines such as A375. Ganetespib alone also downregulated the IRF-1 as compared to DMSO control. These data also demonstrate that IRF1 suppression forms another biomarker of HSP90 inhibition. Doxorubicin (DOX) is a commonly used chemotherapy in human cancers. Recently, several clinical trials with doxorubicin were performed on dogs, which helped to design human phase 1 clinical studies (Jennifer A. MacDiarmid, 2016). OSA31 cell lines were treated with DOX in a cell viability assay and the IC50 was recorded to be 0.62 uM (Figure 35d).

I then wanted to explore if the canine osteosarcoma cells displayed any interaction with HSP70/MDM2. To analyse this, OSA31 cell lines were treated with either DMSO or Ganetespib (100nM) for six hours, followed by a proximal ligation assay (PLA) according to manufactures instruction. The results indicated that there was strong interaction when the cells are treated with Ganetespib as compared to the DMSO control (Figure 36).

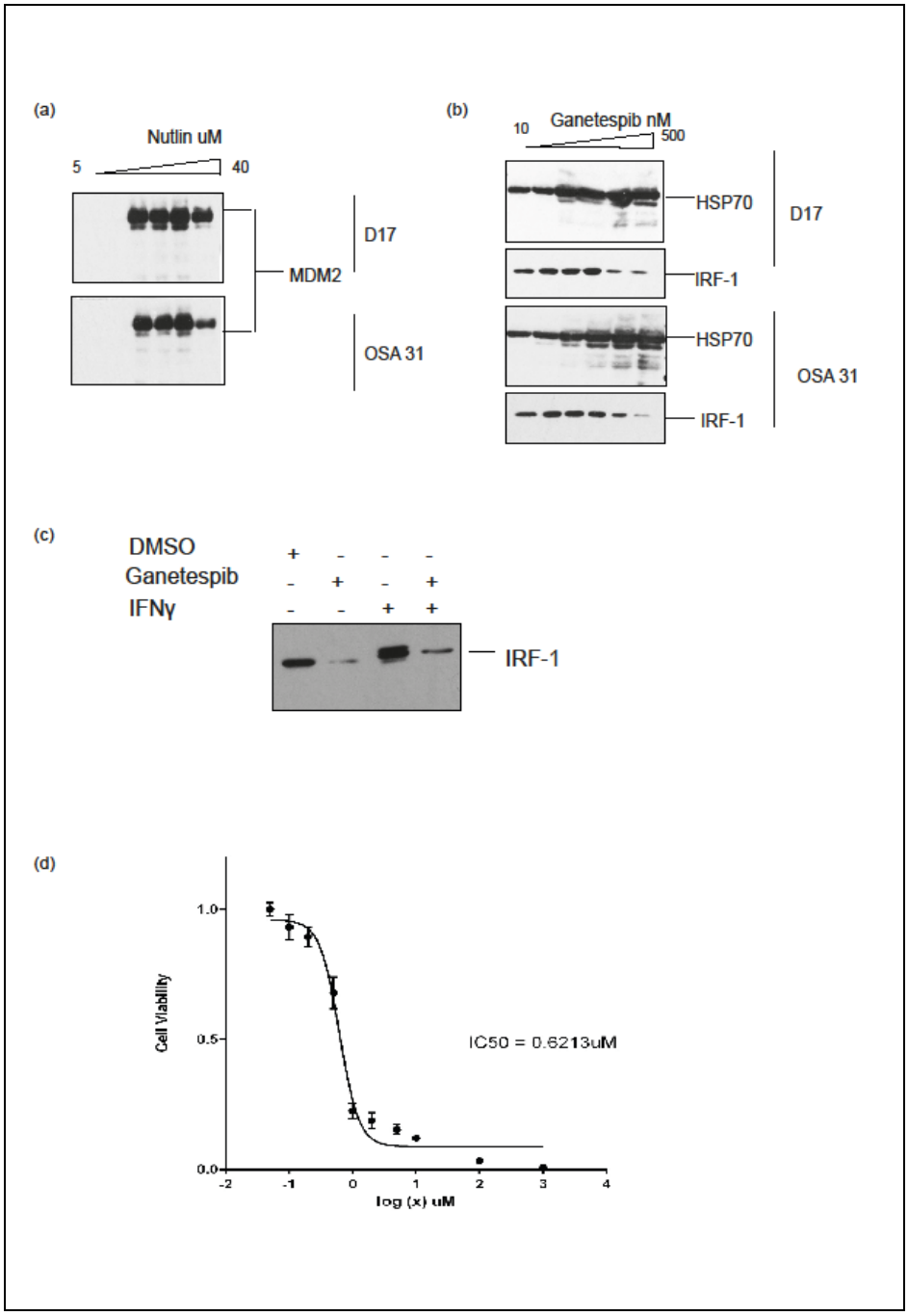

Figure 35OSA and D17 treated with Ganetespib and nutlin

(a) & (b) OSA31 and D17 cell lines treated with a titration of either Ganetespib (0,10,25,50,100,500nM) or Nutlin(0,5,10,20,40uM) for 16 h and 6 h respectively. Total cell lysates analysed for HSP70, IRF-1 and MDM2 by Western blotting. (c) OSA31 cells were treated with Ganetespib, IFNγ, or both, for 16 h. The cell lysates were analysed for IRF-1. The data are representative of at least three independent experiments. (d) Cell viability assay performed by prof Geoffrey A wood (university of Guelph) for OSA 31 cells with DOX, IC50 0.621uM.

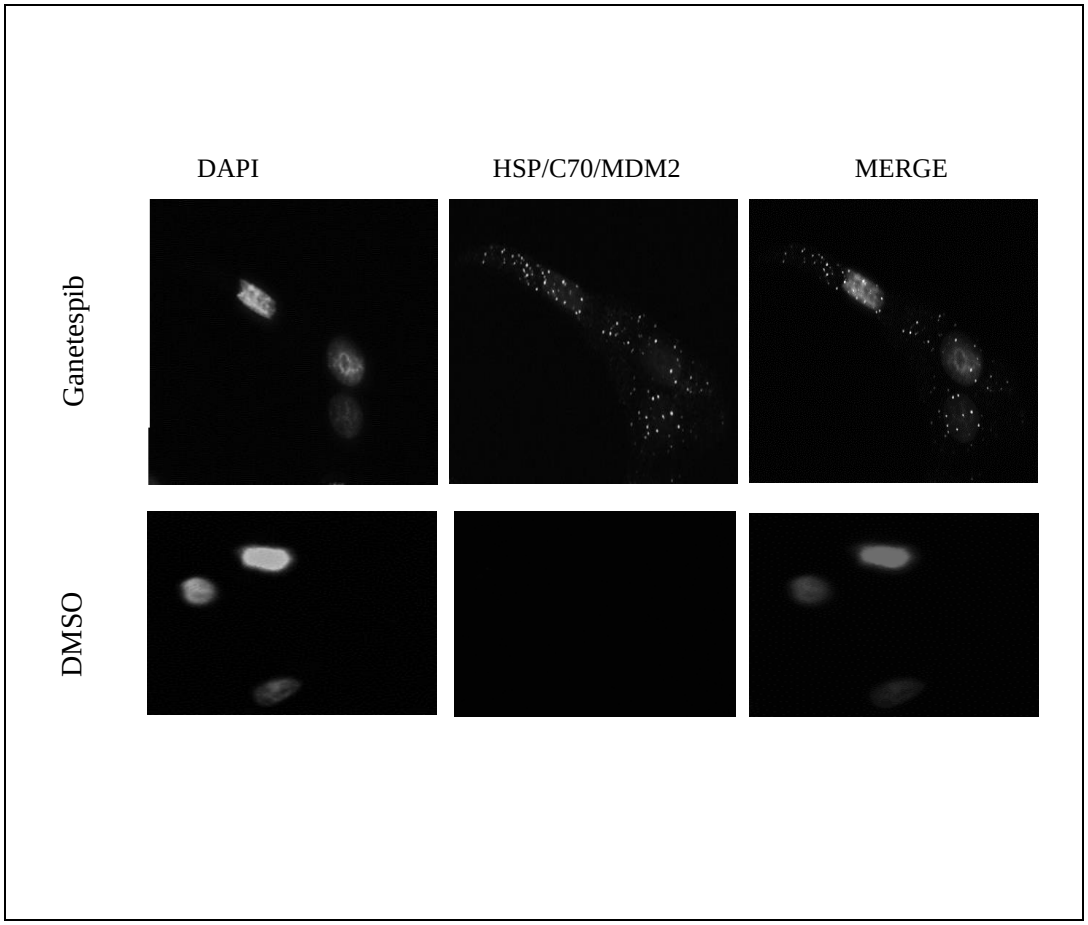

Figure 36 PLA system detects canine HSP/C70/MDM2 interactions

OSA31 cells were treated with DMSO or Ganetespib (100 nM) for 6 h, and a proximity ligation assay (PLA) using only HSP70, or both HSP70 and anti-MDM2 antibodies, was performed. Cells were stained with DAPI (1:5000 in mounting media) and visualised using an Axioplan2 (Zeiss) fluorescent microscope (100 x magnification). Representative PLA images are shown. . The data are representative of at least three independent experiments.

3.2.4 Proteomics on drug-treated canine osteosarcoma cell lines to develop biomarkers of drug responsiveness

The data above indicated that the OSA31 cell line shows responsiveness to Nutlin-3 resulting in activation of p53 and also shows responsiveness to Ganetespib as defined by induction of HSP70, downregulation of IRF1, and induction of the HSP70-MDM2 protein complex. We next aimed to define the global mechanism of how these drugs might function in signal transduction, to identify potential novel biomarkers that could be used to measure drug-responsiveness in canine cancer biopsies in the future. Proteomics is a very efficient technique used for the identification of protein pattern changes in a large variety of diseases, including neoplastic disorders. Using proteomic techniques, a tumour-specific protein expression profile for certain pathologies can be established, which will increase the discovery of novel biomarkers with predictive and prognostic value for more accurate diagnoses. In addition, proteomic techniques could provide an important tool for understanding the tumour's pathogenesis. In human neoplasias, proteomics analyses are routinely used, but are rarely used in the case of canine cancer investigation. In recent years, tumour protein profiling has become another important focus in cancer research, hence cancer cell lines are regarded as a suitable tool for proteomics analyses since they hold an important source of protein (VISAN, 2015).

Proteomics study was performed on canine osteosarcoma cell line (OSA31) which was treated with either Ganetespib, nutlin-3 or DMSO. The cell lines were treated for 6 and 16 hours of nutlin (10uM) and Ganetespib (100nM) respectively. A test western blot was performed before the samples were processed for mass-spectrometric analysis (Figure 37). The results indicated that the 6 hours of nutlin or DMSO didn't induce HSP70 protein levels while 16hours of Ganetespib showed high induction of hsp70 (Figure 37). There was also minor induction of hsp70 with 16hours of DMSO. When the cells were treated with 6 hours of Nutlin a significant upregulation of MDM2 was observed as compared to DMSO control. On the other hand, treatment with Ganetespib lowered the MDM2 expression levels after 16 hours which was similar result observed in human cell lines (chapter 3).Duplicate set for each of the treated samples were processed for TMT mass-spectrometry analysis.

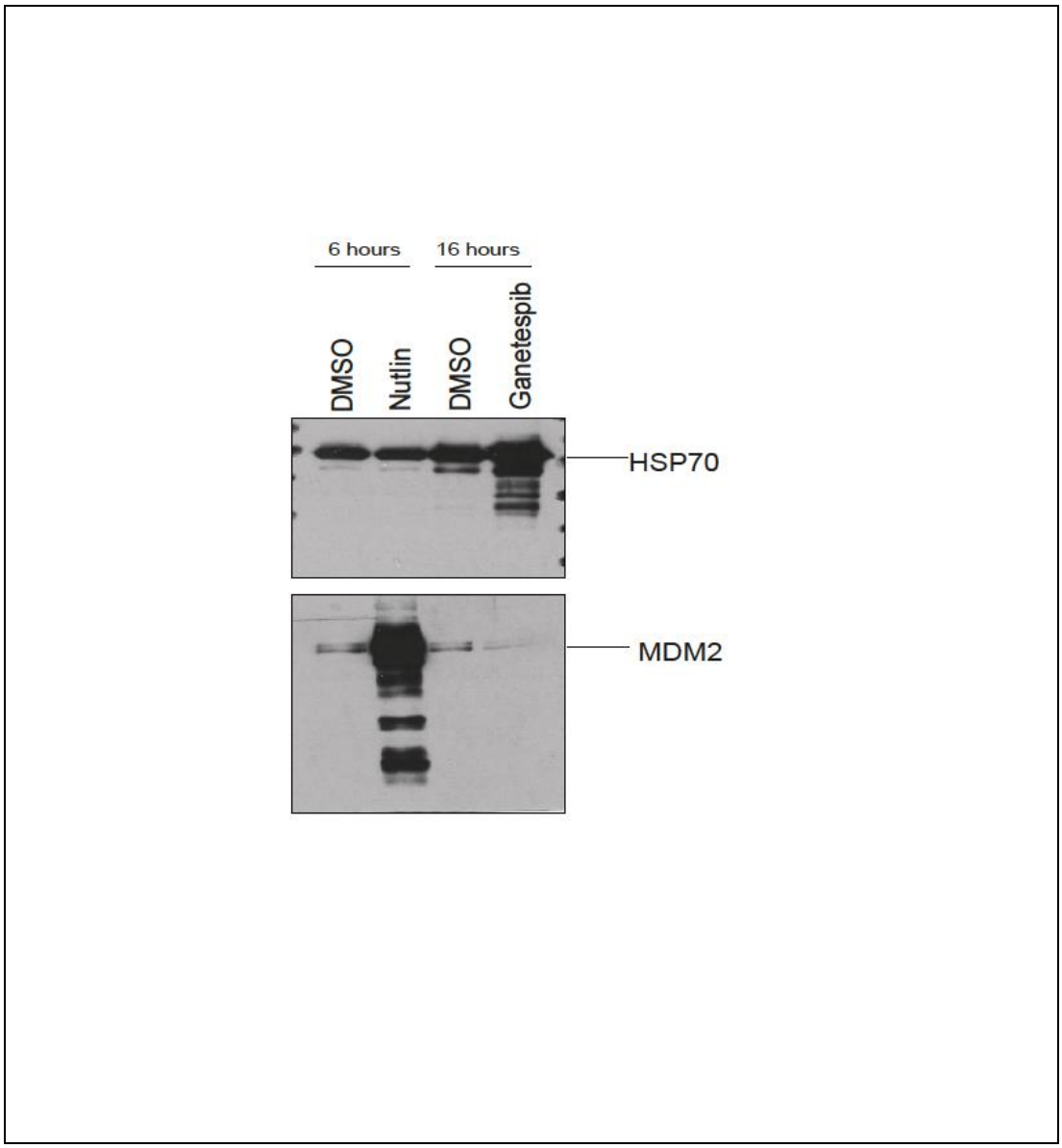

Figure 37 Western blot analysis of proteomics samples

OSA31 cell line treated with titration of either Ganetespib (100nM) or Nutlin (10uM) for 16 h and 6 h respectively. Total cell lysates analysed for HSP70 and MDM2 by Western blotting. TMT mass spectrometry was performed on biological duplicates of the above samples.

3.2.5 Summary of the Ganetespib treatment responses

The proteins upregulated/downregulated with Ganetespib by TMT analysis is represented by scatter plot (Figure 38). The proteins and pathways implicated will be discussed below:

3.2.6 Upregulated proteins with Ganetespib treatment

Thirty of the top upregulated proteins from each duplicate set was compared and 11 proteins were common between them (Figure 39a). Most of the upregulated proteins were related to the chaperone family (Figure 39b) and to the TNF alpha–NFKB biological pathway (Figure 39c). Transcription factor identified was HSF-1 whose molecular functions are chaperone and heat shock activities (Figure 40). Some of the key proteins upregulated are discussed below:

A growing body of evidence suggests that HSPs are implicated in all phases of cancer from proliferation, impaired apoptosis and sustained angiogenesis, to invasion and metastasis. In particular, several studies have investigated the expression and prognostic significance of HSPs in human osteosarcoma. HSP expression has also been demonstrated in preliminary studies carried out on canine neoplasms, which show an abnormal expression pattern similar to that observed in human neoplasms. These parallel findings underline the relevance of studying the multiple roles of HSPs in carcinogenesis in animal models as an additional source of information for clinical cancer research. (Romanucci, 2012). Romanucci and group demonstrated that high expression of HSP90 in canine osteosarcoma suggested hsp90 to be a potential prognostic predictive and therapeutic target (Romanucci, 2012). In my study I observed upregulated HSP70 protein in both duplicate samples. This high induction of HSP70 with Ganetespib treatment indicates the inhibition of HSP90 protein.

Data analysis demonstrated HSF1 to be a transcription factor for the top upregulated protein (Figure 40a). There are some studies indicating that HSF1 can be overexpressed in certain cancers, and inhibiting HSF1 induces apoptosis and partial depletion of HSP90 client proteins. (Ganguly S, 2015). The majority of the upregulated proteins belonged to chaperone functions and a minority to heat shock activity (Figure 40b).Another protein upregulated was SERPINH1. The functions of SERPINH1 contribute significantly to collagen biosynthesis. Overexpression of SERPINH1 was observed in clinical specimens of lung cancer, suggesting that these proteins are involved in the pathogenesis of this disease (Kamikawaji K, 2016). Chi

and group demonstrated that different tumours revealed differences in gene expression. Stress induced the expression of genes such as MMP-3, SERPIN family members and inflammatory and immune responses in only one group of tumours. (Chi, 2012) . These results indicate that Ganetespib could be used based on the gene profiling of group of patients.

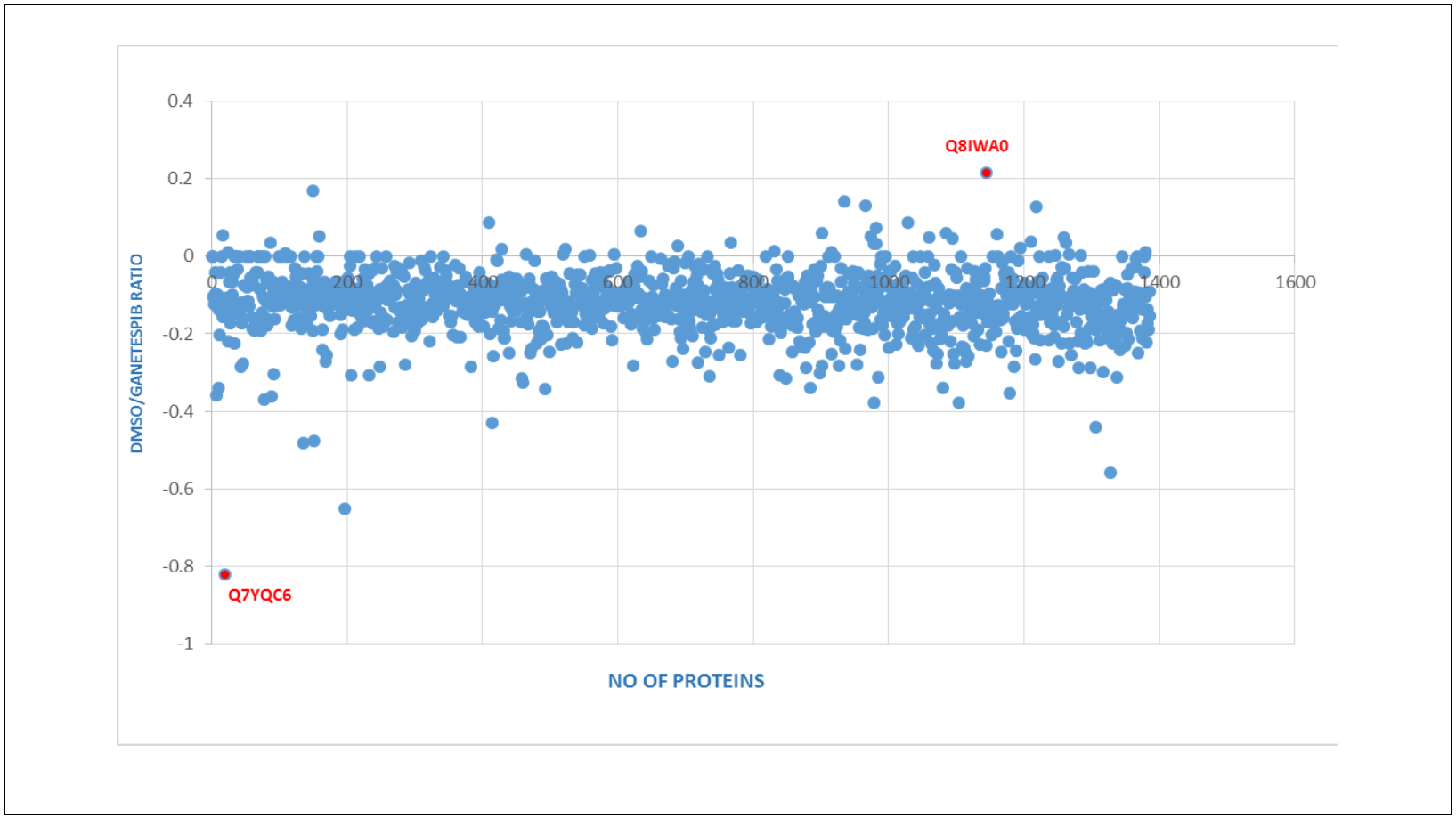

Figure 38 Scatter plot indicating proteins upregulated/downregulated with Ganetespib treatment

Scatter plot of log2 (relative protein quantity) with Ganetespib. The x axis = no. of proteins and y axis DMSO/Ganetespib ratio. Data analysed using FUNRICH software.Q7YQC6 –HSP70 protein and Q8IWA0-WDR75 protein

(a)

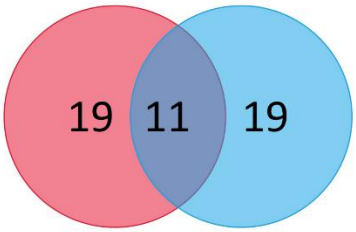

(b)

Search ID	Gene Symbol	Gene description
Q7YQC6	HSP71	Heat shock 70 kDa protein 1 OS=Canis familiaris
P42929	HSPB1	Heat shock protein beta-1 OS=Canis familiaris
Q5R606	HS105	Heat shock protein 105 kDa OS=Pongo abelii
Q0IIM3	HS105	Heat shock protein 105 kDa OS=Bos taurus
Q58FF6	H90B4	Putative heat shock protein HSP 90-beta 4 OS=Homo sapiens
Q1H2K2	HTPG	Chaperone protein HtpG OS=Methylobacillus flagellatus
P50454	SERPINH1	serpin peptidase inhibitor, clade H (heat shock protein 47)
Q2KJH6	SERPH	Serpin H1 OS=Bos taurus
P07900	HSP90AA1	heat shock protein 90kDa alpha (cytosolic)
O46392	CO1A2	Collagen alpha-2(I) chain OS=Canis familiaris
A2Q0Z1	HSP7C	Heat shock cognate 71 kDa protein OS=Equus caballus

(c)

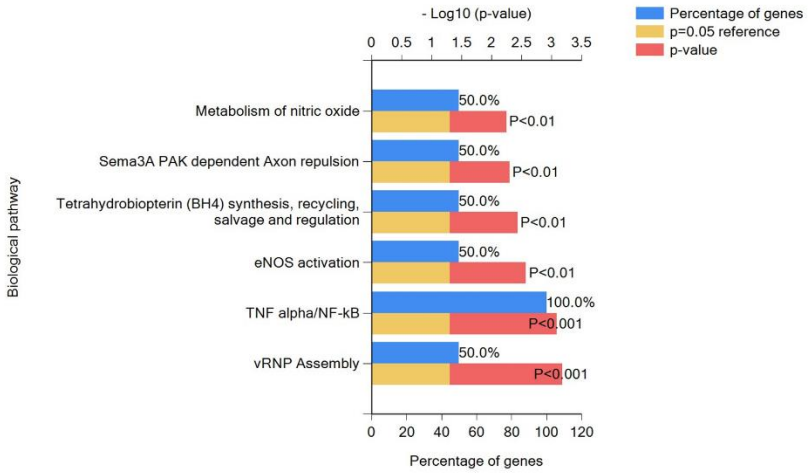

Figure 39 Upregulated proteins in a canine osteosarcoma cell line treated with Ganetespib

(a) Venn diagram of the upregulated genes after Ganetespib treatment of biological replicates. (b) List of upregulated genes with Ganetespib(c) Biological pathway of upregulated genes analysed using FUNRICH software

(a)

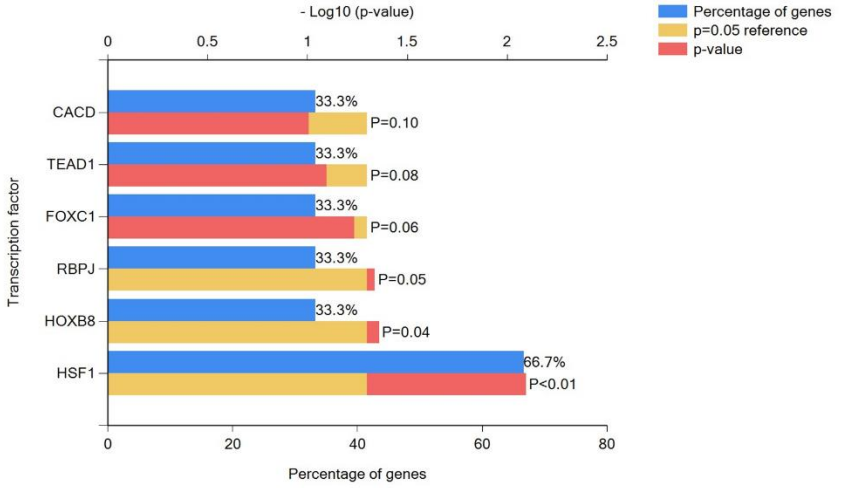

(b)

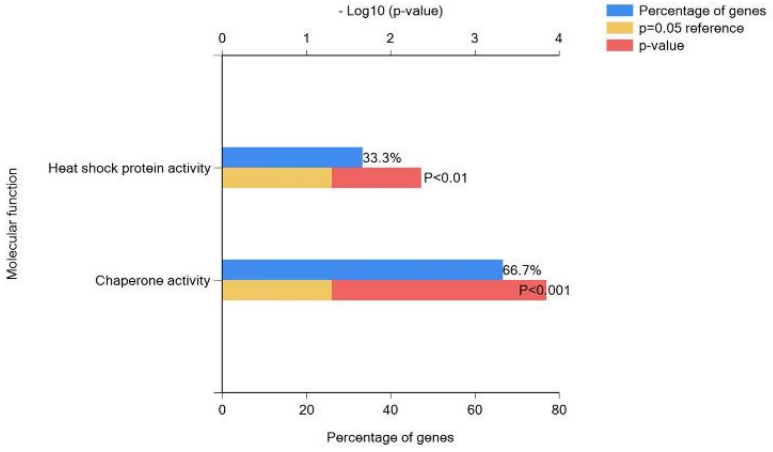

Figure 40 Upregulated proteins with Ganetespib

Transcription factors (a) and molecular functions (b) of upregulated proteins in OSA31 cell lines analysed using FUNRICH software

3.2.7 Downregulated proteins upon treatment with Ganetespib

There were four proteins downregulated common to both the biological sets. Some of the proteins downregulated with Ganetespib in the biological duplicates compared to the DMSO control are discussed below (Figure 41a -b). WDR-75 and HYPK are shown to be upregulated in many cancers, such as breast and thyroid respectively (http://www.proteinatlas.org). Therefore the downregulation of these proteins with Ganetespib would be of great therapeutic benefit. Chang L and group demonstrated that downregulation aldolase A (ALDOA) increases radio-sensitivity in prostate cancer cells, suggesting that controlling these identified proteins or signalling pathways in combination with radiotherapy may hold promise for overcoming radiation resistance (Chang L, 2017).

RanGTPase belongs to the Ras superfamily of small GTPases. It is known to regulate nucleocytoplasmic trafficking as well as mitotic spindle and nuclear envelope formation. RanGTPase has been reported to be essential for cell viability and its over-expression is linked to tumourigenesis. Thus, RanGTPase plays a crucial role in regulating key cellular events, and alterations in its expression may lead to cancer development and/or progression (Lui K, 2009). Lin et al. showed that downregulation of RanGTP eventually led to the apoptosis of cancer cells. (Lin TY L. C., 2015).. Most of the proteins downregulated belong to cell communication and signal transduction pathways, thereby downregulating the signalling pathway between tumour cells (Figure 41C).

Other pathways downregulated with Ganetespib involved HIF-1 alpha, HDAC class II and RanBP2 (Figure 42a). HDAC is a very good therapeutic target, and down regulation is key in Ganetespib treatment. (Jennifer L. Guerriero, 2017). Harnessing both the innate and adaptive arms of the immune system might produce superior tumour reduction and elimination. Guerriero JL and group demonstrated class IIa HDAC inhibition as a means to harness the anti-tumour potential of macrophages to enhance cancer therapy. Furthermore, combining HDAC inhibitor with chemotherapy regimens or T-cell checkpoint blockade significantly enhanced the durability of tumour reduction in their model (Guerriero JL, 2017). Lim YS et al showed that knocking down HIF alpha using siRNA blocked invasion in adecystic carcinoma

and exhibited therapeutic potential for inhibition of metastasis when used in combination with HSP90 inhibitors such as 17AAG (Lim YS, 2017).

The majority of the downregulated proteins were GTpase activator or lyase activity in molecular activity (Figure 42c). The main transcription factors involved in the downregulated genes were TCF3, NFIC and ZFP161. The transcription factor TCF3/E2A drives p21 expression while repressing PUMA across cancer cell types of multiple origins. Accordingly, TCF3/E2A depletion impairs the cell cycle arrest response and promotes apoptosis upon p53 activation by chemotherapeutic agents (Zdenek Andrysik, 2013). Bileck and group identified previously unrecognized inflammation-associated nuclear translocation events of proteins such as ZFP161 (Bileck A1, 2017).

(a)

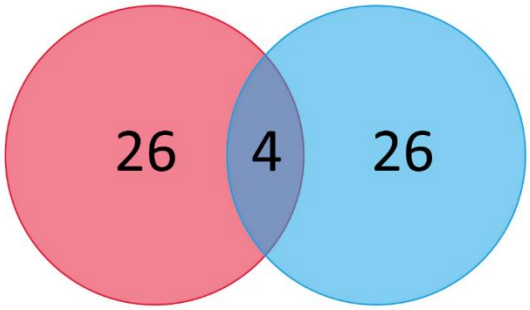

(b)

Search ID/	Gene Symbol	Gene description
Q8IWA0	WDR75	WD repeat domain 75
P04075	ALDOA	aldolase A, fructose-bisphosphate
P46060	RANGAP1	Ran GTPase activating protein 1
Q9CR41	HYPK	Huntingtin-interacting protein K OS=Mus musculus

(c)

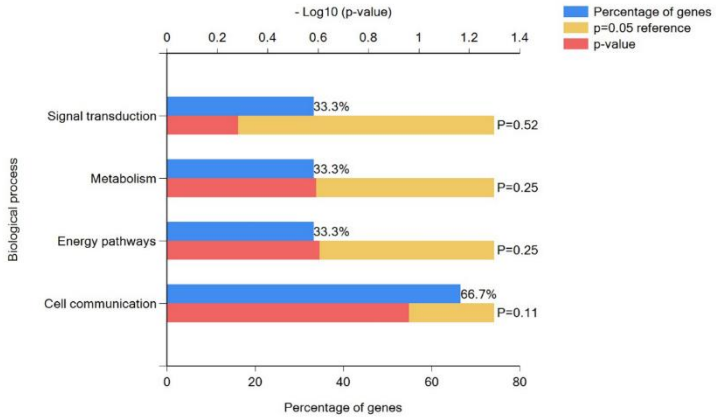

Figure 41 Downregulated proteins in OSA31 cells with Ganetespib treatment

(a) Venn diagram of the downregulated genes after Ganetespib treatment of biological replicates. (b) List of downregulated genes with Ganetespib (c) Biological processes of upregulated genes analysed using FUNRICH software

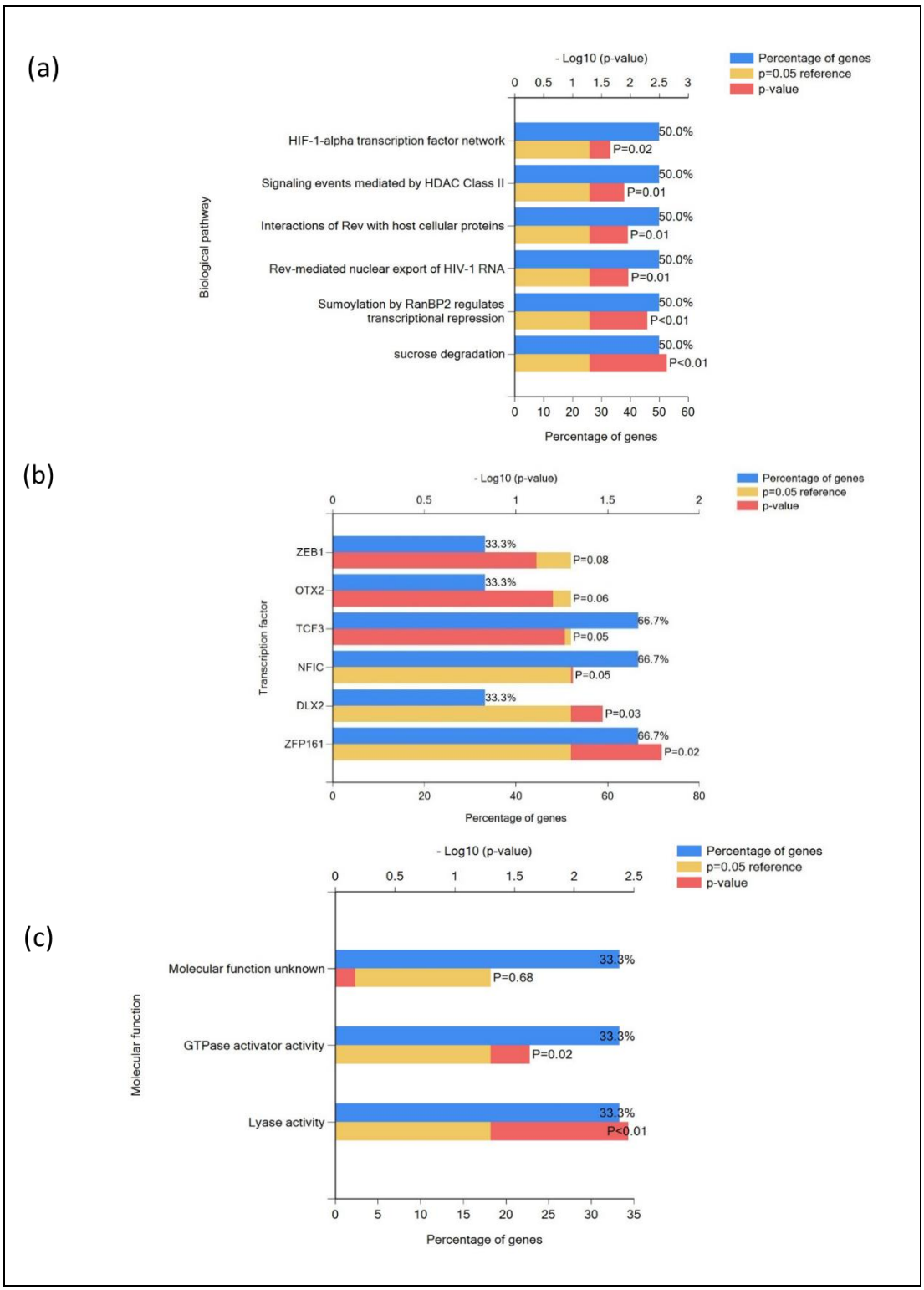

Figure 42 Downregulated proteins in OSA31 cells with Ganetespib treatment

(a) Biological pathways (b) Transcription factors (c) and Molecular functions of downregulated proteins in OSA31 cell lines analysed using FUNRICH software

3.2.8 Proteomic changes upon Nutlin-3 treatment.

Canine cancer is of major significance in terms of animal health and welfare, and soft tissue sarcomas are an important group of tumours accounting for approximityly 15% of all canine tumours presented. Osteosarcoma is common in individuals inheriting mutant p53 or Rb genes. Osteosarcoma in dogs is similar to humans by histology, site, gender ratio and several other biological parameters (Mendoza S1, 1998). Abnormal p53 protein expression and gene mutations have been identified in a number of different canine tumour types and canine p53 homologues have been identified and show a high level of sequence homology to human p53. However, MDM2 gene amplification has only been investigated in a limited number of canine osteosarcomas. (L. Nasira, 2001). A recent review of the spectrum of MDM2 abnormalities has shown that hdm2 gene amplification occurs in approximityly 7% of human cancers, with the highest frequency reported in soft tissue tumours (20%), osteosarcomas (16%) (Nasir L. , 1999). The proteins upregulated/downregulated with Nutlin by TMT analysis is represented by scatter plot (Figure 43). The proteins and pathways implicated will be discussed below:

MDM2 protein was upregulated in the nutlin treated canine OSA31, which indicates the cell line to contain wild type p53. Two other proteins shown to be upregulated with nutlin, and common between the two biological duplicates, were PRDX3 and GSPT1 (Figure 44a - b). Peroxiredoxin (PRDX3) is a mitochondrial peroxide reductase that regulates cellular redox state. It has been reported that PRDX3 is overexpressed in liver cancer and involved in carcinogenesis. PRDX3 promotes tumour growth and mediates cell migration and invasiveness and is a potential therapeutic target for cancer treatment (Liu Z, 2016). Eukaryotic release factor 3a (eRF3a) is a translation termination protein that is encoded by G1 to S phase transition 1 gene (GSPT1). Miri and group demonstrated the differential allele expression of GSPT1 in cancer. (Miri M, 2012) (Malta-Vacas J, 2009)

The molecular function for the proteins were mainly ubiquitin specific protease activity and GTPase activity. (Figure 44 c). Some of the biological pathways upregulated were PIP3, PI-3K and RanBP2 (Figure 45a). Dong and group demonstrated suppression of metastasis by blocking PI-3K/AKT signalling pathway (Dong F1, 2017). PIP_3 functions to activate downstream signalling components, the most notable being the protein kinase AKT, which activates downstream anabolic signalling pathways required for cell growth and survival. Aberrations in the production and metabolism of PIP3 (phosphatidylinositol 3, 4, 5-

trisphosphate) have been implicated in many human diseases including cancer (Goldsmith JR1, 2017). Packham et al demonstrated that RANBP2 had a potential role in nuclear translocation of IGF-1R, thereby contributing to development of new therapeutic strategies (Packham S, 2015).

Signal transduction was the major biological process for most of the proteins upregulated by Nutlin treatment (Figure 45b). HNF4A was one transcription factor upregulated with nutlin (Figure 45c). Significant heterogeneity between different tumours prevents the discovery of cancer driver genes, especially in a patient-specific manner. Liang and group observed the potential role of HNF1A in their studies. (Liang L, 2016). Guo and group identified HNF4A as one of the signature genes in gene expression profiles for adenocarcinoma (Guo M, 2017). Xu et al. demonstrated that HNF4A gene is over expressed and expression level correlates with patient survival. (Xu D1, 2016). Hence the treatment with nutlin could potentially lead to upregulation of several genes that are closely linked to tumour pathogenesis.

Only two proteins, ATPB and HTPG, were observed to be common between the duplicate sets of downregulated genes with nutlin (Figure 46a -b). Pendharkar and group demonstrated that ATPB serves as a bio signature for breast cancer. ATPB is also a potential biomarker and therapeutic target for the immunotherapy of various cancers. (Lu ZJ1, 2009) (Pendharkar N, 2016). Hence downregulation of ATPB by Nutlin could be of great potential in therapy.

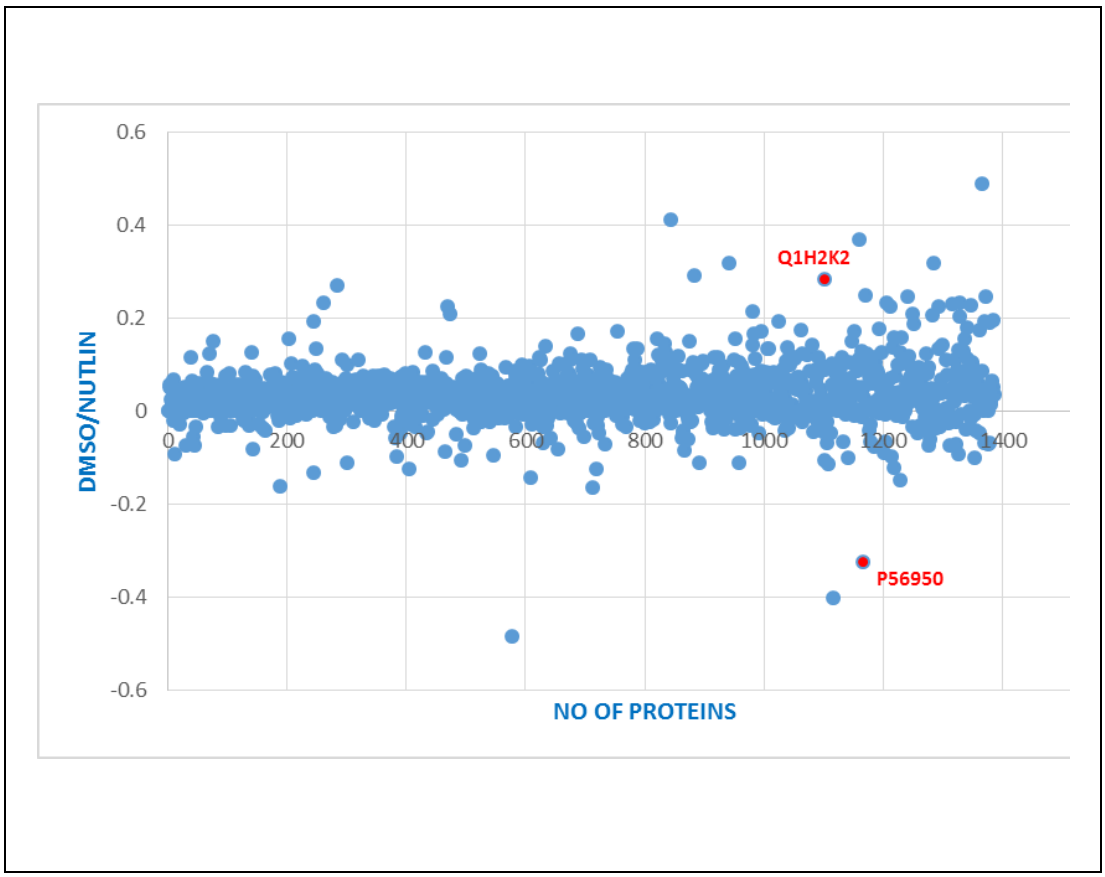

Figure 43 Scatter plot indicating genes upregulated/downregulated with Nutlin treatment

Scatter plot of log2 (relative protein quantity) with Nutlin; x axis = no of proteins and y axis = DMSO/Ganetespib ratio. Data analysed using FUNRICH software.Q1H2K2 is HTP5 and P56950 is MDM2 protein

(a)

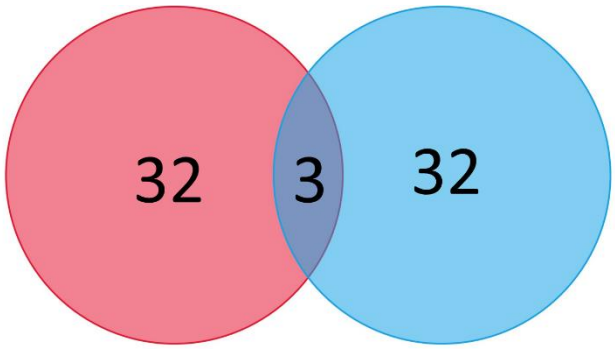

(b)

Search ID/	Gene Symbol	Gene description
P56950	MDM2	E3 ubiquitin-protein ligase Mdm2 OS=Canis familiaris
P35705	PRDX3	Thioredoxin-dependent peroxide reductase, mitochondrial OS=Bos taurus
P15170	GSPT1	G1 to S phase transition 1

(c)

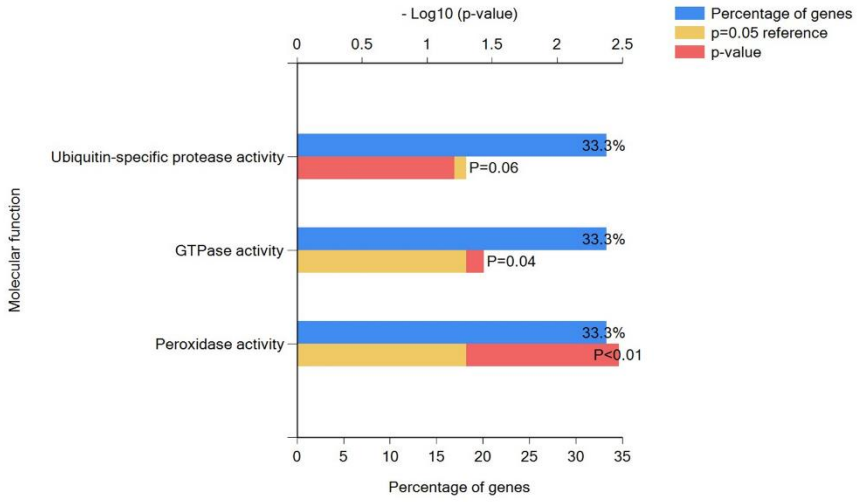

Figure 44 Upregulated genes with nutlin treatment in OSA31 cells

(a) Venn diagram on the upregulated genes after Nutlin treatment in biological replicates. (b) List of upregulated genes with Nutlin (c) Molecular functions of upregulated genes analysed using FUNRICH software

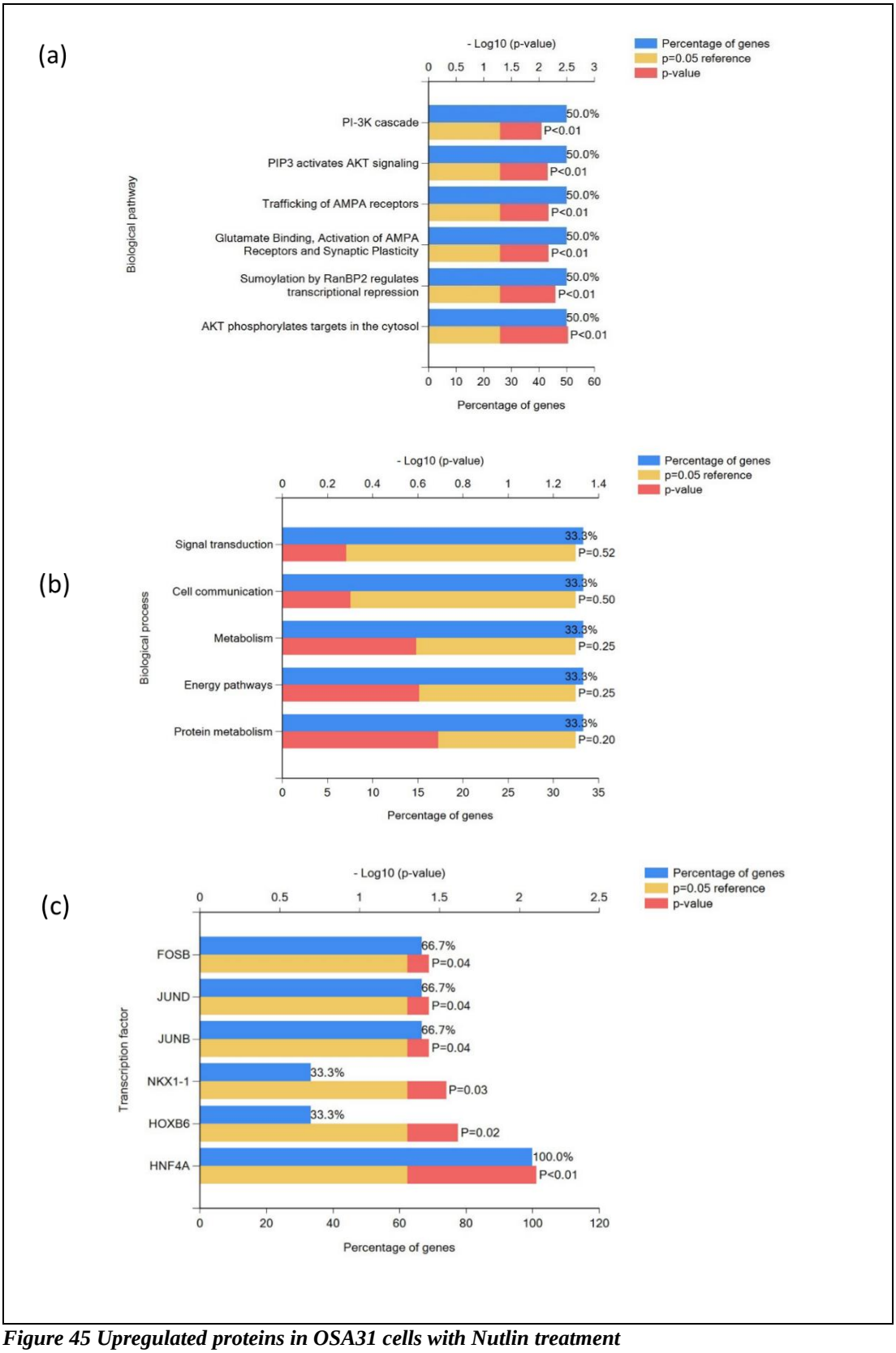

Figure 45 Upregulated proteins in OSA31 cells with Nutlin treatment

Biological pathways (a) Biological process (b) and Transcription factor (c) of upregulated proteins in OSA31 cell lines analysed using FUNRICH software.

(a)

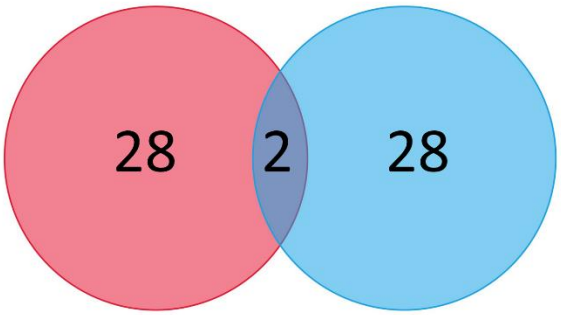

(b)

Search ID	Gene Symbol	Gene description
Q1H2K2	HTPG	Chaperone protein HtpG OS=Methylobacillus flagellatus
P49376	ATPB	ATP synthase subunit beta, mitochondrial OS=Kluyveromyces lactis

Figure 46 downregulated genes with nutlin in OSA31 cells

(a) Venn diagram of the downregulated genes after Nutlin treatment on biological replicates. (b) List of upregulated genes with Nutlin. Data analysed using FUNRICH software

3.2.9 Summary of characterisation of the OAS31 cell line as a model for drug testing.

We have tested two key anti-cancer drugs that affect MDM2-inhibition and HSP90-inhibition to determine whether pathway biomarkers can be identified in canine cells. Using proteomics we have identified key responses that provide a pathway drug response signature in this cell line. We predict that such approaches could be used in future to test new anti-cancer drugs in vitro, identify biomarkers that can be used in canine cancer in vivo, and to develop better models for human medicine. For example, Nutlin-3 shows a "cytostatic" response in human sarcoma patients and the ability to test Nutlin-3 in canine sarcoma cells will open the door to test MDM2-inhibitors in such sporadic cancer patients, develop biomarkers of resistance or response, and use this information to stratify future canine, as well as human, cancers.

Osteosarcoma tumours display a compendium of genetic abnormalities with a high degree of inter-tumour heterogeneity. Classically defined modes of genetic mutation are known to occur in osteosarcoma (McCleese JK, 2009) (Lin TY B. M., 2008) (Cheryl A London, 2011). Various studies have demonstrated the selective cytotoxicity of the novel Hsp90 inhibitor Ganetespib for human and canine OSA cell lines. The widespread expression of HSP90 observed both in primary tumours and in tumour cell lines strongly highlights the possibility of using a canine model for further testing of Hsp90-targeted cancer therapy. (Romanucci, 2012)**.** Because no gold standard treatments exist for pet animals with cancer, new treatments can be provided to pet dogs with cancer at earlier stages of progression than can be introduced in human trials. Cancer progresses at a faster rate in dogs than in humans; accordingly, these studies can be completed without interrupting the existing development path. The intramural NCI's Centre for Cancer Research established the comparative oncology program (COP) to develop this novel cancer drug development opportunity, address potential risks with this approach, and establish the organizational infrastructure to undertake translational clinical trials in pet dogs. (Stroud, 2016)

My study provides evidence that Ganetespib exhibits biological activity in a relevant large animal model of cancer. Given the similarities of canine and human cancers with respect to tumour biology and HSP90 activation, it is likely that Ganetespib will demonstrate comparable anti-cancer activity in human patients. The results also indicate that genes that code for the

proteins targets of most successful drugs, or are highly specific for osteosarcoma, are quite evolutionarily conserved between human and canines.

Stroud and group demonstrated that veterinary and human cancer centres can effectively collaborate and develop therapeutics which lead to governmental licensure and commercial success (Stroud, 2016). Dickinson demonstrated that whole genome sequencing of canine cancers revealed key pathways in human cancers (Dickinson, 2016). For humans, a period of personalized medicine, which uses genomic data to determine disease risk, select specific and effective treatment regimens, and predict relapse, is rapidly becoming state of the art, particularly in the field of cancer. Although the scope and depth of available canine genomic data pales compared with what is currently available for humans, directed or personalized treatments will soon become a reality for pets (Davis, 2014). Despite the commonality of cancer with human medicine, there are still very few experimental models that can effectively test the metastatic cascade or novel treatments. Cancer occurs twice as frequently in dogs as in humans and the histological types and biological behaviour of tumours are very similar. This suggests that the underlying mechanisms in canine carcinogenesis may be similar to those in humans and may represent a good model for this disease (Nasir L. , 2001).

Collaborative efforts among research scientists, clinician scientists, clinicians, and veterinarians is essential for building multifaceted trials that systematically progress from preclinical stages, to canine trials, then to successful human trials. A major proposed benefit is decreased failure rate in human clinical trials. Spontaneous canine osteosarcoma models can effectively bridge the translational gap between preclinical mouse studies and human clinical trials. Developing a systematic and multidisciplinary approach to incorporate this model is likely to result in speedy development of effective therapies and improved care for both human and canine cancer patients (R. Timothy Bentley, 2016) (Bray, 2014). For example, the ability to define the expressed mutated RNA species in cancer facilitates the prediction of mutated proteins that might be produced. Some of these mutant proteins can be presented by the MHC Class I/II system and can form future efforts to define mutated neoantigen therapies. Such an RNAseq driven pipeline has already been performed in syngenic mouse models to drive concepts of cancer vaccinology in such systems ((Yadav M, 2014).

In addition to using such cell models to test new anti-cancer drugs, another emerging therapeutic strategy to treat human cancer will involve immune therapies. It is though that immune therapies will be augmented, in part, by the use of patient-specific neoantigen

vaccines that stimulate tumour rejection. In this chapter, I have used next generation sequencing of DNA and RNA of canine sarcoma cell model in order to define parameters for producing peptide lists that might form the basis for neoantigen vaccines. However, the data on comparative oncology in this chapter could have improved if there wasn't constraint in time and canine samples in this project. There should be a much more elaborative comparison with human models. Canine cancer studies using spontaneous tumour models could potentially exploit patient-specific information to drive vaccinology.

4 MDM2 interactome

4.1 Introduction

In normal cells, p53 is kept inactive through a number of mechanisms, including the activity of the oncoprotein murine double minute 2 (MDM2), a key negative regulator of p53. However, MDM2 also functions as an E3 ligase, covalently attaching ubiquitin molecules to p53, which leads to both the export of p53 to the cytoplasm and its proteasomal degradation. Although MDM2 plays an important role in regulating p53 stability, a number of other E3 ligases have recently been identified that can promote the degradation of p53 independently of MDM2. These include Pirh2, Cop1, TOPORS, ARF-BP1, Synoviolin, Carps, and CHIP (Lukashchuk, 2007).

The p53 gene is mutated in nearly 50% of all human cancers. While wild-type p53 is normally a rapidly degraded protein, these mutant p53 proteins lose the ability to activate transcription, and they often become stable and so accumulate to high levels in tumour cells. Since MDM2 has been shown to retain the ability to bind and degrade mutant p53, the inability to transactivate the expression of MDM2 has been proposed to underlie the stability of mutant p53 proteins (Lukashchuk, 2007)**.** Kathryn Ball's group have demonstrated that MDM2-mediated ubiquitination of the p53 tumour suppressor requires interaction with the ligase at two distinct binding sites that form general multiprotein docking sites for the p53 protein. The first MDM2-binding site resides in the transactivation domain of p53 and is an allosteric effector site for MDM2-mediated p53 ubiquitination; the second site requires the acid domain of MDM2 to recognize an 'ubiquitination signal' within the DNA-binding core of p53 (Susanne Pettersson, 2009).

The aim of the project was to study MDM2 and its interactome in cancer cell lines particularly in sarcomas, using novel drugs such as nutlin (Ladanyi M, 1995). Sarcomas were chosen as these are observed to contain many amplifications of the MDM2 gene. Nutlins are cis-imidazoline analogues that inhibit the interaction between MDM2 and p53. I also focus on chaperone therapeutics using the heat shock protein 90 (HSP90) inhibitor drug Ganetespib, studying the mechanism of action of the drug on its client proteins and also investigate whether the drug has any impact on MDM2 E3 ligase.

An HSP90 inhibitor is a substance that inhibits that activity of the HSP90 heat shock protein. Since HSP90 stabilizes a variety of proteins required for survival of cancer cells, these inhibitors may have therapeutic benefit in the treatment of various types of malignancies. A number of HSP90 inhibitors are currently undergoing clinical trials for a variety of cancers. HSP90 inhibitors include the natural products geldanamycin and radicicol as well as semisynthetic derivatives 17-N-Allylamino-17-demethoxygeldanamycin (17AAG). Most of the inhibitors of HSP90 block the N terminal ATP binding pocket and prevent the conformational changes that are essentially required for the loading of co-chaperones and client proteins. However several other inhibitors have been reported to disrupt the chaperone cycle in ways other than binding to the N-terminal ATP binding pocket.

Heat shock protein 90 (HSP90) is one of the most highly conserved and abundant proteins in mammalian cells, where it serves as a molecular chaperone to maintain the stabilization of intracellular and extracellular proteins. Hundreds of HSP90 clients have been identified to date, many of which play critical roles in signal transduction, cell cycle control and DNA repair including: mutant p53, AKT, ATR, mutant BRAF, BRCA1, CDK1/4, CHK1, EGFR, EML4-ALK, HER2, HIF1-α, IGF-1R, MET, VEGFR, and steroid receptors . It has recently been shown that >60% of human kinases are clients of HSP90 ((Solit DB R. N., 2011); (Whitesell L, 2005); (Taipale M, 2012). (Haque A, 2016).

HSP90 is overexpressed in a range of cancers (such as breast, lung, colon, prostate, leukaemia and skin) and may contribute to tumour cell survival and metastasis by stabilizing aberrant signalling proteins, interfering with apoptosis and promoting migration and invasion ((Solit DB C. G., 2008); (Tsutsumi S, 2009); (workman, 2004)).Thus, one unique characteristic of targeting HSP90 in cancer is that inhibition results in the simultaneous degradation of hundreds of client proteins and combinatorial blockade of multiple signal transduction cascades, thereby potentially bypassing pathway redundancies often found in cancer cells (Friedland JC, 2013); (He S Z. C., 2013); (Proia DA F. K., 2011); (Sang J, 2013); (Shimamura T, 2012); (Xu W, 2007))

This strategy is quite distinct from other targeted inhibitors (i.e., kinase inhibitors), which typically are designed to block a single oncoprotein/pathway. Another unique feature of HSP90 inhibitors is their tumour selectivity. Small molecule inhibitors of HSP90, including Synta Pharmaceuticals' drug candidate Ganetespib, are retained in tumours for as much as twenty-times longer than in blood or normal tissue (Shimamura T, 2012). Recently published work suggests that cellular transformation is accompanied by a post-translational modification

of HSP90 (SUMOylation) which enhances the recognition of HSP90 by ATP competitive inhibitors, thus providing an explanation for the sensitivity of cancer cells to HSP90 inhibitors relative to normal cells (Mollapour M, 2014). Ganetespib (formerly called STA-9090) is a novel, injectable resorcinolic triazolone small molecule inhibitor of HSP90. Ganetespib inhibits the growth of many tumour types in vitro and in vivo including AML, ALL, CML, NHL, neuroblastoma, Ewing sarcoma, rhabdoid cancer, rhabdomyosarcoma, melanoma, and carcinomas of the breast, lung, prostate, bladder and colon (Friedland JC, 2013) (Sang J, 2013) (Proia DA F. K., 2011) (He S Z. C., 2013)) (Acquaviva J S. D., 2014); (Acquaviva J S. D., 2012) (Bansal H B. S., 2010) (Bansal H Y. Q., 2014) (Ganji PN, 2013); (He S S. D., 2014); (Liu H, 2013); (Nagaraju GP, 2013); (Proia D, 2012); (Proia DA Z. C., 2014); (Ying W, 2012); (Lock RB, 2013).

4.2 Results

4.2.1 MDM2 interactome and p53 ubiquitination

MDM2 has been extensively studied in the Ball laboratory. I wanted to further explore the interactions of MDM2 with other proteins and its role in p53 ubiquitination (Maura wallace, 2006). The A375 cell line has been well characterised and thus I used this line to study the preliminary responses. To demonstrate p53 ubiquitination, the cells were treated with either DMSO or 10 μM nutlin for six hours and the cell lysates were analysed by Western blotting. The results showed that with DMSO treatment, MDM2 and p53 expression was low and only weak ubiquitination bands observed for p53, whereas nutlin induced MDM2 protein levels and increased the ubiquitination of p53 (Figure 47a).

I then determined the effect of knockdown of MDM2 on p53 ubiquitination or p53 status. I used siRNA targeting MDM2 and treated A375 cells for 48 hours prior to the addition of nutlin or DMSO for further six hours. The results demonstrated that using MDM2 siRNA I was able to knock down MDM2 by ~65% compared to the no treatment control (Figure 47b). Nutlin treatment increased the levels of both MDM2 and p53 even when MDM2 siRNA was used. When nutlin was used along with siRNA against MDM2 there was no significant knockdown of MDM2; only about 16% reduction of MDM2 expression for nutlin+MDM2siRNA as compared to nutlin+control siRNA. GAPDH was used as a loading control and the levels were equal in all the samples.

The data indicate that there is increased expression of MDM2 with nutlin, and p53 is stably mono-ubiquitinated following activation by nutlin3. My results also suggest that it is challenging to study p53 ubiquitination using nutlin and MDM2 siRNA and requires an alternative approach.

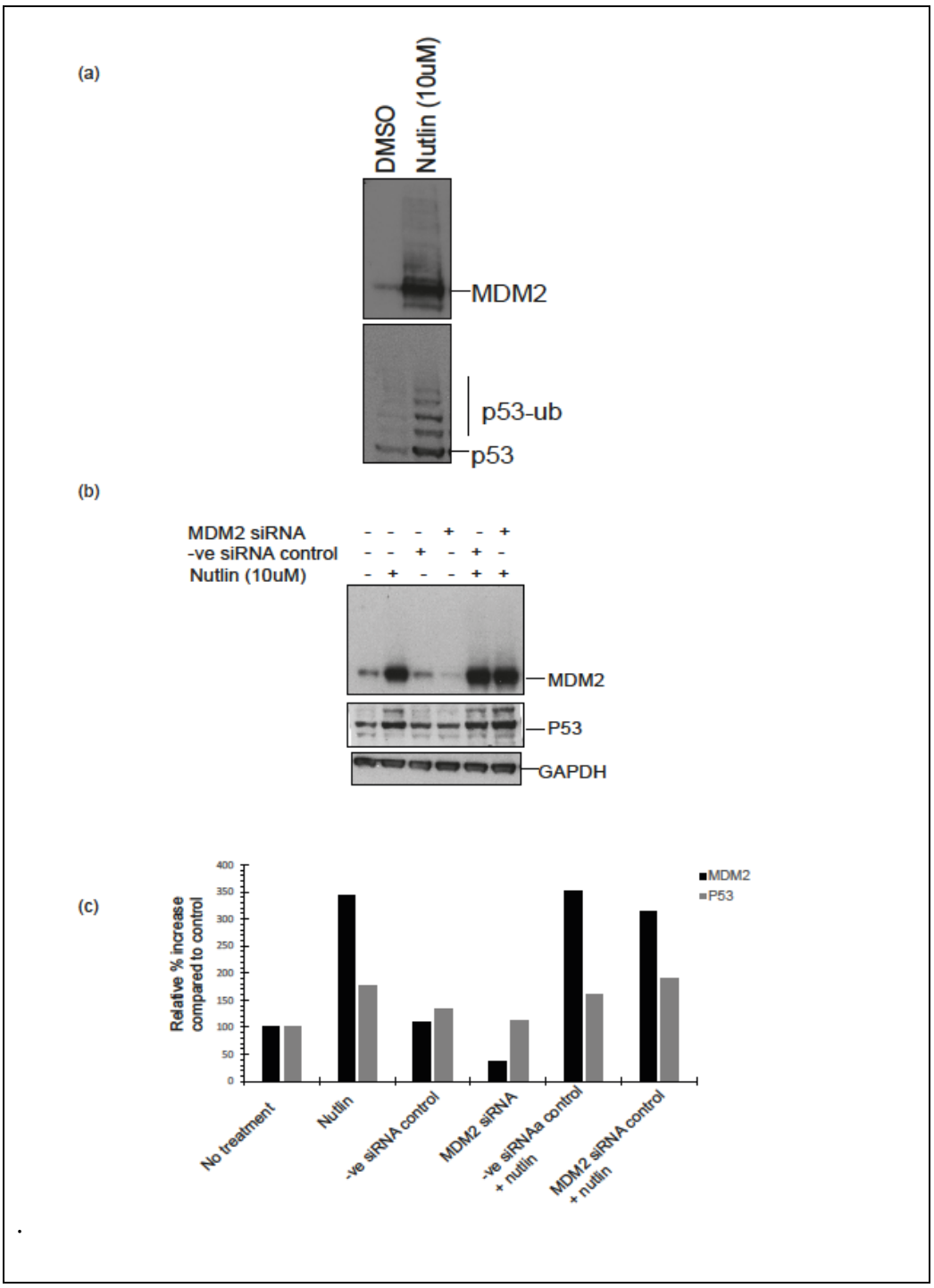

Figure 47 MDM2 interactome and p53 ubiquitination

(a) A375 melanoma cells were treated with either DMSO, or nutlin (10 μM) for 6 h. The cells were isolated and the total proteins extracted; p53 and MDM2 levels were determined by Western blot analysis. (b) A375 cells were treated with either control siRNA or siRNA to MDM2 (60nM) for 24 h and then treated as indicated on the panel. Total cell lysates analysed for p53, MDM2 and GAPDH by Western blotting. (c) Graphical representation of the siRNA treatment on A375 cell lines from (b). The data are representative of at least three independent experiments.

Since I was unable to prevent significant increase in MDM2 protein levels in response to nutlin-3 under conditions where about 70% knockdown of MDM2 was achieved in the controls, I used the MDM2 inhibitor protein p14ARF to determine that ubiquitination of p53 is MDM2-mediated. Hence p14ARF was chosen as a tool instead of knocking down MDM2 by siRNA.

For this experiment I used a p14ARF plasmid vector and transfected a titration of plasmid into both A375 and HCT 116+/+ cell lines prior to nutlin treatment (Figure 48a). The results indicated that there was a loss of p53 ubiquitination with increase in p14ARF plasmid in both nutlin-treated and DMSO-treated cells. This was similar in both the cell lines. The highest dose of ARF plasmid was 2 µg. The titration also indicated that at least 500 ng of plasmid is required to show a significant loss of p53 ubiquitination (Vivien Landré, 2017).

The results indicated that p14ARF could overcome the effect of nutlin3 on p53 ubiquitination. This confirms the hypothesis that nutlin-3 enhances p53 mono-ubiquitination through a process that involves MDM2 (Vivien Landré, 2017).

I observed that p53 ubiquitination could also be affected by the cell lysis conditions, such as the type of buffer used to lyse the cells. Duplicate sets of A375 cell lines were treated with either DMSO or nutlin for 2, 4, 6, 8 and 16 hours, then harvested using PBS. Each of the cell pellets was lysed using either NP40- or urea-containing lysis buffer. The results indicated that urea lysed cells contained strongly-ubiquitinated p53 bands with nutlin, and this increased with nutlin treatment duration, compared to samples lysed with NP40 buffer (Figure 48b). This difference could be due to composition of the buffer. For example Christoph and group demonstrated that protein ubiquitination is reversible, and this modification can therefore easily be lost through the hydrolysis of ubiquitin chain linkages, which is catalysed by protein ubiquitin hydrolases, termed de-ubiquitylases (DUBs). For this reason it is essential to include DUB inhibitors in the buffers used for cell lysis, to preserve proteins in the state of ubiquitination present in the intact cell.

To block DUB activity, EDTA or EGTA must be included in the lysis buffer to remove traces of heavy metal ions, and iodoacetamide (IAA) or N-ethylmaleimide (NEM) must also be added to alkylate the active site cysteine residues of DUBs. High concentrations of NEM are better at preserving K63-Ub chains and M1-Ub chains than high concentrations of IAA, probably due to the instability of the latter compound. (Christoph H. Emmerich, 2015). Therefore it is essential to maintain optimal buffer conditions when studying ubiquitination.

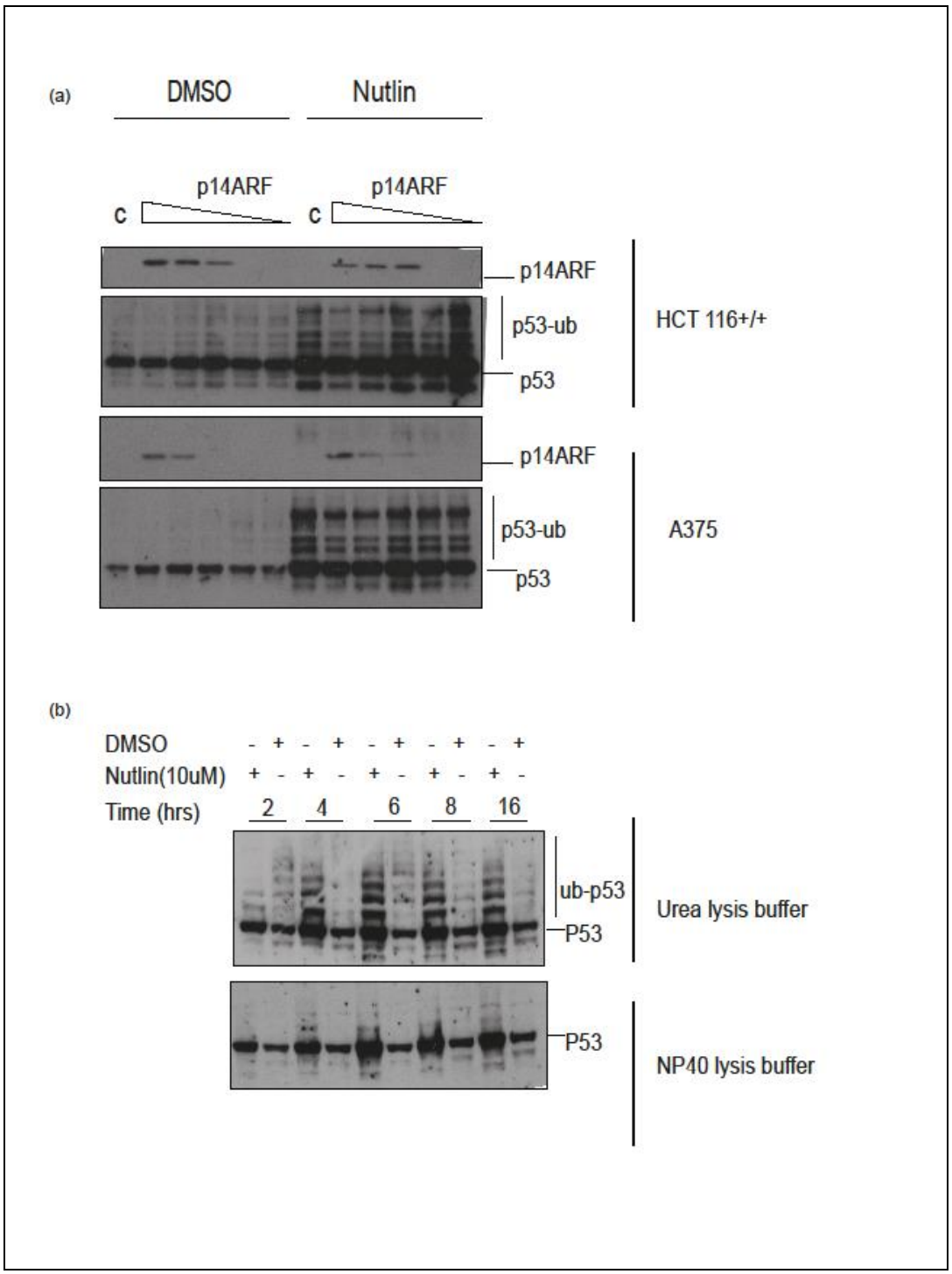

Figure 48 Components regulating p53 ubiquitination

a) A375 and HCT116 p53+/+ cells were transfected with titration of p14ARF (0, 2, 1, 0.5, 0.25ug) for 16 h, followed by treatment with either DMSO, or nutlin (10uM) for 6 h. The cells were isolated and total proteins extracted; p53 and p14ARF levels were determined by Western blot analysis. (b) A375 cells were treated with either DMSO or nutlin (10uM) for 2, 4, 6, 8 and 16 hours. Cells were lysed using either urea or NP40 lysis buffer. Total cell lysates were analysed for p53 ubiquitination by Western blotting. The experiments are representative of three independent experiments.

4.2.2 Ewing sarcoma and HSP90 inhibitors

Ewing sarcoma is the second most frequent primary bone tumour among teenagers and young adults. In 85% of cases, Ewing sarcoma is characterized by the expression of the EWSR1–FLI1 chimeric protein resulting from the chromosomal translocation t (11; 22) (q24:q12), which links the transcription regulating domain of Ewings Sarcoma RNA binding protein 1(EWSR1) to the ETS DNA-binding domain of Friend leukemia integration 1 transcription factorFLI1. The EWSR1-FLI1 fusion protein behaves as an aberrant transcriptional factor modulating the expression of specific target genes. EWSR1–FLI1 expression promotes oncogenesis of Ewing sarcoma (G-A Franzetti1, 2017), (David Herrero-Martin, 2011) (Folpe AL, 2000) (Siddhartha Mani, 2011) (Jambhekar, 2010)

Amplification of the MDM2 gene has been observed in various bone and soft tissue sarcomas particularly Ewing sarcoma (ES) or peripheral neuroectodermal tumour (PNET) (Ladanyi M, 1995). Ewing sarcoma is characterized by multiple deregulated pathways, which mediate cell survival and proliferation. Since HSP90 is a critical component of the multi-chaperone complexes that regulate the disposition and activity of a large number of proteins involved in cell-signalling systems, blocking HSP90 has shown, in various studies, to reduce the cell line growth and survival (Martins AS, 2008), (Srikanth R. Ambati, 2014).I wanted to study the effect of HSP90 inhibitor drug Ganetespib on two Ewing sarcoma cell lines. I used two cell lines, TC32 (primitive neuroectodermal tumour (PNET) and TC71 (Ewing sarcoma), both containing non-functional p53. First I analysed MDM2 expression in these cell lines; I treated both the cell lines with either DMSO or a nutlin titration for six hours. The resulting Western blots indicated that nutlin induced MDM2 in both cell lines, and there was also increased p53 with increased nutlin concentration (Figure 49a). I also observed a higher basal level of MDM2 expression in TC71 as compared to TC32. I was unable to detect any p53 in TC71 using the D01 antibody. I then tested Ganetespib on both the cell lines. I performed a dose titration of Ganetespib for 16 hours on both the cell lines. The drug depleted FLi-1 at the highest dose of 100 nM for TC71, whereas very low expression of FLi-1 was seen in TC32 cells (Figure 49b). HSP70 induction was observed with Ganetespib treatment in both the cell lines. GAPDH was used as a loading control.

The results indicated that Ganetespib could be effective for Ewing sarcoma and could be used either alone or in combination with other treatments. Since the drug does not require functional p53 to lower EWS-FLi1, Ganetespib could potentially be used for both WT and mutant p53 sarcomas.

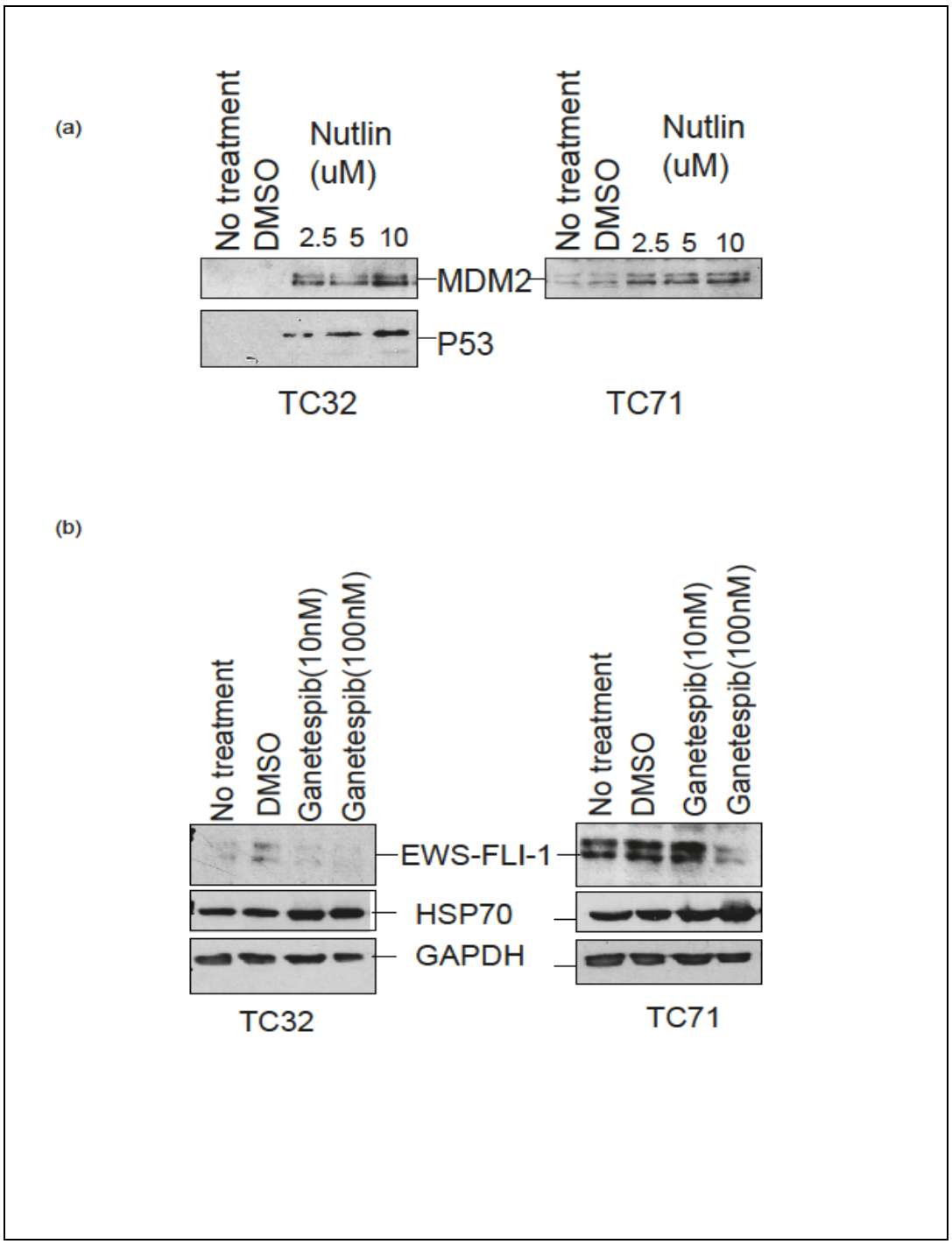

Figure 49 Ewing sarcoma and HSP90 inhibitors

(a) TC32 and TC71 cells were treated with either DMO or nutlin at 2.5, 5 and 10 µM. The cells were isolated and total proteins extracted; MDM2 and p53 levels were determined by Western blot analysis. (b) TC32 and TC71 cells were treated with either DMSO or 10 and 100nM Ganetespib. Total cell lysates were analysed for EWS FLI1, HSP70 and GAPDH by Western blotting. The experiments are representative of three independent experiments

4.2.3 Characterisation of osteosarcoma cell lines in association with MDM2 expression

Since sarcomas, particularly osteosarcomas, have high amplification of the MDM2 gene, I wanted to characterise osteosarcoma cell lines to determine if cell density had any impact on the expression levels of MDM2 protein. For this purpose I used three different cell types: MHM, SJSA (osteosarcoma) and T778 (liposarcoma), which are different categories of sarcomas. I also analysed the effect of nutlin on these cell types. Cell lines T778 and MHM were kind gift from Oslo University, and SJSA was from ATCC.

Time course experiments (2, 4 and 6 hours) with 10 µM nutlin were performed on low density (about 40% confluency and high density (~80% confluency). There was strong induction of MDM2 in all three lines (Figure 50a). At two hours of nutlin treatment there was low induction for all the cell lines at both the cell densities. With increased duration of nutlin treatment there was also an increase in MDM2 induction. I also observed that at low density, T778 cell lines gave steady MDM2 expression, as compared to the high-density cultures. This supports the data of the Hupp group, which shows that MDM2 exhibits higher steady state levels at lower cell densities, after nutlin treatment (Luke Way, 2016), however, this is not true for all the cell types, as SJSA and MHM behaved similarly for both the cell densities, i.e. higher induction with higher cell density. The data also showed that four hours of 10 µM nutlin was sufficient to induce MDM2, for all the cell lines except T778 high density. While for the high density of T778 requires optimisation for better MDM2 induction. The drug titration was performed for all three cell lines, at both low and high densities, with concentrations of 2.5, 5 and 10 µM for six hours. For T778 and MHM, MDM2 expression was steady across the titration range (Figure 50b), whereas for SJSA, a low cell density gave better induction, compared to a high density. In general 5 µM for six hours was sufficient for all cell lines and cell densities to induce high MDM2 expressions.

Ganetespib drug titration was performed for all the three cell lines. The T778 showed a low basal HSP70 induction whereas MHM and SJSA HSP70 induction even in non-treated samples (Figure 50c). This suggests that Ganetespib could potentially work better in T778 cell types than in either of the others, as induction in HSP70 indicates inhibition of HSP90.

These results indicate MDM2 expression after nutlin treatment is determined by two factors: the cancer cell type and the cell density at which the drug treatment is performed. Hence these need to be optimised for each experiment.

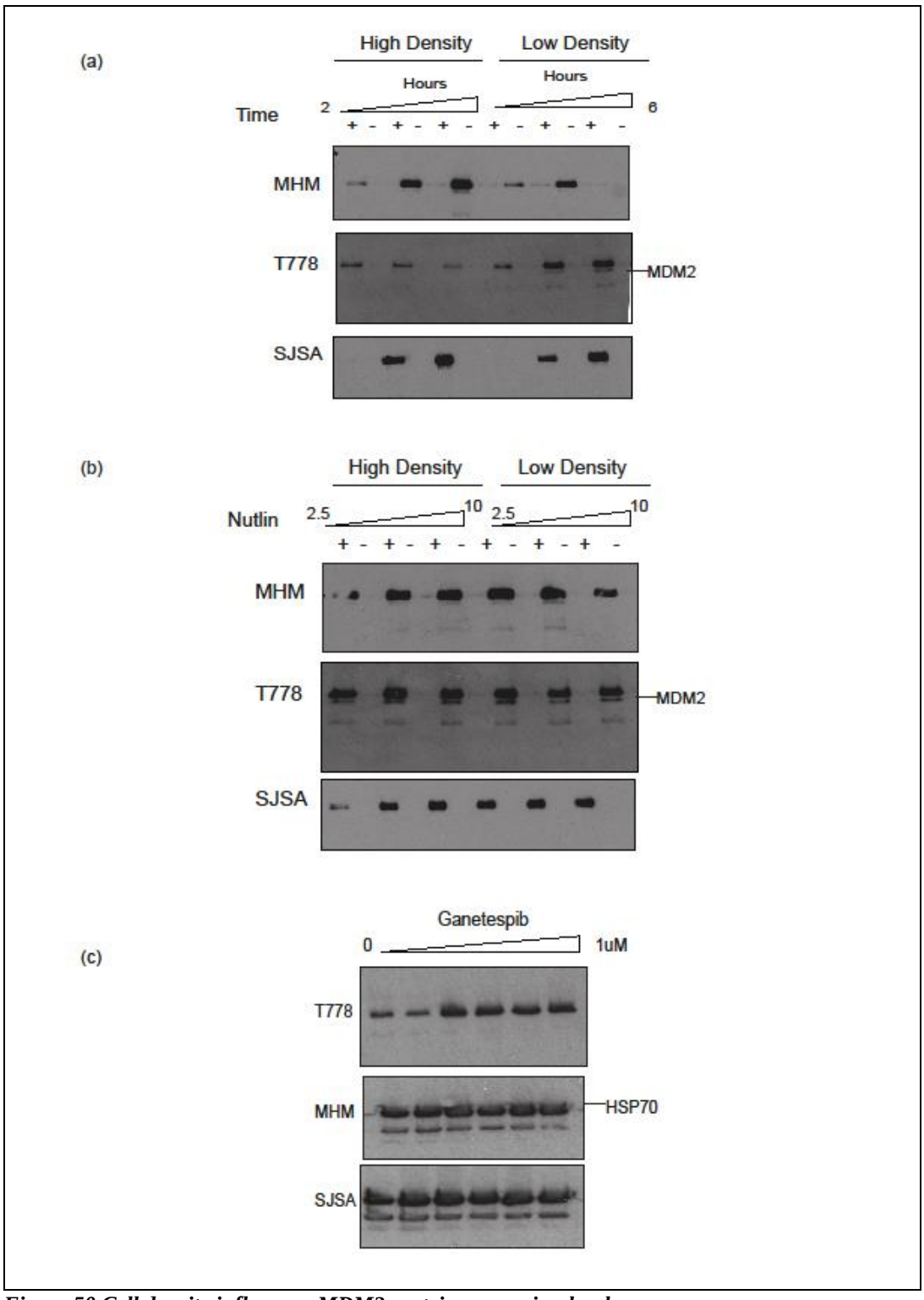

Figure 50 Cell density influences MDM2 protein expression levels

a) MHM, T778 and SJSA low and high density cells were treated with nutlin (10 uM) for 2, 4 and 6 h .The cells were isolated and total proteins extracted; MDM2 levels were determined by Western blotting (b) High (50k) and low density (10k) cells were treated with nutlin titration (2.5, 5, 10uM) as indicated on the panel. Total cell lysates were analysed for MDM2 by Western blotting. (c) The cells were treated with a Ganetespib titration (0, 25, 50,100,500,1000nM) and cell lysates analysed for HSP70.The data are representative of at least three independent experiments.

4.2.4 Ganetespib stabilises HSP/C 70 and MDM2 interaction

As the above results indicated HSP70 upregulation with Ganetespib, I wanted to determine if MDM2 had any specific interaction with HSP70. For this purpose I studied the interaction using a proximal ligation assay (PLA) assay. A375 cells were treated with either DMSO or Ganetespib for six hours prior to the PLA assay.

The results indicated a strong interaction between HSP/C70 and MDM2 (Figure 51). DMSO treatment showed interaction mainly in the cytoplasm, but with the addition of Ganetespib the number of was increased, as compared to controls, and were concentrated more in the cytosol. Nutlin treatment reduced this interaction (Figure 51a). I also examined HSP90 and MDM2 interactions as a control for the assay. The results indicated less of an interaction, compared to HSP/C70/MDM2 complexes (Figure 51b). HSP90/MDM2 interactions were in the cytosol with DMSO treatment but more nuclear when treated with Ganetespib. nutlin treatment also showed interactions between HSP90 and MDM2, and these were more nuclear in localisation. Negative controls for the assay were single antibody and BSA controls, and they gave no signal, indicating no background from the assay. The above assays were also performed on TC32 sarcoma cells with similar results (data not shown).

I also wanted to determine if these treatments changed the localisation of the HSP70 and MDM2. For this I performed an immunofluorescence localisation assay. Results indicated that MDM2 was found both in the nucleus and cytosol with DMSO and Ganetespib treatment (Figure 52a). However, with nutlin treatment I observed induction of MDM2, as compared to the DMSO control, and localisation was tightly within the nucleus. In comparison, I observed HSP70 to be exclusively within cytosol for both DMSO and Ganetespib treatments, whereas with nutlin treatment HSP70 was observed also within nucleus (Figure 52b). A secondary antibody only control gave no signal, showing that the assay didn't give any background signal. The results indicate that there is interaction between HSP70 and MDM2, and this interaction is increased by treatment of cells with Ganetespib.

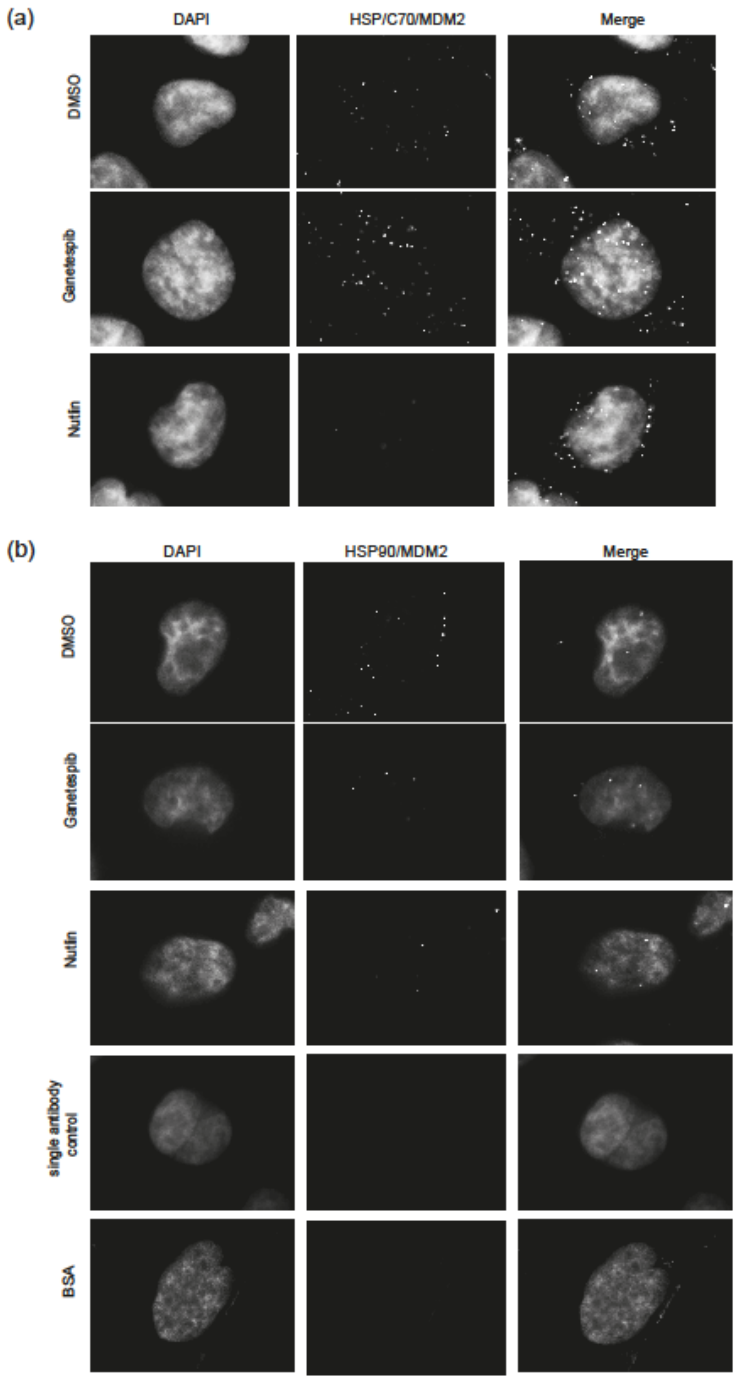

Figure 51 Ganetespib stabilises HSP/C70 and MDM2 complexes.

A375 cells were treated with1 µM nutlin, 100nM Ganetespib or DMSO for 16 h, and a proximity ligation assays (PLA) were performed using either only (a) anti-HSP70 or (b) both anti-HSP70 and anti-MDM2 antibodies. Cells were stained with DAPI (1:5000 in mounting media) and visualised using an Axioplan2 (Zeiss) fluorescent microscope (100 x magnification). Representative PLA images are shown.

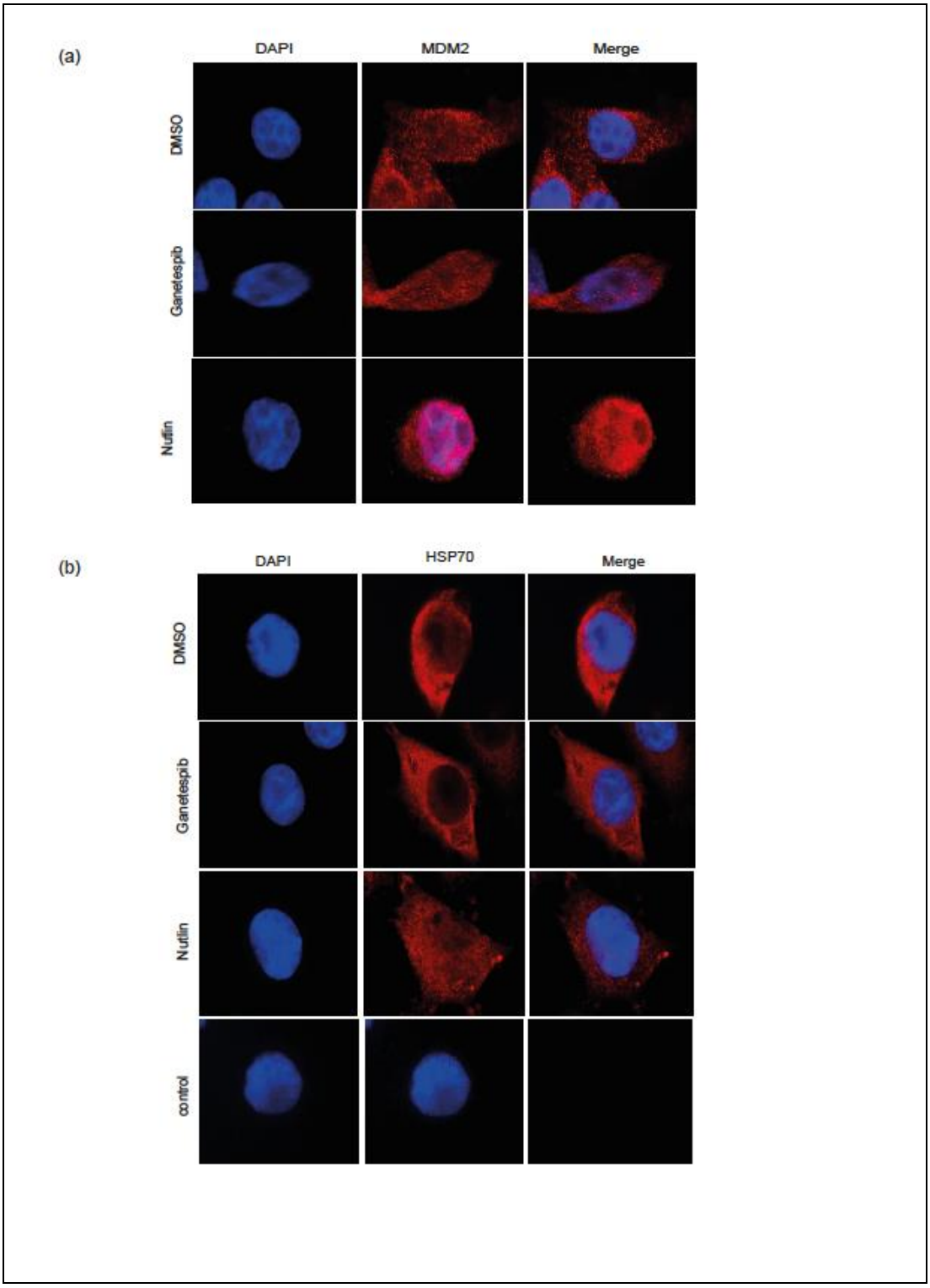

Figure 52 MDM2 and HSP70 localisation with drug treatments

A375 cells were treated with DMSO, nutlin or Ganetespib for 16 h. Cells were fixed, stained with either anti HSP70 or anti MDM2 antibody and then with secondary Alexa fluor 594 antibody, and DAPI, and visualised by IF microscopy.

4.2.5 Validation of HSC/P70 and MDM2 interaction

To detect and validate the protein–protein interaction of the E3 ligase MDM2 with HSP70, I initially performed an immunoprecipitation (co-IP) using antibody- coupled Protein G-sepharose . A375 cells were grown and harvested as per protocol. Cell pellets lysed and the pre-cleared lysate was incubated with beads bound to anti-MDM2 antibody. The eluate from the beads was run on a gel and HSP70 detected by Western blotting using anti-HSP70 antibody. There was a significant amount of HSP70 detected by Western blotting (Figure 53). The same Co-IP was performed with anti-HSP70 bound to beads and detection with MDM2 antibody. This resulted in no pull down of MDM2; this could be due to the low amount of MDM2 in A375 cells (data not shown).

To check the specificity of this interaction, Streptavidin-Binding Peptide (SBP) constructs encoding mutant HSP70 proteins were prepared (I164D, T204, D529A, V438F). The mutation V438F has a phenylalanine sterically blocking the substrate cavity, hence it is a mutant that doesn't bind substrate proteins, and thus is vital for distinguishing between specific HSP70 binders and HSP70 substrates. Its allostery and conformational changes are preserved. In contrast, I164D mutants do not induce ATP-bound HSP70 conformation changes but still bind to substrates. (Matthias P. Mayer, 2000)

I transfected the constructs into A375 cells and performed SBP pulldowns after either nutlin or Ganetespib treatment. The results indicated that the mutant proteins had altered affinity for MDM2, when compared to WT HSP70 protein. In this experiment I could pull down MDM2 with HSP70 bound to beads when cells were transfected with WT HSP70 (Figure 53b), whereas no pulldown was observed with V438F transfected samples. This mutant is unable to bind substrate and thus indicated that MDM2 was not able to bind this mutant after the sterical conformational change. In contrast, the mutants I164D, T204, and D529A, behaved similarly to the WT HSP70.

Since HSP70 binds to its substrates in the presence of ATP, the pulldown was performed with/without the presence of ATP. However this made no significant difference in the pulldown results. With DMSO and Ganetespib treatment I observed less pulldown of MDM2 for WT and I164D mutant HSP70 while high and none for D59V and V438F constructs respectively. With nutlin treatment I observed high levels of MDM2 expression for WT and I164D and low levels for D59V.There was no MDM2 pulldown with V438F. These results

were in the presence of ATP; in the absence of ATP the pulldown showed similar results but with lower expression of protein in general. Based on these results, WT HSP70 and I164D performed very similarly whereas D59V had lower MDM2 pulldown, and V438F indicated it was unable to bind to MDM2. Lysates for HSP70 and MDM2 showed high induction for all treatments. I also had two controls for transfection: a non-transfected control (c) and the pcDNA MDM2 vector control. My results indicate that MDM2 could potentially be a substrate for HSP70.

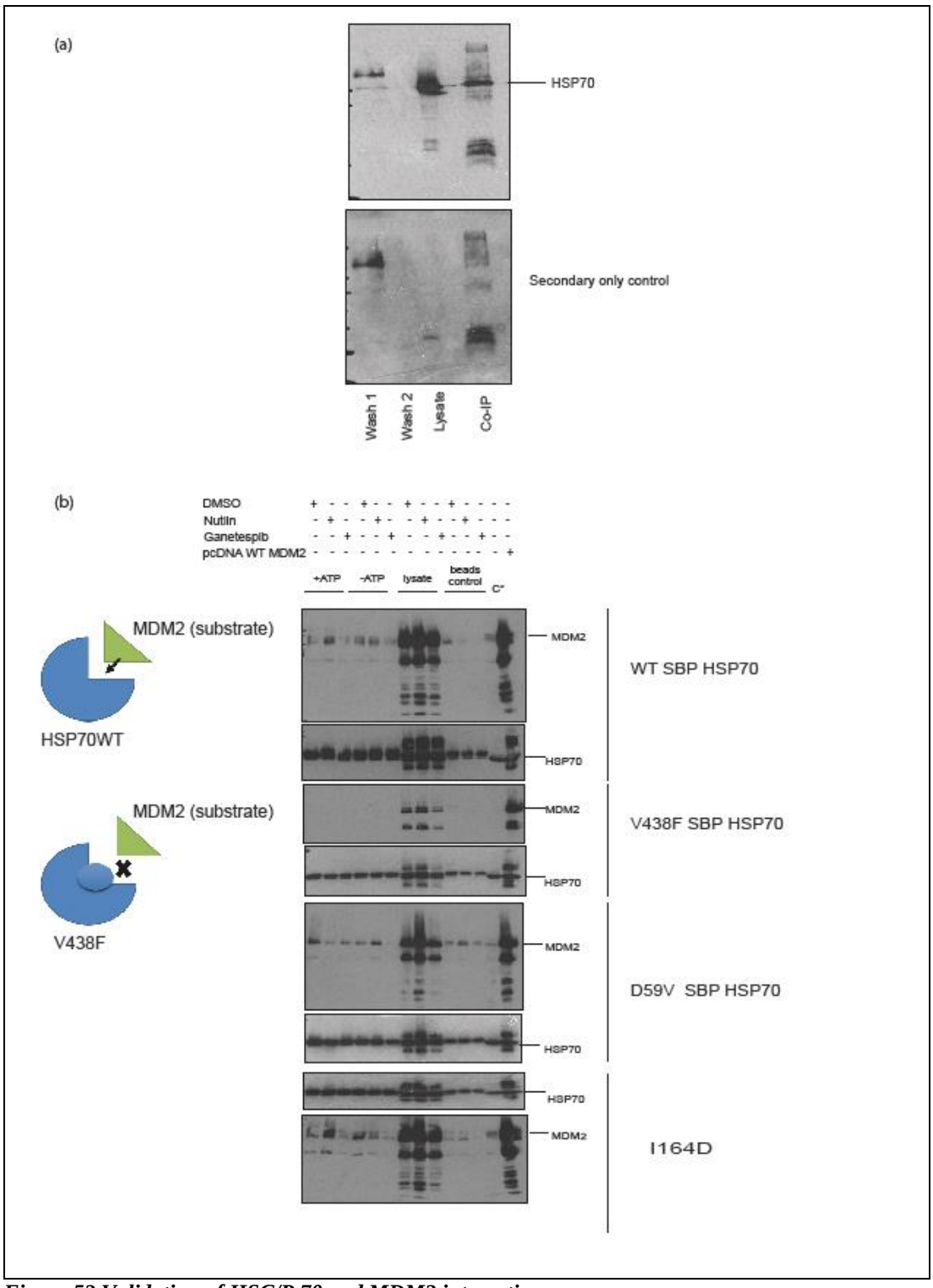

Figure 53 Validation of HSC/P 70 and MDM2 interaction

(a) Co-Immunoprecipitation assay: lysate from A375 cell lines were incubated with MDM2 antibody-bound beads. The eluate was analysed for HSP70 by Western blotting. (b) SBP pulldown assay: A375 cell lines were transfected with either WT or mutant HSP70 for 24 h then treated with either nutlin (10 uM), DMSO or Ganetespib (100 nM) for a further six and 24 h respectively. The cells were harvested and the total lysates analysed by Western blot for MDM2 and HSP70. The experiments are representative of three independent experiments.

4.2.6 Combinatorial treatment of Ganetespib with nutlin

I wanted to study whether the HSP70/MDM2 interaction had any synergistic effect with nutlin and what effect Ganetespib had on its client proteins, such as IRF-1. To determine this, I treated A375 cells with Ganetespib titration either alone, or in combination with 10uM nutlin for 16 hours. The results indicated that there was a steady loss of IRF-1 with increase in Ganetespib drug concentration (Figure 54a). When there was no nutlin treatment, the loss of IRF-1 was greatest with 100nM and almost 80% loss with doses of 50nM and 25nM and no loss of IRF-1 with 12.5nM Ganetespib. Interestingly, when nutlin was used in combination with Ganetespib there was loss of IRF-1 even with the 12.5 nM Ganetespib, compared to the DMSO control. This indicated a synergistic effect of both the drugs on IRF-1. Another interesting feature was that Ganetespib increased the total MDM2 level when used alone. MDM2 level of expression with a combination of nutlin and Ganetespib was also higher than with nutlin alone. GAPDH was used as a loading control and was similar across in all samples.

I also wanted to test the effect of the drug combination on p53, and if this effect could be seen with a shorter duration of drug treatment. I treated two sets of A375 cell lines with nutlin, DMSO or Ganetespib for six or 16 hours. The effect of Ganetespib was shown only at 16 hours and not much at 6 hours. IRF-1 depletion was seen at 16 hours and none at six hours (Figure 54b). I could also see clear induction of HSP70 with every Ganetespib treatment. At 16 hours of treatment, a combination of nutlin and Ganetespib completely reduced IRF-1, again indicating that the combination has a better effect on IRF-1 than the drugs alone. IFNγ treatment was used as a control for IRF-1 induction. P53 ubiquitination was observed with the addition of nutlin and interestingly this was attenuated when Ganetespib was used in combination for 16 hours. Similar results were observed with MDM2: induction with nutlin treatment and expression of MDM2 also increased with 16 hours of Ganetespib treatment.

I wanted to determine if these treatments changed the localisation of the proteins in the cells. For this purpose I performed immunofluorescence on A375 cell lines. Cells were treated with a titration of Ganetespib, either alone or in combination with nutlin. The results showed that IRF-1 was localised within the cytosol and membrane-bound, and the total amount decreased with increased concentration of Ganetespib (Figure 55). IRF-1 was also observed to be granulated in appearance with the drug, as compared to DMSO control. Nutlin treatment increased the IRF-1 but it was localised within cytosol and nuclear. The combination of nutlin and Ganetespib localised IRF-1 partially in cytosol and particularly in nucleus. With increased concentration of Ganetespib along with nutlin, the IRF-1 was re-localised back into the

cytosol. A BSA control gave no fluorescence, indicating that there was no background signal from the secondary antibody.

My results indicate a possible synergic effect on HSP90 client proteins when Ganetespib and nutlin are used in combination, but further work is required to confirm this conclusion.

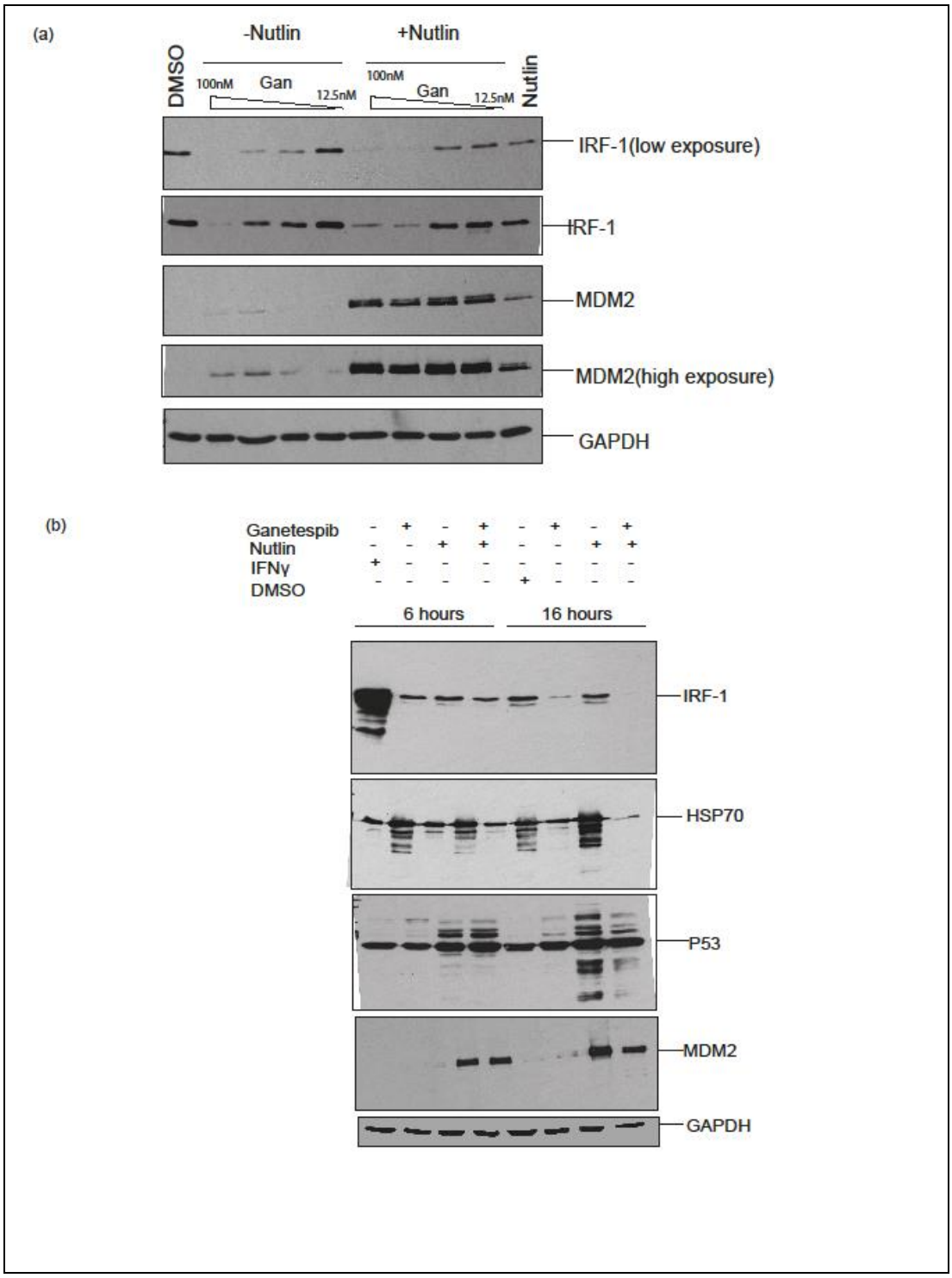

Figure 54 Combinatorial effects of nutlin and Ganetespib on IRF-1 depletion

a) A375 cells were treated with Ganetespib drug titration(12.5,25,50,100nM) +/-nutlin (10 uM) for 16 h. The cells were isolated and the total proteins extracted; MDM2, IRF-1 and GAPDH levels were determined by Western blotting. (b) A375 cells were treated with a time course of Ganetespib (6 or 16 h) +/- nutlin (10 uM). Total cell lysates were analysed for MDM2, p53, HSP70 and GAPDH by Western blotting. The data are representative of at least three independent experiments.

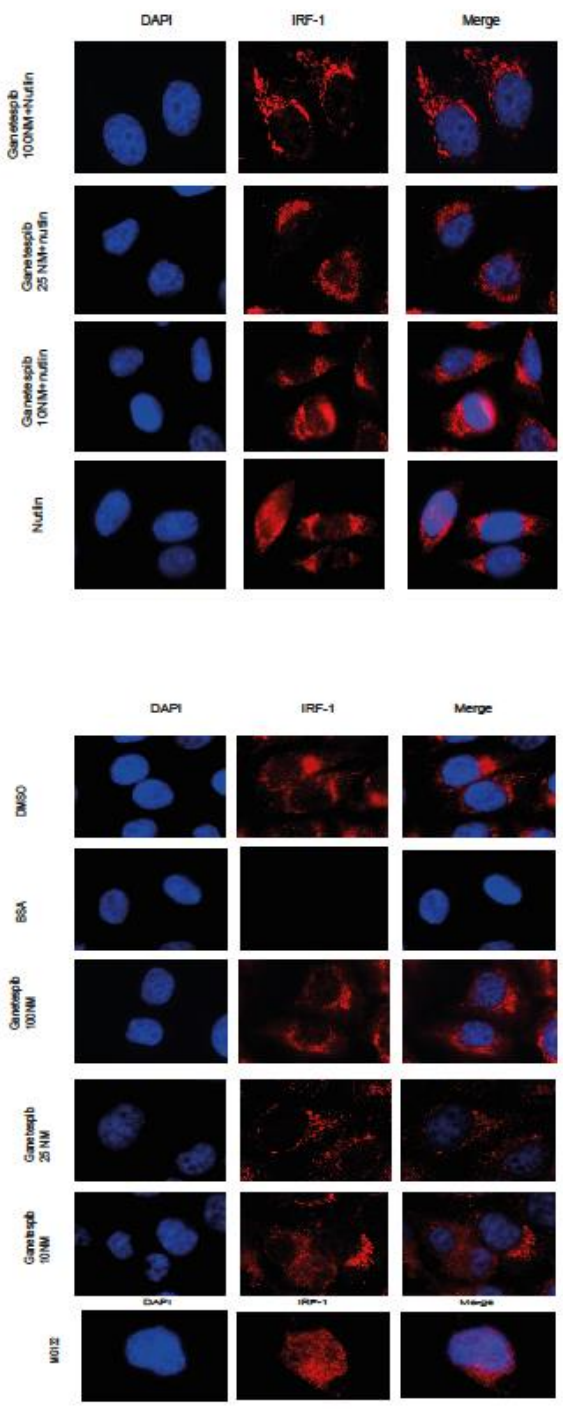

Figure 55 Effect of combinatorial treatment on IRF-1 localisation

A375 cells were treated with DMSO, nutlin or Ganetespib alone, or in combination, for 16 h as indicated in the panel. Cells were fixed, stained with anti IRF-1 antibody and secondary DAPI Alexa fluor 594, and visualised by IF microscopy.

4.2.7 Cell viability with Ganetespib and nutlin treatments

I wanted to determine the cell viability and the cell cycle checkpoint activity in the presence of Ganetespib and nutlin were used. I treated A375 cells with DMSO, Ganetespib, nutlin or combinations. Cells were washed with PBS, fixed and stained with DAPI. The stained cells were then analysed for viability and cell cycle phase using flow cytometry. There is an increase in cells at G2/M when Ganetespib is used (Figure 56a - b). The combined treatment increased the number of cells in G2/M compared with DMSO, but the number was lower than Ganetespib alone and higher than nutlin alone. The number of cells in G0/G1 was decreased significantly with Ganetespib treatment whereas nutlin increased the number of cells in this phase, and the combined treatment showed a number of cells in a range between both the treatments. Cell number in S phase was significantly lower for nutlin and combined treatment; Ganetespib treatment was similar to no treatment.

To determine cell viability we performed AlamarBlue assay using Ganetespib, nutlin and 17AAG, another class of HSP90inhibiotr drug, extensively studied in our laboratory (Narayan, 2009). The highest dose of nutlin (40uM) was highly toxic leaving only 11% live cells, while cells were unaffected in concentrations below 20µM (Figure 56c and d). 17AAG was toxic up to 2.5uM, which left only 55% live cells. In contrast, Ganetespib was safe even at 5uM. This shows that Ganetespib is less toxic than other commercially available HSP90 drugs. This also shows that Ganetespib could be used in combination therapy and would be less toxic to human cells when used with drugs such as nutlin.

The cell cycle data indicates that with Ganetespib treatment, cells are in G1 for a shorter duration, compared to nutlin- or DMSO-treated cells. Cell viability results demonstrate that Ganetespib is less toxic to the cells, compared with 17AAG, at a given concentration, and nutlin is toxic to cells at concentrations above 20uM.

(a)

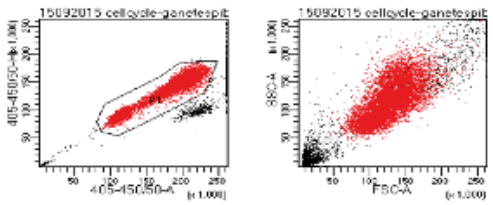

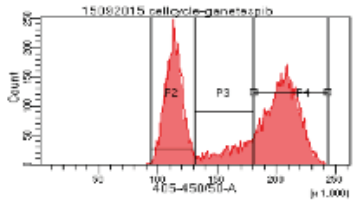

Tube: ganetespib

Population	#Events	%Parent	%Total
All Events	13,625	####	100.0
P1	10,139	74.4	74.4
P2	3,851	38.0	28.3
P3	1,271	12.5	9.3
P4	4,988	49.2	36.6

(b)

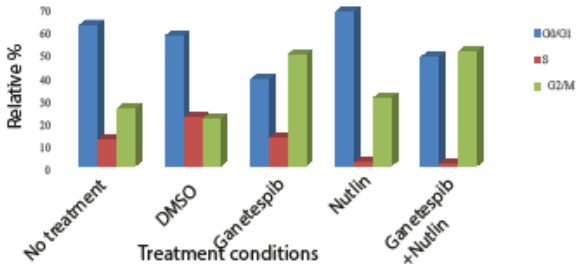

(c)

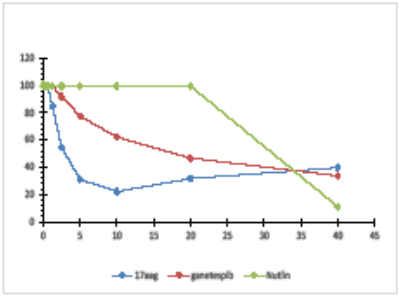

(d)

	40	20	10	5	2.5	1.25	0.625	0.3125	0.15625	0.078125	0.039063
17aag	40	32	22	31	55	85	99	99	99	99	100
ganetespib	34	47	62	78	92	99	100	99	100	100	100
Nutlin	11	99	99	99	99	99	99	99	100	100	100

Figure 56 Cell viability with nutlin and Ganetespib treatments.

A375 cells are treated with either nutlin (10 uM) or Ganetespib (100 nM) for six and 16 h respectively. The cells were resuspended and the mean fluorescence intensity (MFI) was measured using flow cytometry (a) Gates and MFI results (b) graphical representation of the data from (a). (c) And (d) Alamar blue assay to determine the cell viability of A375 cells when the cells are treated with a drug titration (40 uM–40nM) of nutlin, 17AAG or Ganetespib for 16 h.

4.2.8 Discussion

The results indicated that there is increased expression of MDM2 with nutlin, and p53 is stably monoubiquitinated, following activation by nutlin-3. My results also suggested using pARF to overcome the effect of nutlin-3 on p53 ubiquitination through a process that involves MDM2. I have also discussed the importance of buffer conditions for studying ubiquitination. My results indicated that the HSP90 inhibitor drug Ganetespib can be effective for Ewing sarcoma, and could be used either alone or in combination with other treatments. Since the drug does not require functional p53 to lower EWS-FLi1, Ganetespib could potentially be used for both WT and mutant p53 sarcomas. The expression of MDM2 with nutlin activation will be governed by several factors such as the tumour type and cell density at which the drug treatment is performed and hence each experiment must be optimised based on these considerations. My results indicate that there is a novel interaction between HSP/C70 and MDM2, and this interaction is stabilised with Ganetespib. This interaction was also validated using HSP70 WT and specific mutants lacking substrate-binding capability. Cell viability results demonstrate that Ganetespib is less toxic to the cells, compared with 17AAG at a given concentration, and nutlin is toxic to cells at concentrations above 20uM. I have also shown that there is a potential synergistic effect on HSP90 client proteins when Ganetespib and nutlin are used in combination.

5 Mechanism of downregulation of IRF-1 with ganetespib

5.1 Introduction

5.1.1 IRF-1

Interferon regulatory factor -1 (IRF-1), is the founding member of the interferon (IFN) regulatory factor family and was originally identified as a key regulator of type I interferons. IRF-1 levels are regulated at the transcriptional level in response to various stimuli such as IFNs (type I and type II), double-stranded RNA, cytokines, and hormones. By virtue of its affinity for a specific DNA sequence, IRF-1 participates in the transcription of various IRF-1-inducible genes. Through the activities of its various functional domains, IRF-1 is suggested to provide a link between innate and adoptive immune systems and plays a critical role in various physiological and pathological aspects, including viral infection, oncogenesis, proinflammatory injury, development of immune system and autoimmunity (Dou, 2014)

IRF-1 inactivation by deletion of one or more exons, or loss of one IRF-1 allele, has been reported in various cancer types. Unlike the classic tumour suppressor genes, loss of IRF-1 alleles alone rarely induces tumour development, however, IRF-1 deficiency significantly increases the incidence of tumours in combination with other genetic alterations. The mechanisms by which IRF-1 mediates tumour suppression is thought to be via activation of target genes associated with regulation of the cell cycle, apoptosis and the immune response to impact on tumour susceptibility and progression. IRF-1 and p53 regulate DNA damage-induced apoptosis, both cooperatively and independently, depending on the type and differentiation stage of the cell (Dou, 2014). In certain cancer types IRF-1 acts as a tumour promoter rather than tumour suppressor (Gerard M. Doherty, 2001)

5.1.2 Molecular chaperons and IRF-1

The early clinical hypothesis for inhibiting HSP90 in cancers was based on the dependence of certain key client proteins in malignant cells – including a host of well-characterized oncoproteins – on the activity of HSP90 for their function and stability. An additional concept

that has been established is that cancer cells have heightened dependence on the efficient maintenance of intracellular proteomic homeostasis, the central components of which are HSP90 and other heat shock proteins (Travers, 2012). In this chapter I investigate the loss of IRF-1 using the HSP90 inhibitor Ganetespib to explore if the downregulation of IRF-1 with Ganetespib is via autophagy and/or the proteosomal degradation pathway.

Autophagy is a highly regulated catabolic pathway responsible for the degradation of long-lived proteins and damaged intracellular organelles, and thereby maintains cellular homeostatsis. A key biological marker identifying autophagy in mammalian systems is the microtubule associated protein 1A/1B-light chain 3 (LC3). During autophagy, cytosolic LC3-1 is conjugated to phosphatidylethanolamine to form LC3-II. This is then recruited and incorporated into the autophagosomal membrane. Methods that have traditionally been used to measure LC3 include Western blot analysis and fluorescence microscopy (Pugsley, 2016) (Qian, 2016) (Schaaf, 2016). The cargo signals that are selectively recognized by autophagy receptors are diverse but can be broadly grouped into two classes: ubiquitin-dependent cargo recognition and ubiquitin-independent recognition. (Mancias, 2016).

Here I investigate the role of IRF-1 as a client of HSP90 and ask what is the mechanism involved in the downregulation of the protein in response to the HSP90 inhibitor Ganetespib.

5.2 Results

5.2.1 Inhibition of HSP90 leads of reduction of client protein levels

It has been demonstrated previously by various groups that HSP90 inhibitors (HSP90i) can lead to the loss of HSP90 client proteins (Narayan, 2009) (Seo, 2015). In the previous chapter I established that there is a downregulation of IRF-1 at the protein level with Ganetespib treatment and therefore I wanted to compare Ganetespib with previously used HSP90 inhibitors belonging to different classes of drug (for example 17AAG and radicicol). The rationale behind this was to determine whether the loss of IRF-1 I observed was specific to Ganetespib or if other inhibitors also had the same effect.

I used two well-studied HSP90 inhibitor drugs, 17AAG and radicicol. 17AAG is a derivative of the antibiotic geldanamycin, while radicicol is a natural product, which binds to HSP90 and alters its function (national cancer institute, 2016) (Narayan, 2009). These represent different classes of HSP90 drugs. The A375 cell line was chosen for these assays and a range of doses for both drugs was tested, with the highest dose being 100 nM. Cells were treated for six hours and were tested initially for HSP70 induction, as this is a sensitive indicator of HSP90 inhibition. HSP70 protein was detected by immunoblot and showed there was enhanced induction with increasing dose for both the drugs (Figure 57a). As both drugs led to a similar induction of the HSP70 protein, only 17AAG was used in subsequent experiments.

I next directly compared Ganetespib with 17AAG to determine if there was a dose dependent effect on IRF-1 similar to that previously reported by the Ball group for 17AAG (Narayan, 2009). A dose titration of both drugs was performed in A375 cells for 16 hours. The results were similar for both of the HSP90 inhibitor drugs; Ganetespib appeared to be more potent as it could downregulateIRF-1 to a greater extent than 17AAG at a given dose (Figure 57b). A low dose of Ganetespib (100 nM) could almost completely downregulate IRF-1 while 17AAG, even the highest dose tested (10 uM), couldn't downregulate IRF-1 to the same extent. HSP90 protein levels showed a decrease with increased drug concentration when cells were treated with Ganetespib and probed with anti-HSP90 polyclonal antibody (Figure 57b) to detect total HSP90 protein. Phosphospecific-HSP90 antibody or anti-HSP90 (alpha+beta isoforms) showed no significant difference across the titration for either drug. By comparison, HSP70 induction was observed for both drugs, but with Ganetespib the induction occurred across all

the concentrations whereas for 17AAG it wasn't observed for higher doses. There was no significant change in p53 levels with either drug, suggesting that IRF-1 is much more sensitive to HSP90 inhibition than p53, which has also been described as an HSP90 client protein. GAPDH was used as an internal control and was consistent throughout all the samples in both the drug treatments.

I wanted to investigate other client proteins of HSP90, and the effect of Ganetespib on them. I selected CDK4 and EGFR, and when A375 cells were treated with (100 nM) Ganetespib for 16 hours both proteins where reduced in level (Figure 57c). In comparison, Nutlin increased EGFR expression and reduced CDK4 expression when compared to DMSO/no treatment controls. A combination of Nutlin and Ganetespib reduced CDK4 expression further than did Ganetespib alone; the same combination increased EGFR when compared to DMSO or Ganetespib treatment. Again, GAPDH was used a control and was consistent in all the different treatments.

The above experiments show that IRF-1 is very sensitive to HSP90 inhibition and is down regulated similarly to the well-characterised HSP90 client proteins like CDK4 and EGFR, at similar doses of Ganetespib, whereas p53 is less sensitive to HSP90 inhibition in the cells used.

To extend my study I next investigated the effect Ganetespib on HSP90 in terms of its localisation within the cell. I performed immunofluorescence microscopy and used three different antibodies that detect different forms of HSP90: a pan-HSP90 polyclonal serum detecting all isoforms; a HSP90 isoform alpha + beta specific antibody; and an anti-phospho-HSP90. In the controls, HSP90 localised in the cytoplasm with all three antibodies. However, when the cells were treated with Ganetespib (100 nM) for six hours I observed HSP90 shift from the cytoplasm into the nucleus with all three antibodies, although to a lesser extent for the phospho-HSP90 isoform (Figure 58). When the cells were treated with Nutlin, the polyclonal and alpha + beta antibodies showed HSP90 in cytoplasm, whereas the phospho-HSP90 antibody showed a more nuclear localisation. This suggests phosphorylation may regulate HSP90 localisation.

These results indicated that Ganetespib performed similarly to other class of HSP90 inhibitors as a modulator of IRF-1 levels. I also showed that Ganetespib is a more potent effector of IRF-1 than 17AAG at a given dose in the nM concentration range.

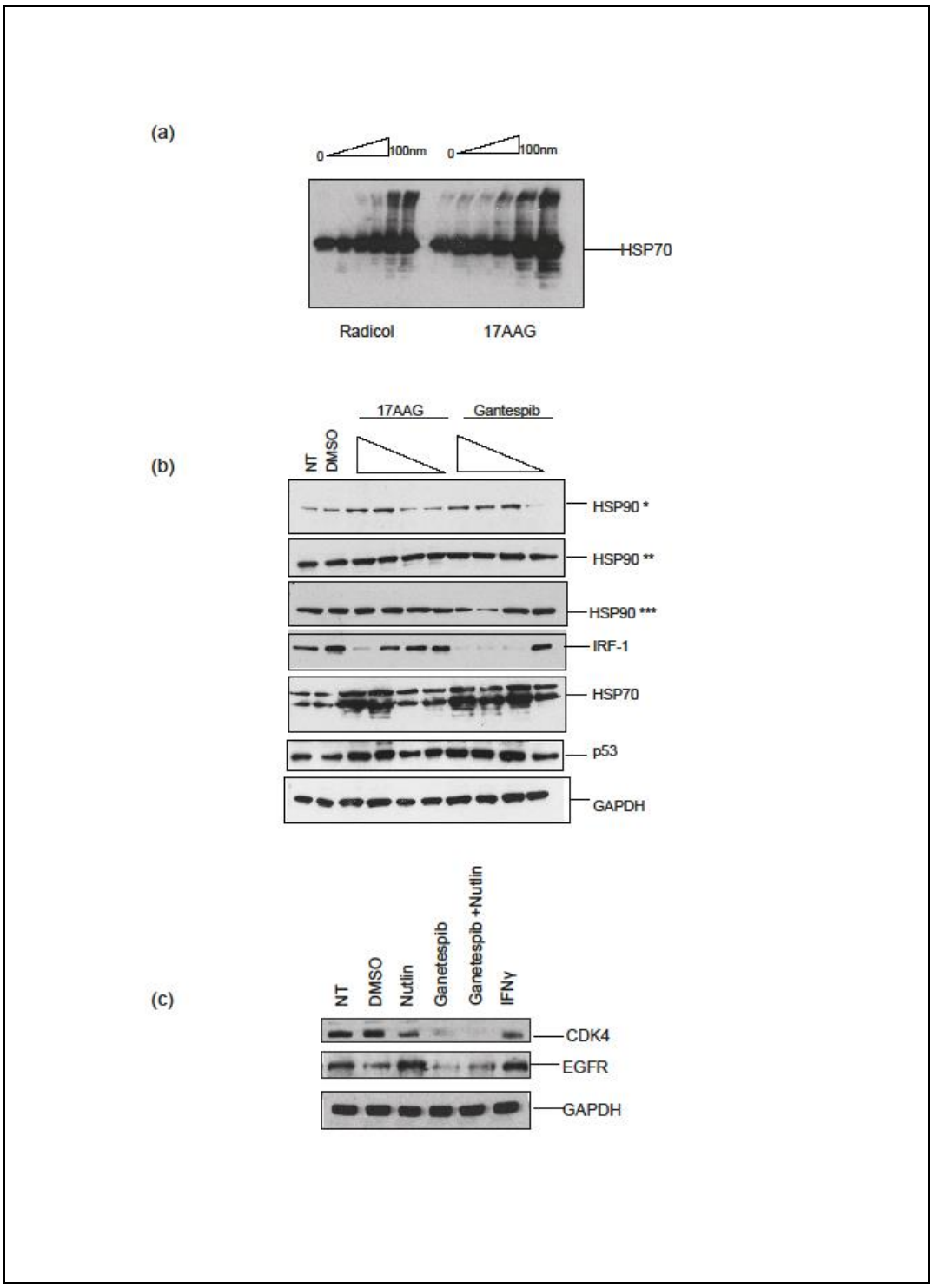

Figure 57 HSP90 inhibitor downregulates client proteins

(a) A375 melanoma cells were treated with a dose titration of 17AAG or Radicol (12.5, 25, 50,100 nM) for six hr. The cells were isolated and total proteins extracted. HSP70 levels were determined by Western blot analysis. (b) A375 cells were treated with a dose titration of Ganetespib or 17AAG (0.1, 1, 10 and 0uM) for 16 h. The cells were isolated and the total proteins extracted. HSP70, HSP90, p53, IRF-1 and GAPDH levels were determined by Western blot analysis. * Hsp90, **Hsp90 phospho, ***Hsp90 (alpha+beta) forms. (c) A375 cells were treated with Nutlin (10μM), Ganetespib (100nM), IFNγ (100 ng/ml) either alone or in combination for 16 h. CDK4 and EGFR levels were determined by Western blot analysis. The data are representative of at least three independent experiments.

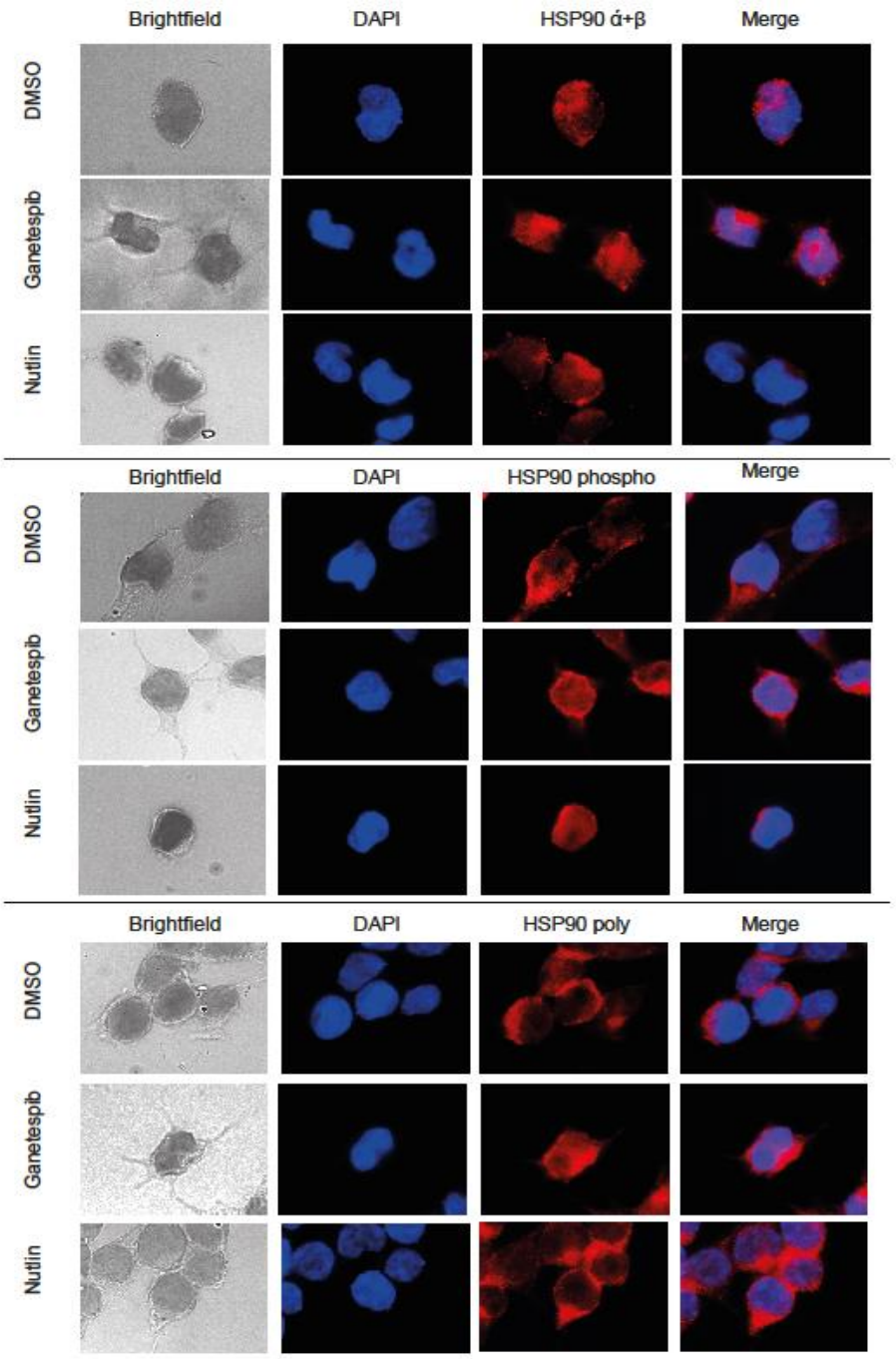

Figure 58 HSP90 localisation in A375 cell lines

(a) A375 melanoma cells were treated with DMSO, Ganetespib (100nM), or Nutlin (10 μM) for six h. Cells were fixed, stained with either anti HSP90 (α+β), or HSP90 phospho or polyclonal antibody and then with appropriate secondary Alexa fluor 594 antibody and DAPI and imaged by IF microscopy. The data are representative of at least three independent experiments.

5.2.2 Attenuation of IRF-1 is p53-independent

Previous studies have showed a cooperative relationship between IRF-1 and p53, and unpublished data from the Ball group found that IRF-1 was a p53 responsive gene in the double-stranded RNA activation pathway. I therefore wanted to establish whether p53 was required for the effect of Ganetespib on IRF-1 protein levels ((David Dornan, 2004).

I was interested to learn if the inhibition of IRF-1 was a p53 dependent pathway. I used an isogeneic p53-null A375 cell line (These are p53 null cells generated by Li R in Prof Ted Hupp's laboratory using CRISPR technology). The cells were treated with Ganetespib, Nutlin or DMSO, alone or in combination for 16 hours. I observed that even in the absence of functional p53, IRF-1 was depleted in the presence of Ganetespib (Figure 59).

A combination of Nutlin and Ganetespib had no significant effect on MDM2 levels in the p53 -/- cells. Nutlin treatment alone did not induce MDM2 in the absence of p53, which is expected as only WT p53 can induce MDM2 (Muller, 2008). HSP70 induction was seen with increasing doses of Ganetespib. GAPDH was used as an internal control and was similar in all samples.

This result indicates that the loss of IRF-1 with Ganetespib treatment is a p53 independent mechanism. This feature makes Ganetespib a versatile treatment, as it has the potential to modulate IRF-1 in both WT and p53 mutant cancer cell backgrounds.

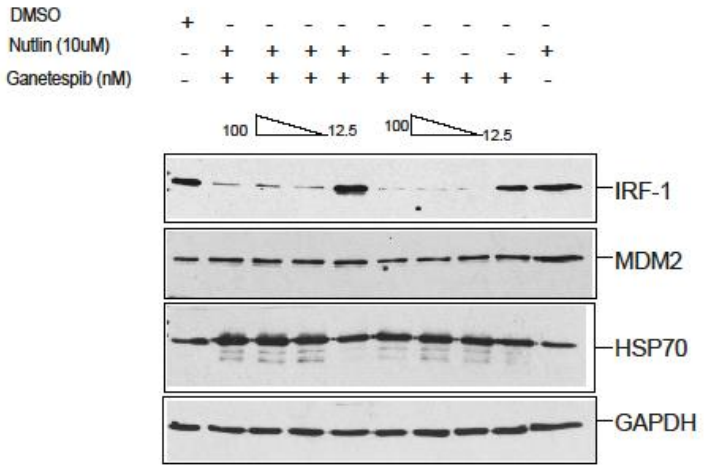

Figure 59 Loss of IRF-1 is a p53 independent mechanism

A375 p53-/- cells were treated with a dose titration of Ganetespib for 16 h (100, 50, 25, 12.5, 0nM) with or without Nutlin (10 μM). The cells were isolated and total proteins extracted. IRF-1, MDM2, HSP70 and GAPDH levels were determined by Western blot analysis. The data are representative of at least three independent experiments.

5.2.3 Downregulation of IRF-1 is affected by proteasome inhibitors

To investigate the mechanism by which IRF-1 protein was lost in Ganetespib treated cells I first determined whether loss of IRF-1 represented a change in its solubility. I analysed both the soluble (cell lysates) and insoluble fractions (cell pellets) after cells were treated with DMSO, Ganetespib, or both. The majority of the IRF-1 protein was in the soluble fractions and a negligible amount was in the insoluble fraction (Figure 60a). IRF-1 expression in the insoluble fraction was not increased by Ganetespib treatment. This ruled out the possibility that Ganetespib altered the solubility ofIRF-1 rather than its absolute levels.

To investigate if the downregulation of IRF-1 by Ganetespib involved a proteasome-dependent mechanism I asked whether blocking the proteasome with an inhibitor would rescue IRF-1 protein levels. I pre-treated A375 cells with Ganetespib for four hours then added MG132 for a further two hours. Cells treated with Ganetespib and MG132 and did not down regulate IRF-1 compared to cells treated with Ganetespib alone, indicating rescue of IRF-1 by MG132 (Figure 60b). By blocking the proteasome, MDM2 levels were also increased, compared to those in the DMSO control, consistent with MDM2 being degraded by the proteasome in control cells. Again, Ganetespib had no significant effect on MDM2 either alone or in combination with MG132.

The data presented here suggests that IRF-1 loss can be rescued by inhibiting the proteasome. As basal IRF-1 is degraded via an ubiquitin-dependent mechanism (Pion, 2009) these data implicated an important role for E3-ubiquitin ligases in the Ganetespib-stimulated loss of IRF-1 protein.

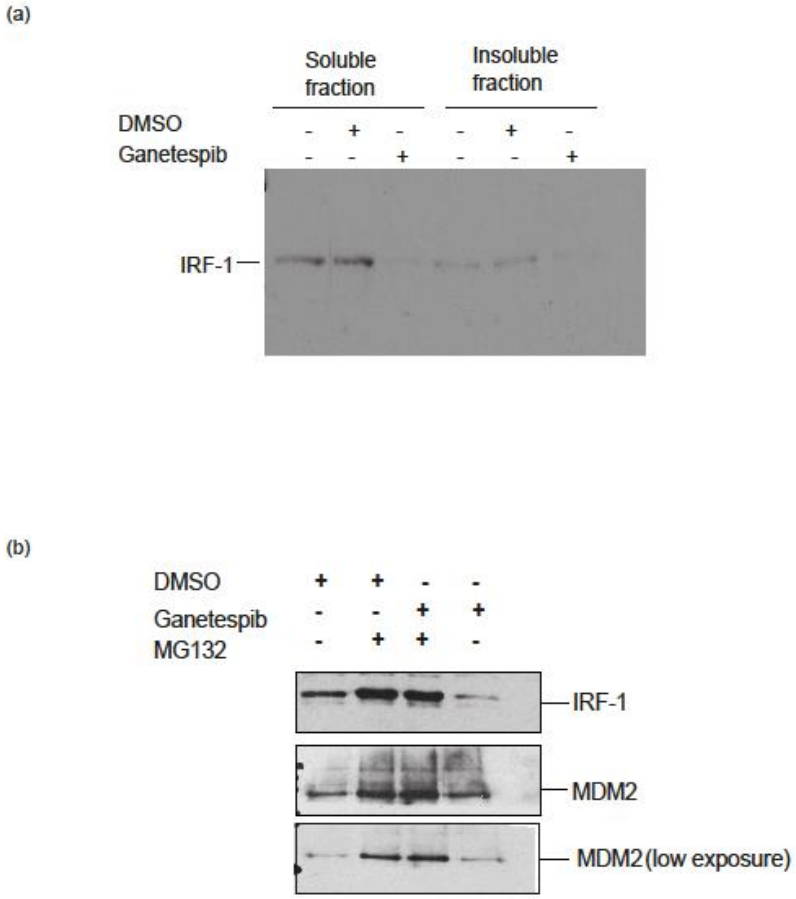

Figure 60 Attenuation of IRF-1 is post-translational

(a) A375 cells were treated with either DMSO or Ganetespib for 16 h. The cell lysates (soluble fraction) and cell pellets (insoluble fraction) were analysed by Western blot for IRF-1 levels. The data are representative of at least three independent experiments. (b) A375 cells were pre-treated with Ganetespib (100 nM) for four h prior to the addition of MG132 (50 µM) for further two hours. Cell lysates were isolated and total protein extracted. IRF-1 and MDM2 levels were analysed by Western blot.

5.2.4 Role of E3 ligases in IRF-1 downregulation

My data indicated that IRF-1 protein levels are very sensitive to HSP90 inhibition by Ganetespib and that this can be rescued by MG132, implicating the ubiquitin-mediated proteosomal degradation pathway. To investigate the mechanism further I evaluated the E3 ligase(s) involved in this degradation pathway.

The two known E3 ligases for IRF-1 are CHIP and MDM2 (Narayan, 2011; Landres, 2013). Both these E3-ligases are known to associate with the core molecular chaperone machinery. CHIP was first identified as an HSP/C70 binding protein that can also bind to HSP90, and MDM2 has been shown to bind both HSP90 and HSP70 ((Burch, 2004)) ((Wiech, 2012). In the absence of HSP90 activity, less stable proteins, like IRF-1, which require chaperoning by HSP90, (Narayan, 2009) can become unfolded and preferentially associate in a complex with HSP70 and chaperone-associated ligases such as CHIP and MDM2 (muller, 2008), which then target them for ubiquitin mediated degradation. I investigated whether these E3 ligases had any interactions with HSP70 in Ganetespib treated cells.

I first performed proximal ligation assays (PLA) for endogenous HSP/C70 and MDM2. I observed a striking induction of HSP/C70/MDM2 complexes when cells were treated with Ganetespib for six hours, compared to the DMSO control (Figure 61a). These complexes were predominantly cytoplasmic. In comparison, in cells treated with Nutlin there were fewer HSP70/MDM2 complexes and they were more nuclear in localisation.

Subsequently I measured complexes between CHIP and HSP70; results indicated no significant increase in total complex number following Ganetespib treatment but complexes were redistributed and found predominantly in the cytoplasm (Figure 62). In cells treated with Nutlin the CHIP/HSP70 complexes were very similar to those in the DMSO control, with few complexes equally distributed between cytoplasm and nucleus.

As both HSP70/MDM2 and HSP70/CHIP complexes were predominantly found in the cytoplasm of Ganetespib treated cells, consistent with a role in IRF-1 degradation which takes place in the cytoplasm (Emmanuelle Pion, 2009), I wanted to study MDM2 and CHIP interaction when A375 cell lines were treated with the drug. In contrast to the HSP70/MDM2 complexes, the CHIP/MDM2 interactions were nuclear and appeared to be membrane bound

in the control DMSO treated cells (Figure 63). With Ganetespib treatment the complexes were observed within the nucleus. The single antibody control gave no PLA signal and the BSA control gave very few PLA spots indicating a low background signal in the assay (Figure 63). Thus, although CHIP and MDM2 can be found in the same complexes, these are in the nucleus whereas the HSP70-E3-ligase complexes are in the cytoplasm, where IRF-1 is degraded.

To complement the PLA analysis I determined the localisation of MDM2 and CHIP using immunofluorescence. MDM2 localisation was strongly cytoplasmic and showed no significant changes with Nutlin or Ganetespib treatment compared to the DMSO control (Figure 64). CHIP was observed to be cytoplasmic with DMSO and Ganetespib treatment, and more nuclear with Nutlin. The secondary-only control showed no signal indicating no background fluorescence from antibodies.

The data in this section suggest that in the presence of Ganetespib the two known E3-ligases for IRF-1, namely CHIP and MDM2, can be found in complex with HSP70. The HSP70/E3-ligase complexes are predominantly found in the cytoplasm consistent with a role in the degradation of HSP90 client proteins under conditions where HSP90 activity has been inhibited, causing them to become unfolded and subsequently detected by HSP70-containing degradation complexes.

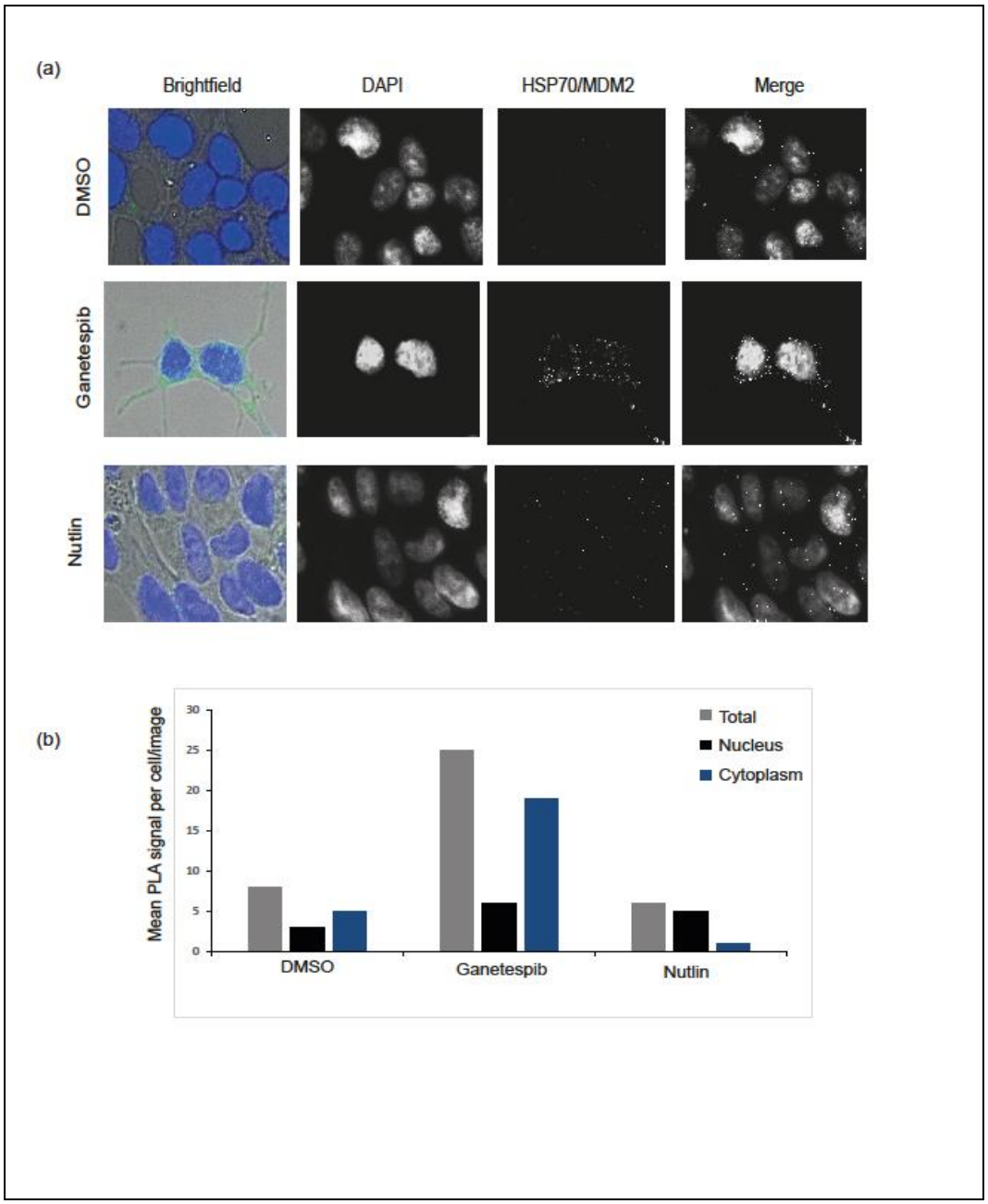

Figure 61Proximity ligation assay system detects induced HSP70 and MDM2 interaction with Ganetespib

(a) A375 cells were treated with DMSO, Ganetespib (100 nM) or Nutlin (10 μM) for six h, and a proximity ligation assay (PLA) using only HSP70 or both HSP70 and anti-MDM2 antibodies was performed. Cells were stained with DAPI (1:5000 in mounting media) and visualised using an Axioplan2 (Zeiss) fluorescent microscope (100 x magnification). Representative PLA images are shown. (b) Graphical quantification of the PLA results from (a). The data are representative of at least three independent experiments and the graphical quantification of PLA results is average of at least 4 different fields.

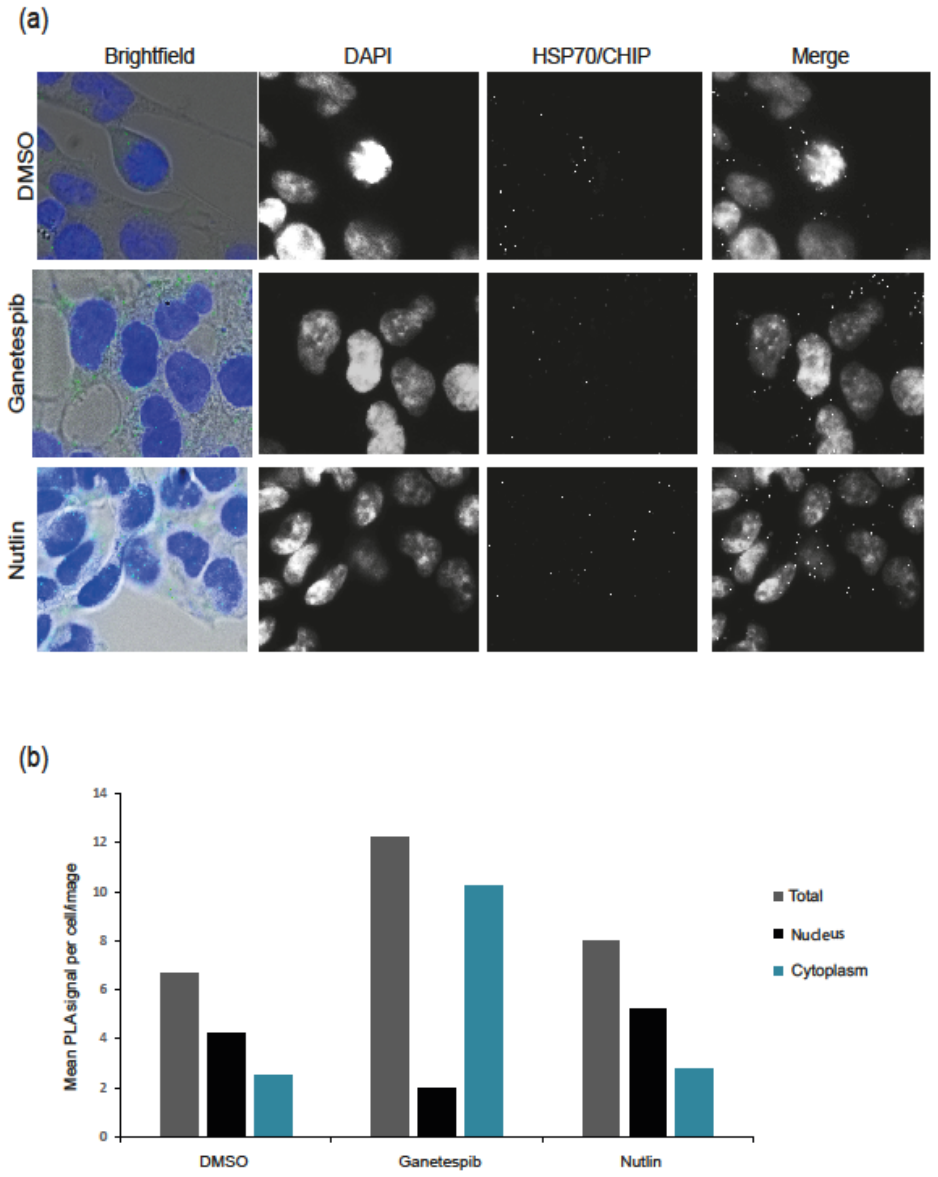

Figure 62 Proximity ligation assay system detects HSP70 and CHIP interaction with Ganetespib and Nutlin treatment

(a) A375 cells were treated with DMSO, Ganetespib (100 nM) or Nutlin (10 μM) for six hours, and a proximity ligation (PLA) assay using either only HSP70 or both HSP70 and anti-CHIP antibodies were performed. Cells were stained with DAPI (1:5000 in mounting media) and visualised using an Axioplan2 (Zeiss) fluorescent microscope (100 x magnification). Representative PLA images are shown. (b) Graphical quantification of the PLA results from (a). The data are representative of at least three independent experiments and the graphical quantification of PLA results is average of at least four different fields.

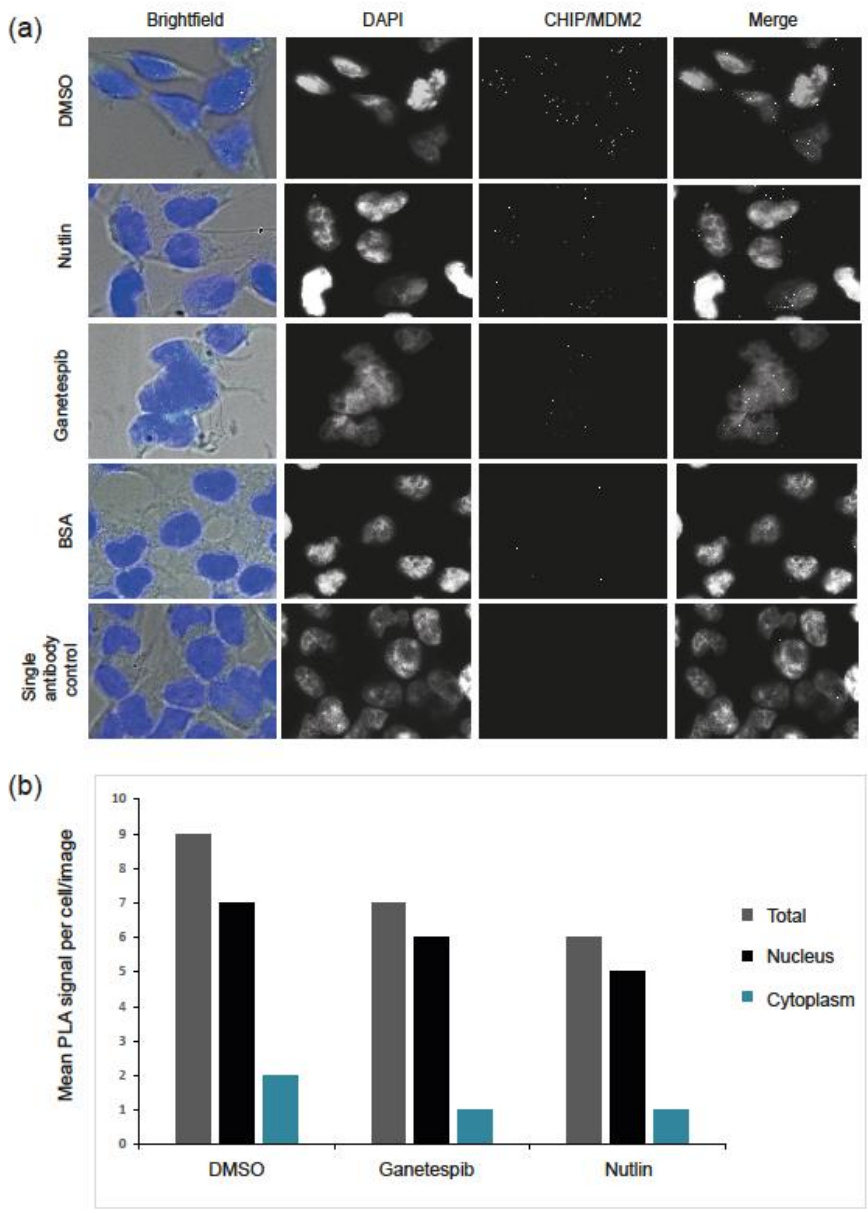

Figure 63 PLA system detects MDM2 and CHIP interaction with Ganetespib and Nutlin treatment

(a) A375 cells were treated with DMSO, Ganetespib (100 nM) or Nutlin (10 μM) for six hours, and proximity ligation assays (PLA) using only CHIP or both CHIP and anti-MDM2 antibodies was performed. Cells were stained with DAPI (1:5000 in mounting media) and visualised using an Axioplan2 (Zeiss) fluorescent microscope (100 x magnification). Representative PLA images are shown. (b) Graphical quantification of the PLA results from (a). The data are representative of at least three independent experiments and the graphical quantification of PLA results is average of at least four different fields.

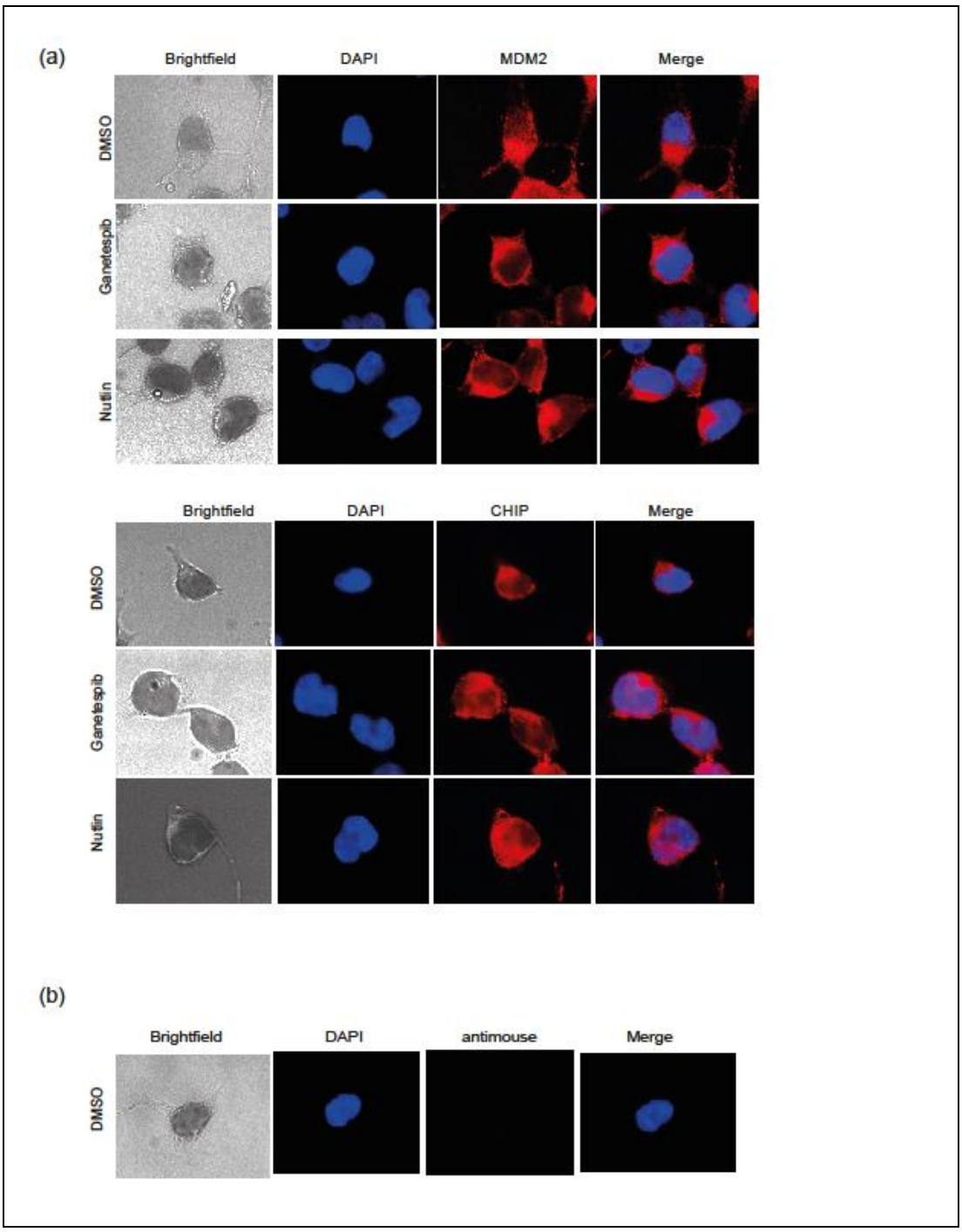

Figure 64 Localisation of MDM2 and CHIP with Ganetespib and Nutlin treatment

(a) A375 cells were treated with either DMSO, Nutlin (10 μM) or Ganetespib (100 nM) for six hours. Cells were fixed, stained with either anti CHIP antibody or anti MDM2 antibody and then with appropriate secondary DAPI Alexa fluor 594 and visualised by IF microscopy. (b) Cells were fixed and stained with only DAPI Alexa fluor 594 secondary antibody. The data are representative of at least three independent experiments.

5.2.5 CHIP and MDM2 Knock-down

The data presented above shows that CHIP and MDM2 are found in association with HSP70 in Ganetespib treated cells. To evaluate if these chaperone/E3 ligase complexes where responsible for the degradation of IRF-1 I wished to knock down these two ligases using siRNA. First, I treated A375 cells with siRNA targeting MDM2 for 24 hours prior to the addition of Ganetespib, which was present for a further 24 hours. The siRNA treatment knocked down MDM2 by at least 50% when compared to the untreated control or the siRNA negative control. The results indicated that down regulation of MDM2 failed to stimulate recovery of IRF-1 protein levels after Ganetespib treatment (Figure 65 a), under conditions where p53 levels where elevated by the down regulation of MDM2. The increase in p53 showed that the 50% decrease in MDM2 was sufficient to affect the levels of its major E3-ligase activity target. This suggests that MDM2 probably is not the E3-ligase involved in IRF-1 loss. Rather, loss of MDM2 cooperated with Ganetespib, and IRF-1 protein levels decreased even further with the combined treatment. This result was consistently reproducible.

The next E3 ligase to study was CHIP; I knocked down CHIP in A375 cells using siRNA. The cells were treated with siRNA for 24 hours prior to the addition of Ganetespib for a further 24 hours. There was more than a 90% reduction in the expression of CHIP when the cells were treated with siRNA (Figure 65 b). A negative siRNA control gave the same CHIP expression of as the DMSO control. Again IRF-1 expression could not be recovered by the down regulation of CHIP. This indicated that the downregulation of IRF-1 was not under the control of the CHIP ligase. However, I did observe a small but reproducible effect of combined Ganetespib and CHIP siRNA treatment, compared with Ganetespib alone, where IRF-1 was further reduced consistent with CHIP having a positive regulatory role in IRF-1 steady state levels under some cellular conditions (Narayan, 2011).

Finally, as chaperone associated E3-ligases are thought to be redundant checked if a double knock-down of MDM2 and CHIP could make any difference to the levels of IRF-1 after Ganetespib treatment. The cells were treated with both the siRNA to MDM2 and CHIP for 24 hours prior to the addition of Ganetespib for a further 24 hours. The results indicated that neither the single knock down nor the double knock down of MDM2 and CHIP recovered the downregulated IRF-1 after Ganetespib treatment (Figure 65 C). There was significant knock down of CHIP and MDM2 with the respective siRNAs. Downregulation of IRF-1 was observed with Ganetespib and, as shown above, treatment with both Ganetespib and siRNA to MDM2 had the greatest effect on IRF-1 levels.

The data provide evidence that IRF-1 downregulation was not mediated via CHIP/MDM2 as E3 ligases. However, the data lent support to the theory that MDM2 can support IRF-1 function (Landres, 2013) and that this could be through its chaperone activity when working with HSP90 (Narayan, 2009)((Burch, 2004)((Wawrzynow, 2007) In this case the data suggest that HSP70/MDM2 complexes formed in the cytoplasm are not involved the degradation of IRF-1 but that, in fact, the complex could be inhibitory for the IRF-1 chaperoning function of MDM2, and that this in exaggerated when MDM2 activity is further reduced, for example by using MDM2 targeted siRNA.

To investigate this further I tested whether the HSP70/MDM2 complexes where made up of classic stress-inducible HSP70 isoforms or the constitutive HSP70 isoform, HSC70. The HSP70 antibody detects different forms of HSP70 including HSC70. Since I observed a strong interaction between HSP/C70 and MDM2 with Ganetespib treatment of I wanted to confirm if this was due to HSC70 or HSP70. I used HSC70 and HSP70 specific antibodies for a PLA. The results indicated that there was a robust induction of complexes between MDM2 and HSC70, but not HSP70, when the cells were treated with Ganetespib (Figure 66). Both HSC70 and HSP70 complexes were cytoplasmic with Ganetespib treatment. When cells were treated with DMSO, HSC70/MDM2 complexes were predominantly nuclear and there were no detectable complexes for HSP70/MDM2. BSA controls showed no PLA spots, and the single antibody control gave very few PLA spots.

The above result suggests that MDM2 is specifically associated with HSC70, rather than HSP70, as expected, in cells where HSP90 has been inhibited. These data may therefore explain why MDM2 is not involved in IRF-1 degradation despite being found in HSP70 chaperoning complexes after HSP90 inhibition, as it is HSP70 isoforms rather than HSC70 that are usually associated with detecting and mediating the degradation of unfolded proteins via the proteasome. HSC70, on the other hand, is involved in chaperone-mediated autophagy ((Chiang HL, 1989).

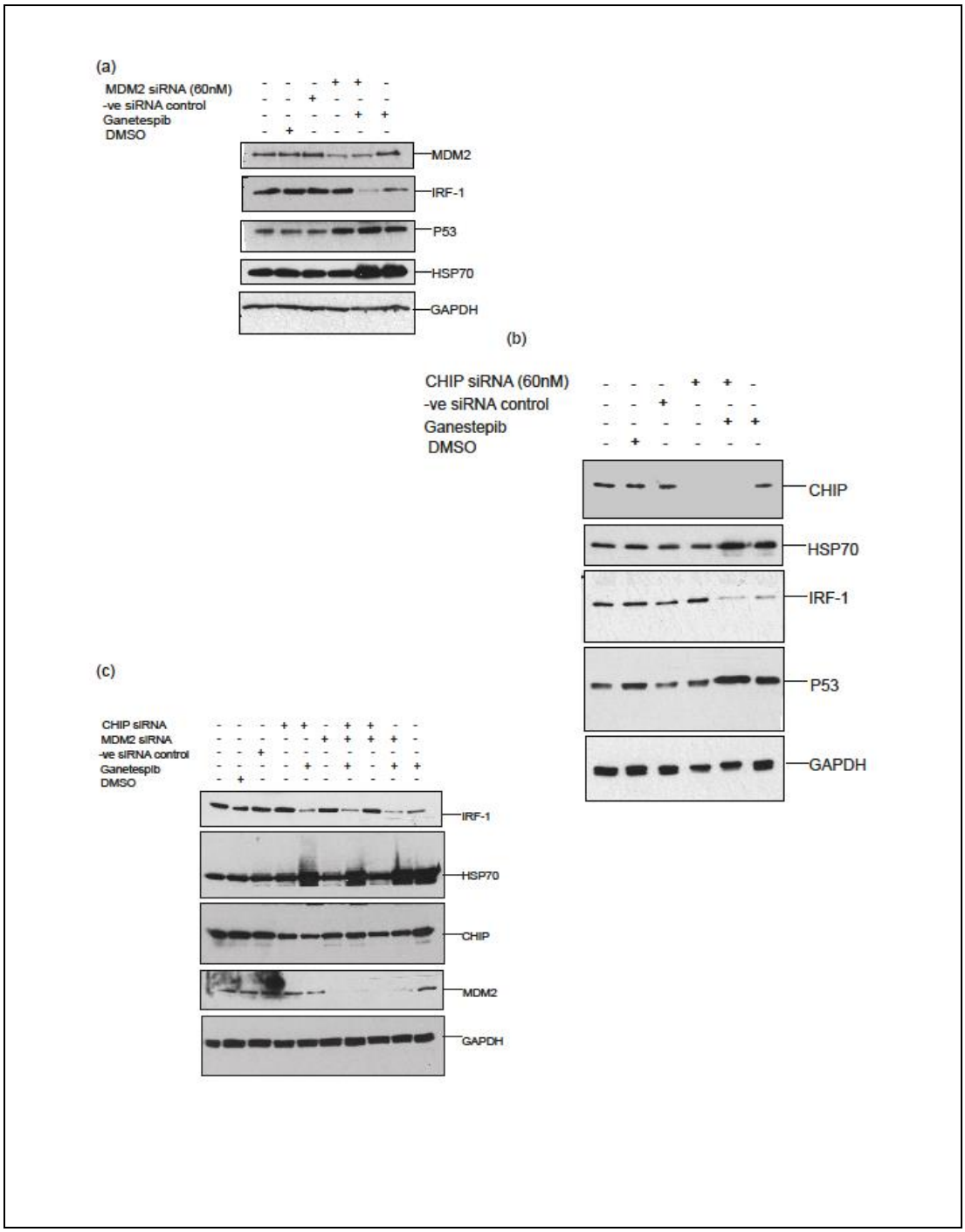

Figure 65 Role of CHIP and MDM2 in downregulation of IRF-1 with Ganetespib treatment

A375 cells were treated with either control siRNA, siRNA to (a) MDM2 (60nM) or (b) CHIP (60 nM) for 24 h and then treated with Ganetespib (100 nM) or DMSO for further 24 h. Total cell lysates analysed for MDM2, CHIP, HSP70, p53, IRF-1 and GAPDH via Western blotting. *(c)* A375 cells were treated with either control siRNA or siRNA to MDM2 (60nM) and CHIP (60 nM) for 24 h and then treated with Ganetespib (100 nM) or DMSO for further 24 h. Total cell lysates analysed via Western blot as above. The data are representative of at least three independent experiments.

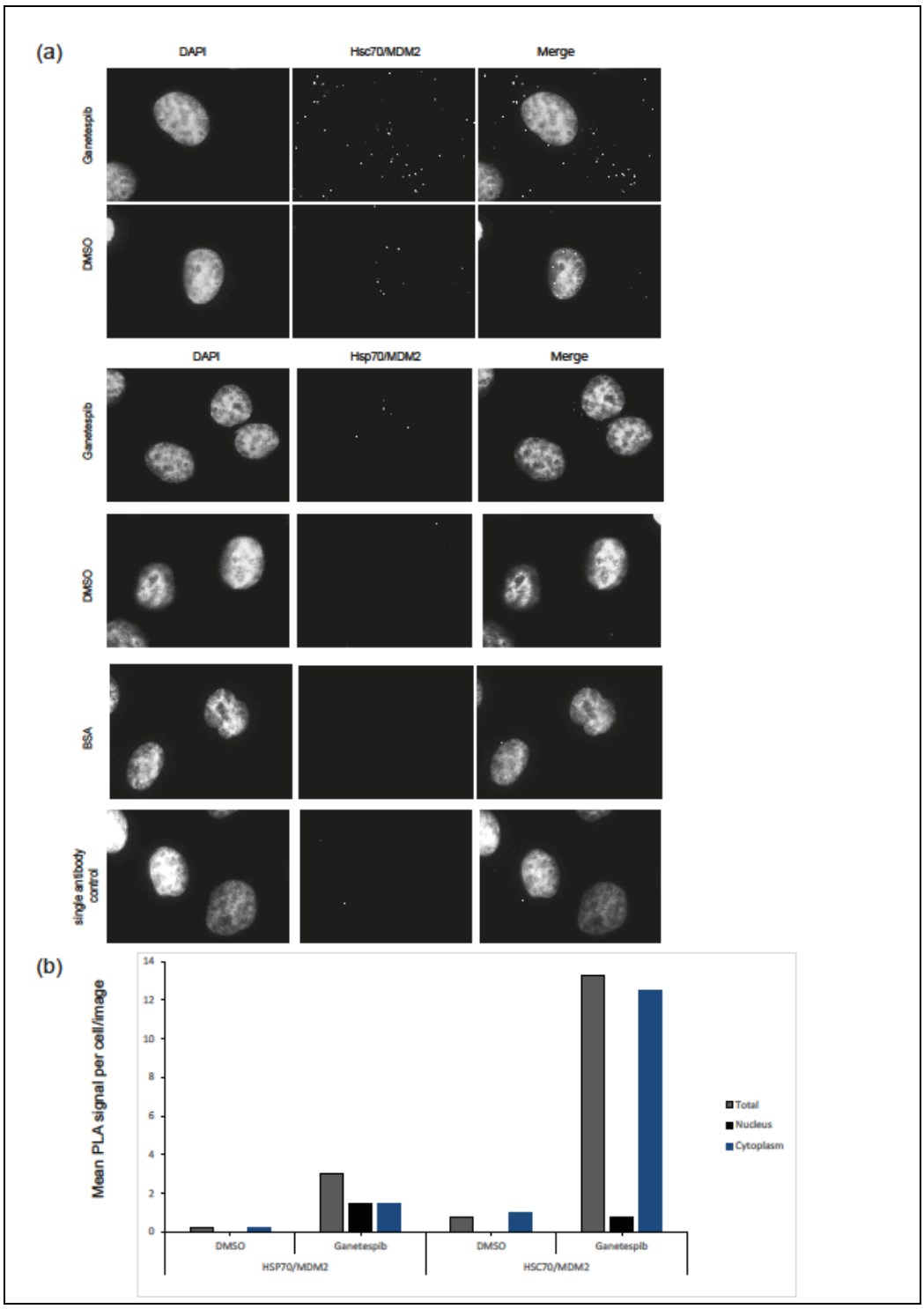

Figure 66 Proximity ligation assay detects induced HSC70/MDM2 interaction with Ganetespib treatment

(a) A375 cells were treated with DMSO, Ganetespib (100 nM) for six hours, and a proximity ligation assay (PLA) using either HSP70/MDM2 or HSC70/MDM2 antibodies were performed. Cells were stained with DAPI (1:5000 in mounting media) and visualised using an Axioplan2 (Zeiss) fluorescent microscope (100 x magnification). Representative PLA images are shown. (b) Graphical quantification of the PLA results from (a). The data are representative of at least three independent experiments and the graphical quantification of PLA results is average of at least four different fields.

5.2.6 Chaperone mediated autophagy

Data in the previous section suggests that IRF-1 degradation is not mediated by the known IRF-1 E3-ligases CHIP and MDM2. This was surprising as both of these ligases are known to mediate the degradation of HSP90 client proteins. This suggests that either a new chaperone associated IRF-1 E3-ligase is involved, or that a novel degradation pathway for IRF-1 has been uncovered. Recent studies suggest that proteasome and autophagy pathways for degradation are highly integrated and interdependent and that inhibition of one pathway can feedback to the other ((Lilienbaum, 2013)). In addition, although I observed that MG132 could rescue IRF-1 loss in some experiments this was not always consistent, and sometimes there was only a partial rescue, suggesting that additional IRF-1 degradation pathways exist.

Melanomas have high levels of basal autophagosomes suggestive of increased autophagy. Patients with melanomas with higher levels of autophagosomes have decreased survival (Amaravadi, 2016). I showed in CHAPTER 6 that PD-L1 was sensitive to autophagy pathway modulation and above I found that HSC70, the major mediator of chaperone mediated autophagy (CMA), formed protein complexes (with MDM2) in response to Ganetespib. I therefore decided to determine if autophagy played a role in the down regulation of IRF-1 as the Ball group have previously shown that IRF-1 contains an HSC70 specific binding sequence (Narayan, 2009) and unpublished data)

I investigated if there was any interaction between IRF-1 and HSP70 using PLA to analysis this. Results indicated induction of IRF-1/HSP70 complexes in Ganetespib treated cells compared to the DMSO control (Figure 67 a). These complexes were cytoplasmic, consistent with a role in IRF-1 degradation. As total IRF-1 protein levels are already decreasing at the time point tested, I wanted to combine Ganetespib with MG132 (to block IRF-1 loss) to get the real picture for HSP70/IRF-1 complex number under conditions where IRF-1 was not being degraded. When the cells were treated with MG132 alone to inhibit basal IRF-1 degradation, which is known to occur through the ubiquitin-proteasome pathway (Pion, 2009), I observed increased number of IRF-1/HSP/C70 complexes but these were more nuclear in

localisation. Addition of MG132 to Ganetespib treated cells showed that Ganetespib could drive IRF-1 into HSP/C70-containing complexes and they were located in the cytoplasm. DMSO treated cells showed no significant interaction between IRF-1 and HSP70.

The data suggest that IRF-1 is specifically found in complex with HSP/C70 in Ganetespib treated cells, and these complexes are in the cytoplasm suggesting they could be involved in IRF-1 degradation. Interestingly, location of HSP/C70/IRF-1 complexes in the cytoplasm in response to Ganetespib takes precedence over MG132, as complexes formed in response to proteasome inhibition are mainly found in the nucleus.

I also wanted to investigate if the localisation of the total proteins changed with drug treatment. For this I performed an immunofluorescence assay. In the DMSO control I observed strong IRF-1 expression in the cytoplasm towards the cell membrane, whereas with Ganetespib treatment there was a loss of IRF-1 staining, consistent with the immunoblot results (Figure 67 b). Treatment with Nutlin also reduced IRF-1 expression compared to the DMSO control, but did not change the localisation. When the cells were treated with Ganetespib along with Nutlin there was no significant change in IRF-1 expression compared to Ganetespib treated cells.

HSP/C70 was observed to be cytoplasmic in DMSO treated cells and with Ganetespib treatment there was induction of HSP/C70 and it was more localised in the nucleus (Figure 67 c). The levels of HSP/C70 with Nutlin treatment were comparable that to DMSO controls. The BSA control showed no background signal from the secondary antibody.

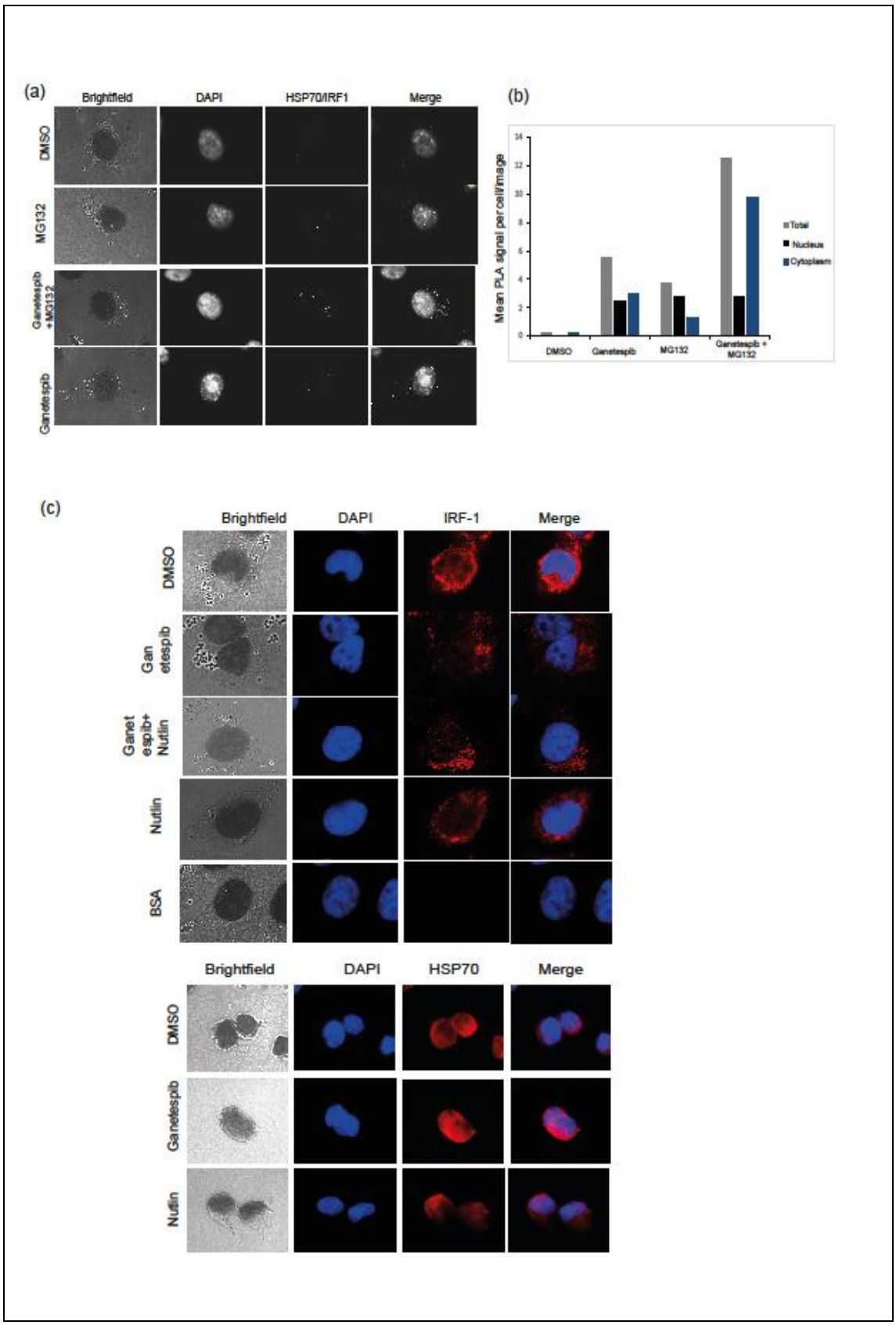

Figure 67 IRF-1 and HSP70 interactions with Ganetespib treatment

(a) A375 cells were treated with DMSO, Ganetespib (100 nM) for four h and then with MG132 (50 uM) for further two h, and a proximity ligation assay (PLA) using only HSP70 or both HSP70 and anti-IRF-1 antibodies was performed. Cells were stained with DAPI (1:5000 in mounting media) and examined using an Axioplan2 (Zeiss) fluorescent microscope (100 x magnification). Representative PLA images are shown. (b) Graphical quantification of results from (a). (c) A375 cells were treated with Ganetespib (100 nM), Nutlin (10μM) or DMSO for six h. Cells were fixed, stained with either anti IRF-1 or HSP70 antibody and then with appropriate secondary DAPI Alexa fluor 594 and visualised by IF microscopy. The data are representative of at least three independent experiments.

5.2.7 HSP90 inhibitors and autophagy

As I observed the induction of IRF-1 and HSP70 complexes under conditions where IRF-1 was being actively degraded by Ganetespib treatment, I wanted to investigate if attenuation of IRF-1 could involve CMA in addition to the ubiquitin–proteasome pathway. For this purpose I used the autophagy inhibitors chloroquine and 3MA.

A375 cells were treated with DMSO, Ganetespib and chloroquine, either alone or in combination, for 16 hours. The results indicated that HSP70 was induced with Ganetespib alone but not with chloroquine (Figure 68 a). I observed LC3 induction with Ganetespib and chloroquine when compared to the DMSO control. Consistent with earlier data showing that Ganetespib promotes HSC70 containing complexes (with MDM2) this result indicated that Ganetespib is either inducing an autophagy pathway, or inhibiting it and increasing the LC3-II levels. The p53 levels were shown to increase to some extent with the use of Ganetespib but not with chloroquine, when compared to the DMSO control. IRF-1 levels were not affected by chloroquine and remained at DMSO control levels. Ganetespib downregulated IRF-1 levels, and using chloroquine in combination with Ganetespib did not recover IRF-1, indicating the downregulation of IRF-1 under the conditions used was not chloroquine sensitive.

To confirm that IRF-1 did not respond to autophagy inhibition I used a second inhibitor 3MA in combination with Ganetespib. The control was DMSO carrier, and IFNγ was used as a positive control for IRF-1 induction as several bands where detected using the IRF-1 MAb in some experiments. Chloroquine and 3MA by themselves induced LC3 when compared to DMSO or no treatment controls (Figure 68 b). I observed that LC3-II induction was higher than LC3-I in both the treatment conditions. There were no significant changes to IRF-1 or HSP70 when cells were treated with either chloroquine or 3MA, compared to no treatment controls. The cells treated with Ganetespib downregulated IRF-1, as expected, and also induced HSP70. Interestingly, I saw a LC3-I induction with Ganetespib, and the combination treatment with chloroquine increased both LC3-I and II. This suggested that chloroquine increased LC3-II while Ganetespib contributed towards the LC3-I induction. The cells treated with Ganetespib, IFNγ and chloroquine had the same LC3 induction as with Ganetespib + chloroquine and the IFNγ made no difference .There was also downregulation of IRF-1 and induction of HSP70 with the above combination treatment. I then used 3MA and Ganetespib together which showed the same effect as Ganetespib alone. The combination of 3MA,

Ganetespib and IFNγ treatments downregulated IRF-1 to a level below that seen with Ganetespib treatment alone. Again the data suggest autophagy is not required for IRF-1 down regulation and that, if anything, inhibition of autophagy enhances IRF-1 loss.

To confirm that an active autophagy pathway was not required for Ganetespib-activated suppression of IRF-1 levels I used ATG5 knock-out cells. The knock-out was performed by Simon Wilkinson's group using CRISPR gene editing in an A549 cell background. When the cells were treated with Ganetespib, I observed downregulation of IRF-1 in both WT and knock-out cell lines, but to a different extent. There was more downregulation of IRF-1 in ATG5 null cells compared to the WT A549 cell lines (Figure 68 c), which is consistent with the observation that autophagy inhibitors may enhance the effect of Ganetespib in the experiments presented above. In general, the downregulation of IRF-1 was less pronounced in A549 cells compared to A375 cells. It could be that the drug requires different optimisation in this cell type or that it works more effectively in a melanoma cell line. I also observed a higher molecular weight IRF-1 band in the WT A549 cell line, but only a single band in the knock-out cell lines. It would be interesting to investigate this further to see if the upper IRF-1 band is a modified form that is lost in the mutant cells, as IRF-1 transcriptional activity has been implicated in autophagy ((Liang J, 2015)). Alternatively the difference could be due to clonal variation, as the knock-out line has been generated from a single knock-out cell.

I wanted to explore the interaction of HSC70/MDM2 in the presence of the autophagy inhibitors and I used PLA to study this interaction in A375 cells treated with Ganetespib, chloroquine and MG132, either alone or in combination. MG132 plus chloroquine were added four hours after Ganetespib treatment. In the DMSO control there were few HSC70/MDM2 complexes and, as expected from earlier experiments, Ganetespib treatment led to an induction of the complexes that were localised in the cytoplasm (Figure 69). Less expected was that chloroquine appeared to prevent the formation of Ganetespib-dependent HSC70/MDM2 complexes, whereas MG132 enhanced complex formation. This is potentially interesting and will be followed up by the Ball laboratory as it could indicate that MDM2 binding to HSC70 plays a role in autophagy and that blocking the autophagy pathway feeds back to prevent complex formation.

In summary, my data show that: (i) MG132 can be used to rescue Ganetespib-induced degradation of IRF-1 under some conditions; (ii) Ganetespib leads to the induction of HSP/C70/IRF-1 complexes whereas complexes between IRF-1 and CHIP or MDM2 are not

induced under these conditions (not shown) and the HSP/C70/IRF-1 complexes can be stabilised by the addition of MG132, suggesting they may be involved in targeting IRF-1 for degradation. However, neither of the known IRF-1 E3-ligases are responsible for IRF-1 degradation and inhibition of the autophagy pathway, if anything, enhances rather than attenuates the effect of Ganetespib on IRF-1 protein levels. Together the data therefore suggest that IRF-1 is degraded by a novel Ganetespib-sensitive pathway. As there are approximityly 500 E3-ubiquitin ligases, it is not feasible to take a systematic approach to identify components of a novel IRF-1 degradation pathway. With only limited time remaining in my PhD I therefore decided to see if I could narrow down potential regulators of IRF-1 by determining the effect of Ganetespib on the whole cell proteome by mass spectrometry.

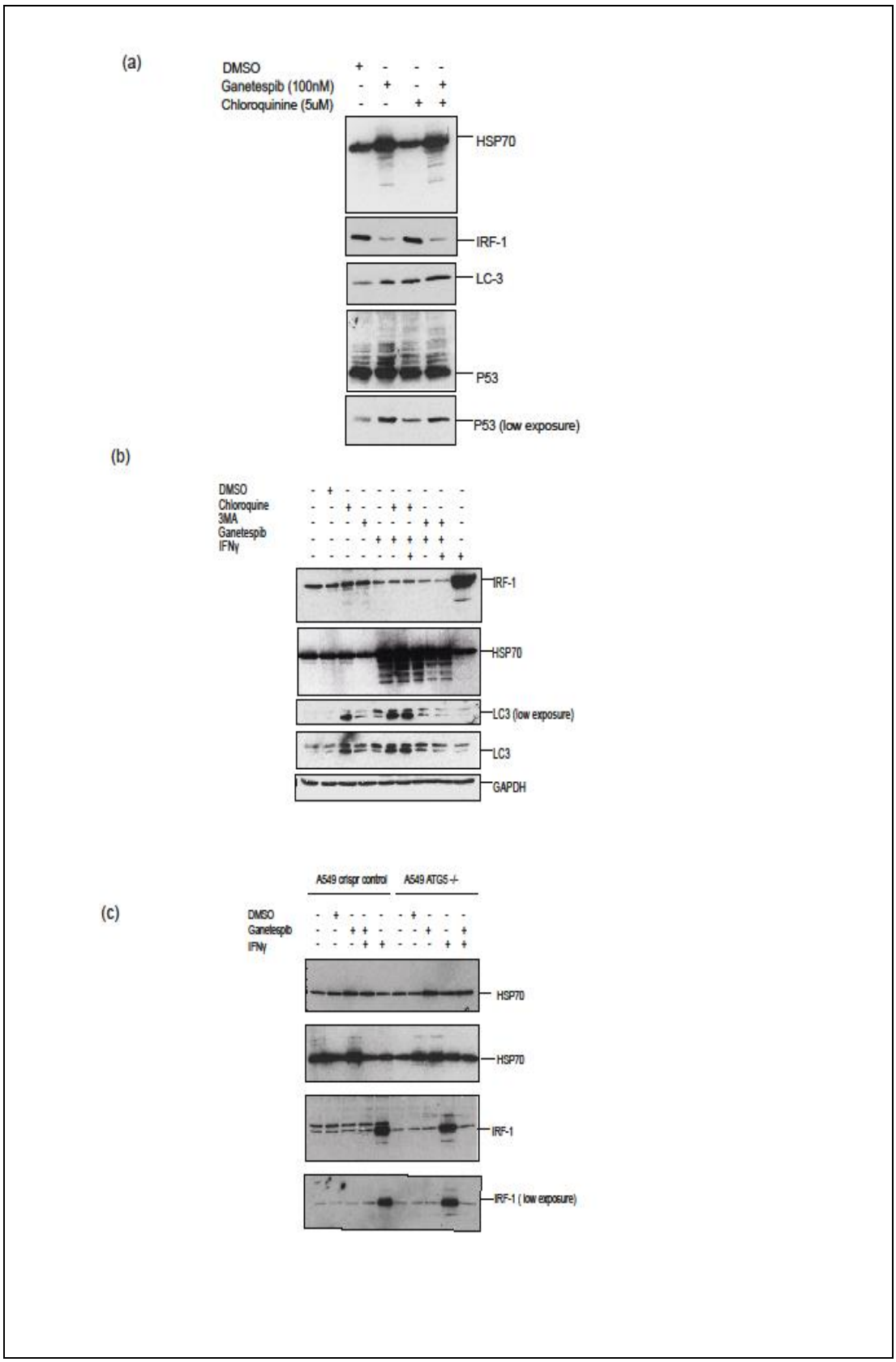

Figure 68 Chaperone mediated autophagy

(a) A375 cells were treated with DMSO, Ganetespib (100 nM) for six h and then treated with chloroquine (5μM) alone or in combination for further 16 h. Total cell lysates analysed for HSP70, p53, IRF-1 and LC-3 via Western blotting. (b) A375 cells were treated with DMSO, Ganetespib (100 nM) for six h and then treated with chloroquine (5μM) or 3MA (5 mM) alone or in combination for further 16 h. IFNγ was used as a control for the assay. Total cell lysates analysed for HSP70, IRF-1, GAPDH and LC-3 via Western blotting. (c) A549 ATG-/- and +/+ cells were treated with DMSO or Ganetespib (100 nM) for 16 h. Total cell lysates analysed for HSP70 and, IRF-1 via Western blotting. The data are representative of at least three independent experiments.

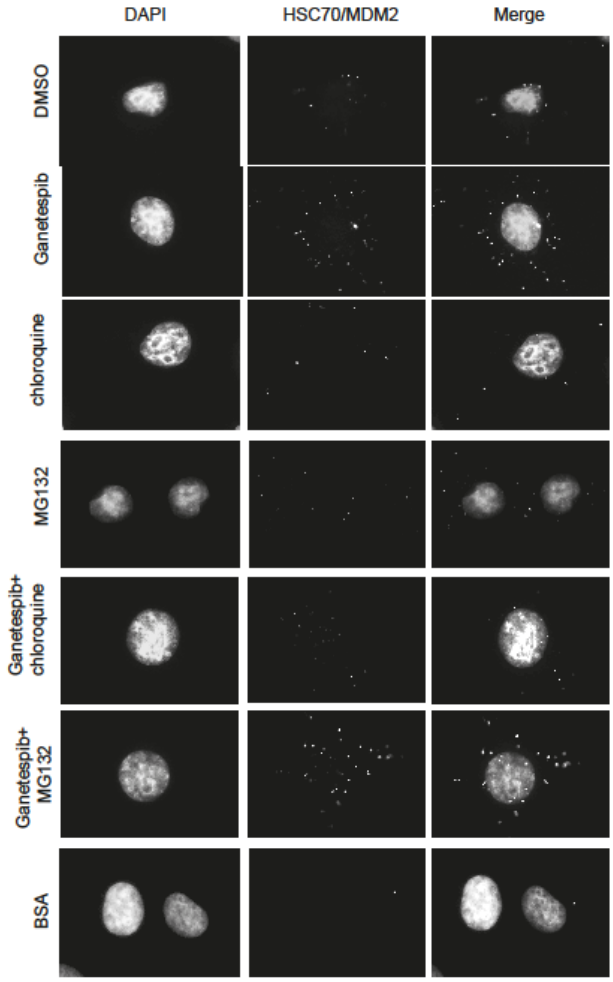

Figure 69 Proximity ligation assay detection of HSC70/MDM2 with autophagy and proteasome inhibitors

(a) A375 cells were treated with DMSO, Ganetespib (100 nM) for 16 h and then treated with either MG132 (50 µM) or Chloroquine (5µM) for further four h, and a proximity ligation assay (PLA) using either only HSC70 or both HSC70 and MDM2 antibodies were performed. Cells were stained with DAPI (1:5000 in mounting media) and visualised using an Axioplan2 (Zeiss) fluorescent microscope (100 x magnification). The data are representative of at least three independent experiments.

5.2.8 Proteomic screen

A proteomic screen was performed to analyse changes in the proteome of melanoma cells after treatment with Ganetespib to see if there were any significant changes in proteins associated with protein degradation.

Quantitative proteomics requires the identification and quantitation of proteins within the biological system under study. Liquid chromatography–mass spectrometry (LC–MS) is one of the most widely used methods in current technology that results in both identification and quantification of the proteins. In order to quantitate and compare the proteomic profiling of two different biological systems, several different tags are used. Relative quantitation methods include SILAC (stable isotope labelling with amino acids in cell culture), ICAT (isotope-coded affinity tagging), and label-free quantification metal-coded tags (MeCAT), MCAT (mass-coded abundance tagging), ITRAQ (isobaric tags for relative and absolute quantification) and TMT (tandem mass tagging). However, SILAC, ICAT and other enzyme or chemical based tagging methods have limitations, such as growth conditions of cells in medium containing the labels, along with practical implications (Ressom, 2009). Rather than introduce a tag into the growing cells I chose to use TMT–MS in which the proteins are labelled following cell lysis, so that the changes in cell growth rate in response to the introduction of, for example SILAC media, are not a factor (Figure 70 TMT mass spectrometry)

In this assay, A375 cells were treated with DMSO, Nutlin, Ganetespib or Nutlin + Ganetespib for 16 hours. Cell lysates were fractionated, labelled, and processed in RECAMO, Masaryk Memorial Cancer Institute, Czech Republic, where I performed the mass spectrometric analysis using an LC–MS spectrophotometer in collaboration with Prof. Ing. Lenka Hernychova. Schematic representation of the fractionation and TMT–mass spectrometric analysis is given in Figure 70a.The cells treatments (DMSO, Ganetespib, Nutlin or both) were performed in triplicate. To confirm that the cells for MS responded to treatment I carried out Western blot analysis. The Nutlin treated cells showed induction of MDM2 while the Ganetespib treated cells downregulated IRF-1 and induced HSP70 when compared to DMSO control. The loading control GAPDH showed no change in protein levels (Figure 70b).

The data analysis for MS is based on a comparison between duplicate sets of treated cell lysates. A protein is regarded as upregulated for MS analysis if the ratio between non-treated and treated sample is greater than 2, and if the ratio is less than 0.5 the protein is regarded as being downregulated. Only the top 50 proteins from each duplicate data set were considered.

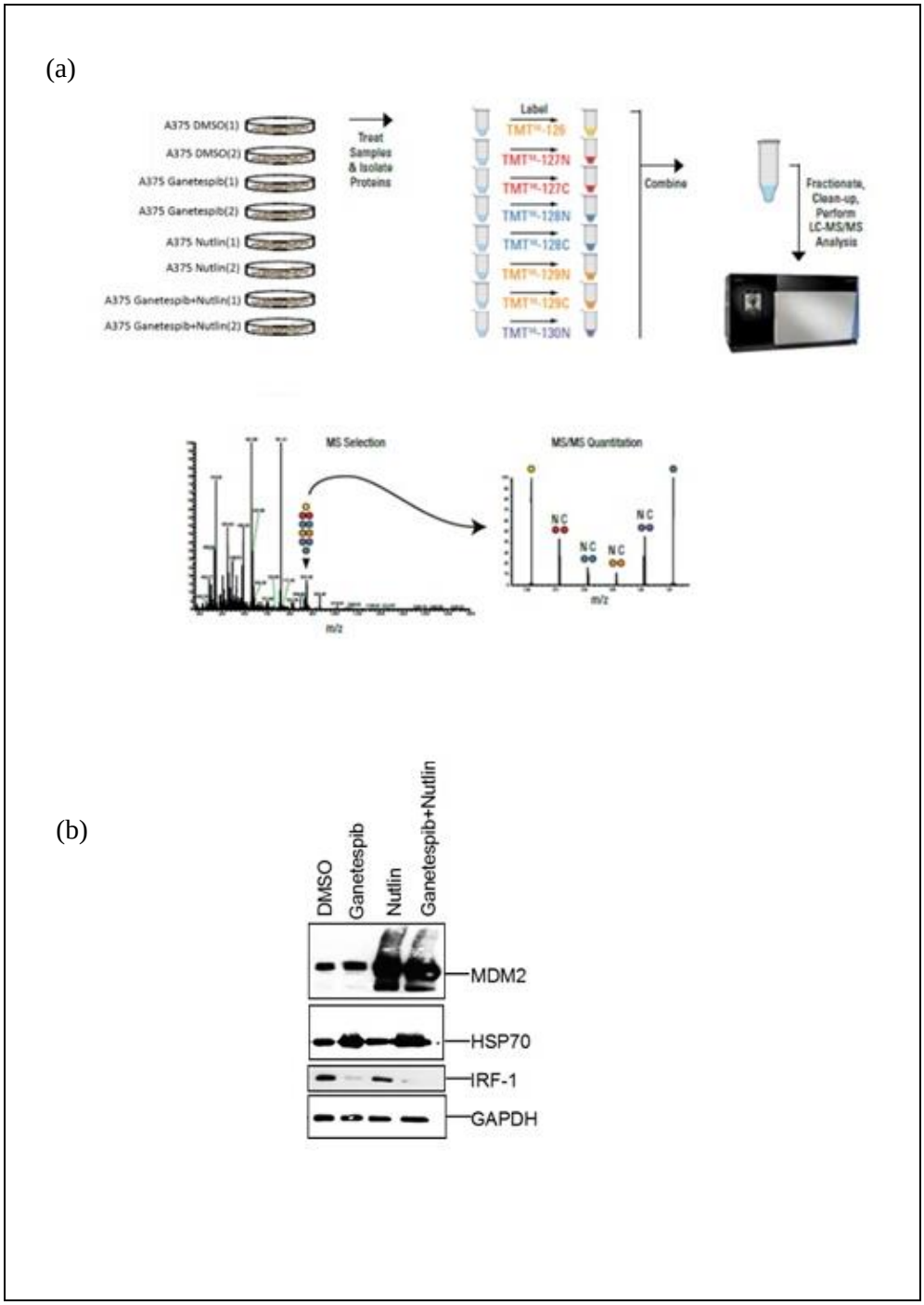

Figure 70 TMT mass spectrometry

(a) Schematic representation of steps involved in the TMT –mass spectrometry based proteome profiling to compare the differential distribution of proteins either upregulated or downregulated with drug treatments in A375 cell lines. (b) Western blot analysis on A375 cell lines treated with nutlin and Ganetespib for TMT mass spectrometry analysis.

5.2.8.1Effects of Ganetespib treatment on A375 proteome

I wanted to analyse the proteins that were upregulated with the treatment of Ganetespib. From the proteins common between the duplicate sets I found five proteins that were upregulated with Ganetespib treatment (Figure 72 a - b). Among these proteins was HSP70, which acted as an internal control as this was seen to be upregulated in cell assays. Another protein of interest was UBA3. This is an E1 ubiquitin activating enzyme and is upregulated in the mass spec. analysis data. The data were also analysed based on molecular function of the proteins identified, and were mainly enriched in chaperone activity and heat shock proteins (Figure 72 -c). The major transcription factors involved where SP1, HSF1etc (supplement data Figure 96). The cellular components that responded to HSP90 inhibition were mainly cytoplasmic proteins, whereas the majority of the proteins were involved in protein metabolism (supplement data Figure 96 b and c).

I studied the proteins that were downregulated in cells treated with Ganetespib. I analysed 50 proteins from each data set and found only one common protein between the duplicate data sets (Figure 73-b). EPHA2 was the protein downregulated with Ganetespib in both the sets. This protein has clinical significance in several cancer types. The gene is shown to be upregulated in various cancers and often leads to poor prognosis (hasegawa, 2016). This could be of clinical importance especially in combinatorial therapy, as lowering EPHA2 could provide a treatment for cancers such as bladder cancer, melanoma etc.

The molecular function of the downregulated proteins was mainly shown to be kinase activity (supplement data Figure 98 - C); the biological process highlighted was cell communication and signal transduction (supplement data Figure 98 -b); the cellular component was plasma membrane (supplement data Figure 98-a)

The complete set of upregulated and downregulated proteins are also represented on a scatter plot where x and y axes are the duplicate sets and the values are represented as log2 of the ratio of DMSO over Ganetespib treatment (Figure 71)

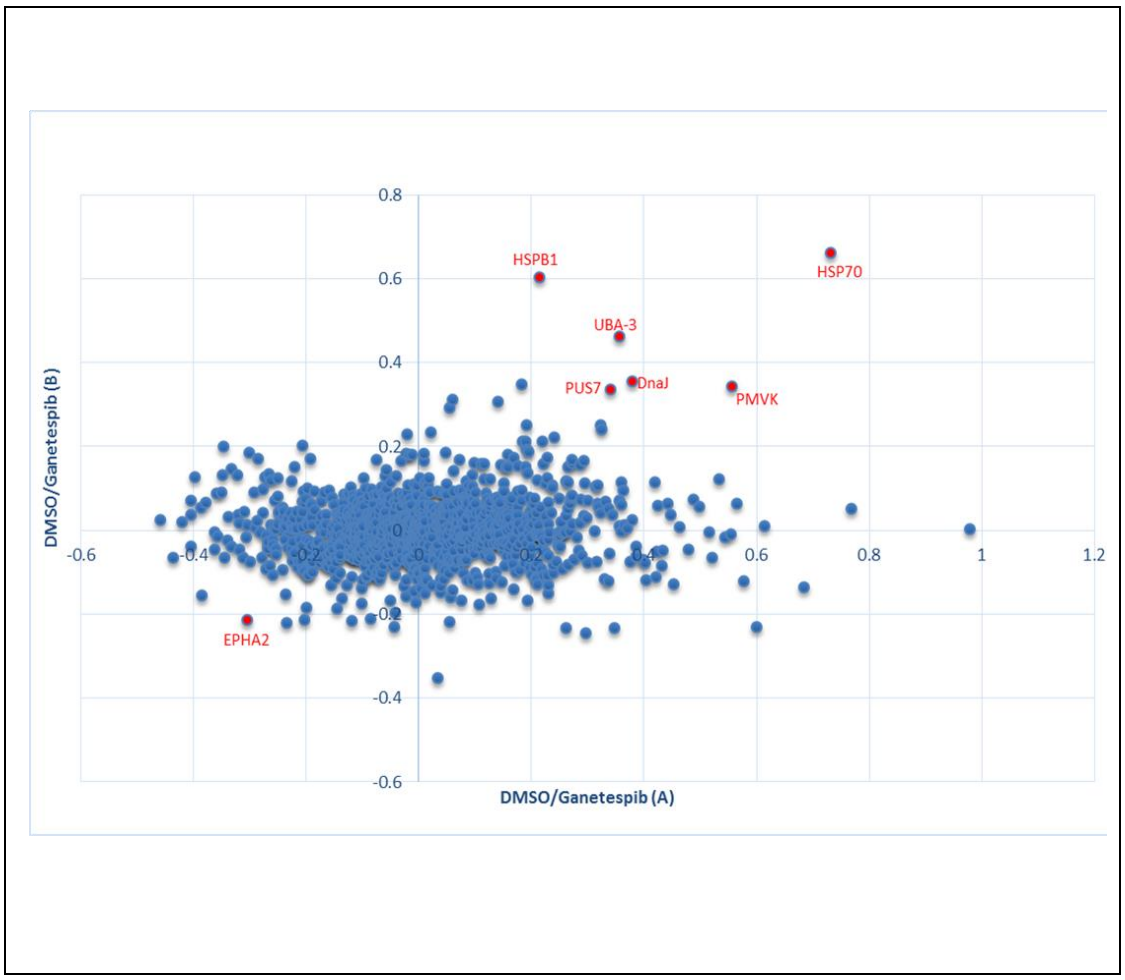

Figure 71 Scatter plot indicating genes upregulated/downregulated with Ganetespib treatment

Scatter plot of log2 (relative protein quantity) with Ganetespib, with x axis DMSO/Ganetespib (A) and y axis DMSO/Ganetespib (B) Data analysed using FUNRICH software.

(a)

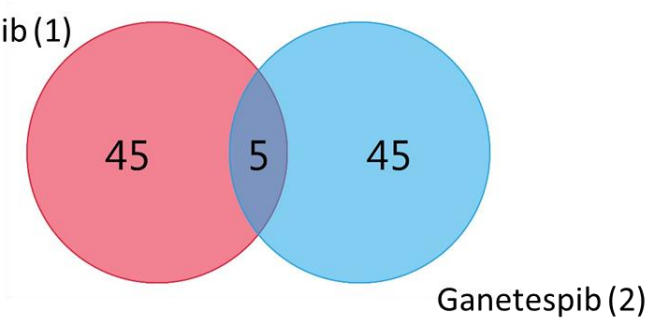

(b)

Search ID/Accessions	Gene Symbol	Gene description	Map location
P08107	HSPA1A	heat shock 70kDa protein 1A	6p21.3
Q15126	PMVK	phosphomevalonate kinase	1q22
P25685	DNAJB1	DnaJ (Hsp40) homolog, subfamily B, member 1	19p13.2
Q8TBC4	UBA3	ubiquitin-like modifier activating enzyme 3	3p14.1
Q96PZ0	PUS7	pseudouridylate synthase 7 (putative)	7q22.3

(c)

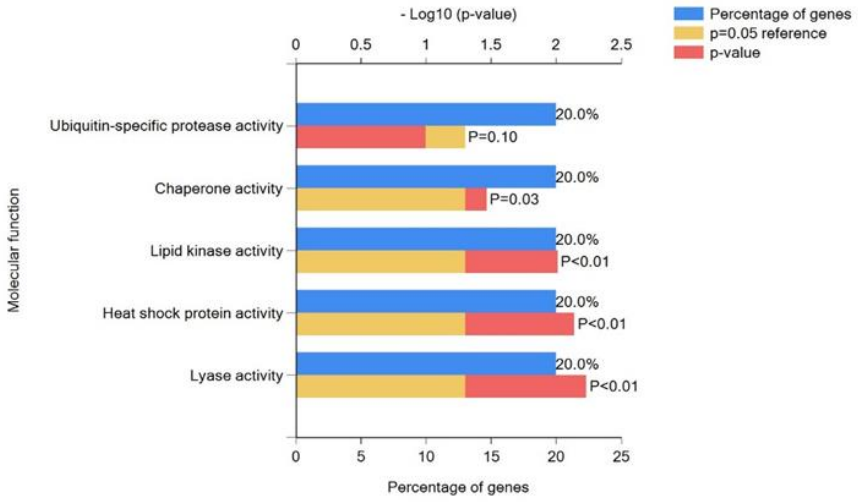

Figure 72upregulated genes with Ganetespib

(a) Venn diagram of the upregulated genes after Ganetespib treatment on biological replicates. (b) List of upregulated genes with Ganetespib(c) molecular functions of upregulated genes analysed using FUNRICH software.

(a)

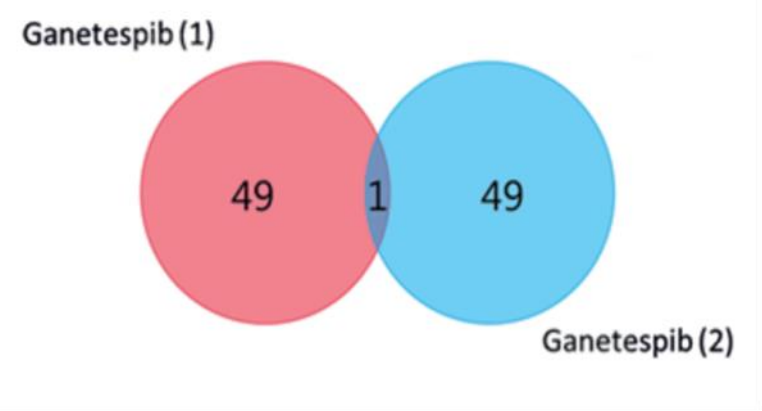

(b)

Search ID/Accessions	Gene Symbol	Gene description	Map location
P29317	EPHA2	EPH receptor A2	1p36

(c)

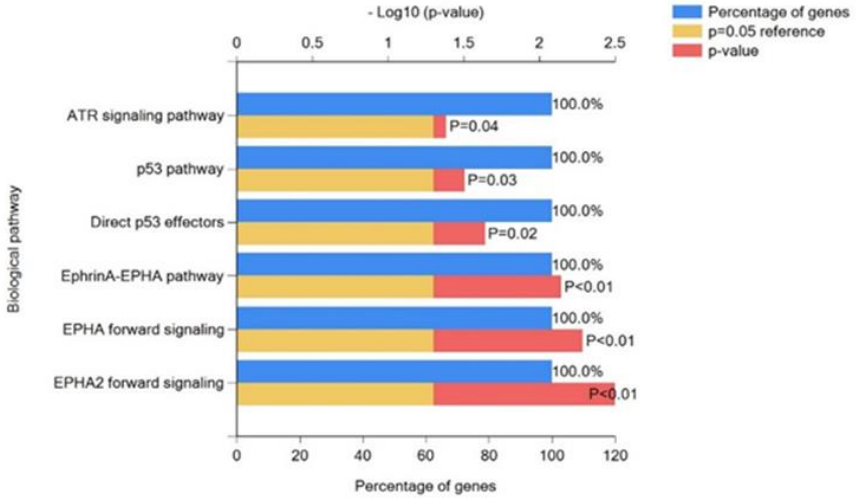

Figure 73 Downregulated genes with Ganetespib

(a) Venn diagram of the downregulated genes after Ganetespib treatment on biological replicates.
(b) List of downregulated genes with Ganetespib(c) biological pathways of downregulated genes analysed using FUNRICH software.

5.2.8.2Effects of Nutlin treatment on the A375 proteome

I extended the proteomic study by determining the proteins up or downregulated when cells were treated with Nutlin or Nutlin + Ganetespib. With Nutlin treatment I observed several proteins to be upregulated but, most importantly, some of them were apoptosis/cell death related, such as annexin. This may indicate that Nutlin treatment primes cells for apoptosis. One of the interesting proteins upregulated is RPS27L (Figure 75 a - b). This protein is a direct p53-inducible target. It is mainly localized in the cytoplasm but, upon p53-activating signals, a portion of RPS27L shuttles to the nucleoplasm where it co-localises with MDM2. Xiong and group demonstrated that both the cytoplasmic and the nuclear p53, induced by ribosomal stress, were reduced upon RPS27L silencing, thus describing a multi-level interplay between RPS27L and the p53-MDM2 axis, with RPS27L functioning as a p53 target, a MDM2 substrate and a p53 regulator (X Xiong, 2011).

Another protein upregulated with Nutlin treatment was TP53I3. The p53-inducible gene 3 (PIG3 or TP53I3) can be involved in apoptosis induced by p53 via the production of reactive oxygen species (ROS). Xu J and group showed that PIG3 plays an oncogenic role in thyroid cancer via the regulation of the PI3K/AKT/PTEN pathway and this supports the exploration of PIG3 as a novel biomarker for patients with thyroid cancer (Xu J, 2015). Herraiz and group also emphasised the clinical importance of the PIG3 gene in their studies (Herraiz C, 2015).

Biological pathway analysis for the Nutlin upregulated proteins indicated that the majority belonged to p53 and ATM pathways (Figure 75 c). In addition, the majority of the upregulated proteins had molecular functions such as ligase activity or aminopeptidase. Major transcription factors seen to change were HSF1, MYF5 etc. (supplement data Figure 97 a-b). Key upregulated proteins were localised in the cytoplasm and exosomes. Protein metabolism and signal transduction were the major biological process for the upregulated proteins in Nultin treated cells (supplement data Figure 97 c and d).

There were 11 proteins selected between the duplicate sets that were observed to be downregulated (Figure 76 a-b). One of the key proteins was NFATc2. Ding and group indicated a reciprocal regulatory relationship between the NFATc1 and p53 pathways. In patients with colon cancer, expression of nuclear NFATc1 correlated with inferior survival (Ding W, 2016). Hence downregulation of this protein with Nutlin could improve prognosis for colon cancers. Some of the transcription factors for the downregulated protein identified

in the screen were GABPA and NRF1 (supplement data Figure 99-a). The biological process highlighted was regulation of nucleotide and nucleic acid metabolism (supplement data Figure- b).

The complete set of proteins are also represented on a scatter plot where x and y axis are the duplicates sets and the values are represented as log2 of the ratio of DMSO over Nutlin treatment (Figure 74).

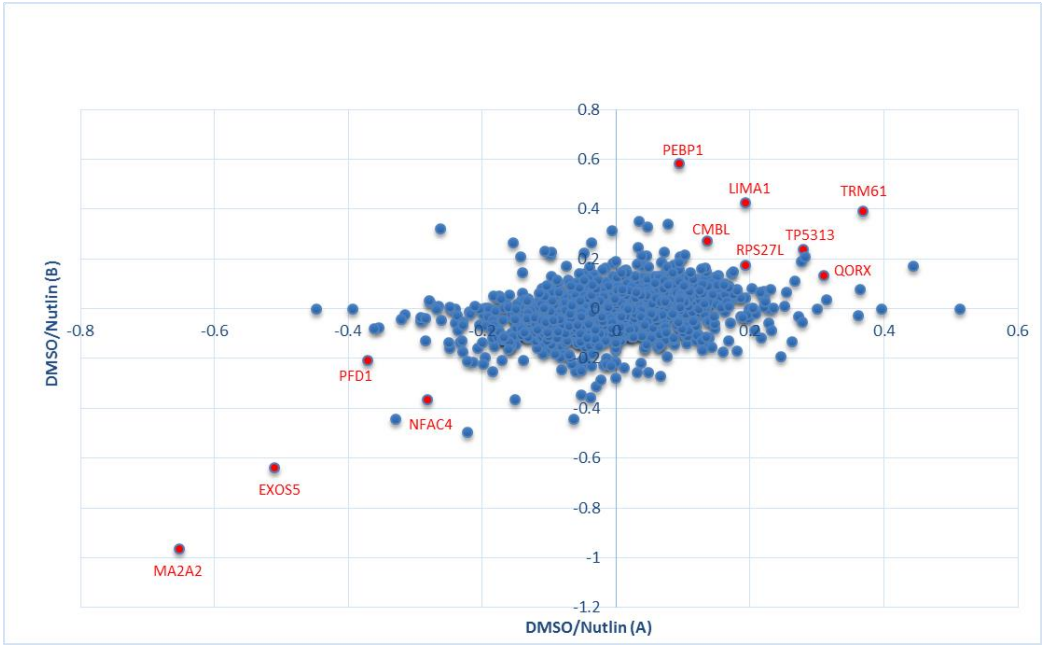

Figure 74 Scatter plot indicating genes upregulated/downregulated with Nutlin treatment

Scatter plot of log2 (relative protein quantity) with nutlin; x axis DMSO/nutlin (A) and y axis DMSO/nutlin (B). Data analysed by FUNRICH software.

(a)

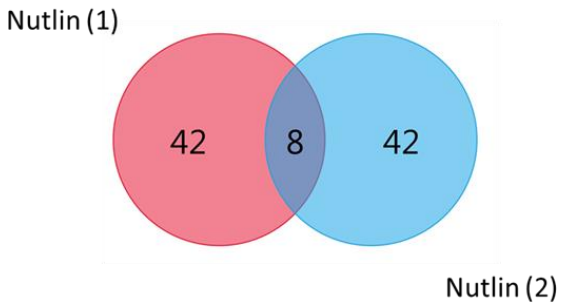

(b)

Search ID/Accessions	Gene Symbol	Gene description	Map location
Q7L576	CYFIP1	cytoplasmic FMR1 interacting protein 1	15q11
Q9NQW7	XPNPEP1	X-prolyl aminopeptidase (aminopeptidase P) 1, soluble	10q25.3
Q53FA7	TP53I3	tumor protein p53 inducible protein 3	2p23.3
Q9Y285	FARSA	phenylalanyl-tRNA synthetase, alpha subunit	19p13.2
P09525	ANXA4	annexin A4	2p13
Q9UHB6	LIMA1	LIM domain and actin binding 1	12q13
Q96DG6	CMBL	carboxymethylenebutenolidase homolog (Pseudomonas)	5p15.2
Q71UM5	RPS27L	ribosomal protein S27-like	15q22.2

(c)

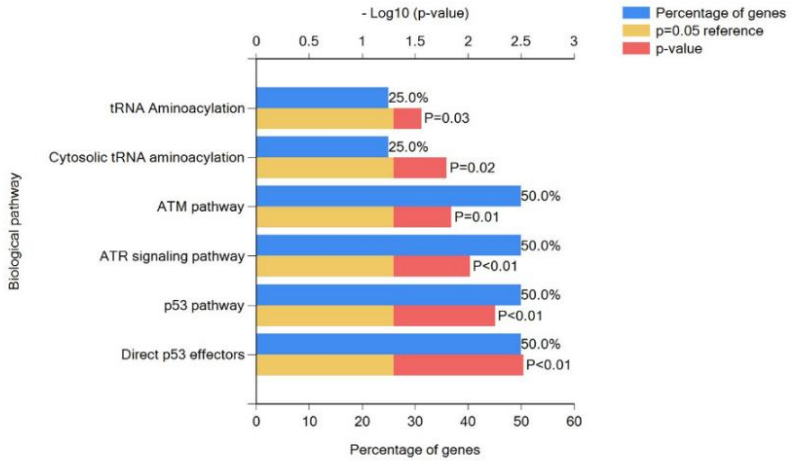

Figure 75 Upregulated genes with Nutlin

(a) Venn diagram of upregulated genes after Nutlin treatment on biological replicates. (b) List of upregulated genes with nutlin (c) Biological pathways of upregulated genes analysed using FUNRICH software.

(a)

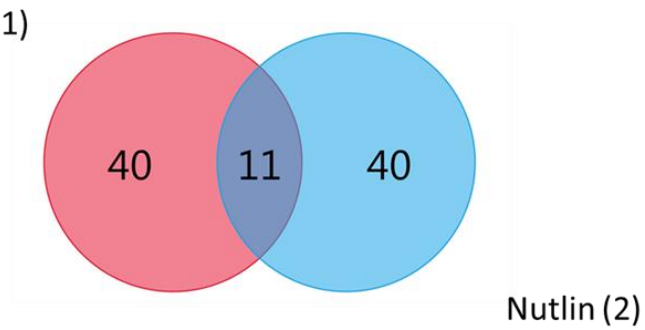

(b)

Search ID/Accessions	Gene Symbol	Gene description	Map location
P49641	MAN2A2	mannosidase, alpha, class 2A, member 2	15q26.1
Q9NQT4	EXOSC5	exosome component 5	19q13.1
O60925	PFDN1	prefoldin subunit 1	5q31
Q8IUE6	HIST2H2AB	histone cluster 2, H2ab	1q21
Q14934	NFATC4	nuclear factor of activated T-cells, cytoplasmic, calcineurin-dependent 4	14q11.2
O60869	EDF1	endothelial differentiation-related factor 1	9q34.3
Q13015	MLLT11	myeloid/lymphoid or mixed-lineage leukemia (trithorax homolog, Drosophila); translocated to, 11	1q21
Q9BQ61	C19orf43	chromosome 19 open reading frame 43	19p13.2
Q6UN15	FIP1L1	factor interacting with PAPOLA and CPSF1	4q12
P06899	HIST1H2BJ	histone cluster 1, H2bj	6p22.1
Q8TAQ2	SMARCC2	SWI/SNF related, matrix associated, actin dependent regulator of chromatin, subfamily c, member 2	12q13.2

(c)

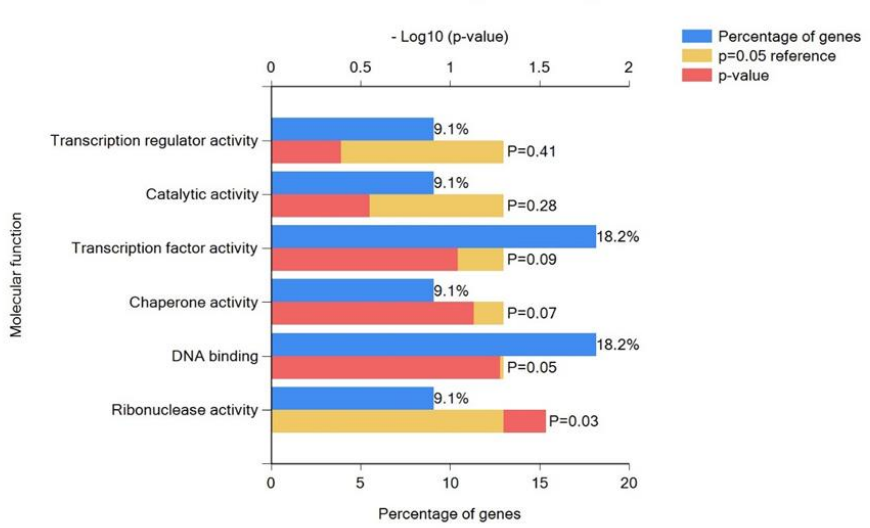

Figure 76 Downregulated genes with nutlin

(a) Venn diagram of the downregulated genes after nutlin treatment on biological replicates. (b) List of downregulated genes with nutlin (c) Molecular functions of downregulated genes analysed using FUNRICH software.

5.2.8.3 Effects of combinatorial treatment on the A375 proteome

When I analysed the combined treatment data (Nutlin + Ganetespib) several proteins were upregulated and common between the Ganetespib + Nutlin treatment duplicates (Figure 78 a-b). One of these was BAG3.BAG3, a nucleotide exchange factor of the heat shock protein HSP70, has been implicated in cell signalling. Colvin and group demonstrated that BAG3 is a critical factor in HSP70-modulated signalling and offered a preclinical proof-of-concept that the HSP70-Bag3 complex may offer an appealing anticancer target. (Colvin TA, 2014)

Interestingly Behl and group showed that overexpression of BAG3 is responsible for the resistance to chemotherapy in small cell lung cancer and hence BAG3 could be a marker of poor prognosis in certain cancer patients (with abnormalities in p53). In addition, in patients of a subgroup of stage III melanoma, survival is influenced by the expression of BAG3 (Behl, 2016). Investigating a potential correlation between BAG3 expression and response to therapeutic agents might result in the ability to predict treatment outcome. BAG3-positive tumours could constitute candidates for BAG3-based therapeutic approaches (Franco, 2012).

The molecular function analysis for the upregulated proteins in cells exposed to the combined drug treatment showed heatshock activity and chaperone activity (Figure 78 c), in agreement with results from the analysis of Ganetespib treatment only.

The cellular components analysis showed mainly cytosol and exosome distribution (supplement data Figure 100- a), and biological processes again highlighted metabolism, cell communication and signal transduction (supplement data Figure 100- b). The major transcription factors observed to change where HSF1, HOXB4 and CREB1 (supplement data Figure 100-c).

There were 12 downregulated proteins common between the duplicate sets of data (Figure 79a- b). The major biological pathways involved with the downregulated proteins were the E2F transcription factor network at G0 and early G1 pathway (Figure 79 c). CDK1 is one of the proteins downregulated with the combinatorial treatment. CDK1 may be required for apoptosis induction in some particular pathways of cell killing. This applies to several clinically important settings, for instance to paclitaxel-induced killing of breast cancer cells, in which the ErbB2 receptor kinase can mediate apoptosis inhibition through inactivation of CDK1. (Min Lu 1. H., 2013)

Some of the major transcription factors downregulated in the combinatorial treated samples were MEF2A, NFYA and PU2F1 (supplement data Figure 101- a) with biological process mainly being regulation of nucleotide and nucleic acid metabolism (supplement data figure 6 b). The major molecular function for the downregulated proteins is DNA binding (Figure 101- c).

The complete set of proteins is represented on a scatter plot, where the x and y axes are the duplicate sets and the values are represented as log2 of the ratio of DMSO over Nutlin + Ganetespib treatment (Figure 77).

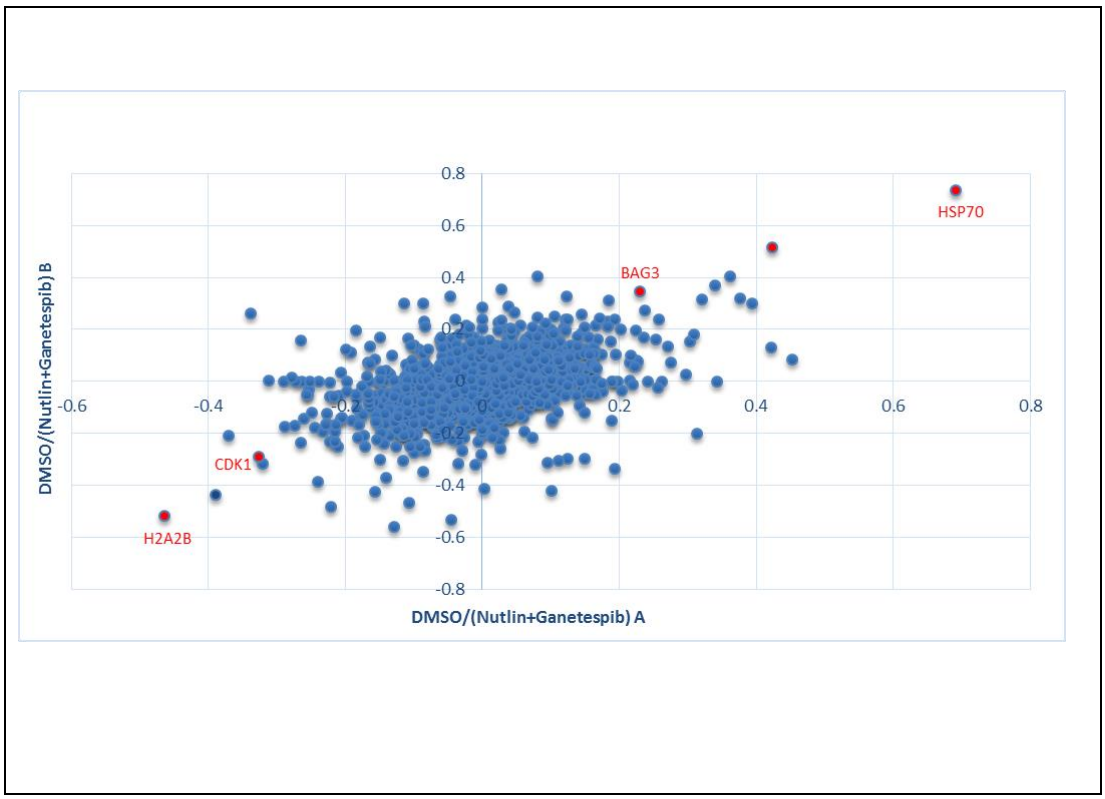

Figure 77 Scatter plot indicating genes upregulated/downregulated with combinatorial treatment

Scatter plot of log2 (relative protein quantity) with nutlin + Ganetespib; x axis DMSO/ nutlin + Ganetespib (A) and y axis DMSO/ nutlin + Ganetespib (B). Data analysed using FUNRICH software.

(a)

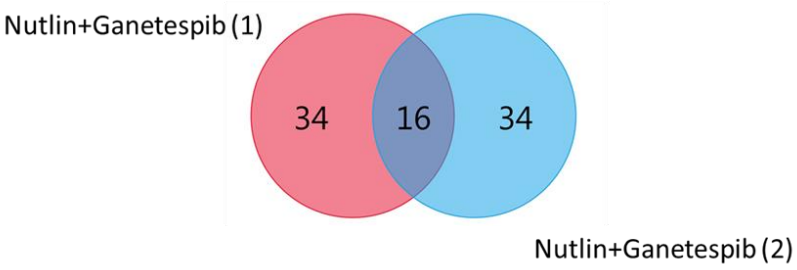

(b)

Search ID/Accessions	Gene Symbol	Gene description	Map location
P08107	HSPA1A	heat shock 70kDa protein 1A	6p21.3
P04792	HSPB1	heat shock 27kDa protein 1	7q11.23
Q96PZ0	PUS7	pseudouridylate synthase 7 (putative)	7q22.3
P09525	ANXA4	annexin A4	2p13
Q92598	HSPH1	heat shock 105kDa/110kDa protein 1	13q12.3
Q14573	ITPR3	inositol 1,4,5-trisphosphate receptor, type 3	6p21
Q8WUM0	NUP133	nucleoporin 133kDa	1q42.13
P25685	DNAJB1	DnaJ (Hsp40) homolog, subfamily B, member 1	19p13.2
P04217	A1BG	alpha-1-B glycoprotein	19q13.4
P19623	SRM	spermidine synthase	1p36-p22
O95817	BAG3	BCL2-associated athanogene 3	10q25.2-q26.2
P07900	HSP90AA1	heat shock protein 90kDa alpha (cytosolic), class A member 1	14q32.33
O00300	TNFRSF11B	tumor necrosis factor receptor superfamily, member 11b	8q24
P34931	HSPA1L	heat shock 70kDa protein 1-like	6p21.3
P19525	EIF2AK2	eukaryotic translation initiation factor 2-alpha kinase 2	2p22-p21

(c)

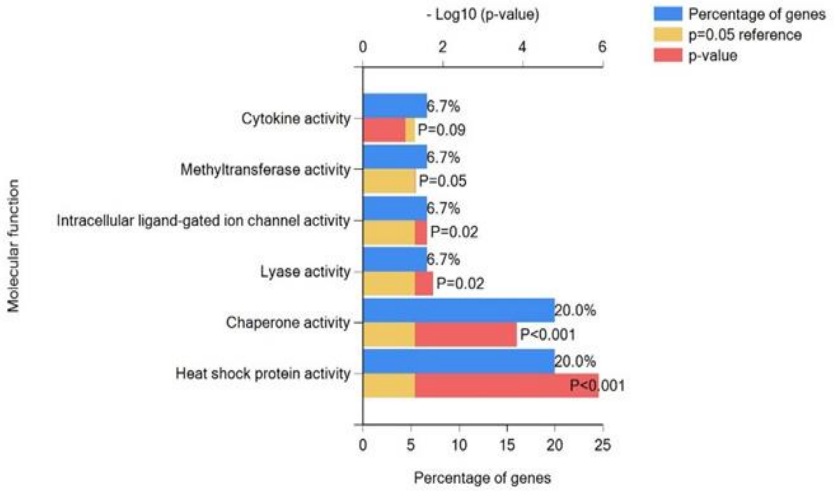

Figure 78 Upregulated genes with combinatorial treatment

(a) Venn diagram of the upregulated genes after Ganetespib + nutlin treatment on biological replicates. (b) List of upregulated genes with Ganetespib + nutlin (c) Molecular functions of upregulated genes analysed using FUNRICH software.

(a)

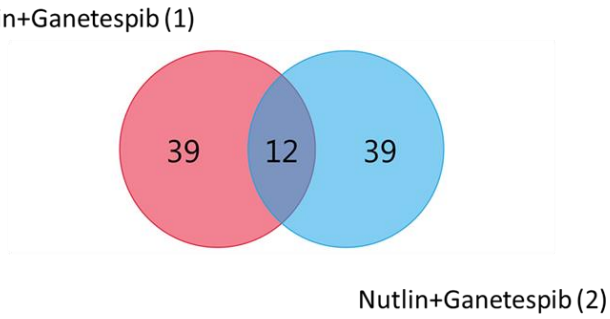

(b)

Search ID/Accessions	Gene Symbol	Gene description	Map location
Q8IUE6	HIST2H2AB	histone cluster 2, H2ab	1q21
Q9NQT4	EXOSC5	exosome component 5	19q13.1
O43818	RRP9	ribosomal RNA processing 9, small subunit (SSU) processome component, homolog (yeast)	3p21.2
P06493	CDK1	cyclin-dependent kinase 1	10q21.1
Q16777	HIST2H2AC	histone cluster 2, H2ac	1q21.2
Q7Z3B4	NUP54	nucleoporin 54kDa	4q21.1
P06899	HIST1H2BJ	histone cluster 1, H2bj	6p22.1
O43790	KRT86	keratin 86	12q13
O60814	HIST1H2BK	histone cluster 1, H2bk	6p21.33
Q6UN15	FIP1L1	factor interacting with PAPOLA and CPSF1	4q12
Q09028	RBBP4	retinoblastoma binding protein 4	1p35.1
P08670	VIM	vimentin	10p13

(c)

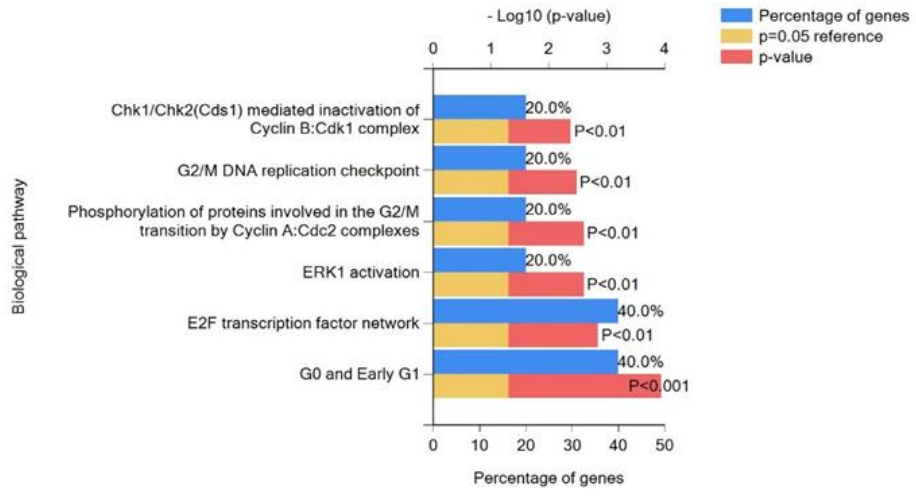

Figure 79 Downregulated genes with combinatorial treatment

(a) Venn diagram of the downregulated genes after Ganetespib + nutlin treatment on biological replicates. (b) List of downregulated genes with Ganetespib + nutlin (c) Biological pathways of upregulated genes analysed using FUNRICH software.

5.2.8.4UBA 3 analysis

Based on the mass spectrometric analysis data, UBA3 protein was shown to be upregulated in the Ganetespib treated cells. As UBA3 is a E1-ubiquitin activating enzyme family member which can also activate NEDD8, I wanted to investigate whether it could be a component of a novel pathway for down regulation of IRF-1.

Ubiquitination and neddylation are necessary for a number of biological processes and have been implicated in numerous diseases, particularly in cancer. The process of ubiquitination has been identified as the mechanism that labels proteins for degradation by the 26s proteasome. Conjugation of ubiquitin to its substrate requires three enzymes, ubiquitin-activating enzyme E1, ubiquitin-conjugating enzyme E2 and ubiquitin ligase enzyme E3. The neural precursor cell-expressed developmentally downregulated (NEDD8) protein is 60% identical to ubiquitin and also conjugates to target proteins. This process is termed neddylation and is similar to ubiquitination. NEDD8 is activated by the E1 enzyme (APPBP1/UBA3 heterodimer), whereby a thioester bond is formed with the cysteine residue of the UBA3 subunit (FANG CHENG, 2014). I used siRNA targeting of UBA-3 to knock this down in A375 cell lines. Cells were treated with siRNA for 24 hours prior to the addition of Ganetespib.

The results indicated that loss of UBA3 didn't rescue the downregulation of IRF-1 and suggested that probably this E1, and therefore Neddylation are not involved in the degradation of IRF-1 (Figure 80). I observed more than 80% knockdown of the UBA 3 levels with siRNA when compared to the controls. The negative siRNA control had no significant effect on UBA 3 when compared to the control and positive knockdown cells. Downregulation of IRF-1 was observed when cells were treated with Ganetespib either alone or in combination with UBA 3 siRNA.

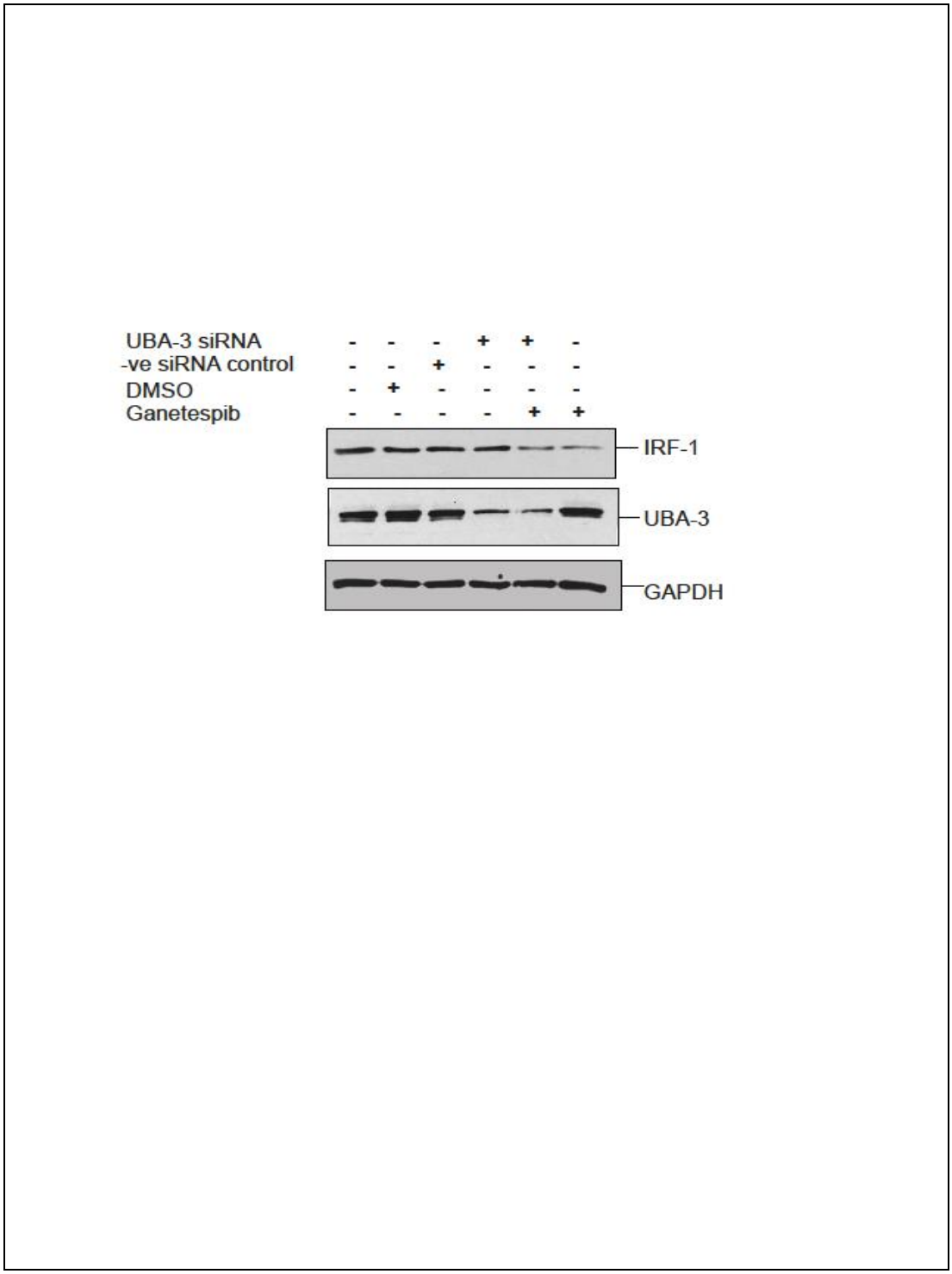

Figure 80 Western blot analysis of the role of UBA-3 as potential E1 ligase

A375 cells were treated with either control siRNA or siRNA to UBA-3 (60nM) for 24 h and then treated with Ganetespib (100 nM) for further 16 h. Total cell lysates analysed for UBA-3, IRF-1 and GAPDH via Western blotting.

5.3 Discussion

Some of the key proteins analysed by masspectrometry are detailed below.HSP70 protein was upregulated with the treatment of Ganetespib which demonstrates the inhibition of HSP90.EPHA2 was one of the protein downregulated with Ganetespib treatment. As described earlier EPHA2 protein is shown to be a biomarker for various cancers such as bladder and melanoma and its downregulation could be beneficial in combinatorial therapy.

RPS27L protein was upregulated with nutlin. It has dual functions in p53 regulation; in a $Trp53^{+/+}$ background, Rps27l disruption triggers ribosomal stress to induce p53 and apoptosis, whereas in a $Trp53^{+/-}$ background, Rps27l disruption triggers genomic instability and Trp53 deletion to promote tumourigenesis (Xiong X, 2014). Elevated RPS27L may improve the prognoses of certain colorectal cancer (CRC) patients by enhancing the DNA repair capacity of their colonic cells; it can be measured in faeces. Huang and group demonstrated that by integrating clinical, molecular, and cellular data, faecal RPS27L may be a useful index for predicting prognoses and guiding personalized therapeutic strategies, especially in patients with intermediate-stage CRC (Huang CJ, 2013).

In Combinatorial treatment of Ganetespib and nutlin BAG3 was shown to be upregulated.BAG3, also known as CAIR-1 or Bis, mediates protein delivery to the proteasome and modulates apoptosis by interfering with cytochrome c release, apoptosome assembly and other events in the cellular death programme. Moreover, it takes part in the processes of cell adhesion and migration. It has been shown that, in human cancer cells including lymphocytic and myeloblastic leukemic cells, BAG3 sustains cell survival and underlies resistance to chemotherapy, through down-modulation of apoptosis. Zhu and group described BAG3 in their studies as a potential therapeutic target of human malignancy (Zhu H, 2012). Guerriero and group also described the gene as a pro-survival factor in several tumour types including melanomas (Guerriero, 2014).The discovery of its role in selective autophagy and the description of BAG3-mediated selective macroautophagy as an adaptive mechanism to maintain cellular homeostasis, under stress as well as during aging, make BAG3 a highly interesting target for future pharmacological interventions.

CDK1 was one of the downregulated proteins. Nearly 90% of human melanomas contain inactivated wild-type p53. Min lu and group showed that cyclin B1/CDK1-phosphorylates

iASPP, which leads to the inhibition of iASPP dimerization, promotion of iASPP monomer nuclear entry, and exposure of its p53 binding sites, leading to increased p53 inhibition. Nuclear iASPP is enriched in melanoma metastasis and associates with poor patient survival. Most wild-type p53-expressing melanoma cell lines co-express high levels of phosphorylated nuclear iASPP, MDM2, and cyclin B1. Inhibition of MDM2, and iASPP phosphorylation, with small molecules induce p53-dependent apoptosis and growth suppression (Min Lu 1. H., 2013) (Bresler, 2016). Concurrent p53 reactivation and CDK1 inhibition by combinatorial therapy could provide alternatives for melanoma therapy.

To conclude this chapter I have identified a new proteasome dependent degradation pathway for IRF-1 where CHIP and MDM2 are not required and where formation of IRF-1/HSP/C70 complexes in the cytoplasm preceded degradation. . The proteomic analysis using TMT mass spectrometry emphasised the importance of combinatorial treatment in cancer and how different proteins respond the drugs used.

6 HSP90 inhibitors in immune surveillance

6.1 Introduction

6.1.1 The Interferon system

IFNs belong to the large class of proteins known as cytokines. Interferon signalling pathways are critical to both innate and adaptive immunity. Interferons (IFNs) provide defence against viral and bacterial infections, as well as tumour surveillance. IFNs are divided into two main categories: type I and type II.

The two major members of type I IFNs (IFNα and IFNβ) are universally expressed and signal through the type I receptor. IFNs are differentiated primarily through their amino acid sequence. Interferons α and-β, which have relatively similar amino acid sequences, are classified as type I interferons. Interferon γ is a type II interferon. Interferons of type III signal through a receptor complex consisting of the interleukin 10 receptor (IL10R2) and the interferon lambda receptor (IFNLR1) and are predominately important in viral infections. (Zaidi MR, 2011) (Murtas D, 2013).

6.1.1.1Interferon γ

Interferon gamma (IFN γ) is the only type II interferon, classified as such because of its unique amino acid sequence. This interferon is known for its ability to regulate overall immune system functioning. IFNγ is a cytokine whose biological activity is associated with cytotoxic and antitumour mechanisms during cell-mediated adaptive immune response. It has been used clinically to treat a variety of malignancies, although with mixed results and side effects that can be severe. IFNγ is an important activator of macrophages and inducer of Class II major histocompatibility complex (MHC) molecule expression. IFNγ is produced predominantly by natural killer (NK) and natural killer T (NKT) cells as part of the innate immune response, and by CD4Th1 and CD8 cytotoxic T lymphocyte (CTL) effector T cells once antigen-specific immunity develops (Zaidi MR, 2011).

IFNγ is structurally and functionally different from the type I IFNs and has its own receptor, consisting of IFN-gR1 and IFN-gR2 subunits. The intracellular carboxyl termini of IFN-gR1

and IFN-gR2 bind the non-receptor tyrosine kinases Janus-activated kinase (JAK) 1 and JAK2, respectively, which phosphorylate the receptor upon ligand binding. This phosphorylation forms binding sites for the STAT proteins (Abroun S, 2015).

Activation of the JAK/STAT pathway occurs by binding of ligands to their receptors. These ligands can activate different JAKs and STATs. In addition to JAKs, other non-receptor tyrosine kinases (TKs) can be phosphorylated and activated by interaction between ligands and their receptors in the JAK/STAT pathway. Once activated, JAKs can phosphorylate additional targets, which include both the receptors and their major substrates, the STATs. In normal cells, after modulating gene expression, STATs become dephosphorylated by tyrosine phosphatases and are thus free for subsequent rounds of stimulation (Abroun S, 2015).

IFNγ regulates the differentiation and function of many types of immune cells. It is intimately involved in all aspects of Th1-mediated immune responses by regulating the differentiation, activation, and homeostasis of T-cells. One of the major primary response genes transactivated by IFNɣ–activated JAK/STAT signalling is the transcription factor IFN response factor 1 (IRF-1). IRF-1, in turn, activates a large number of secondary response genes. The antitumour activity of IFNγ is mediated in part through IRF-1 and may be blocked by IRF-2. The effects of IFNγ have been shown to involve upregulation of MHC class I genes, which increase tumour immunogenicity ((Shang L, 2006); (Connett JM, 2005); (Lowney JK, 1999); (Murtas D, 2013)).

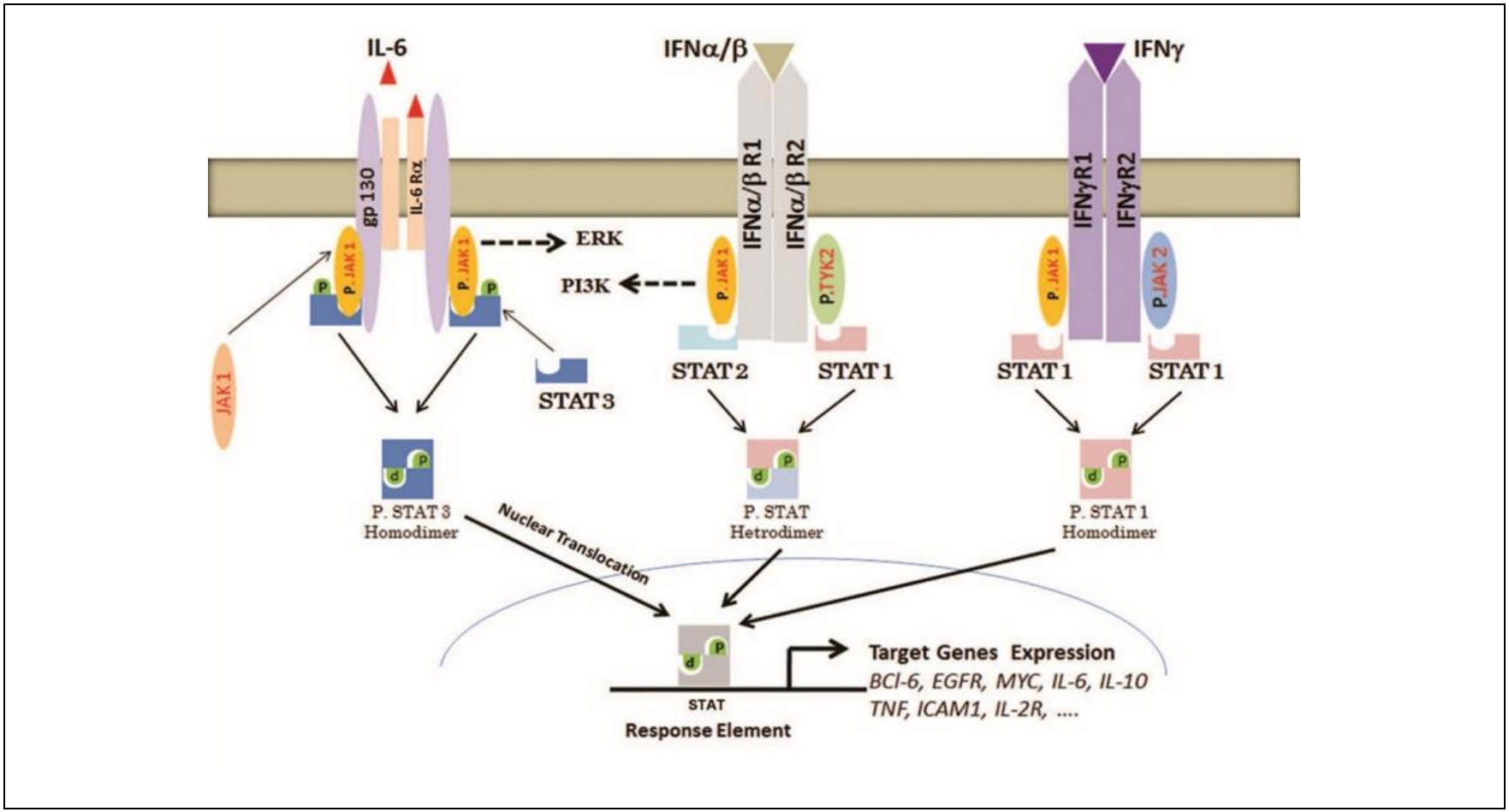

Figure 81 Cytokines induce Janus kinase/signal transducers and activators of transcription (JAK/STAT) pathway activation

Expression of STAT target gene is dependent on STAT types as well as cell types. IL; Interleukin, INF; Interferon, ERK; Extracellular regulated MAP kinase, PI3K; Phosphoinositide 3-kinase and TYK; Tyrosine kinases (Abroun S, 2015)

6.1.2 Therapeutic targets for cancer immunotherapy

Recognition of the major histocompatibility complex (MHC) is key in both innate and adaptive immune recognition. The function of innate immune cells e.g. natural killer (NK) cells and the adaptive immune cells e.g. T-cells relies on recognition of MHC-1 molecule expression on aberrant cells (figure82). Tumours escape the immune response by mechanisms such as inhibition of tumour antigen presentation, secretion of immunosuppressant factors, and inhibition of attack by immune cells or recruitment of immunosuppressant cell types.

6.1.2.1Immune checkpoints

Immune checkpoints are molecules in the immune systems that are either stimulatory (turn up a signal) or inhibitory (turn down signal). Five stimulatory checkpoint molecules are members of the tumour necrosis factor (TNF) receptor superfamily: CD27, CD40, OX40, GITR and CD137. Another two stimulatory checkpoint molecules belongs to the B7-CD28 superfamily: CD28 itself and ICOS (Suzanne L. Topalian, 2016).

6.1.2.1.1 CD28

This molecule is constitutively expressed on almost all human $CD4^+$ T cells and on around half of all CD8 T cells. Binding with its two ligands CD80 (B7-1) and CD86 (B7-2), expressed on dendritic cells, prompts T cell expansion (Figure 82).

Many cancers protect themselves from the immune system by inhibiting the T cell signal. Some of the major inhibitory checkpoint molecules are: A2AR, B7-H3 (CD276), B7-H4, BTLA (CD272), CTLA-4 (CD152), IDO, KIR, LAG3, PD-1, TIM-3, and VISTA (Suzanne L. Topalian, 2016).

Inhibitory checkpoint molecules are increasingly considered as new targets for cancer immunotherapies due to the effectiveness of two checkpoint inhibitor drugs that were initially indicated for advanced melanoma. Yervoy is a monoclonal antibody targeting CTLA-4, produced by Bristol-Myers Squibb (Copur MS, 2017), and Keytruda is an anti-PD1 antibody from Merck (Addeo, 2017).

6.1.2.1.2 PD-1

Programmed cell death protein 1 (PD-1) is an immune checkpoint receptor showing great promise as a therapeutic target. The protein is part of a complex system controlling T-cell activation in the periphery during an inflammatory response. PD-1 also interacts with other activated non-T-cell subsets, including B-cells and NK cells, limiting their lytic activity. Chronic antigen exposure, as seen in cancer, may result in persistently high PD-1 levels, leading to anergy among antigen-specific T-cells. The PD-1 pathway can also shift the balance from T-cell activation to tolerance early in the course of the T-cell response to antigens within secondary lymphoid tissues. In solid tumour cells, PD-ligand 1 (PD-L1) is the major ligand expressed(figure 82) limiting local antitumour T-cell mediated responses. Thus, it is clear that blockade of PD-1, and its ligands (PD-L1, PD-L2), is an attractive therapeutic option (O'Byrne, 2015) (Ting Huyan, 2016)

6.1.2.1.3 CTLA-4

The over proliferation of cytotoxic T-lymphocyte (CTL) A-4 on the surface of T-cells is yet another mechanism that has not been entirely investigated. This dampens activation of the T-cells by outcompeting CD28 in binding CD80 and CD86. CTLA-4 also delivers inhibitory signals to T-cells. Thus, CTLA-4 blockade has emerged as another attractive option for cancer immunotherapy (O'Byrne, 2015) (Garcia-Carbonero R, 2013).

$CD8^+$ T effector (T_{eff}) cells are thought to be the major type of immune cell affected by the programmed cell death protein 1 (PD1) immunosuppressive checkpoint pathway. In contrast CTLA4 predominantly regulates the activity of both effector and regulatory (T_{reg}) $CD4^+$ T cell subtypes. Priming of T-cells requires the recognition of processed tumour antigens presented by antigen presenting cells (APCs) such as monocytes and dendritic cells through a unique T-cell receptor (TCR) that binds to a major histocompatibility complex (MHC) molecule and tumour-derived peptide antigens (figure 82) (Suzanne L. Topalian, 2016). Such antigens may be generated from mutant or non-mutated tumour-associated proteins. Priming of T cells generally occurs in lymphoid tissue, and $CD4^+$ T cells provide help for $CD8^+$ T cell priming in the form of cytokines. Both $CD4^+$ and $CD8^+$ T cells are then activated through co-stimulatory pathways such as CD28–B7-1 and CD28–B7-2, causing them to proliferate, secrete inflammatory cytokines, acquire cytolytic properties and migrate to sites of antigen display i.e. tumour deposits. Within hours to days, activated T cells also begin to express the co-inhibitory receptor PD1 (figure 82) (Suzanne L. Topalian, 2016).

The recognition that a network of immune checkpoints need to be passed in order for effective immune responses to proceed has led to a focus on inhibitors of these checkpoints. Tumours may take over some of these checkpoints, contributing to immune resistance. Targeting checkpoints is an evolving approach to cancer immunotherapy, designed to foster an immune response. (Ting Huyan, 2016)

6.1.2.2Combined therapies

The immune blockade approaches are just emerging as compelling therapeutics. Pathways that mediate resistance to primary immune blockade antibodies are also emerging. Targeting these resistance pathways using combination therapies might be promising. Examples of this include targeting of CDK5 and ATG5, whose inhibition can impact on the efficacy of immune blockade antibodies. Identification of new targets for combined therapies or resistance factors will help to improve immune blockade therapies (O'Byrne, 2015).

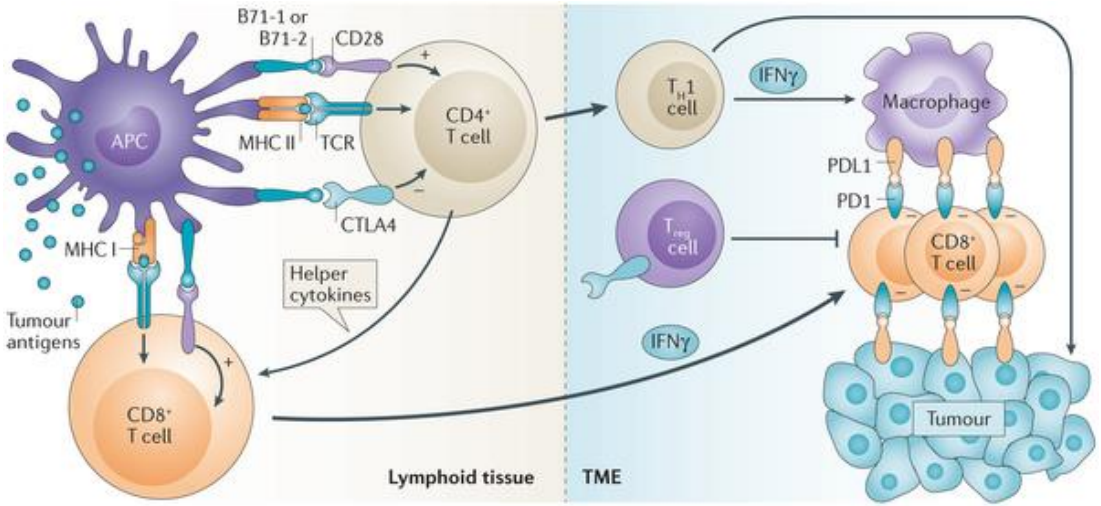

Figure 82 Immune checkpoint pathways

$CD4^+$ T helper 1 (T_H1) cells and $CD8^+$ T cells in the tumour microenvironment (TME) produce interferon-γ (IFNγ), which, on the one hand, activates tumour killing by macrophages and antigen display by tumour cells, but on the other hand, induces PDL1 expression by these same macrophages and tumour cells. Tumour-specific $PD1^+$ $CD8^+$ T cells encountering $PDL1^+$ cells within the TME will be functionally disabled. CTLA4 expressed by T_{reg} cells in the TME enhances their ability to suppress $CD8^+$ T cell-dependent cytokine production and direct tumour cell killing. Drugs blocking the immune checkpoints CTLA4, PD1 and PDL1 interrupt these immunosuppressive interactions and restore the ability of T cells to eliminate antigen-expressing cancer cells (Suzanne L. Topalian, 2016).

6.1.3 HSP90 and the immune system

Molecular chaperones, many of which are heat shock proteins (HSPs), are an important class of molecules with various functions. Many oncogenes, including tyrosine kinases, transcription factors, and cell-cycle regulatory proteins, are client proteins of HSP90. Drug candidates that target HSP90 can result in degradation of oncogenic kinases and thus hold therapeutic promise.

Inflammation is increasingly recognized as a factor in tumour initiation and progression. Due to the interaction of HSP90 with many pro-inflammatory kinase cascades such as IL-1 and TNF alpha, inhibition of HSP90 may provide a novel approach to reducing chronic inflammation (Rappa F, 2012); (Garcia-Carbonero R, 2013).

It is known that HSP90 is required for signal transducers and activators of transcription factor? 1 phosphorylation and, in its absence, JAK1/2 are degraded by the proteasome. HSP90 is also important for the conformation of the MHC complex, receptors and other important immune cell function proteins, including client proteins that are involved in human malignancies such as breast cancer, multiple myeloma and Ewing's sarcoma (Shimp SK, 2012) (Shang L, 2006) .

6.2 Aim

Due to the published links between the HSP90 system, interferon signalling and cancer development, I set out to determine how HSP90 targeted drugs can impact on oncogenic pathways in the immune receptor landscape.

I used several approaches to ask the following questions:

1. What was the effect of Ganetespib on its client proteins, particularly IRF-1

2. Does Ganetespib have any an effect on immune checkpoints such as PDL-1/PD-1 complexes in melanoma?

3. If Ganetespib has effects on PDL-1 levels in melanoma, to investigate the possible role of IRF-1 in this mechanism.

6.3 Results

6.3.1 Ganetespib downregulates IFNγ -induced IRF-1 expression

Interferon gamma is implicated as one of the many signals that can have an impact on immune blockade receptor functions. Our laboratory has previously discovered that HSP90 inhibitors can affect IRF-1 protein turnover. We aimed to understand whether HSP90 inhibitors can therefore impact on interferon induced immune blockade receptor function through the IRF-1 pathway.

My studies show that, when A375 melanoma cells with WT p53 were treated with Ganetespib (a HSP90 inhibitor drug) and IFNγ in combination for 16 hours, there was reduction in IFNγ-induced IRF-1 expression (Figure 83). HSP70 induction is normally observed in cells treated with HSP90 inhibitor as an indicator of inhibition of HSP90. I observed that HSP70 protein levels were induced after treatment with Ganetespib compared to control cells treated with DMSO (carrier for Ganetespib). Using IFNγ in combination with Ganetespib did not alter the levels of HSP70 significantly when compared to Ganetespib treated cells alone, but did increase production of lower molecular weight forms of HSP70. I observed no significant change in p53 expression between the IFN γ and DMSO treated cells, which indicates that when cells are treated only with IFNγ, their p53 status is unaltered whilst IRF-1 is upregulated.

Tumour-associated antigens (TAA) are the basis for antigen-specific immunotherapy. I investigated the protein levels of one such TAA, MDM2 a negative regulator of p53. Levels of MDM2 increase with addition of either Ganetespib alone or in combination with IFNγ, but not in cells treated with IFN-γ alone (Figure 83). This elevated MDM2 with IFNγ has been previously shown by various other studies (Mayr C1, 2006); (Yuan XW, 2008). GAPDH was used as a loading control and was similar across all the samples.

Overall these data show that Ganetespib can downregulate IFNγ-induced IRF-1 expression.

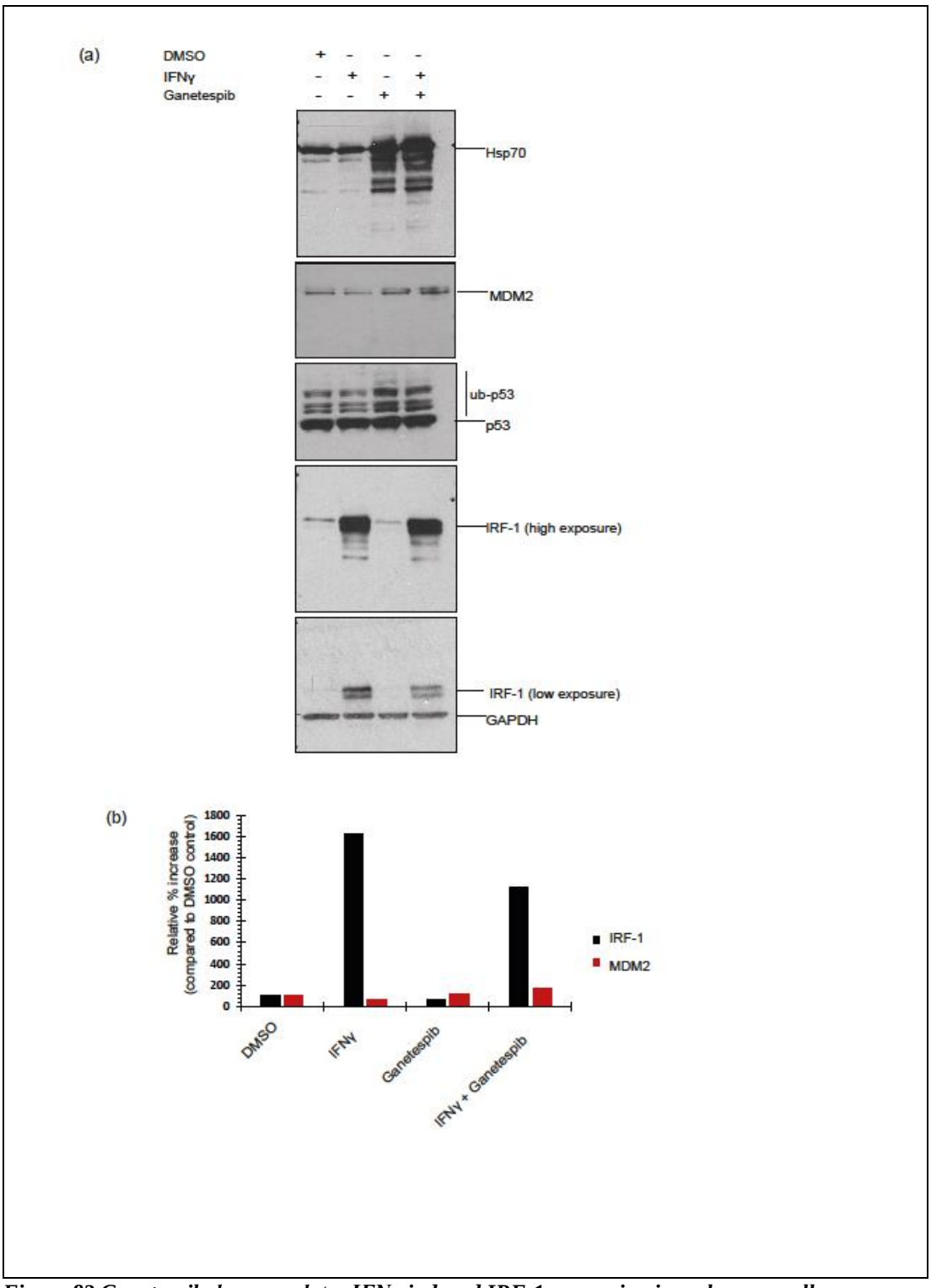

Figure 83 Ganetespib downregulates IFNγ-induced IRF-1 expression in melanoma cells.

(a) A375 melanoma cells were treated with DMSO, Ganetespib or IFNγ for 16 h, alone or in combination as indicated. Ganetespib was used at a final concentration of 100 nM, and IFNγ at 6 nM (100 ng/ml). Cells were isolated and total proteins extracted; IRF-1 levels were determined by Western blot analysis. (b) Quantification of results from (a) using Image J. The relative % increase of MDM2 and IRF-1 with respect to the DMSO control was calculated and is shown. The data are representative of at least three independent experiments.

6.3.2 Upregulation in IRF-1 expression with IFNγ is dose and time dependent

To determine if the combinatorial effect of IFNγ and Ganetespib on IRF-1 was dose or time dependent, I performed an IFNγ dose titration and time course assay. These treatments were done without the removal of IFNγ from culture medium prior to the addition of Ganetespib. Additional experiments were also performed, adding fresh medium before treatment with Ganetespib and these produced similar results (data not shown). A time course (1, 2 and 4 hours) of IFNγ treatment did not show any significant difference in IRF-1 induction (Figure 84-a), indicating that a one-hour treatment with IFN γ at100 ng/ml is sufficient to induce IRF-1 and saturate the expression level. In comparison, the time course or IFNγ in combination with Ganetespib induced a significant decrease in IRF-1 compared to the control of Ganetespib treatment alone. However, the loss of IRF-1 was again similar in all three of the IFNγ time course with Ganetespib combinations, suggesting Ganetespib can downregulate the IRF-1 protein even after up to 4 hours of IFNγ treatment prior to the addition of Ganetespib (Figure 84–a).

An IFNγ titration between 100–400 ng/ml was performed to determine whether the effect of Ganetespib on IRF-1 after IFNγ treatment was dose dependent. The cells were treated with IFNγ with Ganetespib for 16 hours. The results show that even all concentrations of IFNγ from 100–400 ng/ml produced similar induction of IRF-1 (Figure 84-b). All combinations of IFNγ and Ganetespib reduced IRF-1 to a level equivalent to control or baseline IRF-1. These results show that even the lowest dose of IFNγ used here (100 ng/ml) can induce IRF-1 within one hour, and that this induced IRF-1 can be downregulated with Ganetespib. Induction of IRF-1 suggests that there is de novo synthesis in 1 hour after cytokine stimulation.

To study if the time dependent effect of IFNγ on IRF-1 had any effect on the localisation of available IRF-1, I performed an immunofluorescence assay. The results showed an upregulation of IRF-1 over the time course of IFNγ treatment, and that the longer the treatment with IFNγ, the more intense the signal for IRF-1 (Figure 85-a).

At two hours post IFNγ treatment IRF-1 was detected in both the cytoplasm and the nucleus, but after four hours IRF-1 protein was detected almost exclusively in the nucleus.

When IRF-1 is primarily localised in the cytosol, its ability to regulate gene transcription would be limited. Treatment with IFNγ appears to induce IRF-1 and its translocation into nucleus thus enhancing its role in gene transcription. Blocking the activity of the proteasome with MG132 (a specific, potent and cell permeable proteasome inhibitor) after four and six hours of IFNγ treatment didn't change the localisation of IRF-1, compared with treatment with IFNγ only (Figure85).

Overall these data show that IFNγ has a time and dose dependent effect on both total IRF-1 protein expression and localisation of IRF-1 within the cell.

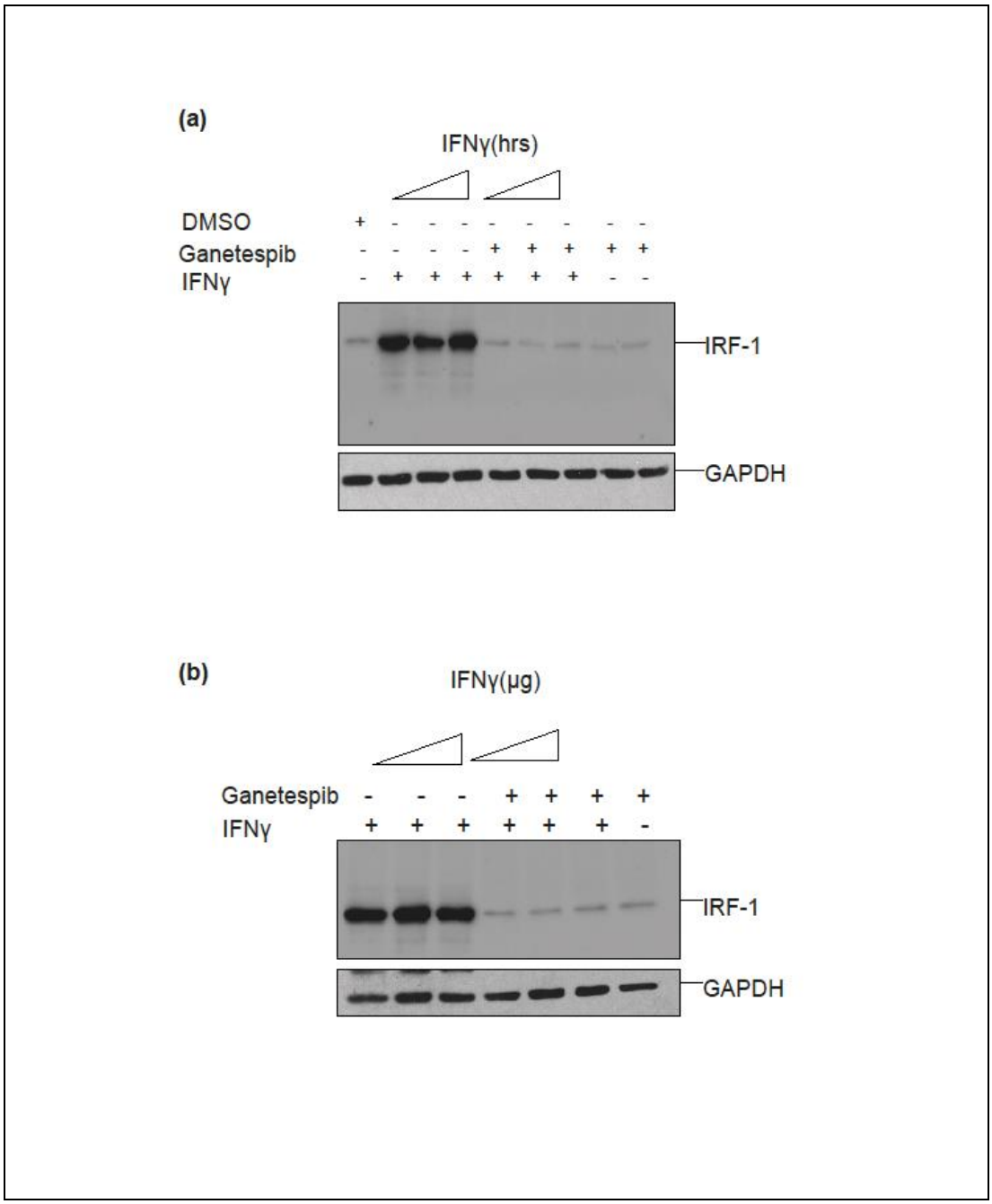

Figure 84 IRF-1 activation via IFNγ is dose and time dependent

(a) A375 cells were treated with IFN*γ* (100 ng/ml) for 1, 2 or 4 h prior to the addition of Ganetespib (100 nM) or vehicle (DMSO) for 16 hours. Cell lysates were prepared and assayed by Western blot. *(b)* A375 cells were treated with either Ganetespib (100 nM), DMSO or IFN*γ* (100, 200 or 400 ng/ml) alone or in combination for 16 hours. Cell lysates were prepared and assayed by Western blotting. The data are representative of at least three independent experiments.

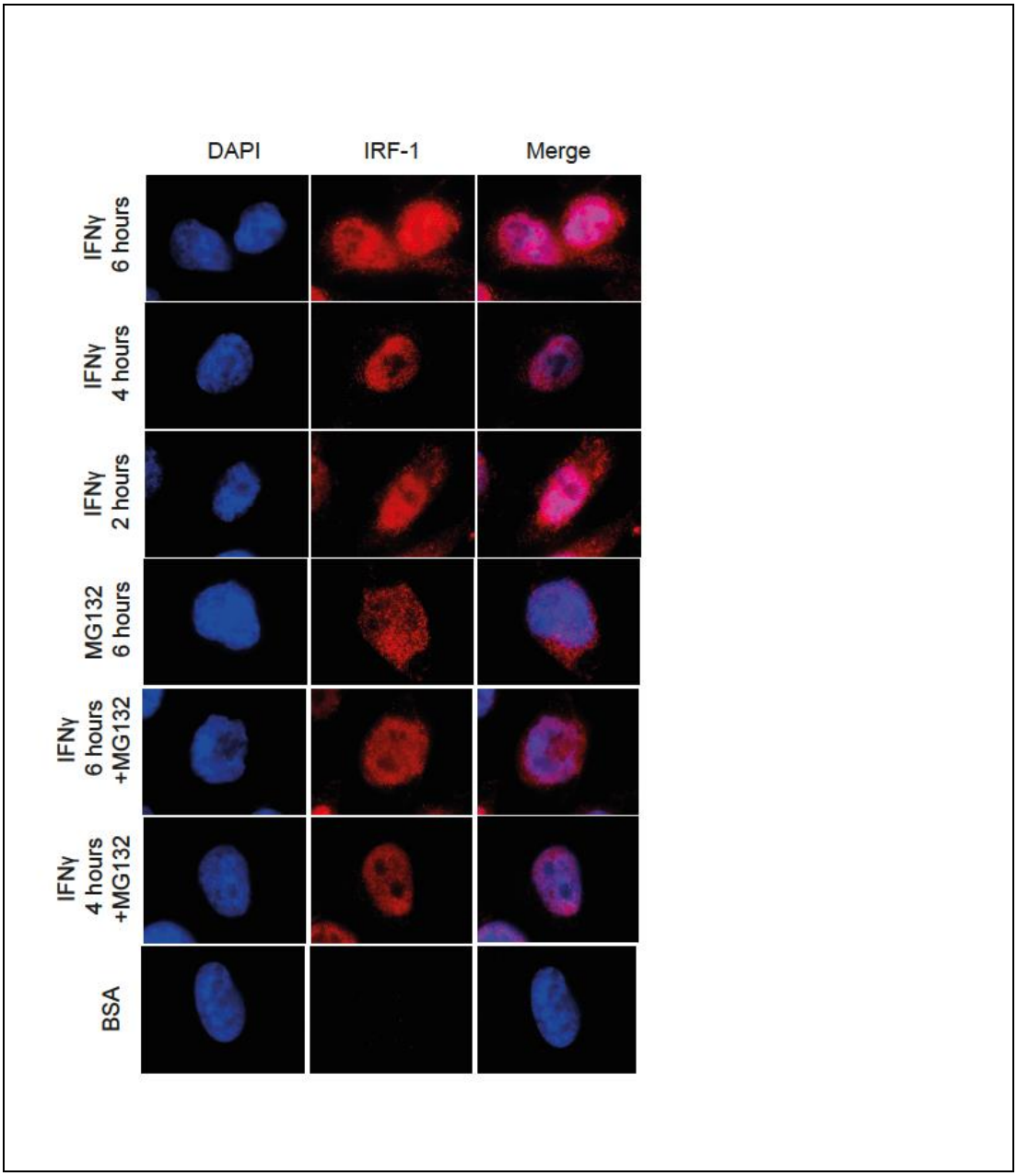

Figure 85 IRF-1 localisation with IFNγ time course

A375 cells were pre-treated with IFNγ (100 ng/ml) for 2, 4 and 6 h prior to the addition of MG132 (50 μM) for a further 2 h. Cells were fixed, stained with anti IRF-1 polyclonal antibody and then with secondary goat anti-rabbit Alexa fluor 594 and DAPI, then visualised by IF microscopy. The data are representative of at least three independent experiments.

6.3.3 Downregulation of IFNγ-induced PD-L1 expression by Ganetespib

In patients treated with IFNs who are immune-compromised as a result of cancer treatment, there is likely to be an elevated expression of PD-L1 complexes, thereby making their tumours more susceptible to immune evasion. I show that total PD-L1 levels are significantly elevated after IFNγ treatment and that inhibition of the IFNγ effect with Ganetespib partially prevented the induction of PD-L1 (Figure 86). This effect was more noticeable if the cells were pre-treated with Ganetespib prior to the treatment with IFNγ (Figure 86-a). Pre-treating the cells with Ganetespib for six hours and then treating with IFNγ reduced the PD-L1 protein level to that of the vehicle control. There is a small increase in PD-L1 with Ganetespib alone when compared to untreated samples. These results were analysed by Western blotting of whole cell lysates, probing for PD-L1.

The above result was confirmed using flow cytometric analysis using APC mouse anti-human PD-L1 monoclonal antibodies to detect cell surface membrane bound PD-L1. This analysis also indicated that pre-sensitizing the cells with Ganetespib (six hours in this instance) prior to treatment with IFNγ decreased the amount of antibody accessible PD-L1 on the membrane (Figure 86-b). Pre-treating the cells with Ganetespib downregulated the expression of PD-L1 below the level in control samples. When the cells were pre-treated, PD-L1 expression after IFNγ treatment was reduced by 70% compared to cells treated with Ganetespib and IFNγ at the same time. Expression levels in the latter were reduced by 50% compared to the IFNγ only control. An isotype control was included as an indication of nonspecific antibody binding (Figure 86–b).

To determine if IFNγ-dependent attenuation of PD-L1 was time dependent, I performed a time course of IFNγ treatment with Ganetespib, where the cells were treated first with IFNγ (30 mins to two hours) prior to the treatment with Ganetespib (six hours). There were no significant changes in total PD-L1 protein expression levels over the time course (Figure 86-c), but IRF-1 levels were significantly changed. It is worth noting that as we increase the duration of cells' exposure to IFNγ, the action of Ganetespib is overcome by IFNγ**.** However a treatment of either 30 mins or 1 hour of IFNγ, along with subsequent 6 hours of Ganetespib, can still lower the levels of IRF-1 but after two hours there are no significant changes. PD-L1

does not increase during a short time-course, suggesting that this mechanism is downstream of IRF-1, i.e. IRF-1 is induced and activated prior to increased expression of PD-L1.

Comparing these results to those in Figure85, where IFNγ and Ganetespib were added together and produced substantial IRF-1 downregulation, suggests that pre-treating the cells with IFNγ reduces the effectiveness of Ganetespib to reduce IRF-1. I also observed that incubating cells with Ganetespib for 16 hours after the cells were pre-treated with IFNγ had a greater impact on IRF-1 protein levels compared to 6 hours of Ganetespib treatment. In this case, PD-L1 is observed as two bands. The higher band is predominant when cells are treated with Ganetespib alone, whereas both bands are equally intense when cells are treated with IFNγ. This suggests that the lower form of PD-L1 is lost preferentially and it will be of interest to determine what causes this difference in molecular mass.

To evaluate whether drug administration with or without IFNγ affected the localisation of PD-L1 within the cell, immunofluorescence assays were conducted. PD-L1 was shown cytoplasmic and membrane bound in the Ganetespib and DMSO controls, whereas a more dense and nuclear localised PD-L1 was observed with IFNγ treatment (Figure 87). When IFNγ is combined with Ganetespib there was a shift of PD-L1 localisation and it appeared to be more concentrated in the cytoplasm.

In summary, Ganetespib downregulates IFNγ-induced PD-L1 expression and pre-sensitisation of the cells with Ganetespib prior to the addition of IFNγ increases the efficacy of the drug. A 16-hour treatment with 100nM of Ganetespib is more effective than a six-hour treatment. IFNγ treatment re-localises the PD-L1 to the nucleus.

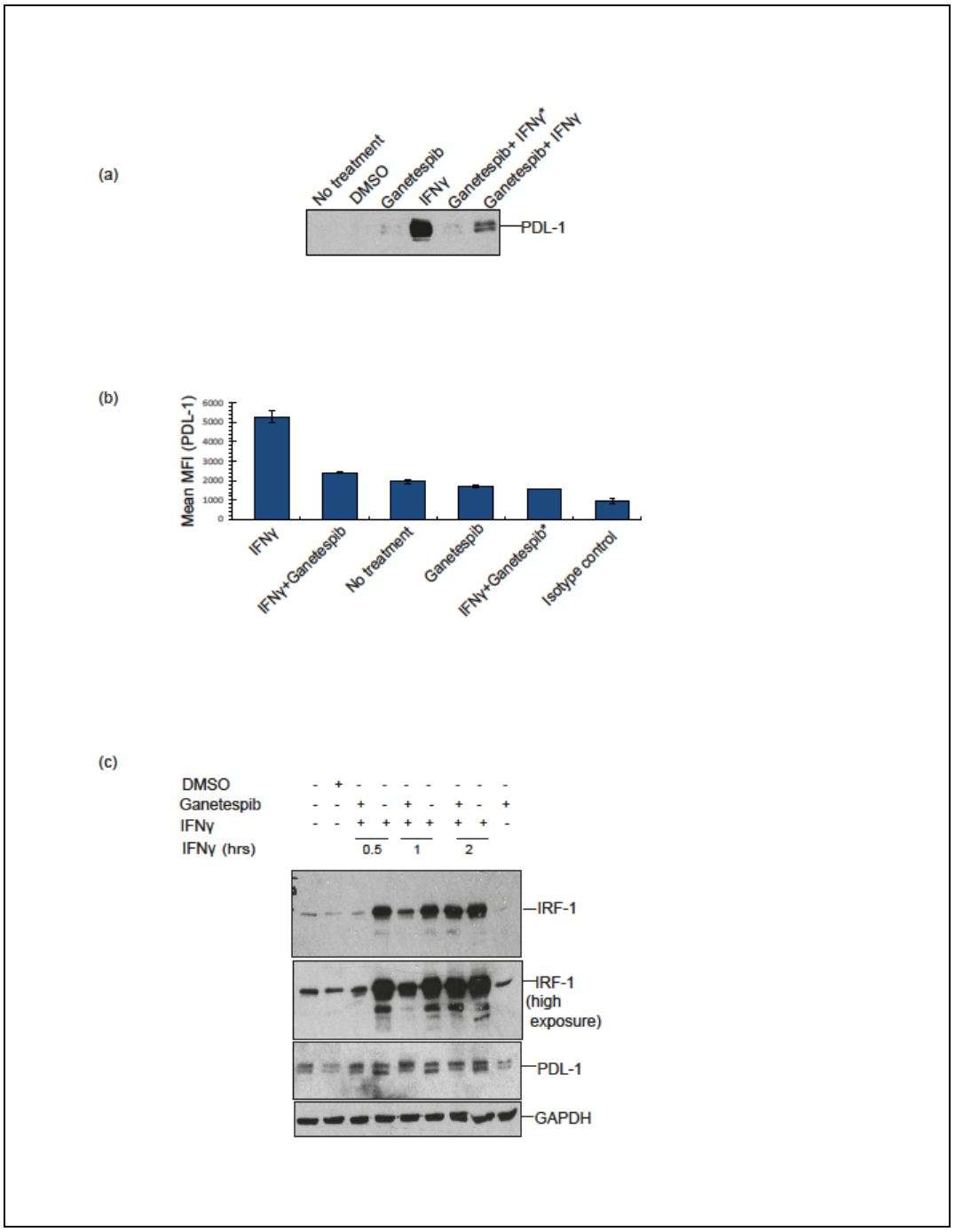

Figure 86 Ganetespib downregulates IFNγ induced PD-L1 expression.

(a) A375 cells were treated with either Ganetespib (100nM), DMSO or IFNγ (100 ng/ml) alone or in combination for 16 hours. Cell lysates were prepared and analysed by Western blot. Total PD-L1 was detected using rabbit monoclonal anti human PD-L1. *(b)* The cells were resuspended and the mean fluorescence intensity (MFI) was measured using flow cytometry. Graphical representation of MFI. *(c)* Cells were treated with a time course of IFNγ (100 ng/ml) at 0.5, 1 and 2 h prior to the addition of Ganetespib for 6 h. Total PD-L1 and IRF-1 were determined by Western blot analysis. *Ganetespib pre-treated for 6 hours prior to the stimulation with IFNγ. The data are representative of at least three independent experiments.

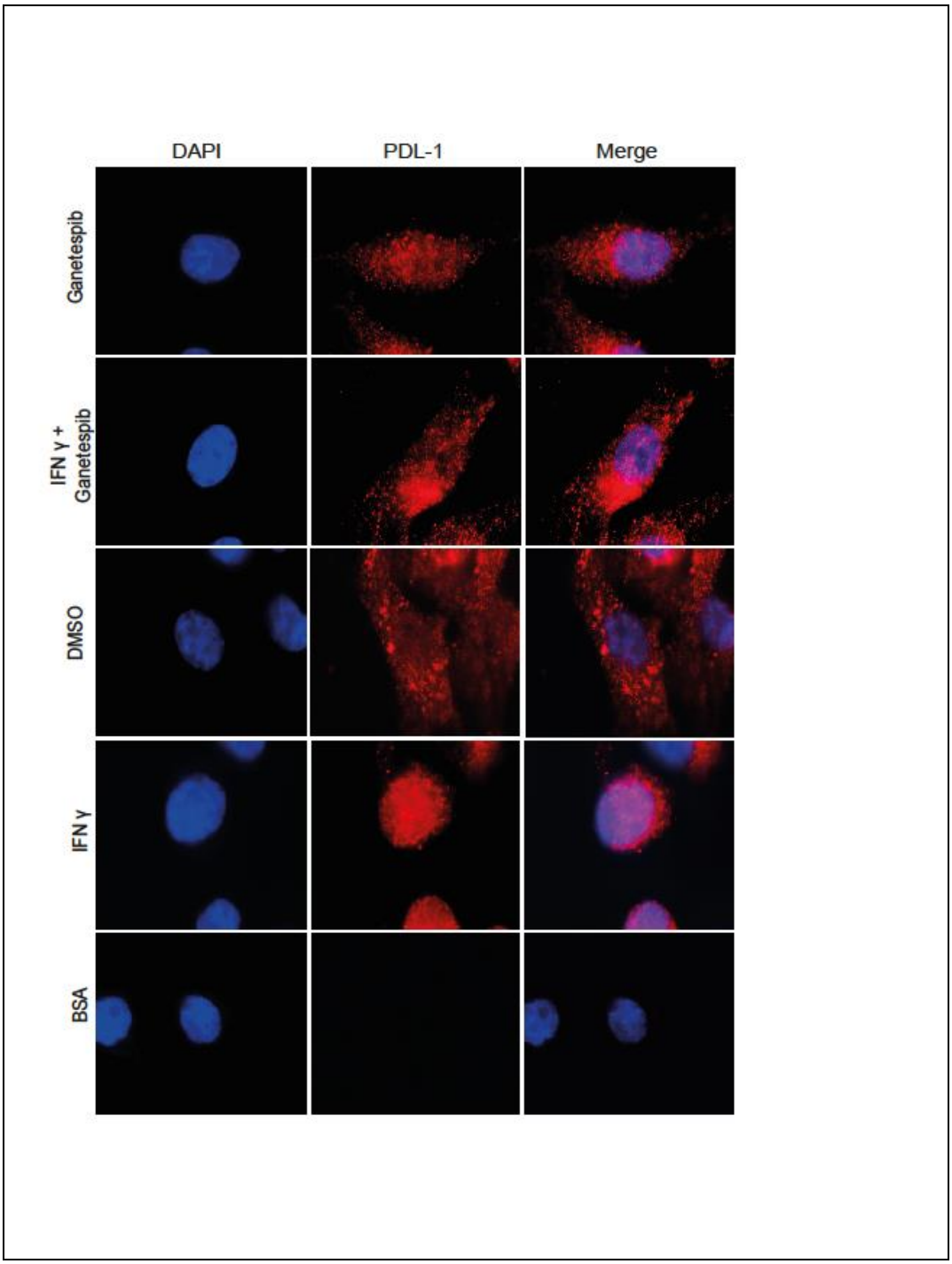

Figure 87 Localisation of PD-L1

Cells were treated as per panel and stained with anti PD-L1 polyclonal antibody and then with secondary Alexa fluor goat anti-rabbit 594 and detected by IF microscopy. *Ganetespib (100 nM) pre-treated for 6 h prior to the stimulation with IFNγ (100 ng/ml). The data are representative of at least three independent experiments.

6.3.4 Ganetespib inhibits PD-L1 expression induced by INFγ pre-treatment

I wanted to determine if the action of Ganetespib on PD-L1 was still effective after cells were pre-treated with IFNγ. Previously I have shown that a two-hour treatment with IFNγ was sufficient to induce IRF-1 and saturate the effect of Ganetespib, and it was important to determine whether this was similar for PD-L1. I pre-treated the cells with IFNγ for four hours then incubated cells with Ganetespib for 16 hours. Interestingly, even after pre-sensitizing with IFNγ, Ganetespib was able to still reduce PD-L1 expression by 43%, as compared to an IFNγ only control. When cells were treated with IFNɣ and Ganetespib together there was a 53% reduction of PD-L1 expression, compared to IFNγ treatment (Figure 88-a).

To further validate this data, I studied IFNγ pre-treatment with a time course of Ganetespib. Cells treated overnight (16 hours) with IFNγ and then treated with Ganetespib for four hours, showed a 9% reduction of IFNγ-induced PD-L1 expression as compared to IFNγ control whereas there was a 20% reduction in induced PD-L1 expression when cells were pre-treated with IFNγ for only two hours. As previously shown, when cells were treated with both Ganetespib and IFNγ together we observed a 52 % reduction in IFNγ-induced PD-L1 expression (Figure 88-b). These results suggest that the mechanism of Ganetespib action is dependent on the duration of exposure of cells to IFNγ; when used in combination, the levels of PD-L1 is still comparable to controls.

Overall, the pre-treatment of the cells with IFNγ does restrict the action of Ganetespib on PD-L1. In contrast, simultaneously administrating IFNγ and Ganetespib extensively downregulated IFNγ-induced PD-L1 expression compared with IFNγ controls.

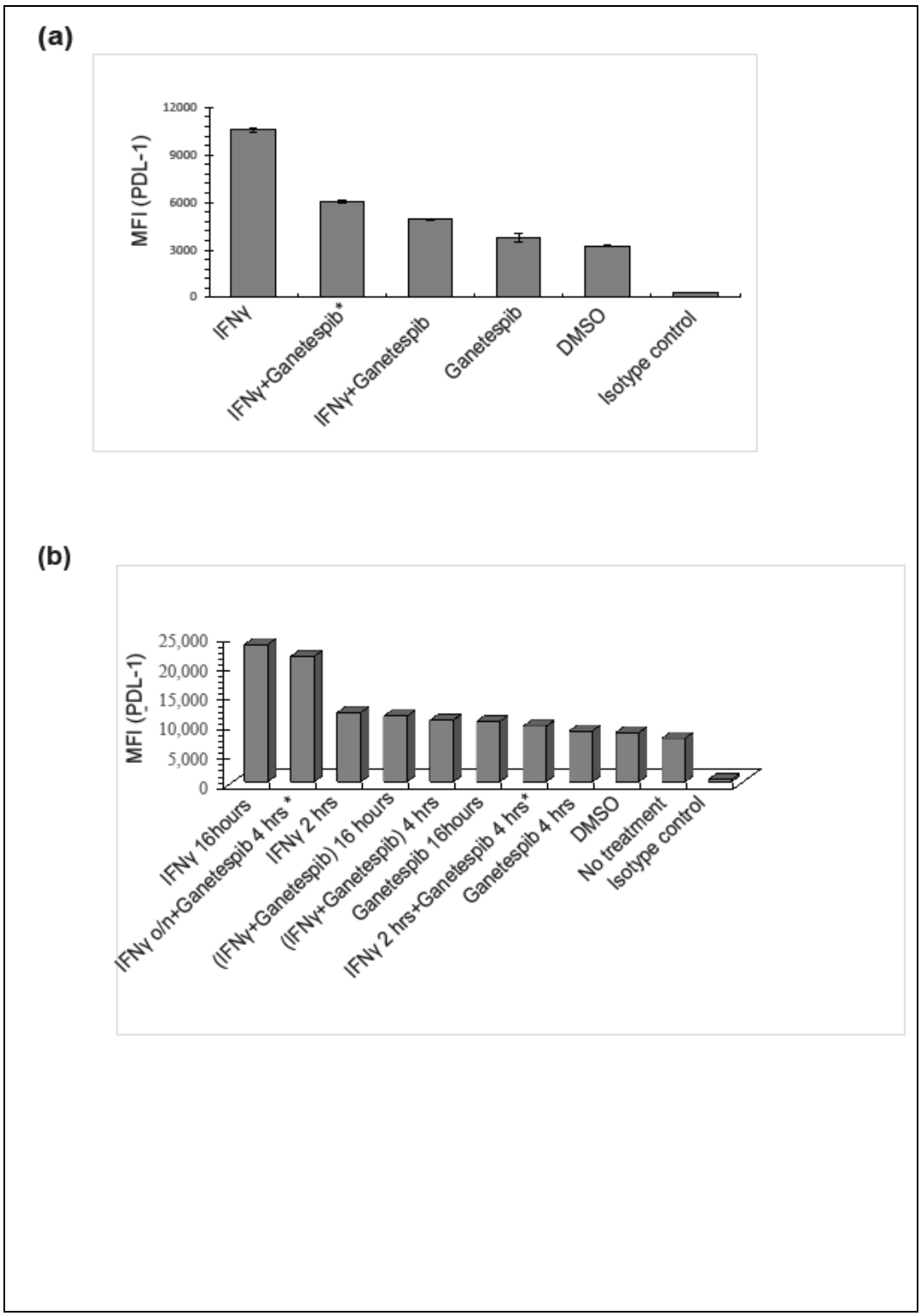

Figure 88 Ganetespib downregulates pre-treated IFNγ-induced PD-L1 expression.

(a) A375 cells treated with IFNγ (100 ng/ml for 4 h), DMSO or Ganetespib(100 nM) either alone or in combination with Ganetespib for further 16 hours *(b)* A375 cells treated as per panel. The cells were re-suspended and the mean fluorescence intensity (MFI) measured using flow cytometry. *IFNγ pre-treated before the addition of Ganetespib. The data are representative of at least three independent experiments.

6.3.5 Loss of PD-L1 is via an IRF-1-dependent pathway

In the previous chapter I have shown that Ganetespib can inhibit IRF-1 expression levels in cancer cell lines such as A375, and have investigated the mechanism of loss of IRF-1. Here I wanted to determine if PD-L1 downregulation was an IRF-dependent process.

I addressed this, first by using flow cytometric assays, in which I knocked down IRF-1 expression in cells using siRNA, and analysed membrane bound PD-L1 after IFNγ treatments.

My results indicated that knocking down IRF-1 using siRNA decreased PD-L1 expression by ~61%, compared to that in IFNγ treated control cells (Figure 89-a). This reduction in PD-L1 expression was similar to when IFNγ and Ganetespib were used in combination, indicating that the loss of IRF-1 by Ganetespib was probably contributing towards the downregulation of PD-L1. All the controls including the siRNA negative control gave low and similar PD-L1 expression.

Total PD-L1 protein after siRNA treatment was also assessed. The results supported the data from flow cytometric analysis, indicating that the high levels of induced PD-L1 by IFNγ were downregulated by the loss of IRF-1, as determined using immunoblotting of whole cell extracts (Figure 89-b). Using IRF-1 siRNA I was able to knock down IRF-1 by approximityly 93%, compared to the DMSO control. When the cells were treated with Ganetespib after siRNA treatment, knockdown of IRF-1 was >95%. In cells treated with IFNγ + IRF-1 siRNA, PD-L1 protein expression was comparable to that in controls. Treatment with Ganetespib and IRF-1 siRNA together resulted in here was significant loss of IRF-1 when compared to cells treated with IRF-1 siRNA alone. IFNγ-induced IRF-1 levels were therefore downregulated by the treatment of Ganetespib. To determine the effect of siRNA on IRF-1 intracellular localisation I performed immunofluorescence. IFNγ treatment re-localised IRF-1 into the nucleus, whereas treatment with IFNγ plus Ganetespib reduced the total IRF-1 but it was still localised within the nucleus (Figure 90). IRF-1 knockdown using siRNA didn't alter the localisation of IRF-1, compared with control negative siRNA, DMSO or Ganetespib treated cells. Although immunoblotting showed a significant effect of IRF-1 siRNA on IRF-1 protein levels (lanes4 and 5), the difference was less evident by immunofluorescence. This could reflect that the IRF-1 antibody used for immunofluorescence gave a weak signal and thus a relatively poor signal to noise ratio. In conclusion, the results suggest that IRF-1 might stabilise PD-L1 expression and that Ganetespib inhibits IFNγ-induced PD-L1 expression by inhibiting IRF-1.

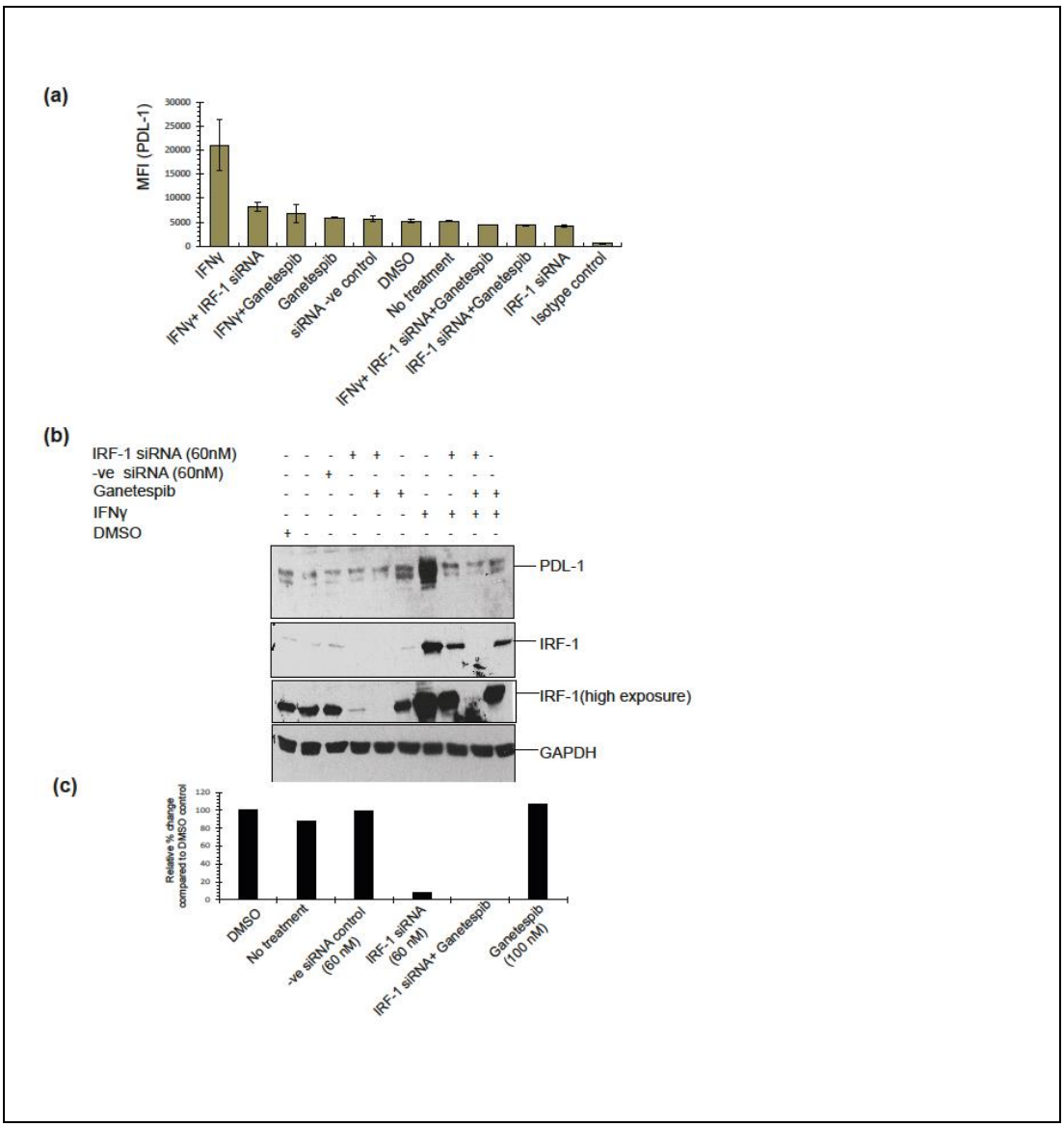

Figure 89 IFNγ-induced expression of PD-L1 is IRF-1 dependent

(a) A375 cells were treated as per panel. The cells were resuspended and the mean fluorescence intensity (MFI) was measured using flow cytometry *(b)* A375 cells were treated with either control siRNA or siRNA to IRF-1 (60nM) for 24 h and then treated as indicated on the panel. Total cell lysates were analysed for PD-L1 or IRF-1 via Western blotting. *(c)* Quantification of results from (b) using Image J.

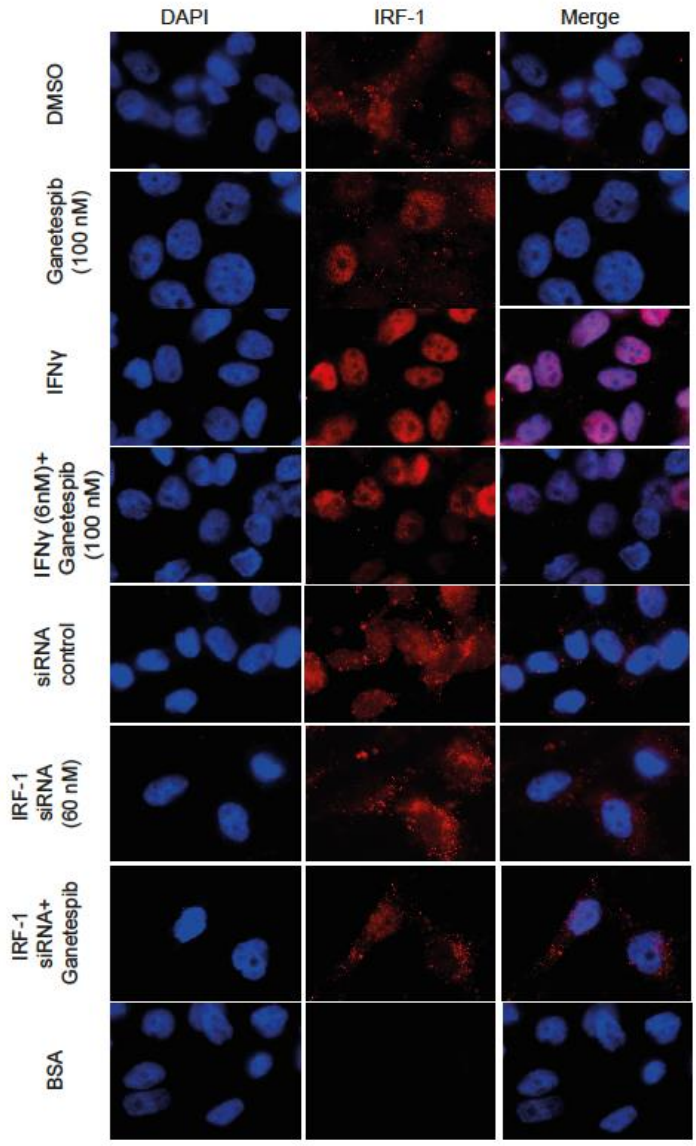

Figure 90 IRF-1 localisation after IFNγ stimulation

(a) A375 cells were treated with either non-targeting control siRNA or siRNA to IRF-1 (60nM) for 24 h and then treated as indicated on the panel. Cells were stained with anti-polyclonal IRF-1 antibody and secondary Alexafluor 594 goat anti rabbit and visualised by IF microscopy

6.3.6 The dose dependency of PD-L1 expression on Ganetespib depends on cell type

Given that different cell lines have a different amplitude of response to cytokine stimulation, I wanted to determine whether the activation of IRF-1 by IFNγ is different for different cancer cell types.

For this experiment I used the A375 melanoma and the A549 human lung carcinoma cell lines. I have shown that the loss of PD-L1 by Ganetespib is IRF-1 dependent. Next, I wanted to evaluate if this loss was drug dose dependent. As previously shown, the optimal dose of Ganetespib used in the assays was 100 nM, and this was sufficient to reduce IFNγ-induced PD-L1 expression. This concentration was determined based on the dose response for IRF-1. I conducted a titration of Ganetespib (10–10 μM) with and without pre-treatment with IFNγ and analysed PD-L1 expression levels. Concentrations of 10 μM, 1 μM and 100 nM gave similar effects on PD-L1 expression after IFN γ treatment of A375 cell lines, but the lowest dose (10 nM) didn't downregulate PD-L1 and was similar to the IFNγ-only controls (Figure 91-a). A titration of Ganetespib alone gave only low PD-L1 expression, comparable to the control DMSO and no treatment samples. I observed an 80.4% reduction of IFNγ induced PD-L1 expression with 100 nM Ganetespib and his was similar with 10 μM and 1 μM concentrations.

The results for A549 cells were different. There was only 55% reduction of induced PD-L1 expression for the highest dose, and 47.5% reduction with the lowest dose of 10 nM (Figure 91-b). Ganetespib concentrations of 10nM to 10 μM had similar effects in A549, whereas in A375 cell lines 10 nM had no effect on PD-L1 expression.

In brief, this data indicates that Ganetespib has different kinetics based on the cell type and probably requires optimisation for its maximum effect on the cells.

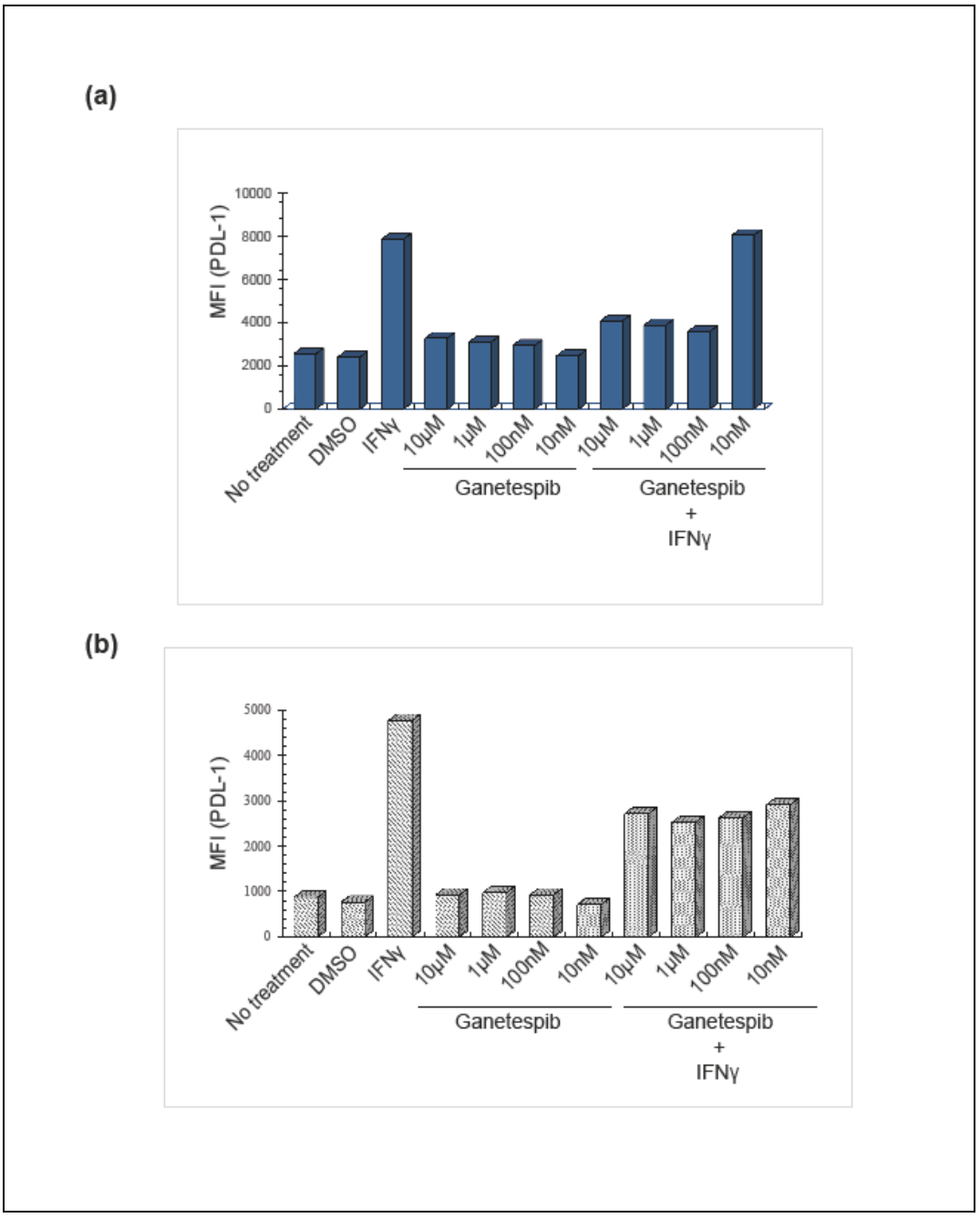

Figure 91 Attenuation of IFN-induced PD-L1 is cell type dependent

(a) A375 cells were treated with a titration of Ganetespib (10 μM–10 nM) either alone or in combination with 100 ng/ml of IFNγ for 16 h. The cells were resuspended and mean fluorescence intensity of membrane bound PD-L1 measured by flow cytometry. *(b)* WT A549 cells treated and analysed as above. The data are representative of at least three independent experiments.

6.3.7 PD-L1 expression is regulated by the autophagy protein ATG5

In the previous chapter I showed that down-regulation of IRF-1 by Ganetespib could be associated with the proteasome activity. In this chapter I aimed to discover whether loss of PD-L1 is linked to the autophagy pathway. When cell death is induced, Atg5 (an E3 ubiquitin ligase) plays a supportive role in the apoptosis process, indicating its role in autophagy/apoptotic cell death (Chandra B Lebovitz, 2015).

For this purpose I used three A549 cell lines: WT, KO (ATG5 CRISPR) and Rescue (ATG5 rescue) cell lines (Kind gift from Simon Wilkinson's laboratory). In CRISPR rescue A549 cell line, the ATG5 gene is replaced back into the cell KO line and there is a partial recovery of the autophagic capacity of the cell (Wilkinson, personal communication).

In WT A549 cell lines, the levels of membrane surface-expressed PD-L1 was low in untreated or DMSO treated cells compared to the ATG5 KO cells (Figure 92-a). When the cells were treated with IFNγ + Ganetespib, the PD-L1 signal was downregulated by 43% in the WT A549 cells compared to the IFNγ-only treated cells. When ATG5 KO cells were treated with IFN γ +Ganetespib, the cells were able to attenuate the PD-L1 expression by only 24% compared to the IFNγ-only controls, indicating that Ganetespib inhibition of IFNγ –induced PD-L1 expression is ATG5-dependent. The isotype controls gave low PD-L1 expression levels indicating very low non-specific binding of the flow cytometric PD-L1 antibody. When treated with Ganetespib alone each cell lines gave PD-L1 expression comparable to the basal level and only slight increase in expression as compared to DMSO control.

Downregulation of ATG5 gene expression upregulates PD-L1 in the KO cell lines, compared to the WT. This indicates that ATG5 deletion might enhance pathways which upregulate PD-L1 expression. Yang et al also demonstrated that deletion of ATG5 enhanced activation of the IκB kinase (IKK)-related kinase TBK1 in vivo, which is associated with PD-L1 upregulation (Yang S, 2016). The mechanism of action of Ganetespib might be via ATG5, hence knocking the ATG5 gene out reduces the drugs ability to downregulate PD-L1 as compared to the WT control. PD-L1 expression in the rescue cell lines revealed that when the cells were treated

with Ganetespib, PD-L1 expression was reduced by 34% as compared to the IFN γ alone control .This range is higher than the knockout but still lower than the WT, suggesting there is probably only partial recovery of ATG5 and hence not enough ATG5 gene in the system to keep a tight control of regulation of PD-L1 expression.

The results suggest that the basal expression of PD-L1 is enhanced in the KO, suggesting autophagy plays a role in normal turnover of PD-L1, however the Ganetespib effect could partly involve autophagy in combination with IRF-1 dependent modulation of PD-L1 gene expression; this requires further investigation. Therefore this data indicates that expression of PD-L1 is ATG5 dependent and the loss of PD-L1 by Ganetespib could be via activation of ATG5 gene.

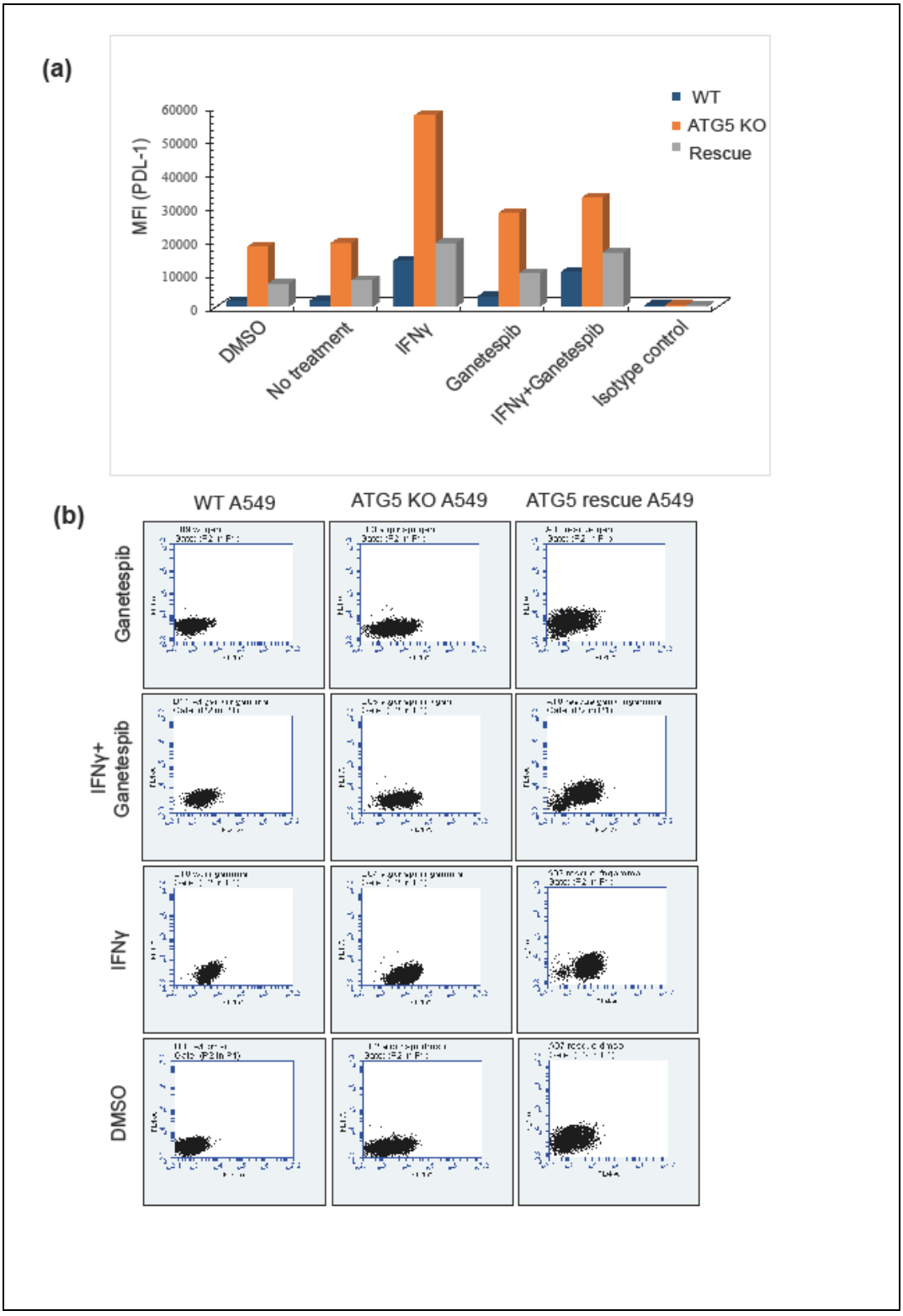

Figure 92 Downregulation of IFNγ-induced PD-L1 by Ganetespib is regulated via the ATG5 gene

(a) WTA549, ATG5 KO A549 and Rescue ATG5 A549 cells were treated with DMSO, IFNγ (100ng/ml), Ganetespib (100nM) either alone or in combination for 16 h. The cells were resuspended and mean fluorescence intensity of membrane bound PD-L1 measured by flow cytometry. *(b)* Gates for flow cytometry

6.3.8 HSP90 inhibitors in IFNα signalling

IRF-1 is an activator of IFNα transcription (Yuan XW, 2008). IFNα induces cell cycle arrest and triggers apoptosis; it also enhances transcription of the tumour suppressor gene p53. Here I wanted to study the role of a HSP90 inhibitor within the IFNα system as a control for comparison to the effects of INFγ in the experiments described above.

Titration of IFNα was performed and compared to the standard dose of IFNγ (100ng/ml) as control. There was no effect of IFNα (400 ng/ml) on levels of IRF-1, whereas IFNγ at 100 ng/ml showed intense upregulation of IRF-1 protein (Figure 93–a**).** HSP70 expression was shown to be stable in both IFNα and IFNγ treatments, however p53 expression was different between the two treatments: there were stronger ubiquitination bands of p53 in IFNα-treated cells compared to IFNγ treated cells.

In the previous section I demonstrated that pre-treating cells with Ganetespib prior to the addition of IFNγ could downregulate the induced PD-L1 expression efficiently and effectively. I also evaluated this effect with IFNα treatment. A375 cells were treated with Ganetespib and IFNα, either alone or in combination, for 16 hours. There was no change in IRF-1 expression when cells were treated with IFNα and Ganetespib together, compared to controls (Figure 93-b). However, when cells were pre-treated with Ganetespib prior to addition of IFNα, Ganetespib could downregulate the IRF-1 levels. There was negligible difference between IRF-1 expression when IFNα and Ganetespib were added simultaneously as compared to controls (Figure 93-b). Ganetespib treatment alone reduced IRF-1 to basal levels and here acted as a control for the assay.

When flow cytometric analysis of PD-L1 expression with IFN α and IFNγ treatments, similar results were obtained. The data indicated that IFNα-induced PD-L1 expression by was also lowered after the treatment with Ganetespib. (Figure 93-c). Control cells treated with IFNγ +/- Ganetespib were included in the same assay. IFNγ, as expected, induced much higher PD-L1 expression than did IFNα.

When cells are treated with IFNα there is an increase of only 5.2% in PD-L1 expression, compared to the basal level. When Ganetespib was added with IFNα, PD-L1 expression was

reduced by 10.3%, bringing the total PD-L1 levels lower than the basal levels. Ganetespib reduced the induced PD-L1 by 5.6% as compared to the levels of controls DMSO/no treatment.

In comparison, there was an 86% increase in PD-L1 expression with IFNγ, compared to control untreated cells. There was about 41% reduction in the IFNγ-induced PD-L1 expression when Ganetespib is used in combination. Ganetespib + IFNɣ treatment increases only 10% of the PD-L1 expression when compared to DMSO control.

As shown in the former segment, PD-L1 loss was IRF-1 dependent. I wanted to determine if IFNα-induced PD-L1 loss with Ganetespib treatment also followed the same pathway. There was a 41.5% decrease in PD-L1 expression when IRF-1 was knocked down and a further 48% decrease in IFNα-induced PD-L1 expression when compared to cells treated with IFNα alone (Figure 93-d). There was only 10% drop in PD-L1 expression when Ganetespib was treated in combination with IFNα, compared to the IFNα induced PD-L1. A slightly lower reduction was obtained when IFNα + Ganetespib and siRNA to IRF-1 where used in combination. I observed only 33.5% reduction of PD-L1 compared to IFN alpha only treated cells.

Overall I have shown that both the IFNα- and IFNγ-dependent pathways could be altered by Ganetespib treatment, and the PD-L1 expression increased with both IFNs could be reduced by Ganetespib. The above data demonstrates that HSP90 inhibition by treatment with drugs such as Ganetespib causes a decrease in IRF-1 protein levels and this effect is not mediated via inhibition of p53.

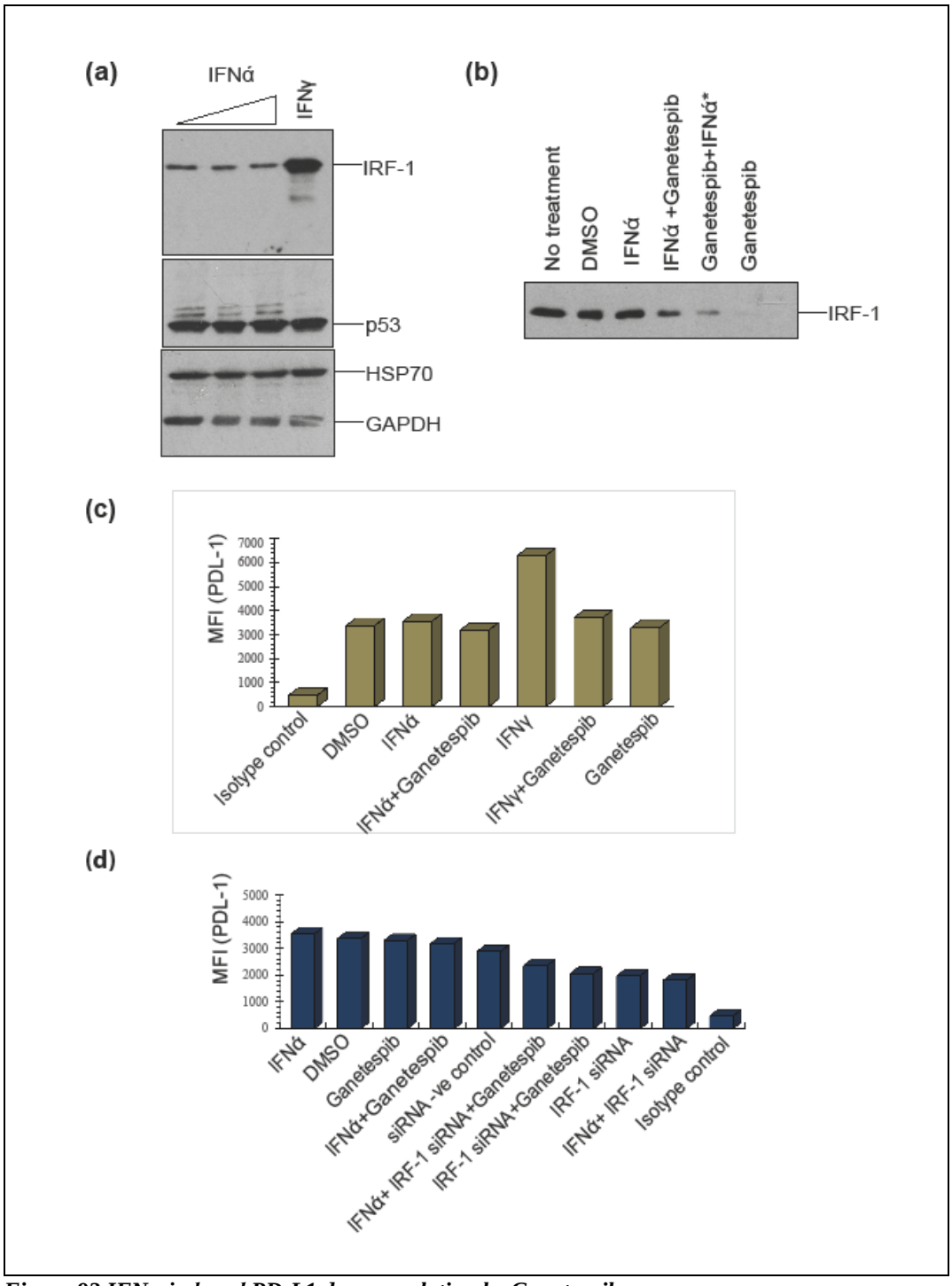

Figure 93 IFNα induced PD-L1 downregulation by Ganetespib

(a) A375 cells were treated with either titration of IFNα (100, 200 and 400ng/ml) or IFNγ (100ng/ml) and the total cell protein analysed for IRF-1, p53 and HSP70 by Western blotting. *(b)* Cells treated with either DMSO or IFNα with pre-treatment of Ganetespib and total cell lysate analysed for IRF-1. *(c) & (d)* The cells were treated as the panel and the cells resuspended and mean fluorescence intensity (MFI) of membrane bound PD-L1 measured by flow cytometry.

6.4 Discussion

HSP90 functions as an immune capacitor and maintains critical immune network components of the IFNγ pathways. IFNγ has a central role in the immunologically active cancer phenotype characterised by improved expression of IRF-1, and plays an important role in IFNγ-induced apoptosis in tumour cells (Murtas D, 2013).HSP90 associates with signalling molecules implicated in the aberrant survival of tumour cells, such as mutant and WT p53. HSP90 client proteins that influence p53 stability include MDM2, the E3 ligase that directly ubiquitylates and promotes the degradation of p53 (Olivier Ayraulta, 2009).

My results show that IRF-1 protein levels are upregulated, in a dose- and time-dependent manner, when melanoma cells A375 are treated with IFNγ, and that this IFNγ induced IRF-1 expression is downregulated when the cells were treated with an HSP90 inhibitor drug (Ganetespib). MDM2 expression levels in non-treated A375 cell lines were low, and treatment with IFNγ did not alter protein levels. The downregulation of IRF-1 increased the expression levels of MDM2 when the cells were treated with Ganetespib either alone or in combination with IFNγ. I also observed marginally stronger bands for ubiquitinated p53 in Ganetespib treated cells. Ganetespib could be altering the interaction between MDM2 and p53, thereby increasing the total available p53 in the cells.

There was an induction of HSP70 with Ganetespib implying the inhibition of HSP90. Lazenby et al. have shown that upregulation of HSP70 is a cytoprotective function in response to hp90 inhibition by sustained induction of the HSP transcription factor HSF1 (M. Lazenby, 2015).The IFNγ titration assays have shown that incubating cells with 100ng/ml for 1 hour induces IRF-1 is sufficient to induce IRF-1, and Ganetespib could downregulate IRF-1 even after a 4-hour IFNγ induction, at the highest doses of IFNγ, (400ng/ml) at four hours. These data suggest that Ganetespib activity was potent and robust. However, IFNγ doesn't suppress Ganetespib at 400ng/ml for 4 hours or 100ng/ml for 16 hours. Study of the localisation of IRF-1 with IFNγ titration indicated that IRF-1 expression increased with the duration of IFNγ treatment and extended duration resulted in IRF-1 localisation from the cytoplasm to the nucleus. Blocking the proteasome made no difference to the localisation of IRF-1; possibly the cells required a longer treatment with MG132 for efficient proteasome inhibition.

Blocking checkpoints that allow cancer cells to evade patients' immune responses holds great promise for achieving durable antitumour responses. In the tumour microenvironment,

research has been focused on blockading the PD-1/PD-L1 pathway, and in the lymph nodes the focus has been on blocking the CTLA-4 pathway (O'Byrne, 2015). A substantial proportion of human melanomas harbour IFNγ-producing macrophages, and thereby have upregulated PD-L1 expression. (Hatem Soliman, 2014) .I have found that Ganetespib downregulated IFNγ-induced PD-L1 expression, and this was downregulated even further if cells were pre-sensitised with Ganetespib prior to addition of IFNγ. This could indicate that inhibition of HSP90 blocks the IFN system. With IFNγ treatment, PD-L1 was localised to the nucleus, whereas in Ganetespib treated cells PD-L1 was localised to the cytoplasm and membrane. The IFNγ time course didn't significantly change the total PD-L1 expression in the cells. Pre-sensitising cells with IFNγ prior to treatment with Ganetespib also resulted in downregulated PD-L1 expression but to a lesser extent than when treatments were applied at the same time. Similar results were obtained from the Ganetespib time course with IFNγ pre-treatment. This indicates that there is probably a threshold of IFNγ which Ganetespib can endure, beyond which it suppresses Ganetespib drug action but still lowers PD-L1 to lesser extent. Hence Ganetespib action depends on how long cells are pre-sensitised with IFNγ prior to drug treatment for effective downregulation of PD-L1. Su –kil et al. demonstrated that an antitumour drug can suppress IFNγ-elicited PD-L1 expression by inhibiting IRF-1 transcription via the Jak/STAT signalling pathway (Su-Kil Seo a, 2013).

My results also indicate that downregulation of PD-L1 is regulated by IRF-1. This was confirmed by knocking down IRF-1 cells and analysing the expression of total and membrane surface bound PD-L1 by Western blotting and flow cytometry respectively. Knockdown of IRF-1, by siRNA, downregulated PD-L1 expression, both alone and in combination with IFNγ treatment, suggesting that downregulation of PD-L1 is in an IRF-1-dependent pathway, or that IRF-1 could be stabilising PD-L1. Figure 94a demonstrates the effects of interferon on IRF-1 and expression levels of PD-L1, and Figure 94b summaries the potential effects Ganetespib might have on tumour cells after downregulating PD-L1 expression.

IRF-1 localisation after treatment with IRF-1-targeting siRNA revealed lower expression of IRF-1, and this effect was increased when cells were treated with both Ganetespib and siRNA against IRF-1. With siRNA the IRF-1 was more cytoplasmic while with IFN treatment, IRF-1 was tightly nuclear localised. A high expression of IRF-1 was observed with IFN γ when compared to DMSO control. IRF-1 is known to have tumour suppressive properties, and IRF-2 expression correlates with its role opposing IRF-1 effects. Subtle differences in IRF-1/IRF-2 ratios or posttranslational modification may determine the fate of a cancer cell (JUDITH M. CONNETT, 2005).

To determine if the effects of Ganetespib were cell type dependent we used two different cell lines: the A375 (melanoma) cell line that has high basal level of PD-L1 and A549 (lung carcinoma) that has a low PD-L1 expression. Both cell lines have WT-p53. Ganetespib downregulated PD-L1 at the higher doses in both cell lines. At low doses (10 nM) Ganetespib downregulated PD-L1 in A375 to a lesser extent than in A549 cell lines. This could be due to the higher basal levels of PD-L1 in A375 cells. It could also be due to the variable genetic mutations in the two cancer cell lines, such as higher levels of STAT1 and lower levels of IRF2 expression. A549 cells also have an activated RAS mutation, which might contribute to alterations between the melanoma and lung cancer cell line. Both IFNs α and γ are used to treat cancer patients. p53 plays a pivotal role in IFNα-induced apoptosis through transcriptional activation of CD95. In contrast, IFNγ induces apoptosis in a p53-independent manner. CD95 and IRF-1 are directly upregulated by IFNγ, leading to caspase activation and IFNγ-induced apoptosis. (Porta C, 2005)

I tested the effects of Ganetespib on cell lines treated with IFNα. When A375 cell lines were treated with IFNα there was no significant induction of IRF-1. Interestingly there was more ubiquitination of p53 in cells treated with IFNα than with IFNγ. STAT1 is a key mediator of the IFNα-induced pathway. It can promote elevation of p53 protein levels through downregulating MDM2 and increasing apoptosis in response to DNA damage. IRF-1 has been reported to participate in modulating p53 activity in response to DNA damage (Yuan XW, 2008). Pre-sensitising the cells with Ganetespib prior to the addition of IFNα does downregulate IRF-1 compared to the controls.

From these experiments, both IFNα and IFNγ pathways could be altered using Ganetespib, but the PD-L1 expression induced by IFNα was reduced by Ganetespib to a lesser extent then that induced by IFN γ. When A375 cells were treated with nutlin (MDM2 antagonist) there was an increase in PD-L1 expression compared to the basal level. There was a drop in this expression level when cells were treated with nutlin together with Ganetespib. This indicated that nutlin had an Antagonist effect with Ganetespib on PD-L1 expression levels. Vaseva et al. have also demonstrated that HSP90 inhibitors (17AAG) destabilised MDM2 and synergized with nutlin to induce apoptosis (A V Vaseva, 2011).

Autophagy is a self-digesting process that is primarily accountable for the eradication and recycling of long-lived proteins and damaged organelles to maintain the homeostasis of the cell. Tumour cells employ autophagy to seize and degrade damaged cell contents to provide energy and promote cell survival. ATG5 is an E3 ubiquitin ligase, which is necessary

for autophagy (Takeshi Matsuzawa E. F., 2013). IFNγ induces autophagy through the IRF-1 signalling pathway and the induction of autophagy contributes to the growth-inhibitory effect of IFNγ with cell death in human cancer cells. (Chandra B Lebovitz, 2015)

To determine whether downregulation of PD-L1 was mediated by autophagy via ATG5 we used A549 ATG5 null, rescue and WT cell lines. In WT A549 cells the basal PD-L1 expression is low compared to that in ATG5 KO cell lines. IFNγ induced PD-L1 expression to a greater extent in KO cells compared to WT cells. In the rescue cell lines, IFNγ-induced PD-L1expression is lower than in the KO but still higher than in WT cells. This might be due to the partial, rather than complete rescue of ATG5 gene. Interestingly, the same trend is followed when all three cell lines were treated with Ganetespib + IFNγ; Ganetespib reduced the induced PD-L1 expression to a different extent in each line. These results indicate that ATG5 gene regulates PD-L1 expression and its loss has a synergistic effect on Ganetespib in downregulating PD-L1 expression. IFNγ-induced expression of PD-L1 is dependent on ATG5.

Conclusion

The demonstration that immune checkpoint inhibition can meaningfully improve outcomes for cancer patients has transformed the field of immuno-oncology. Accumulating evidence suggests that tumour-based HSP90 inhibition can directly influence, and is compatible with, T-cell–mediated antitumour immunity and may promote enhanced tumour surveillance and recognition through exploitation of client protein-dependent and -independent mechanisms (Tsirigotis P, 2016) (Proia DA K. G., 2015).Ganetespib has also shown to have synergistic effect with other drugs when used in mutant EGFR driven xenograft tumours where the combination treatment resulted in significant tumour regressions (Proia DA K. G., 2015). Although HSP90 inhibitors have a high therapeutic value with limited effects on normal cells, they have been described to inhibit dendritic cell function. Therefore, these observations demonstrate the need to closely monitor immune function in patients being treated with an HSP90 inhibitor.HSP70 plays a crucial role in antigen cross-presentation from treated tumour cells and is normally indicated as a tumour promoter.

As HSP90 inhibitors causes induction of HSP70, using HSP90 inhibitors in combination with HSP70 inhibitors or blockers could solve this issue. Lin et al. demonstrated that HSP90 inhibitors downregulated overexpressed mutant p53 and upregulated WT p53. The upregulation of WT p53 was accompanied by downregulation of MDM2.

In summary, our findings reveal important consequences of inhibiting HSP90 in cancer cells and strongly support the therapeutic evaluation of HSP90 inhibitors in poor-prognosis patients with p53 defects.

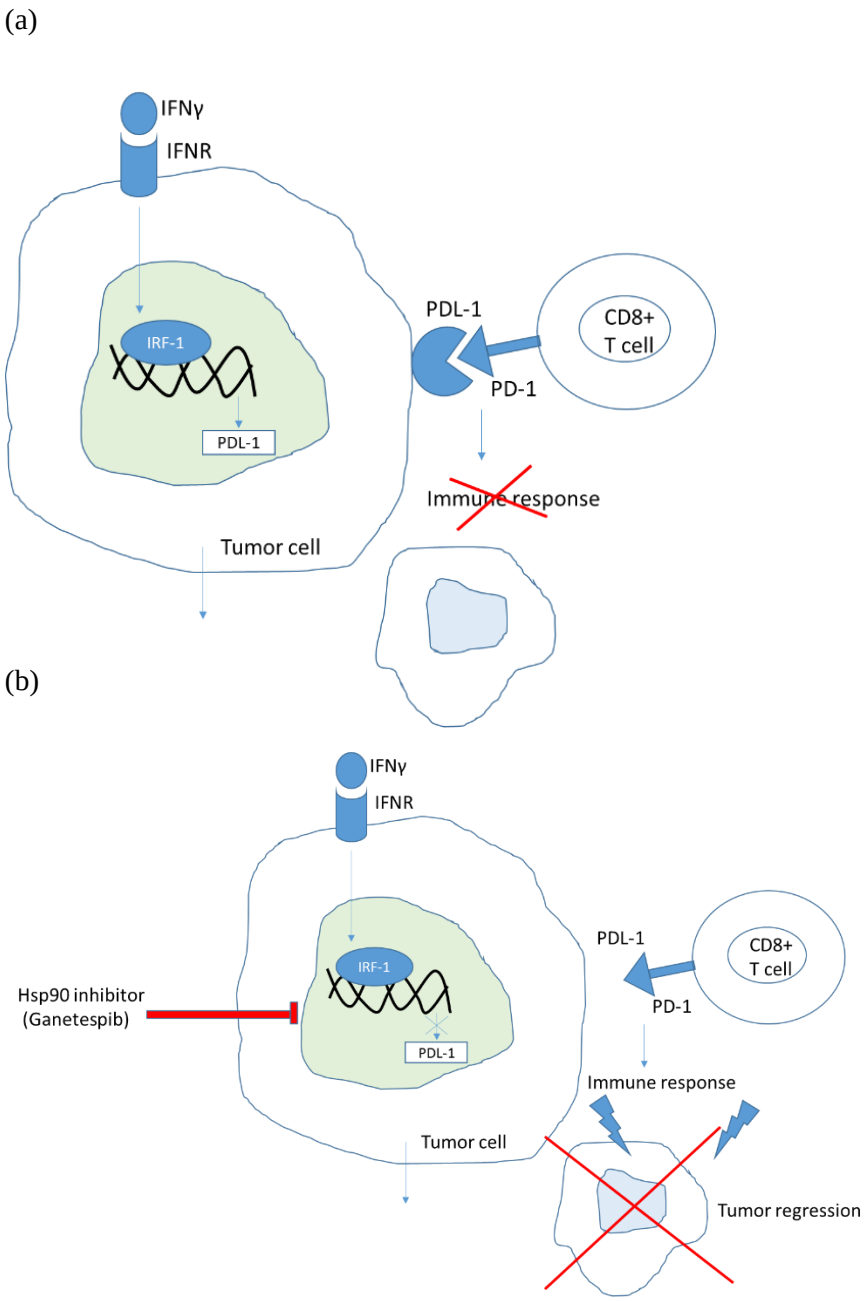

Figure 94 Summary for potential effects of Ganetespib on tumour cells

(A)In tumour cells IFNγ stimulation leads to IRF-1 mediated transcription of PD-L1 and expression of PD-L1 at the tumour cell.PD-L1 binds to PD-1 at CD8+ T cells which inhibits antitumor immune response and results in tumour initiation and growth. (B)When Ganetespib is used, PD-L1 transcription by IRf-1 is inhibited and results in reduced expression of PD-L1.This induces immune response and results in tumour rejection.

7 Conclusion and future work

Since the early 2000s, there has been renewed interest in the development of Hsp90 inhibitors in oncology, with more than 15 compounds currently under evaluation in clinical trials. As we enter the era of targeted therapy and personalised medicine, development of biomarkers to help select the most appropriate patient population for a specific therapy is key. HSP90 tumour expression, as the main target of these drugs, might seem a suitable strategy to select patients most likely to benefit. The advantage of HSP90 inhibitors may lie precisely in their pleiotropic activity. The dual inactivation cell cycle checkpoints, but not nucleases, by HSP90 inhibition results in a highly effective chemosensitization. Various HSPs are nowadays considered biomarkers of carcinogenesis, and their expression is correlated with the degree of differentiation and aggressiveness of certain tumors(Rappa F, 2012) (Daniela Kramer, 2017) (esfahani K, 2015).

Canine OSA data analysis indicated that the highest rate of mutations was observed in chromosome 1 and the majority of the mutations being SNV (single nucleotide variations) .In canine OSA RBM10, which acts like a tumour suppressor, was observed to be mutated.. Gene sequencing revealed a deletion in CCNB1IP1 which is correlated significantly with relevant prognostic factors, and with clinical outcome (Confalonieri S, 2009). IRF-1, CDKN2A and HSP90ab1 all expressed with an SNV. These all form drugable target pathways that could be used in our strategy to match drug leads to mutated expressed pathways. There were 74 genes shortlisted based on expressed mutations and mass spectrometric analysis. We approached the use of genetics to identify drugable pathways as a personalized approach by focussing on the p53 and HSP90/IRF1 pathways. I aimed to define the global mechanism of how these drugs might function in signal transduction, to identify potential novel biomarkers that could be used to measure drug-responsiveness in canine cancer biopsies in the future. The majority of the upregulated canine proteins belonged to chaperone functions and a minority to heat shock activity.

WDR-75 and HYPK are overexpressed in many cancers and hence its downregulation with Ganetespib is of clinical importance. Therefore the downregulation of these proteins with Ganetespib proved of great therapeutic benefit. Two proteins, ATPB and HTPG, were downregulated with nutlin . Pendharkar and group demonstrated that ATPB serves as a bio signature for breast cancer. ATPB is also a potential biomarker and therapeutic target for the immunotherapy of various cancers. (Lu ZJ1, 2009) (Pendharkar N, 2016). Hence downregulation of ATPB by Nutlin could be of great potential in therapy.

Zhang F and group also demonstrated that ALDOA could contribute to the progress of cancer, at least partially through its association with genes relevant to cell cycle independent of glycolysis. (Zhang F, 2017). Thus ALDOA represents a potential new signature for development and prognosis in several cancers, and its downregulation with drugs such as Ganetespib would be advantageous. RanGTP was another protein downregulated with Ganetespib. Yeun HF and group demonstrated that Ran is required for, and is a potential therapeutic target of, Myc-driven cancer progression in both breast and lung cancers (Yuen HF, 2013). Hence Ran downregulation with Ganetespib could be vital in the therapy of various cancer types. Two other proteins shown to be upregulated with nutlin, and common between the two biological duplicates, were PRDX3 and GSPT1 .PRDX3 seems to confer increased treatment resistance and aggressive phenotypes. PRDX3 has substantial clinical impact on the progression of cancers (Zhang H, 2017) (Pendharkar N, 2016).

As is the case with all targeted therapies, there is a pressing need to develop companion diagnostics such as canine models or predictive biomarkers to better select patients who might derive the most benefit from ganetespib therapy. My study provides evidence that Ganetespib exhibits biological activity in a relevant large animal model of cancer. Given the similarities of canine and human cancers with respect to tumour biology and HSP90 activation, it is likely that Ganetespib will demonstrate comparable anti-cancer activity in human patients. In summary my data indicated that the OSA31 cell line shows responsiveness to Nutlin-3 resulting in activation of p53 and also shows responsiveness to Ganetespib as defined by induction of HSP70, downregulation of IRF1, and induction of the HSP70-MDM2 protein complex. The results also indicate that genes that code for the proteins targets of most successful drugs, or are highly specific for osteosarcoma, are quite evolutionarily conserved between human and canines.

My results from melanoma cell lines indicated that there is increased expression of MDM2 with Nutlin, and p53 is stably monoubiquitinated, following activation by Nutlin-3. My results also suggested using pARF inhibition to overcome the effect of nutlin-3 on p53 ubiquitination through a process that involves MDM2. I have demonstrated that Ganetespib can be effective for Ewing sarcoma, and could be used either alone or in combination with other treatments. Since the drug does not require functional p53 to lower EWS-FLi1, Ganetespib could potentially be used for both WT and mutant p53 sarcomas. My results indicate that there is a novel interaction between HSP/C70 and MDM2, and this interaction is stabilised with

Ganetespib. I have also shown that there is a potential synergistic effect on HSP90 client proteins when Ganetespib and Nutlin are used in combination.

The proteomic analysis of melanoma cell lines using TMT mass spectrometry emphasised the importance of combinatorial treatment in cancer and how different proteins respond the drugs used. Overall I observed the downregulation of EPHA2 protein with Ganetespib which possess clinical importance in therapy. I also demonstrated the overexpression of RPS27L protein which is a positive prognosis in tumour regression. Combinatorial treatment using Ganetespib and Nutlin downregulated CDK1 which would help in the reduction of tumour growth as CDK1 is associated with tumour proliferation. On the contrary, combinatorial treatment also increased PIG3 which is regarded a biomarker for certain cancer types such thyroid cancer. Hence it is essential to regulate and optimise combinatorial treatment for each cancer type and personalise the treatment as per patient gene and protein profile.

I have showed that Ganetespib is a more potent effector of IRF-1 than 17AAG at a given dose in the nanomolar concentration range .My result indicates that the loss of IRF-1 with Ganetespib treatment is a p53 independent mechanism. This feature makes Ganetespib a versatile treatment, as it has the potential to modulate IRF-1 in both WT and p53 mutant cancer cell backgrounds. My results suggest that MDM2 is specifically associated with HSC70, rather than HSP70, as expected, in cells where HSP90 has been inhibited. However, neither of the known IRF-1 E3-ligases are responsible for IRF-1 degradation and inhibition of the autophagy pathway, if anything, enhances rather than attenuates the effect of Ganetespib on IRF-1 protein levels. Together the data therefore suggest that IRF-1 is degraded by a novel Ganetespib-sensitive pathway.

The immuno-oncology landscape is presently undergoing a major transformation due to advancements in immunotherapeutic drug development, best exemplified by the clinical introduction of targeted biologics against the CTLA-4 and PD-1/PD-L1 immune checkpoints. (David A. Proia 2015).This inhibition of PDL1 is likely responsible for the ability of the MHC II vaccines to efficiently activate and maintain tumor-specific effector T cells and suggests new therapeutic avenues for preventing tumor cell PDL1-induced immune suppression (Haile ST, 2011). Blocking checkpoints that allow cancer cells to evade patients' immune responses holds great promise for achieving durable antitumour responses. I have found that Ganetespib downregulated IFNγ-induced PD-L1 expression, and this was downregulated even further if cells were pre-sensitised with Ganetespib prior to addition of IFNγ. My results also indicate that downregulation of PD-L1 is regulated by IRF-1. The results also indicate that ATG5 gene

regulates PD-L1 expression and its loss has a synergistic effect on Ganetespib in downregulating PD-L1 expression. IFNγ-induced expression of PD-L1 is dependent on ATG5.

Synergistic combinatorial benefit between HSP90 inhibitors and taxanes (antimitotic agents) has been described in different cancer models, suggesting that their nonoverlapping but complementary mechanisms of action are conserved across tumor types.(Yifan Wang, 2016).HSP inhibitors could act as potential sensitisers for many anticancer drugs that would otherwise have limited therapeutic efficacy. Clinically, HSP inhibition will probably have the greatest effect in tumours addicted to particular driver oncogene products that are sensitive HSP90 clients. Moreover, studies have suggested that in tumours, HSP90 forms multichaperone, biochemically distinct complexes that specifically interact with oncogenic proteins and have higher affinity than HSP90 in normal tissues for specific small-molecule inhibitors. (Rocio Garcia-Carbonero, 2013) (Ganji Purnachandra Nagaraju, 2016) (Garcia-Carbonero R, 2013).My results also show beneficial antagonistic activity of Ganetespib and nutlin when treated together. Melanoma cancer cell lines, though very powerful tools to study this disease at the molecular and cellular biology levels, are clearly incomplete models.One cannot be expected to accurately gauge the effect of inhibitors on a complex tumor microenvironment in a monolayer of cancer cells, or be able to extrapolate the effect of inhibitors on distal metastatic sites. My data also suggest that using better models suchas canine would help to develop personalized medicine.(Komal Jhaveri, 2015)

Future work:

For the canine model further experiments have to be performed to validate and confirm the potential vaccine list. Cell based assays on molecular biology for the selected lead targets should be conducted to authenticate the DNA and RNA seq data. The validated vaccine list could potentially be used as vaccine trials on canine. However, there are so many mutations identified for this one patient's tumour that orthogonal assays need to be performed in order to stratify the mutated genes and to focus on developing potential therapeutic strategies.

Although HSP90 inhibitors have a high therapeutic value with limited effects on normal cells, they have been described to inhibit dendritic cell function. Therefore, these observations demonstrate the need to closely monitor immune function in patients being treated with an HSP90 inhibitorThe anticancer effects of Hsp90 inhibitor have been well studied in malignant cells, but their impact on human effector cells has not been well characterized. Several studies

have shown that Hsp90 inhibition leads to a significant and irreversible decrease in expression of critical Ags on human T lymphocytes at protein and mRNA levels. Therefore, these results suggest that Hsp90 inhibition disrupts functional activities of both T lymphocytes and NK cells, and highlights the relevance of potential impact of Hsp90 inhibitors on effector cell function in cancer patients during clinical trials (Jooeun Bae, 2013).Hence, future experiments particularly T cell assays to determine the effect of Ganetespib on T cell killing, would be vital.

Based on the autophagy and Ganetespib data it would be interesting to evaluate if the downregulation of IRF-1 is via autophagy pathway. For this purpose further experiments such as to check for the co-localisation of Lamb2A and IRF-1 using immunofluorescence would be valuable. This would help us to confirm if the downregulation of IRF-1 is via chaperon mediated autophagy (CMA).The role of lamp2A and HSC70 in CMA is mentioned in Figure 95.Also, repeating the autophagy experiment with alterative autophagy inhibitor such as bafilomycin which is known to inhibit late phase of autophagy when compared to chloroquine.

While the challenge remains to identify which specific client proteins may ultimately serve as predictive biomarkers for those cancers likely to respond to HSP90 inhibitor treatment, my findings underscore the therapeutic potential of Ganetespib for treatment of metastatic disease in patients with specific biomarkers (David Proia, 2014).In summary, our findings reveal important consequences of inhibiting HSP90 in cancer cells and strongly support the therapeutic evaluation of HSP90 inhibitors in poor-prognosis patients with p53 defects.

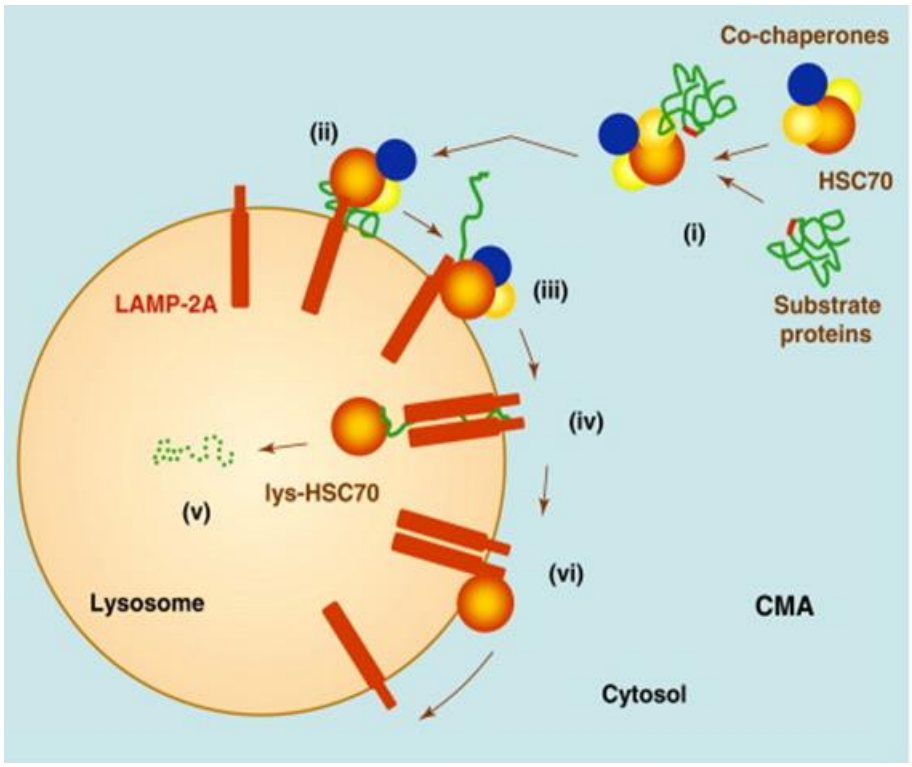

Figure 95Chaperon mediated autphagy

Figure 1. Hypothetical model of the steps and components of chaperone-mediated autophagy (CMA). (i) Substrate proteins bearing a targeting motif are recognized by HSC70 and co-chaperones in the cytosol. (ii) The chaperone–substrate protein complex is delivered to the surface of lysosomes where it binds to the cytosolic tails of LMAP- 2A monomers. (iii) Substrate binding drives multimerization of LAMP-2A into a translocation complex. In between this and the next step, the substrate is unfolded by yet unknown mechanisms. (iv) The substrate crosses the lysosomal membrane assisted by a luminal form of HSC70. (v) Once inside the lysosome, the substrate is rapidly degraded (dotted structure). (vi) HSC70 promotes disassembly of LAMP-2A from the translocation unit, now devoid of substrate, to provide monomeric forms of LAMP-2A for a new cycle of substrate binding and translocation. (Cuervo, 2009)

8 Bibliography

(2017). Retrieved from https://www.otogenetics.com/.

A V Vaseva, A. R. (2011). Blockade of Hsp90 by 17AAG antagonizes MDMX and synergizes with Nutlin to induce p53-mediated apoptosis in solid tumors. *Cell Death and Disease*.

Abroun S, S. N. (2015). STATs: An Old Story, Yet Mesmerizing. *cell*.

Acquaviva J, H. S. (2014). . mTOR Inhibition Potentiates HSP90 Inhibitor Activity via Cessation of HSP Synthesis. . *Molecular cancer research :*.

Acquaviva J, H. S. (2014). FGFR3 Translocations in Bladder Cancer:Differential Sensitivity to HSP90 Inhibition Based on Drug Metabolism. . *Molecular cancer research :*.

Acquaviva J, S. D. (2012). Targeting KRAS-Mutant Non-Small Cell Lung Cancer with the Hsp90 Inhibitor Ganetespib. *Molecular cancer therapeutics* .

Acquaviva J, S. D. (2014). Overcoming acquired BRAF inhibitor resistance in melanoma via targeted inhibition of Hsp90 with ganetespib. . *Molecular cancer therapeutics* .

Addeo, R. (2017). A new frontier for targeted therapy in NSCLC: clinical efficacy of pembrolizumab in the inhibition of programmed cell death 1 (PD-1). *Expert Rev Anticancer Ther.*

Alexandrova, E. M. (2015). Improving survival by exploiting tumour dependence on stabilized mutant p53 for treatment. *nature*.

Al-Lazikani, B. (2012). Combinatorial drug therapy for cancer in the post-genomic era. *nature biotechnology*.

Amaravadi, R. (2016). Recent insights into the function of autophagy in cancer. *GENES & DEVELOPMENT*.

Angstadt, A. Y. (2012). A genome-wide approach to comparative oncology: high-resolution oligonucleotide aCGH of canine and human osteosarcoma pinpoints shared microaberrations. *cancer genetics*.

Ayraulta, O. (2009). Inhibition of Hsp90 via 17-DMAG induces apoptosis in a p53-dependent manner to prevent medulloblastoma. *PNAS*.

Bae J, M. A. (2013). Heat shock protein 90 is critical for regulation of phenotype and functional activity of human T lymphocytes and NK cells. *journal of immunology*.

Ballestar, E. a. (2008). Epigenetic gene regulation in cancer. *Adv Genet*.

Bansal H, B. S. (2010). Heat shock protein 90 regulates the expression of Wilms tumor 1 protein in myeloid leukemias. *Blood* .

Bansal H, Y. Q. (2014). WTAP is a novel oncogenic protein in acute myeloid leukemia. . *Leukemia* .

Bartl, S. e. (2003). Did the molecules of adaptive immunity evolve from the innate immune system? *Integr Comp Biol* , . 43: p. 338–346.

Behl, C. (2016). Breaking BAG: The Co-Chaperone BAG3 in Health and Disease. *trends in pharmacological science*.

Beloueche-Babari, M. (2010). Modulation of melanoma cell phospholipid metabolism in response to heat shock protein 90 inhibition. *oncotarget*.

Bendle GM, H. A. (2004). Induction of unresponsiveness limits tumor protection by adoptively transferred MDM2-specific cytotoxic T lymphocytes. *Cancer research*.

Bileck A1, M. R.-M. (2017). Evaluation of inflammation-related signaling events covering phosphorylation and nuclear translocation of proteins based on mass spectrometry data. *journal of proteomics*.

Bray, J. P. (2014). Canine Soft Tissue Sarcoma Managed in First Opinion Practice: Outcome in 350 Cases. *Veterinary Surgery*.

Bresler, S. C. (2016). Gene expression profiling of anti-CTLA4-treated metastatic melanoma in patients with treatment-induced autoimmunity. *Laboratory Investigation*.

Bu N, W. H. (2015). Exosome from chaperone-rich cell lysates-loaded dendritic cells produced by CELLine 1000 culture system exhibits potent immune activity. *biochemical and biophysical research communications*.

Buferne M, C. L.-V.-A. (2015). IFNγ producing CD8+ T cells modified to resist major immune checkpoints induce regression of MHC class I-deficient melanomas. *oncoimmunology*.

Burch, L. S. (2004). Expansion of protein interaction maps by phage peptide display using MDM2 as a prototypical conformationally flexible target protein. *J Mol Biol* , 337,129-145.

Camicia R, B. S. (2013). BAL1/ARTD9 represses the anti-proliferative and pro-apoptotic IFNγ-STAT1-IRF1-p53 axis in diffuse large B-cell lymphoma. *journaal of cell science*.

Castle, J. e. (2014.). Mutated tumor alleles are expressed according to their DNA frequency. . *Sci Rep,*.

Chandra B Lebovitz, A. G. (2015). Cross-cancer profiling of molecular alterations within the human autophagy interaction network. *autophagy*.

Chang L, N. J. (2017). Identification of protein biomarkers and signaling pathways associated with prostate cancer radioresistance using label-free LC-MS/MS proteomic approach. *Sci Rep*.

Cherukuri Sudhakar, V. V. (2013). IRF-1-binding site in the first intron mediates interferon-c-induced optineurin promoter activation. *Biochemical and Biophysical Research Communications*.

Cheryl A London, M. D. (2011). Phase I Evaluation of STA-1474, a Prodrug of the Novel HSP90 Inhibitor Ganetespib, in Dogs with Spontaneous cancer. *Plos one*.

Chi, J.-T. (2012). Comparison of genomics and functional imaging from canine sarcomas treated with thermoradiotherapy predicts therapeutic response and identifies combination therapeutics. *Clin Cancer Res*.

Chiang HL, T. S. (1989). A role for a 70-kilodalton heat shock protein in lysosomal degradation of intracellular proteins. *science*.

Chiara Gasparinia, A. T. (2012). The MDM2 inhibitor Nutlin-3 modulates dendritic cell–induced T cell proliferation. *Human Immunology*.

Christine Mall, G. D. (2016). Repeated PD-1/PD-L1 monoclonal antibody administration induces fatal xenogeneic hypersensitivity reactions in a murine model of breast cancer. *OncoImmunology*.

Christoph H. Emmerich, P. C. (2015). Optimising methods for the preservation, capture and identification of ubiquitin chains and ubiquitylated proteins by immunoblotting. *Biochemical and Biophysical Research Communications*.

Colvin TA, G. V. (2014). Hsp70-Bag3 interactions regulate cancer-related signaling networks. *cancer research* .

Confalonieri S, Q. M. (2009). Alterations of ubiquitin ligases in human cancer and their association with the natural history of the tumor. *oncogene*.

Connett JM, B. L. (2005). Interferon regulatory factor 1 (IRF-1) and IRF-2 expression in breast cancer tissue microarrays. *journal of interferon and cytokine research*.

Copur MS, R. R. (2017). Ipilimumab Adjuvant Therapy in Melanoma. *N Engl J Med*.

Corey Saba, M. P. (2016). A Comparative Oncology Study of Iniparib Defines Its Pharmacokinetic Profile and Biological Activity in a Naturally-Occurring Canine Cancer Model. *plos one*.

Craig R Brooks, M. Y. (2015). KIM-1-/TIM-1-mediated phagocytosis links ATG5-/ULK1-dependent clearance of apoptotic cells to antigen presentation. *The EMBO journal*.

Cuervo, A. M. (2009). Chaperone-mediated autophagy:selectivity pays off. *cell*.

D Murtas, ,. D. (2013). IRF-1 responsiveness to IFN-c predicts different cancer immune phenotypes. *British Journal of Cancer*.

Dakappagari N, N. L. (2009). An investigation into the potential use of serum Hsp70 as a novel tumour biomarker for Hsp90 inhibitors. *Biomarkers*.

Daniela Murtas, D. M. (2013). IRF-1 responsiveness to immune cytokines predicts different cancer phenotypes. *Journal for ImmunoTherapy of Cancer*.

Davenport, E. (2010). Targeting heat shock protein 72 enhances Hsp90 inhibitor-induced apoptosis in myeloma. *Leukemia*.

David A. Proia, G. F. (2015). Targeting Heat-Shock Protein 90 (HSP90) as a Complementary Strategy to Immune Checkpoint Blockade for Cancer Therapy. *cancer immunology research*.

David Dornan, M. E. (2004). Interferon Regulatory Factor 1 Binding to p300 Stimulates DNA-Dependent Acetylation of p53. *molecular and cellular biology*, 24(22):10083-98.

David Herrero-Martin, A. F. (2011). Factors Affecting EWS-FLI1 Activity in Ewing's Sarcoma. *sarcoma*.

David Proia, R. C. (2014). Ganetespib and HSP90: Translating Preclinical Hypotheses into Clinical Promise. *cancer research*.

Davis, B. W. (2014). Domestic Dogs and Cancer Research: A Breed-Based Genomics Approach. *ILAR Journal*.

Dickinson, P. J. (2016). Chromosomal Aberrations in Canine Gliomas Define Candidate Genes and Common Pathways in Dogs and Humans. *J Neuropathol Exp Neurol*.

Ding W, T. Y. (2016). Study of Arsenic Sulfide in Solid Tumor Cells Reveals Regulation of Nuclear Factors of Activated T-cells by PML and p53. *science reports*.

Donald L. Smith, J. A. (2015). The HSP90 inhibitor ganetespib potentiates the antitumor activity of EGFR tyrosine kinase inhibition in mutant and wild-type non-small cell lung cancer. *targeted oncology*.

Dong F1, L. T. (2017). Chimaphilin inhibits human osteosarcoma cells invasion and metastasis through suppressing the TGF-β1-induced epithelial-to-mesenchymal transition markers via PI-3K/Akt, ERK1/2 and Smad signaling pathways. *Can J Physiol Pharmacol*.

Dou, L. (2014). The regulation role of interferon regulatory factor-1 gene and clinical relevance. *Human Immunology*.

Duhamel LA, Y. H. (2012). Frequency of Mouse Double Minute 2 (MDM2) and Mouse Double Minute 4 (MDM4) amplification in parosteal and conventional osteosarcoma subtypes. *histopathology*.

Eckhardt, A. W. (2014). Identification of IRF1 as critical dual regulator of Smac mimetic-induced apoptosis and inflammatory cytokine response. *cell death and disease*.

Eliane C.M. Zeestraten, F. M. (2012). Addition of interferon-a to the p53-SLPVR vaccine results in increased production of interferon-c in vaccinated colorectalcancer patients: A phase I/II clinical trial. *international journal of cancer*.

Emmanuelle Pion, V. N. (2009). Role of the IRF-1 enhancer domain in signalling polyubiquitination and degradation. *Cellular Signalling*.

esfahani K, C. V. (2015). HSP90 as a novel molecular target in non-small-cell lung cancer. *Lung Cancer: Targets and Therapy*.

Eva Wardelmanna, J. M.-M. (2012). Targeted Therapy of Soft Tissue Sarcomas. *Onkologie*, ;35(suppl 1):21–27.

Evguenia M Alexandrova, S. X. (2017). Ganetespib synergizes with cyclophosphamide to improve survival of mice with autochthonous tumors in a mutant p53-dependent manner. *cell death and disease*.

FANG CHENG, R. H. (2014). Expression of neddylation-related proteins in melanoma cell lines and the effect of neddylation on melanoma proliferation. *ONCOLOGY LETTERS*.

Félix Sauvage a, S. M.-G. (2017). Heat shock proteins and cancer: How can nanomedicine be harnessed? *journal of controlled release*, 133-143.

Flora Zagouri, T. N. (2013). Hsp90 inhibitors in breast cancer: A systematic review. *breast*.

Folpe AL, H. C. (2000). Immunohistochemical detection of FLI-1 protein expression: a study of 132 round cell tumors with emphasis on CD99-positive mimics of Ewing's sarcoma/primitive neuroectodermal tumor. *Am J Surg Pathol.*

Fowles, J. S. (2016). Intra- and interspecies gene expression models for predicting drug response in canine osteosarcoma. *BMC bioinformatics*.

Franco, R. (2012). Expression of the Anti-Apoptotic Protein BAG3 in Human Melanomas . *Journal of Investigative Dermatology*.

Friedland JC, S. D. (2013). Targeted inhibition of Hsp90 by ganetespib is effective across a broad spectrum of breast cancer subtypes. *Investigational new drugs*.

Frith AE, H. A. (2013). Novel pathways and molecular targets for the treatment of sarcoma. *Curr Oncol Rep*, 378-85.

G-A Franzetti1, 2. K.-D.-J. (2017). Cell-to-cell heterogeneity of EWSR1-FLI1 activity determines proliferation/migration choices in Ewing sarcoma cells. *oncogene*.

Gabai, M. S. (2015). Hsp70 in cancer: back to the future. *oncogene*.

Ganguly S, H. T. (2015). Targeting HSF1 disrupts HSP90 chaperone function in chronic lymphocytic leukemia. *oncotarget*.

Ganji PN, P. W. (2013). Antiangiogenic effects of ganetespib in colorectal cancer mediated through inhibition of HIF-1alpha and STAT-3. *Angiogenesis* .

Ganji Purnachandra Nagaraju, A. M. (2016). Targeting the Janus-activated kinase-2-STAT3 signalling pathway in pancreatic cancer using the HSP90 inhibitor ganetespib. *ScienceDirect*.

Garcia-Carbonero R, C. A.-A. (2013). Inhibition of HSP90 molecular chaperones: moving into the clinic. *the lancet oncology*.

Gavin M. Bendle, 1. A.-K. (2004). Induction of Unresponsiveness Limits Tumor Protection by Adoptively Transferred MDM2-Specific Cytotoxic T Lymphocytes. *cancer research*.

Gerard M. Doherty, M. (2001). Interferon Regulatory Factor Expression in Human Breast Cancer. *annals of surgery*.

Gewirtz, D. A. (2016). The Challenge of Developing Autophagy Inhibition as a Therapeutic Strategy. *cancer research*.

Goldsmith JR1, C. Y. (2017). Regulation of inflammation and tumorigenesis by the TIPE family of phospholipid transfer proteins. *Cell Mol Immunol*.

Guerriero JL, S. A. (2017). Class IIa HDAC inhibition reduces breast tumours and metastases through anti-tumour macrophages. *nature* .

Guerriero, L. (2014). BAG3 protein expression in melanoma metastatic. *cell death and disease*.

Guo M, 2. T.-B. (2017). Gene signature driving invasive mucinous adenocarcinoma of the lung. *EMBO mol med*.

Haile ST, B. J.-R. (2011). Tumor cell programmed death ligand 1-mediated T cell suppression is overcome by coexpression of CD80. *journal of immunology*.

Hanahan, D. a. (2011). Hallmarks of cancer: the next generation. *Cell*.

Haque A, A. Q. (2016). Current Understanding of HSP90 as a Novel Therapeutic Target: An Emerging Approach for the Treatment of Cancer. *Current Pharmaceutical Design*.

Harada, H. e. (1989). Structurally similar but functionally distinct factors, IRF-1 and IRF-2, bind to the same regulatory elements of IFN and IFN-inducible genes. *Cell*, 58(4): p. 729-39.

hasegawa, j. (2016). Novel anti-EPHA2 antibody, DS-8895a for cancer treatment. *cancer biology and therapy*.

Hatem Soliman, F. K. (2014). PD-L1 Expression Is Increased in a Subset of Basal Type Breast Cancer Cells. *plos one*.

Hayes, D. C. (2015). Genetic Landscape of Human Papillomavirus-Associated Head and Neck Cancer and Comparison to Tobacco-Related Tumors.. *J Clin Oncol, .*

He S, S. D. (2014). The HSP90 inhibitor ganetespib has chemosensitizer and radiosensitizer activity in colorectal cancer. . *Investigational new drugs* .

He S, Z. C. (2013). Potent activity of the Hsp90 inhibitor ganetespib in prostate cancer cells irrespective of androgen receptor status or variant receptor expression. *International journal of oncology*.

Helman LJ, M. P. (2003). Mechanisms of sarcoma development. *Nat Rev Cancer.*, 3(9):685-94.

Herraiz C, C. F. (2015). Reactivation of p53 by a Cytoskeletal Sensor to Control the Balance Between DNA Damage and Tumor Dissemination. *J Natl Cancer Inst.*

Hiroaki Ikeda, L. J. (2002). *Cytokine & Growth Factor*.

Hiroaki Ikeda, L. J. (2002). *cytokine and growth factor reviews*.

Hongxing Ye, M. C. (2016). Chloroquine, an autophagy inhibitor,potentiates the radiosensitivity of gliomainitiating cells by inhibiting autophagy andactivating apoptosis. *BMC neurology*.

http://www.proteinatlas.org. (n.d.). Retrieved from http://www.proteinatlas.org: http://www.proteinatlas.org/ENSG00000242028-HYPK/cancer

http://www.proteinatlas.org. (n.d.). Retrieved from http://www.proteinatlas.org: http://www.proteinatlas.org/ENSG00000115368-WDR75/cancer/tissue/breast+cancer

Huang CJ, Y. S. (2013). Ribosomal protein S27-like in colorectal cancer: a candidate for predicting prognoses. *Plos one*.

Huang, W. E. (2007). interferon regulatory factor (IRF) 2, and the interferon consensus sequence-binding protein (ICSBP/IRF8) cooperate to activate NF1 transcription in differentiating myeloid cells. *J Biol Chem, ,* . 282(9): p. .

Ito M, B. L.-M. (2011). Comprehensive mapping of p53 pathway alterations reveals an apparent role for both SNP309 and MDM2 amplification in sarcomagenesis. *clinical cancer research*.

J Gao, ,. M. (2010). IRF-1 transcriptionally upregulates PUMA, which mediates the mitochondrial apoptotic pathway in IRF-1-induced apoptosis in cancer cells. *Cell death and differentiation*.

J. P. Frazier, E. B. (2016). Establishment and characterization of a canine soft tissue sarcoma patient-derived xenograft model. *veterinary and comparative oncolgy*.

J. S. Fowles, D. D. (2016). The Flint Animal Cancer Center (FACC) Canine Tumour Cell Line Panel: a resource for veterinary drug discovery, comparative oncology and translationalmedicine. *veterinary and comparative oncology*.

Jambhekar, S. S. (2010). Pathology of Ewing's sarcoma/PNET: Current opinion and emerging concepts. *Indian J Orthop*.

Janz, M. (2007). Pharmacologic activation of p53-dependent and p53-independent apoptotic pathways in Hodgkin/Reed-Sternberg cells. *Leukemia*.

Jennifer A. MacDiarmid, V. L. (2016). Targeted Doxorubicin Delivery to Brain Tumors via Minicells: Proof of Principle Using Dogs with Spontaneously Occurring Tumors as a Model. *plos one*.

Jennifer K. Lowney, M. L. (1999). Interferon Regulatory Factor-1 and -2 Expression in Human Melanoma Specimens. *Annals of Surgical Oncology*.

Jennifer L. Guerriero, A. S. (2017). Class IIa HDAC inhibition reduces breast tumours and metastases through anti-tumour macrophages. *nature letter*.

Jianming Wu, T. L. (2016). Heat Shock Proteins and Cancer. *cellpress*.

Jin Zhang, X. C. (2009). Establishment of a dog model for the p53 family pathway and identification of a novel isoform of p21 cyclin-dependent kinase inhibitor. *molecular cancer research*.

Joe Antony Jacob, J. M. (2017). Autophagy: An overview and its roles in cancer and obesity. *Clinica Chimica Acta*.

Jooeun Bae, A. M. (2013). Heat Shock Protein 90 Is Critical for Regulation of Phenotype and Functional Activity of Human T Lymphocytes and NK cells. *The Journal of Immunology*.

Jooeun Bae, A. M. (2013). Heat Shock Protein 90 Is Critical for Regulation of Phenotype and Functional Activity of Human T Lymphocytes and NK cells. *journal of immunology*.

Jordi Hernández, E. B. (2016). Tumor suppressor properties of the splicing regulatory factor RBM10. *RNA biology*.

Josephine Salimu1, L. K.-T. (2015). Cross-Presentation of the Oncofetal Tumor Antigen 5T4 from Irradiated Prostate Cancer Cells—A Key Role for Heat-Shock Protein 70 and Receptor CD91. *cancer immunology research*.

JUDITH M. CONNETT, L. B. (2005). Interferon Regulatory Factor 1 (IRF-1) and IRF-2 Expression in Breast Cancer Tissue Microarrays. *JOURNAL OF INTERFERON & CYTOKINE RESEARCH*.

Kamikawaji K, S. N. (2016). Regulation of LOXL2 and SERPINH1 by antitumor microRNA-29a in lung cancer with idiopathic pulmonary fibrosis. *J Hum Genet.*

Kämper N, F. S. (2012). γ-Interferon-regulated chaperone governs human lymphocyte antigen class II expression. *FASEB journal*.

Karkoulis, P. K. (2016). 17-DMAG induces heat shock protein 90 functional impairment in human bladder cancer cells: knocking down the hallmark traits of malignancy. *Tumor Biol*.

Khanna, J. J. (2015). Osteosarcoma Genetics and Epigenetics: Emerging Biology and Candidate Therapies. *Critical reviews in oncogenesis*.

Kim KS, K. K. (2009). Interferon-gamma induces cellular senescence through p53-dependent DNA damage signaling in human endothelial cells. *mechanism of aging and development*.

Komal Jhaveri, S. M. (2015). Ganetespib: research and clinical development. *OncoTargets and Therapy*.

Koya T, Y. R. (2017). Interferon-α-inducible Dendritic Cells Matured with OK-432 Exhibit TRAIL and Fas Ligand Pathway-mediated Killer Activity. *science rep*.

Kristoffer R. Brandvold, R. I. (2015). The Chemical Biology of Molecular Chaperones—Implications for Modulation of Proteostasis. *science direct*.

L. Nasira, ,. ,. (2001). Analysis of p53 mutational events and MDM2 amplification in canine soft-tissue sarcomas. *cancer letters*.

Ladanyi M, L. R. (1995). MDM2 and CDK4 gene amplification in Ewing's sarcoma. *J Pathol*.

Ladanyi M, L. R. (1995). MDM2 and CDK4 gene amplification in Ewing's sarcoma. *the journal of pathology*.

Laemmli, U. (1970). Cleavage of structural proteins during the assembly of the head of bacteriophage T4. *nature*.

Leeuwena, I. v. (1997). P53 gene mutations in osteosarcomas in the dog. *cancer letters*.

Lei Wang, L. Y.-Z. (2015). Expression of autophagy-related proteins ATG5 and FIP200 predicts favorable disease-free survival in patients with breast cancer. *Biochemical and Biophysical Research Communications*.

Len Neckers, M. M. (2015). 56 – Heat Shock Protein 90 and the Proteasome: Housekeeping Proteins That Are Also Molecular Targets for Cancer Therapy. In M. M. Len Neckers, *The Molecular Basis of Cancer (Fourth Edition)* (pp. 779–788.e3).

Liang J, P. Y. (2015). Interferon-regulatory factor-1 (IRF1) regulates bevacizumab induced autophagy. *oncotarget*.

Liang L, S. L. (2016). Validation of a multi-omics strategy for prioritizing personalized candidate driver genes. *oncotarget*.

Lilienbaum, A. (2013). Relationship between the proteasomal system and autophagy. *biochemistry and molecular biology*.

Lim YS, C. W. (2017). HIF1α in Tumorigenesis of Adenoid Cystic Carcinoma. *Anticancer Res.*

Lin K, R. N. (2008). Hsp90 inhibition has opposing effects on wild-type and mutant p53 and induces p21 expression and cytotoxicity irrespective of p53/ATM status in chronic lymphocytic leukaemia cells. *Oncogene*.

Lin TY, B. M. (2008). The novel HSP90 inhibitor STA-9090 exhibits activity against Kit-dependent and -independent malignant mast cell tumors. . *Exp Hematol 36: 1266–1277*.

Lin TY, L. C. (2015). Inhibition of RNA transportation induces glioma cell apoptosis via downregulation of RanGAP1 expression. *Chem Biol Interact*.

LIN, Z. (2015). 17-ABAG, a novel geldanamycin derivative, inhibits LNCaP-cell proliferation through heat shock protein 90 inhibition. *INTERNATIONAL JOURNAL OF MOLECULAR MEDICINE*.

Liu H, X. F. (2013). Network analysis identifies an HSP90-central hub susceptible in ovarian cancer. . *Clin Cancer Res* .

Liu Z, H. Y. (2016). Silencing PRDX3 Inhibits Growth and Promotes Invasion and Extracellular Matrix Degradation in Hepatocellular Carcinoma Cells. *J Proteome Res*.

Lock RB, C. H. (2013). Initial testing (stage 1) of ganetespib, an Hsp90 inhibitor, by the Pediatric Preclinical Testing Program. . *Pediatr Blood Cancer* .

Lopez-Santillan M, I. L.-G.-C.-O. (2017). Review of pharmacogenetics studies of L-asparaginase hypersensitivity in acute lymphoblastic leukemia points to variants in the GRIA1 gene. *Drug Metab Pers Ther*.

Lowney JK, B. L. (1999). Interferon regulatory factor-1 and -2 expression in human melanoma specimens. *Annals of surgical oncology*.

Lu M, X. L. (2014). The orally bioavailable MDM2 antagonist RG7112 and pegylated interferon α 2a target JAK2V617F-positive progenitor and stem cells. *Blood*.

Lu ZJ1, S. Q. (2009). Identification of ATP synthase beta subunit (ATPB) on the cell surface as a non-small cell lung cancer (NSCLC) associated antigen. *BMC Cancer*.

Luengo-Fernandez. (2013). Economic burden of cancer across the European Union: a population-based cost analysis. *Lancet Oncol*.

Lui K, H. Y. (2009). RanGTPase: A Key Regulator of Nucleocytoplasmic Trafficking. *mol cell biology*.

Luis Gabriel Rivera-Calderón a, ,. C.-A. (2016). Alterations in PTEN,MDM2, TP53 and AR protein and gene expression are associated with canine prostate carcinogenesis. *Research in Veterinary Science*.

Lukashchuk, N. (2007). Ubiquitination and Degradation of Mutant p53. *MOLECULAR AND CELLULAR BIOLOGY*.

Luke Way, J. F. (2016). Rearrangement of Mitochondrial Pyruvate Dehydrogenase Subunit Dihydrolipoamide Dehydrogenase Protein-Protein Interactions by the MDM2 Ligand Nutlin-3. *proteomics*.

Lyubomir T. Vassilev, *. B. (2004). In Vivo Activation of the p53 Pathway by Small-Molecule Antagonists of MDM2. *science*.

M. Lazenby, R. H. (2015). The HSP90 inhibitor ganetespib: A potential effective agent for Acute Myeloid Leukemia in combination with cytarabine. *Leukemia Research*.

Malta-Vacas J, C. C.-J. (2009). eRF3a/GSPT1 12-GGC allele increases the susceptibility for breast cancer development. *Oncology rep* .

Mancias, J. D. (2016). Mechanisms of Selective Autophagy in Normal Physiology and Cancer. *journal of molecular biology*.

Mark R. Woodford, A. M. (2014). Efficacy of the Hsp90 Inhibitors in Prostate Cancer Therapy. *Journal of Urology and Nephrology*.

Martins AS, O. J.-S.-G. (2008). A pivotal role for heat shock protein 90 in Ewing sarcoma resistance to anti-insulin-like growth factor 1 receptor treatment: in vitro and in vivo study. *Cancer Res*.

Matthias P. Mayer, H. S. (2000). Multistep mechanism of substrate binding determines chaperone activity of Hsp70. *Nature Structural Biology*.

Maura wallace, E. w. (2006). Dual-Site Regulation of MDM2 E3-Ubiquitin Ligase Activity. *Molecular cell*.

Mayr C, B. D. (2006). MDM2 is recognized as a tumor-associated antigen in chronic lymphocytic leukemia by CD8+ autologous T lymphocytes. *Experimental hematology*.

Mayr C1, B. D. (2006). MDM2 is recognized as a tumor-associated antigen in chronic lymphocytic leukemia by CD8+ autologous T lymphocytes. *Experimental Hematology*.

McCleese JK, B. M. (2009). The novel HSP90 inhibitor STA-1474 exhibits biologic activity against osteosarcoma cell lines. *nt J Cancer*.

Mendoza S1, K. T. (1998). Status of the p53, Rb and MDM2 genes in canine osteosarcoma. *Anticancer Res*.

Merlino, M. R. (2011). The Two Faces of Interferon-g in Cancer. *Molecular Pathways*.

Michel Buferne, L. C. (2015). IFNg producing CD8C T cells modified to resist major immune checkpoints induce regression of MHC class I-deficient melanomas. *OncoImmunology*.

Michel Buferne, L. C. (2015). IFNg producing CD8C T cells modified to resist major immune checkpoints induce regression of MHC class I-deficient melanomas. *oncoimmunology*.

Min Lu, 1. H. (2013). Restoring p53 Function in Human Melanoma Cells by Inhibiting MDM2 and Cyclin B1/CDK1-Phosphorylated Nuclear iASPP. *cell*.

Min Lu, L. X. (2016). The orally bioavailable MDM2 antagonist RG7112 and pegylated interferon a 2a target JAK2V617F-positive progenitor and stem cells. *blood journal*.

Miri M, H. S. (2012). GGCn polymorphism of eRF3a/GSPT1 gene and breast cancer susceptibility. *medical oncology*.

Mittra, J. a. (2012). Analysing stratified medicine business models and value systems: innovation-regulation interactions. . *N Biotechnol*.

Mohamed T Hafez, M. A. (2012). Metastatic rhabdomyosarcoma of the thyroid gland, a case report. *head and neck oncology*.

Mollapour M, B. D. (2014). Asymmetric Hsp90 N domain SUMOylation recruits Aha1 and ATP-competitive inhibitors. *mol cell*.

Morimoto, K. R. (2015). The Chemical Biology of Molecular Chaperones—Implications for Modulation of Proteostasis. *journal of molecular biology*.

Morimoto, K. R. (2015). The Chemical Biology of Molecular Chaperones—Implications for Modulation of Proteostasis. *jounral of molecular biology*.

muller, P. (2008). Chaperone-dependent stabilization and degradation of p53 mutants. *Oncogene*.

Muller, P. (2008). Chaperone-dependent stabilization and degradation of p53 mutants. *nature*.

Murtas D, M. D. (2013). IRF-1 responsiveness to IFN-γ predicts different cancer immune phenotypes. *British journal of cancer*.

Murtas D, M. D. (2013). IRF-1 responsiveness to IFN-γ predicts different cancer immune phenotypes. *British journal of cancer*.

Nagaraju GP, P. W. (2013). Antiangiogenic effects of ganetespib in colorectal cancer mediated through inhibition of HIF-1alpha and STAT-3. . *Angiogenesis* .

Nagata, Y. (1999). The stabilization mechanism of mutant-type p53 by impaired ubiquitination: the loss of wild-type p53 function and the hsp90 association. *oncogene*.

Narayan, V. (2009). Cooperative Regulation of the Interferon Regulatory Factor-1 Tumor Suppressor Protein by Core Components of the Molecular Chaperone Machinery. *jbc*.

Narayan, V. (2009). Cooperative Regulation of the Interferon Regulatory Factor-1 Tumor Suppressor Protein by Core Components of the Molecular Chaperone Machinery. *jbc*.

Narayan, V. (2009). COOPERATIVE REGULATION OF THE IRF-1 TUMOUR SUPPRESSOR PROTEIN BY CORE COMPONENTS OF THE MOLECULAR CHAPERONE MACHINERY. *JBC*.

Narayan, V. (2015). Protein–Protein Interactions Modulate the Docking-Dependent E3-Ubiquitin Ligase Activity of Carboxy-Terminus of Hsc70-Interacting Protein (CHIP). *Molecular and Cellular Proteomics*.

Nasir, L. (1999). Cloning, sequence analysis and expression of the cDNAs encoding the canine and equine homologues of the mouse double minute 2 (mdm2) proto-oncogene. *Cancer letter*.

Nasir, L. (2001). Analysis of p53 mutational events and MDM2 amplification in canine soft-tissue sarcomas. *cancer letters*.

national cancer institute. (2016, april). Retrieved from www.cancer.gov: https://www.cancer.gov/publications/dictionaries/cancer-drug?cdrid=43635

Nehyba, J. R. (2009). , Dynamic evolution of immune system regulators: the history of the interferon regulatory factor family. *Mol Biol Evol,*, 26(11): p. 2539-50.

Neil C Chi, J. S. (2004). Molecular determinants of responses to myocardial ischemia/reperfusion injury: focus on hypoxia-inducible and heat shock factors. *Cardiovascular research*.

Nguyen H, J. H. (1997). The growing family of interferon regulatory factors. *Cytokine Growth Factor Rev*, 8(4): p. 293-312.

Nicholson, J. (2014). A systems wide mass spectrometric based linear motif screen to identify dominant in-vivo interacting proteins for the ubiquitin ligase MDM2. *Cellular Signalling*.

Ning Bu, H. W. (2014). Exosome from chaperone-rich cell lysates-loaded dendritic cells produced by CELLine 1000 culture system exhibits potent immune activity. *Biochemical and Biophysical Research Communications*.

O'Byrne, K. (2015). Stimulating immune responses to fight cancer: Basic biology and mechanisms. *asia- pacific jounral of oncology*.

Olivier Ayraulta, ,. M. (2009). Inhibition of Hsp90 via 17-DMAG induces apoptosis in a p53-dependent manner to prevent medulloblastoma. *PNAS*.

Packham S, W. D. (2015). Nuclear translocation of IGF-1R via p150(Glued) and an importin-β/RanBP2-dependent pathway in cancer cells. *Oncogene* .

Pang, L. Y. (2014). Global Gene Expression Analysis of Canine Osteosarcoma Stem Cells Reveals a Novel Role for COX-2 in Tumour Initiation. *plos one*.

Peiyuan Li, Q. D. (2012). Interferon-gamma induces autophagy with growth inhibition and cell death in human hepatocellular carcinoma (HCC) cells through interferon-regulatory factor-1 (IRF-1). *cancer letters*.

Peiyuan Lia, ,. Q. (2012). Interferon-gamma induces autophagy with growth inhibition and cell death in human hepatocellular carcinoma (HCC) cells through interferon-regulatory factor-1 (IRF-1). *cancer letters*.

Peiyuan Lia, Q. D. (2012). Interferon-gamma induces autophagy with growth inhibition and cell death in human hepatocellular carcinoma (HCC) cells through interferon-regulatory factor-1 (IRF-1). *cancer letters*.

Pendharkar N, G. A. (2016). Quantitative tissue proteomic investigation of invasive ductal carcinoma of breast with luminal B HER2 positive and HER2 enriched subtypes towards potential diagnostic and therapeutic biomarkers. *J Proteomics.* .

Porta C, H.-S. R.-A. (2005). Interferons alpha and gamma induce p53-dependent and p53-independent apoptosis, respectively. *oncogene*.

Proia D, A. J. (2012). Preclinical activity of the Hsp90 inhibitor, ganetespib, in ALK- and ROS1-driven cancers. . *J Clin Oncol* .

Proia DA, F. K. (2011). Multifaceted intervention by the Hsp90 inhibitor ganetespib (STA-9090) in cancer cells with activated JAK/STAT signaling. *PloS one* .

Proia DA, K. G. (2015). Targeting Heat-Shock Protein 90 (HSP90) as a Complementary Strategy to Immune Checkpoint Blockade for Cancer Therapy. *Cancer immunology research*.

Proia DA, Z. C. (2014). Preclinical activity profile and therapeutic efficacy of the HSP90 inhibitor ganetespib in triple-negative breast cancer. . *Clin Cancer Res*.

Pugsley, H. R. (2016). Quantifying autophagy: Measuring LC3 puncta and autolysosome formation in cells using multispectral imaging flow cytometry. *methods*.

Qian, H.-r. (2016). Functional role of autophagy in gastric cancer. *oncotarget*.

R. Timothy Bentley, A. U. (2016). Dogs are man's best friend: in sickness and in health. *Neuro-Oncology*.

Ralf Weiskirchen, F. T. (2014). Cellular and molecular functions of hepatic stellate cells in inflammatory responses and liver immunology. *liver immunology*.

Rappa F, F. F. (2012). HSP-molecular chaperones in cancer biogenesis and tumor therapy: an overview. *anticancer research*.

Ressom, L. T. (2009). LC–MS Based Detection of Differential Protein Expression. *journal of proteomics and bioinformatics*.

Rivera-Calderón LG1, F.-A. C.-A. (2016). Alterations in PTEN, MDM2, TP53 and AR protein and gene expression are associated with canine prostate carcinogenesis. *Res Vet Sci.*

Rocio Garcia-Carbonero, A. C.-A. (2013). Inhibition of HSP90 molecular chaperones: moving into the clinic. *Lancet Oncol* .

Romanucci, M. (2012). Heat shock protein expression in canine osteosarcoma. *Cell Stress and Chaperones* .

Rosa Pennisi, P. A. (2015). Hsp90: A New Player in DNA Repair? *biomolecules*.

Rosalba Camicia, S. B. (2013). BAL1/ARTD9 represses the anti-proliferative and pro-apoptotic IFNc–STAT1–IRF1–p53 axis in diffuse large B-cell lymphoma. *journal of cell science*.

S. Hugen, R. E. (2016). Gastric carcinoma in canines and humans,a review. *veterinary and comparaitive oncology* .

S. Parimi, M. *. (2014). Hsp90 inhibitors in oncology: ready for prime time? *current oncology*.

Salimu J, S. L.-T. (2015). Cross-Presentation of the Oncofetal Tumor Antigen 5T4 from Irradiated Prostate Cancer Cells--A Key Role for Heat-Shock Protein 70 and Receptor CD91. *Cancer immunology research*.

Samant, R. S. (2012). The expanding proteome of the molecular chaperone HSP90. *cell cycle*.

Sang J, A. J. (2013). Targeted inhibition of the molecular chaperone Hsp90 overcomes ALK inhibitor resistance in non-small cell lung cancer. *cancer discovery*.

Sasaki, M. (2007). MDM2 Binding Induces a Conformational Change in p53 That Is Opposed by Heat-shock Protein 90 and Precedes p53 Proteasomal Degradation. *THE JOURNAL OF BIOLOGICAL CHEMISTRY*.

Saurabh Jain, L. A. (2016). The Development of a Recombinant scFv Monoclonal Antibody Targeting Canine CD20 for Use in Comparative Medicine. *plos one*.

Schaaf, M. B. (2016). LC3/GABARAP family proteins: autophagy-(un)related functions. *The FASEB Journal*.

Seo, Y. H. (2015). Organelle-specific Hsp90 inhibitors. *Arch. Pharm. Res*, 38:1582–1590.

Shah, S. e. (2012). The clonal and mutational evolution spectrum of primary triple-negative breast cancers. *Nature*.

Shang L, T. T. (2006). The heat shock protein 90-CDC37 chaperone complex is required for signaling by types I and II interferons. *journal of biological chemistry*.

Sharad Verma, S. G. (2016). Hsp90: Friends, clients and natural foes. *Biochimie*.

SHEN-JEU WON, C.-H. Y.-S.-Y. (2015). Justicidin A-Induced Autophagy Flux Enhances Apoptosis of Human Colorectal Cancer Cells via Class III PI3K and Atg5 pathway. *cell physiology*.

Shimamura T, P. S. (2012). Ganetespib (STA-9090), a Non Geldanamycin HSP90 Inhibitor, has Potent Antitumor Activity in In Vitro and In Vivo Models of Non-Small Cell Lung Cancer . *Clin Cancer Res* .

Shimamura, T. (2008). Heat Shock Protein 90 Inhibition in Lung Cancer. *J Thorac Oncol*.

Shimp SK, P. C. (2012). HSP90 inhibition by 17-DMAG reduces inflammation in J774 macrophages through suppression of Akt and nuclear factor-κB pathways. *Inflammation research*.

Shoukath Sulthana, T. B. (2017). Combination Therapy of NSCLC Using Hsp90 Inhibitor and Doxorubicin Carrying Functional Nanoceria. *Molecular pharmaceutics*.

Siddhartha Mani, D. D. (2011). Rare Primitive Neuroectodermal Tumor (PNET) of Liver in a Young Woman. *Gastrointest Cancer Res*.

Solit DB, C. G. (2008). Development and application of Hsp90 inhibitors. *Drug discovery today* .

Solit DB, R. N. (2011). Resistance to BRAF Inhibition in Melanomas. *New england journal of medicine*.

Sreedhar, A. S. (2004). Hsp90 isoforms: functions, expression and clinical importance. *FEBS Letters*.

Srikanth R. Ambati, a. E. (2014). Pre-clinical efficacy of PU-H71, a novel HSP90 inhibitor, alone and in combination with bortezomib in Ewing sarcoma. *molecular oncology*.

Stroikin, Y. (2004). Inhibition of autophagy with 3-methyladenine results in impaired turnover of lysosomes and accumulation of lipofuscin-like material. *cell biology*.

Stroud, C. (2016). A One Health overview, facilitating advances in comparative medicine and translational research. *Clin Trans Med*.

Stuart K. Calderwood, a. J. (2016). Heat Shock Proteins Promote Cancer: It's a Protection Racket. *cell press*.

Su C, R. Z. (2012). PIWIL4 regulates cervical cancer cell line growth and is involved in down-regulating the expression of p14ARF and p53. *FEBS lett*.

Suiquan Wang, M. Z. (2014). Interferon-γ Induces Senescence in Normal Human Melanocytes. *plos one*.

Su-Kil Seo a, ,. D.-I.-K.-S.-G. (2013). Attenuation of IFN-γ-induced B7-H1 expression by 15-deoxy-delta12,14-prostaglandin J2 via downregulation of the Jak/STAT/IRF-1 signaling pathway. *Life sciences*.

Su-Kil Seo a, ,. D.-I.-K.-S.-G. (2014). Attenuation of IFN-γ-induced B7-H1 expression by 15-deoxy-delta12,14-prostaglandin J2 via downregulation of the Jak/STAT/IRF-1 signaling pathway. *life sciences*.

Susanne Pettersson, M. K. (2009). Role of Mdm2 acid domain interactions in recognition and ubiquitination of the transcription factor IRF-2. *biochemical journal*.

Sutter, N. B. (2004). DOG STAR RISING:THE CANINE GENETIC SYSTEM. *nature genetics*.

Suzanne L. Topalian, J. M. (2016). Mechanism-driven biomarkers to guide immune checkpoint blockade in cancer therapy. *NATURE REVIEWS CANCER*.

syntapharmaceuticals. (2016). Retrieved from syntapharmaceuticals.com.

Taipale M, K. I. (2012). Quantitative analysis of HSP90-client interactions reveals principles of substrate recognition. *Cell*.

Takaoka, A. a. (2006). Interferon signalling network in innate defence. . *Cell Microbiol,,* . 8(6): p. 907-22.

Takaoka, A. T. (2008). Interferon regulatory factor family of transcription factors and regulation of oncogenesis. *Cancer Sci, ,* . 99(3): p. 467-78.

Takeshi Matsuzawa, B.-H. K. (2015). IFN-γ elicits macrophage autophagy via the p38 MAPK signaling. *journal of immunology*.

Takeshi Matsuzawa, E. F. (2013). Autophagy activation by interferon-c via the p38 mitogen-activated protein kinase signalling pathway is involved in macrophage bactericidal activity. *immunology*.

Tanida, I. (2004). LC3 conjugation system in mammalian autophagy. *The International Journal of Biochemistry & Cell Biology*.

Taylor BS, B. J. (2011). Advances in sarcoma genomics and new therapeutic targets. *Nat Rev Cancer*, 11(8):541-57.

Ting Huyan, Q. L.-D.-S. (2016). Heat shock protein 90 inhibitors induce functional inhibition of human natural killer cells in a dose dependent manner. *Immunopharmacology and Immunotoxicology*.

Tiwari, A. a. (2012). Progress against cancer (1971-2011): how far have we come? *J Intern Med*.

Travers, J. (2012). HSP90 inhibition: two-pronged exploitation of cancer dependencies. *drug discovery today*.

Tsirigotis P, S. B. (2016). Programmed death-1 immune checkpoint blockade in the treatment of hematological malignancies. *Annals of medicine*.

Tsutsumi S, B. K. (2009). Impact of heat-shock protein 90 on cancer metastasis. *future oncology*.

Tsutsumi S, N. L. (2007). Extracellular heat shock protein 90: a role for a molecular chaperone in cell motility and cancer metastasis. *cancer science*.

Tu, C. X. (2016). Effects of IRF1 and IFN-β interaction on the M1 polarization of macrophages and its antitumor function. *International Journal of molecular medicine*.

Valeria Azzarito, K. L. (2012). Inhibition of α-helix-mediated protein–protein interactions using designed molecules. *nature chemistry*.

Viau, M. a. (2005). B-lymphocytes, innate immunity, and autoimmunity. . *Clin Immunol*, 114(1): p. 17-26.

VISAN, S. (2015). IN VITRO COMPARATIVE MODELS FOR CANINE AND HUMAN BREAST CANCERS. *oncology*.

Vivien Landré, M. B. (2017). Regulation of Transcriptional Activators by DNA-Binding Domain Ubiquitination. *cell death and differentiation*.

Vogelstein, B. a. (2004.). Cancer genes and the pathways they control. . *Nat Med*.

Wang, X. X. (2012). Mdm2 and MdmX partner to regulate p53. *FEBS lett*, 586(10): 1390-1396.

Wawrzynow, B. Z. (2007). MDM2 chaperones the p53 tumor suppressor. *J Biol Chem* , 282, 32603-32612.

Whitesell L, L. S. (2005). HSP90 and the chaperoning of cancer. *nature reviews*.

Wiech, M. (2012). Molecular Mechanism of Mutant p53 Stabilization: The Role of HSP70 and MDM2. *plos one*.

Wilkinson, S. (2010). Autophagy: an adaptable modifier of tumourigenesis. *genetics and development*.

Workman, P. (2003). Overview: translating Hsp90 biology into Hsp90 drugs. *current cancer drug targets*.

workman, P. (2004). Combinatorial attack on multistep oncogenesis by inhibiting the Hsp90 molecular chaperone. *cancer letters*.

Wu, Y.-T. (2010). Dual Role of 3-Methyladenine in Modulation of Autophagy via Different Temporal Patterns of Inhibition on Class I and III Phosphoinositide 3-Kinase. *THE JOURNAL OF BIOLOGICAL CHEMISTRY*.

X Xiong, Y. Z. (2011). Ribosomal protein S27-like and S27 interplay with p53-MDM2 axis as a target, a substrate and a regulator. *oncogene*.

Xi, H. e. (1999). , Co-occupancy of the interferon regulatory element of the class II transactivator (CIITA) type IV promoter by interferon regulatory factors 1 and 2. 3. *Oncogene*, 18(43): p. 5889-90.

Xiaodi Su, Y. Y. (2015). Interferon-γ regulates cellular metabolism and mRNA translation to potentiate macrophage activation. *nature immunology*.

Xiong X, Z. Y. (2014). Ribosomal protein S27-like is a physiological regulator of p53 that suppresses genomic instability and tumorigenesis. *E life*.

Xu D1, J. S. (2016). Small-molecule binding sites to explore protein-protein interactions in the cancer proteome. *Mol Biosyst*.

Xu J, C. J. (2015). PIG3 plays an oncogenic role in papillary thyroid cancer by activating the PI3K/AKT/PTEN pathway. *oncology reports*.

Xu W, N. L. (2007). Targeting the molecular chaperone heat shock protein 90 provides a multifaceted effect on diverse cell signaling pathways of cancer cells. *Clin Cancer Res* .

Yadav M, J. S. (2014). Predicting immunogenic tumour mutations by combining mass spectrometry and exome sequencing.

Yamada-Kanazawa, S. (2017). inhibtion of HSP90 exerts anti-tumor effect on angiosarcoma: Involvement of VEGF signaling. *Br J Dermatol*.

Yang S, I. Y. (2016). Autophagy Inhibition Dysregulates TBK1 Signaling and Promotes Pancreatic Inflammation. *Cancer immunology research*.

Yang, a. X. (2014). Effects of suppressor of cytokine signaling 1 silencing on human melanoma cell proliferation and interferon-γ sensitivity. *molecular medicine reports*.

Yasukazu Takanezawa, R. N. (2016). Atg5-dependent autophagy plays a protective role against. *Toxicology Letters*.

Yifan Wang, H. L. (2016). Hsp90 Inhibitor Ganetespib Sensitizes Non–Small Cell Lung Cancer to Radiation but Has Variable Effects with Chemoradiation. *cancer therapy*.

Ying W, D. Z. (2012). Ganetespib, a unique triazolone-containing Hsp90 inhibitor, exhibits potent antitumor activity and a superior safety profile for cancer therapy. *Molecular cancer therapeutics* .

Youlyouz-Marfak I, G. N.-M. (2008). Identification of a novel p53-dependent activation pathway of STAT1 by antitumour genotoxic agents. *cell death and differentiation*.

Yu Qiao, E. G.-h. (2013). Synergistic Activation of Inflammatory Cytokine Genes by Interferon-g-Induced Chromatin Remodeling and Toll-like Receptor Signaling. *immunity*.

Yuan XW, Z. X. (2008). Interferonalpha enhances etoposide-induced apoptosis in human osteosarcoma U2OS cells by a p53-dependent pathway. *life sciences*.

Yuen HF, G. V.-H.-T. (2013). RanGTPase: a candidate for Myc-mediated cancer progression. *J Natl Cancer Inst*.

Zaidi MR, M. G. (2011). The two faces of interferon-γ in cancer. *clinical cancer research*.

Zdenek Andrysik, J. K. (2013). A genetic screen identifies TCF3/E2A and TRIAP1 as pathway-specific regulators of the cellular response to p53 activation. *cell reports*.

Zhang DZ, C. B. (2017). Basic Transcription Factor 3 is Required for Proliferation and Epithelial-Mesenchymal Transition Via Regulation of FOXM1 and JAK2/STAT3 Signaling in Gastric Cancer. *Oncol Res.* .

Zhang F, L. J. (2017). Elevated transcriptional levels of aldolase A (ALDOA) associates with cell cycle-related genes in patients with NSCLC and several solid tumors. *BioData Min*.

Zhang H, 2. L. (2017). Differential expression of peroxiredoxin 3 in laryngeal squamous cell carcinoma. *Oncotarget.*

Zhang, J. (2009). Establishment of a Dog Model for the p53 Family Pathway and Identification of a Novel Isoform of p21 Cyclin-Dependent Kinase Inhibitor. *molecular cancer research*.

Zhang, K. (2015). Endoplasmic reticulum stress response and transcriptional reprogramming. . *Front Genet*.

Zhang, S. J. (2014). The Significance of Transcriptome Sequencing in Personalized Cancer Medicine.

Zhu H, L. P. (2012). BAG3: a new therapeutic target of human cancers? *Histol Histopathol.*

Ziyan Y. Pessetto, B. C. (2017). In silico and in vitro drug screening identifies new therapeutic approaches for Ewing sarcoma. *oncotarget*.

Supplement data

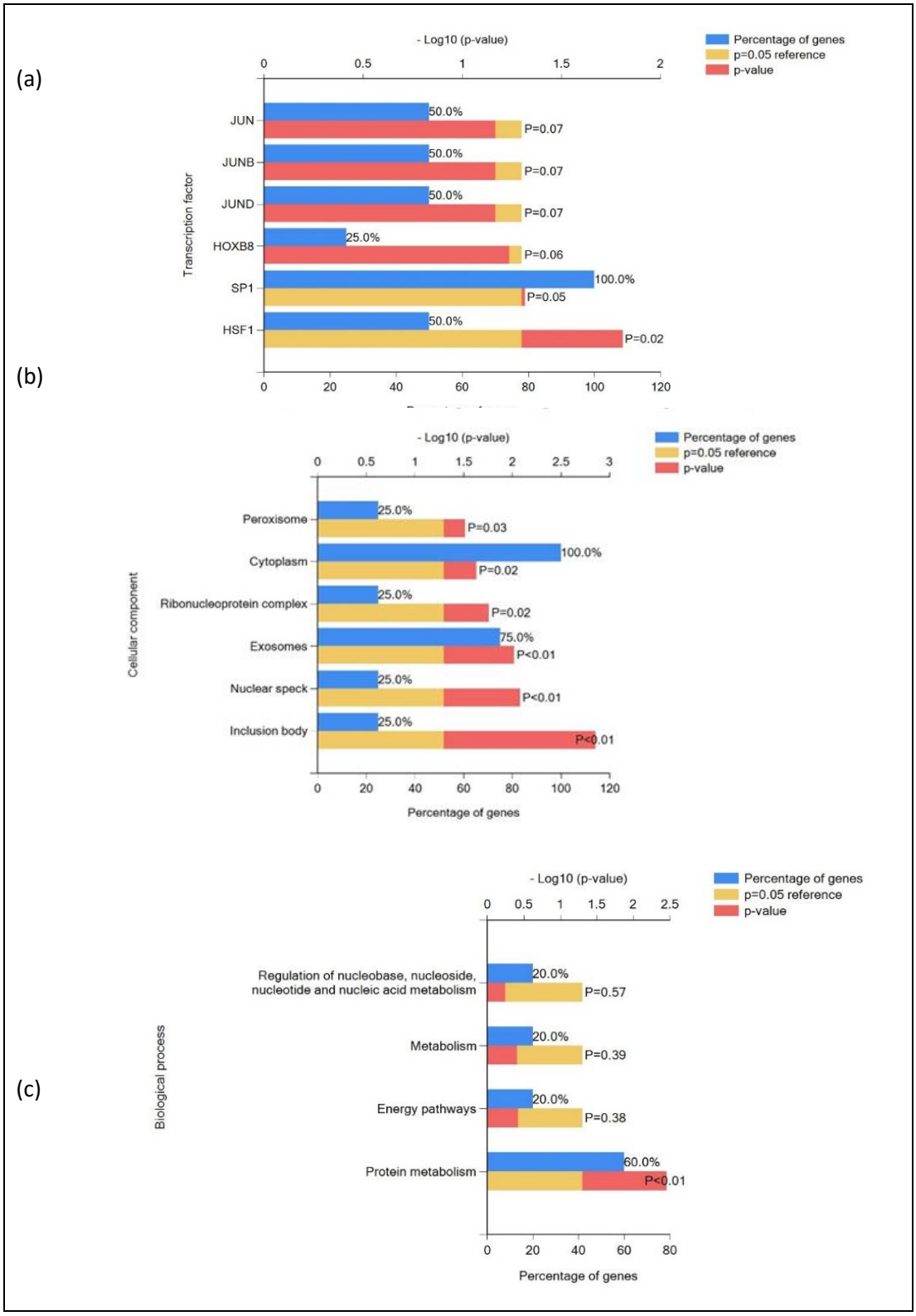

Figure 96 upregulated with Ganetespib

(a)

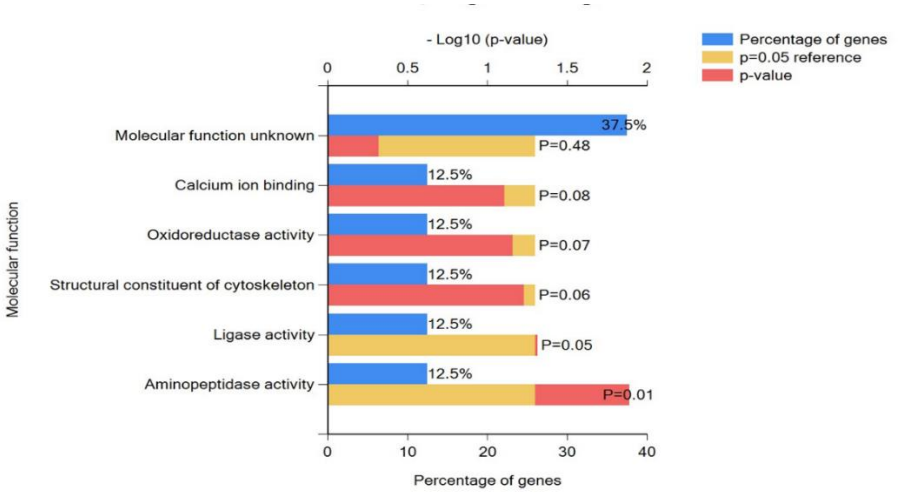
- Log10 (p-value)
0
0.5
1
1.5
2
Percentage of genes
p=0.05 reference
p-value
Molecular function
Molecular function unknown
37.5%
P=0.48
Calcium ion binding
12.5%
P=0.08
Oxidoreductase activity
12.5%
P=0.07
Structural constituent of cytoskeleton
12.5%
P=0.06
Ligase activity
12.5%
P=0.05
Aminopeptidase activity
12.5%
P=0.01
0
10
20
30
40
Percentage of genes

(b)

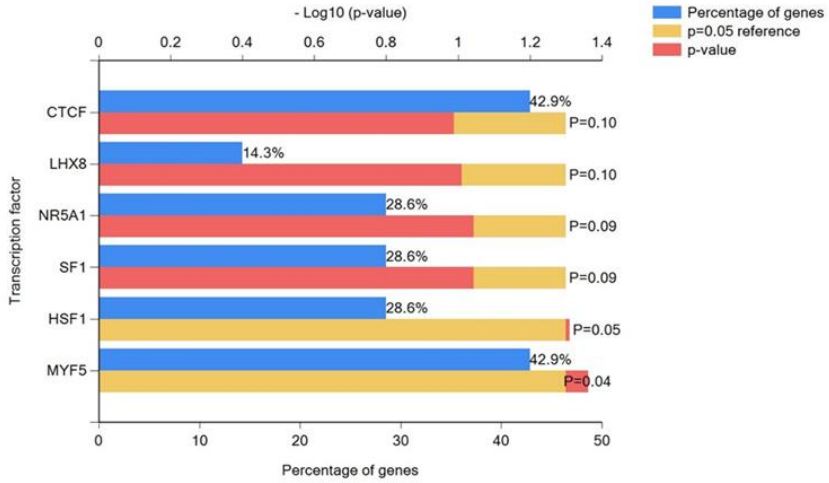
- Log10 (p-value)
0
0.2
0.4
0.6
0.8
1
1.2
1.4
Percentage of genes
p=0.05 reference
p-value
Transcription factor
CTCF
42.9%
P=0.10
LHX8
14.3%
P=0.10
NR5A1
28.6%
P=0.09
SF1
28.6%
P=0.09
HSF1
28.6%
P=0.05
MYF5
42.9%
P=0.04
0
10
20
30
40
50
Percentage of genes

(c)

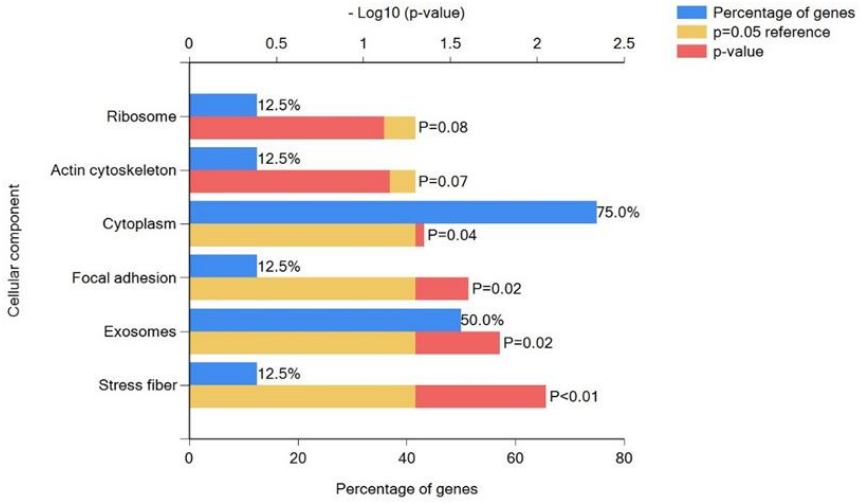
- Log10 (p-value)
0
0.5
1
1.5
2
2.5
Percentage of genes
p=0.05 reference
p-value
Cellular component
Ribosome
12.5%
P=0.08
Actin cytoskeleton
12.5%
P=0.07
Cytoplasm
75.0%
P=0.04
Focal adhesion
12.5%
P=0.02
Exosomes
50.0%
P=0.02
Stress fiber
12.5%
P<0.01
0
20
40
60
80
Percentage of genes

(d)

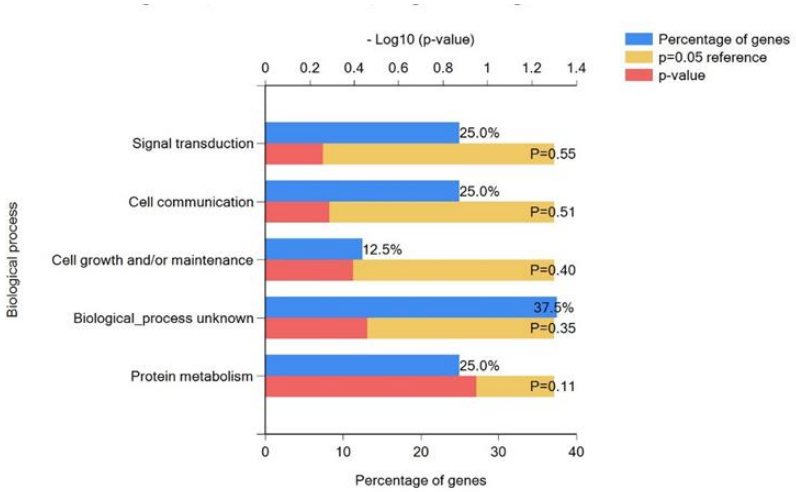

Figure 97 upregulated with nutlin

(a)

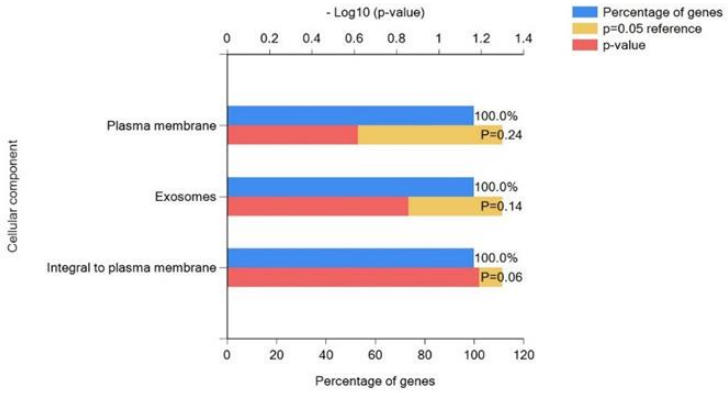

(b)

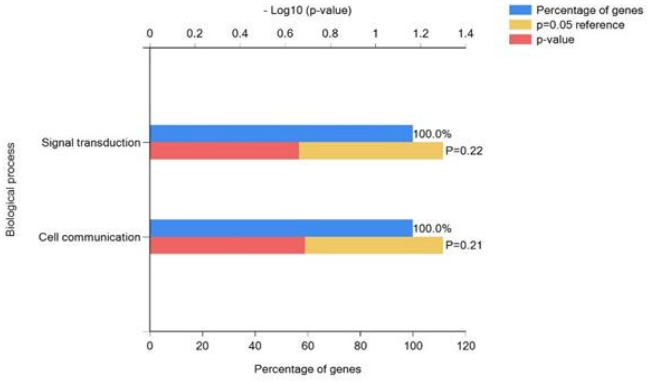

(c)

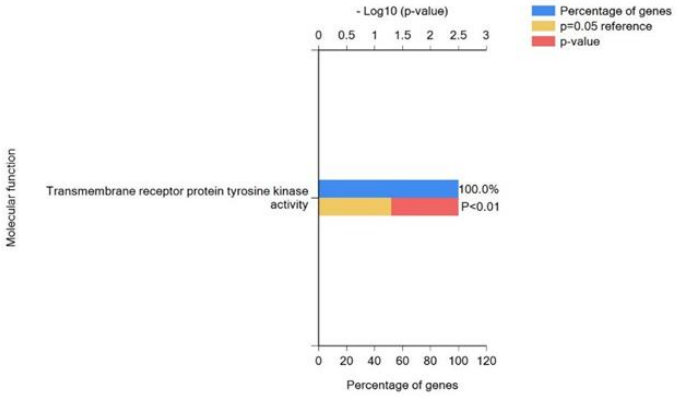

Figure 98 downregulated with Ganetespib

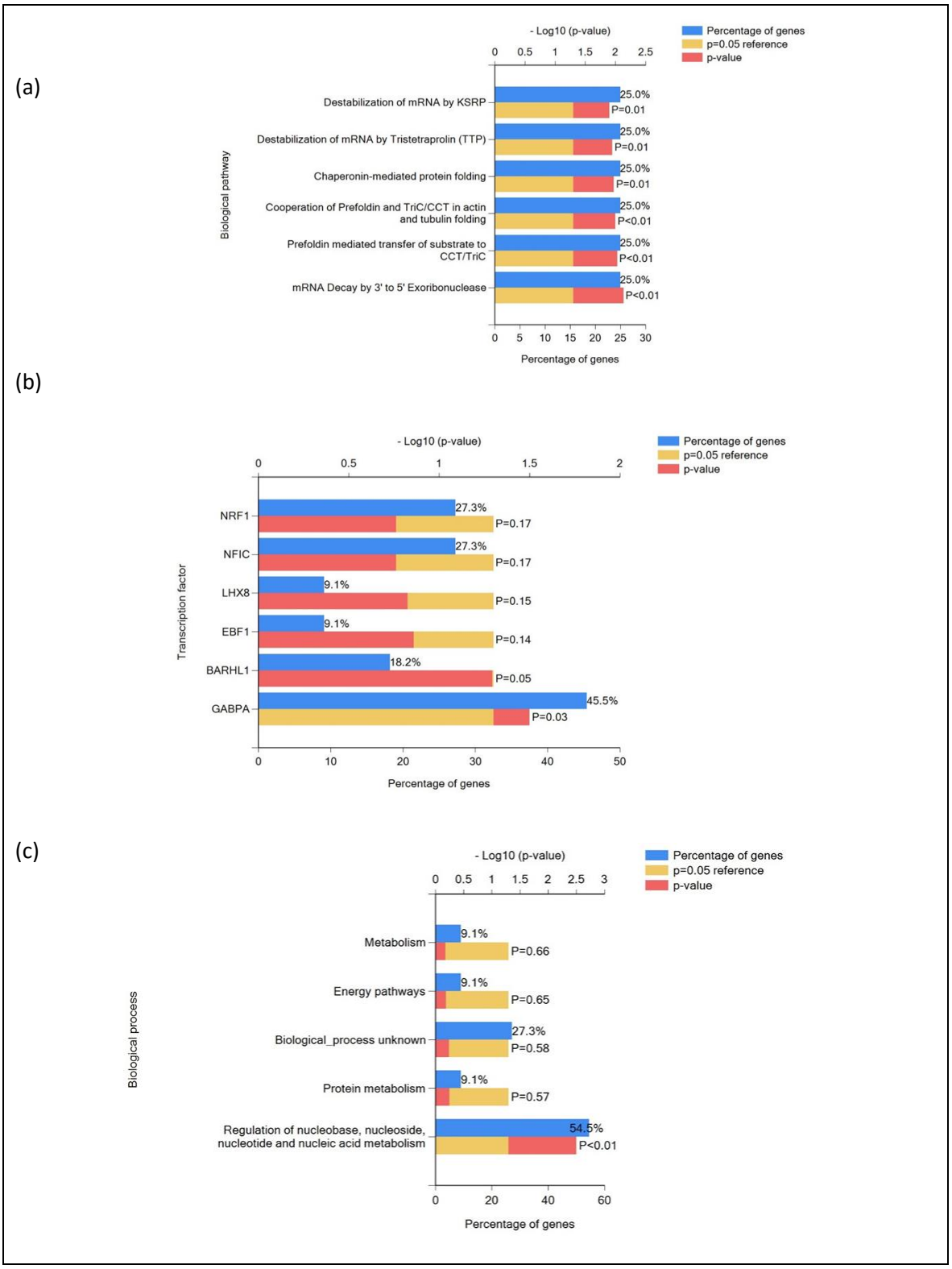

Figure 99downregulated with nutlin

(a)

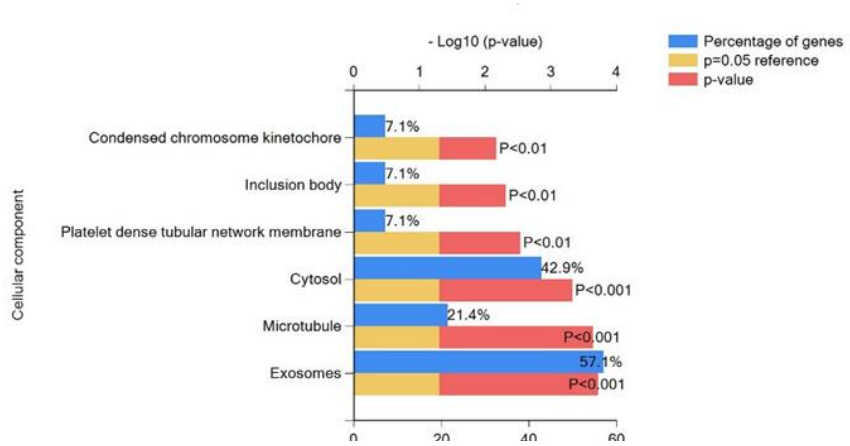

(b)

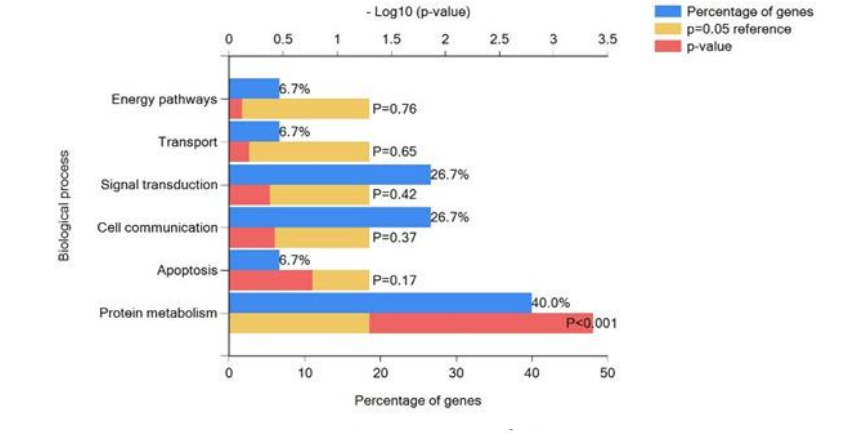

(c)

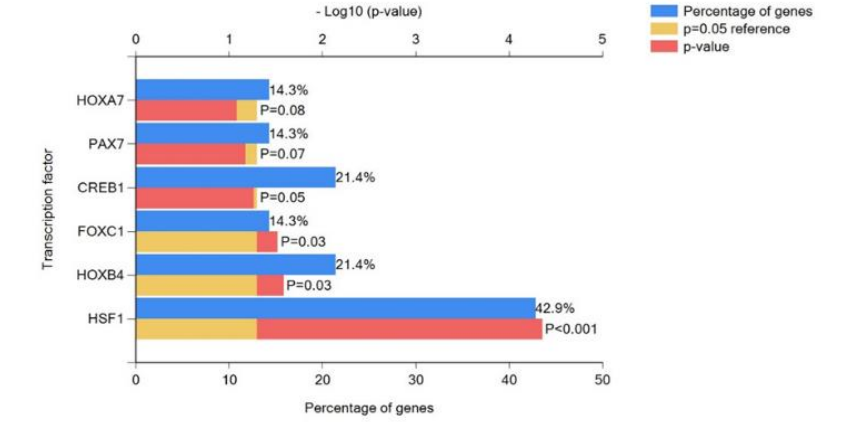

Figure 100gan+nut upregulated

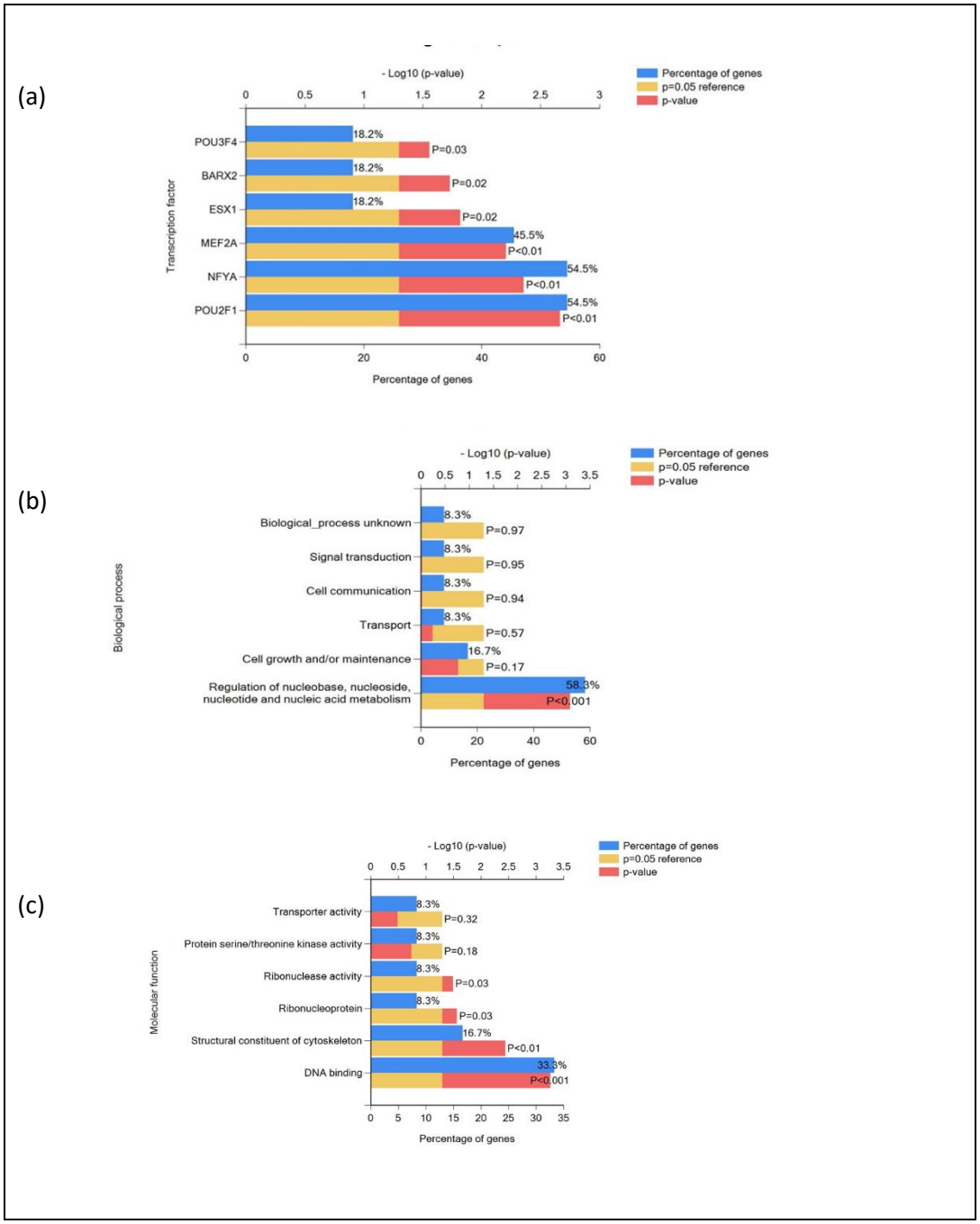

Figure 101nutlin+gan downregulated